

SYNTHESIS OF NEW ORGANOTIN (IV) DERIVATIVES
OF THIO SEMICARBAZIDES AND S, N, O CONTAINING
RELATED LIGANDS: CHARACTERIZATION AND STUDIES
ON THE BIOCIDAL PROPERTIES OF THE NEW COMPOUNDS
WITH SPECIAL REFERENCE TO THEIR AGRICULTURAL
APPLICATIONS

Thesis Submitted for
The Degree of Doctor of Philosophy in Chemistry



By
Bipasa Sarkar , M.Sc.

DEPARTMENT OF CHEMISTRY
UNIVERSITY OF NORTH BENGAL
DARJEELING, WEST BENGAL, INDIA
2010

27 MAY 2017

239345

S245S

S47

TN

Dedicated to my beloved Parents
&
husband Tapan
&
son Vaibhav

DECLARATION

I hereby, declare that the work presented in this thesis entitled "Synthesis of new organotin (IV) derivatives of thio-semicarbazides and S, N, O containing related ligands: characterization and studies on the biocidal properties of the new compounds with special reference to their agricultural applications" is entirely original and was carried out by me under the guidance and supervision of Professor Abhijit Roy (Supervisor, PI), Department of Chemistry, University of North Bengal, Darjeeling and Professor Apurba kumar Chowdhury (Co-supervisor), Department of Plant Pathology, Uttar Banga Krishi Viswavidyalaya, Cooch Behar for the award of Doctor of Philosophy in Chemistry. As far as my knowledge is concerned the contents of this thesis did not form the basis of award of any previous degree to me or to anybody else.

Further, to the best of my knowledge, the thesis has not been submitted previously for the award of any degree to this university or any other university.


Bipasa Sarkar

Siliguri

Date :

CONTENTS

Acknowledgement	I
Preface	III

CHAPTER 1

A SHORT REVIEW ON THE ORGANOTIN(IV) COMPOUNDS

1.1 Introduction	1
1.2 Literature	2
1.3 Bonding in organotin compounds	6
1.4 Structure of organotin compounds	7
1.5 Reactivity of organotin compounds	8
1.6 Analytical techniques applied to determination the structure of organotin compounds	9
1.7 Applications of organotin compounds	9
1.7.1 Biological applications	10
1.7.2 Non biological Applications	11
1.7 References	13

CHAPTER 2

SYNTHESIS AND CHARACTERIZATION OF Mn(II), Fe(II), Co(II), Cu(II), Zn(II) COMPLEXES OF 3,5-DI NITRO BENZOIC ACID, CRYSTAL STRUCTURES OF Co(II) AND Cu(II)

2.1 Introduction	17
2.2 Literature	18
2.3 Scope and objective	31
2.4 Experimental	31
2.4.1 General Comments	31
2.4.2 Materials	31
2.4.3 Measurements	31
2.4.4 Synthetic procedures	32
2.4.4.1 Preparation of sodium salt of 3,5-dinitro benzoic acid (LNa)	32
2.4.4.2 Preparation of Mn(II) complex of 3,5-dinitro benzoic acid (1)	32
2.4.4.3 Preparation of Fe(II) complex of 3,5-dinitro benzoic acid (2)	33
2.4.4.4 Preparation of Co(II) complex of 3,5-dinitro benzoic acid (3)	33
2.4.4.5 Preparation of Cu(II) complex of 3,5-dinitro benzoic acid (4)	33
2.4.4.6 Preparation of Zn(II) complex of 3,5-dinitro benzoic acid (5)	34
2.4.5 Crystal structure determinations	34
2.4.6 Crystallographic data and refinement details for 3 and 4	35
2.4.7 Biological studies	36
2.4.7.1 Antifungal activity	36
2.4.7.2 Phytotoxic effect	36
2.5 Result and discussion	36
2.5.1 Preparation of sodium salt of 3,5-dinitrobenzoic acid	36
2.5.2. Synthesis of transition metal(II) complexes of 3,5-dinitrobenzoic acid (LH)	37
2.5.3 Spectroscopic characterization and X-ray crystal structure determination of	38

transition metal carboxylates, $M(L)_2$ [where $M = Mn, Fe, Co, Cu$ and Zn ; $L = 3,5$ - dinitrobenzoic acid]	
2.5.3.1 IR spectra	39
2.5.3.2 Magnetic moment	40
2.5.3.3 Differential calorimetric analysis	41
2.5.3.4 Electronic spectra	42
2.5.3.5 X-ray Crystal structure	43
2.5.3.5.1 Crystal structure of $Co(II)$ complex of 3,5-dinitrobenzoic acid (3)	43
2.5.3.5.1 Crystal structure of $Cu(II)$ complex of 3,5-dinitrobenzoic acid (4)	47
2.5.4 Biological properties of transition metal carboxylates of 3,5-dinitrobenzoic acid	50
2.5.4.1 Antifungal activities	50
2.5.4.2 Phytotoxic properties	51
2.6 References	52

CHAPTER 3

SYNTHESES AND CHARACTERIZATION OF ORGANOTIN(IV) COMPLEXES OF 2-MARCAPTO ISOTHIOCYANATE

3.1 Introduction	55
3.2 Literature	55
3.3 Scope and Objective	71
3.4 Experimental	71
3.4.1 General comments	71
3.4.2 Materials	72
3.4.3 Measurements	73
3.4.4 Crystallography	73
3.4.5 Synthetic Procedure	79
3.4.5.1 Preparation of 2-marcapto isothiocyanate (LH)	79
3.4.5.2 Preparation of sodium salt of 2-marcapton isothiocyanate (LNa)	80
3.4.5.3 Synthesis of trimethyltin(IV) 2-marcapto isothiocyanate, Me_3SnL (1)	80
3.4.5.4 Synthesis of n-tributyltin(IV) 2-marcapto isothiocyanate, $n-Bu_3SnL$ (2)	80
3.4.5.5 Synthesis of triphenyltin(IV) 2-marcapto isothiocyanate, Ph_3SnL (3)	81
3.4.5.6 Synthesis of tribenzyltin(IV) 2-marcapto isothiocyanate, Bz_3SnL (4)	81
3.4.5.7 Synthesis of tricyclohexyltin(IV) 2-marcapto isothiocyanate, $c-Hex_3SnL$ (5)	82
3.4.5.8 Synthesis of dimethyltin(IV) 2-marcapto isothiocyanate, $Me_2Sn(L)_2$ (6)	82
3.4.5.9 Synthesis of n-dibutyltin(IV) 2-marcapto isothiocyanate, $n-Bu_2Sn(L)_2$ (7)	82
3.4.5.10 Synthesis of diphenyltin(IV) 2-marcapto isothiocyanate, $Ph_2Sn(L)_2$ (8)	83
3.4.5.11 Synthesis of dibenzyltin(IV) 2-marcapto isothiocyanate, $Bz_2Sn(L)_2$ (9)	83
3.5 Result and Discussion	83
3.5.1 Preparation of 2-marcapto isothiocyanate	84
3.5.2 Synthesis of tri- and diorganotin(IV) complexes 2-marcapto isothiocyanate	84
3.5.2.1 Synthesis of triorganotin(IV) complexes of 2-marcapto isothiocyanate (LH)	84
3.5.2.2 Synthesis of triorganotin(IV) complexes of 2-marcapto isothiocyanate (LH)	85
3.5.2.3 Synthesis of diorganotin(IV) complexes of 2-marcapto isothiocyanate (LH)	86
3.5.3 Spectroscopic characterization of tri-and diorganotin(IV) complexes	87
3.5.3.1 Differential calorimetric analysis	87
3.5.3.2 IR Spectra	88
3.5.3.3 NMR Spectra	89
3.5.3.4 A brief note on crystal structure of compound B	94
3.6 References	96

CHAPTER 4

SYNTHESIS, SPECTROSCOPIC CHARACTERIZATION AND X-RAY CRYSTAL STRUCTURES OF SOME DIORGANOTIN(IV) COMPLEXES OF SALICYLALDEHYDE THIOSEMICARBAZONE AND RELATED LIGANDS

4.1 Introduction	100
4.2 Literature	101
4.3 Scope and Objective	132
4.4 Experimental	133
4.4.1 General comments	133
4.4.2 Materials	133
4.4.3 Measurements	133
4.4.4 Synthetic procedure	134
4.4.4.1 Preparation of 4-cyclohexyl thiosemicarbazide	134
4.4.4.2 Preparation of salicylaldehyde 4-cyclohexyl thiosemicarbazone (L ¹ H)	135
4.4.4.3 Preparation of salicylaldehyde ortho-amino thio phenol (L ² H)	135
4.4.4.4 Preparation of 3-bromo-5-Chloro-salicylaldehydethiosemicarbazone (L ³ H)	136
4.4.4.5 Preparation of 3,5-dibromo-salicylaldehydethiosemicarbazone (L ⁴ H)	136
4.4.4.6 Synthesis of dimethyltin(IV) salicylaldehyde 4-cyclohexyl thiosemicarbazonate, Me ₂ SnL ¹ (1)	137
4.4.4.7 Synthesis of n-dibutyltin(IV) salicylaldehyde 4-cyclohexyl thiosemicarbazonate, n-Bu ₂ SnL ¹ (2)	137
4.4.4.8 Synthesis of diphenyltin(IV) salicylaldehyde 4-cyclohexyl thiosemicarbazonate, Ph ₂ SnL ¹ (3)	137
4.4.4.9 Synthesis of n-dibutyltin(IV) salicylaldehyde ortho-amino thio phenol, n-Bu ₂ SnL ² (4)	137
4.4.4.9 Synthesis of dimethyltin(IV) 3-bromo-5-chlorosalicylaldehydethiosemicarbazonate, Me ₂ SnL ³ (5)	138
4.4.4.10 Synthesis of di n-butyltin(IV) 3-bromo-5-chloro-salicylaldehydethiosemicarbazonate, n-Bu ₂ SnL ³ (6)	138
4.4.4.11 Synthesis of diphenyltin(IV) 3-bromo-5-chloro-salicylaldehydethiosemicarbazonate, Ph ₂ SnL ³ (7)	138
4.4.4.12 Synthesis of dibenzyltin(IV) 3-bromo-5-chloro-salicylaldehydethiosemicarbazonate, Bz ₂ SnL ³ (8)	139
4.4.4.13 Synthesis of dimethyltin(IV) 3, 5-dibromo-salicylaldehydethiosemicarbazonate, Me ₂ SnL ⁴ (9)	139
4.4.4.14 Synthesis of di-n-butyltin(IV) 3, 5-dibromo-salicylaldehydethiosemicarbazonate, n-Bu ₂ SnL ⁴ (10)	139
4.4.4.15 Synthesis of diphenyltin(IV) 3, 5-dibromo-salicylaldehydethiosemicarbazonate, Ph ₂ SnL ⁴ (11)	139
4.4.4.16 Synthesis of dibenzyltin(IV) 3, 5-dibromo-salicylaldehydethiosemicarbazonate, Bz ₂ SnL ⁴ (12)	140
4.4.5 Crystal structure determination	140
4.4.6 Crystallographic data and refinement details for 5, 6,7, 9 and 10.	142
4.4.7 Biological studies	147
4.4.7.1 Antifungal activity	147
4.4.7.2 Phytotoxic effect	147
4.5 Result and discussion	148
4.5.1 Syntheses of the Schiff base ligands	148
4.5.2 Syntheses of the diorganotin(IV) complexes of Schiff base ligands	149

4.5.3 Spectral characterization and X-ray structure determination of diorganotin(IV) complexes	153
4.5.3.1 IR spectra	154
4.5.3.2 NMR spectra	155
4.5.3.3 Electronic spectra	162
4.5.3.4 X-ray Crystal Structures	163
4.5.3.4.1 Crystal structure of Me_2SnL^3 (5) and Me_2SnL^4 (9)	163
4.5.3.4.2 Crystal structure of $\text{n-Bu}_2\text{SnL}^3$ (6) and $\text{n-Bu}_2\text{SnL}^4$ (10)	169
4.5.3.4.3 Crystal structure of Ph_2SnL^3 (7)	173
4.5.3.5 Differential calorimetric analysis	176
4.5.4. Biological properties of diorganotin(IV) complexes of substituted salicyldehyde thiosemicarbazone.	177
4.5.4.1 Anti-fungal activities	177
4.5.4.2 Phytotoxic properties	179
4.6 References	181

CHAPTER 5

BIOCIDAL ACTIVITY OF ORGANOTIN(IV) COMPLEXES ON FOLIAR BLIGHT DISEASES OF WHEAT (*Triticum aestivum* L.)

5.1 Introduction	187
5.2 Literature	188
5.2.1 Use of organotin as biocide	188
5.2.2 Economic importance of <i>B. sorokiniana</i>	190
5.2.3 Symptoms of <i>B. sorokiniana</i> infection	193
5.2.4 Management of foliar blight	193
5.2.4.1 Seed treatment	193
5.2.4.2 Chemical Management	194
5.2.4.3 Induced resistance	196
5.2.5 Biochemical changes due to infection	197
5.2.5.1 Phenol	198
5.2.5.2 Ortho-dihydroxyphenol	199
5.2.5.3 Protein	199
5.2.5.4 Polyphenoloxidase	200
5.2.5.5 Peroxidase	200
5.2.5.6 Phenylalanine ammonia-lyase	201
5.2.5.7 Pathogenesis Related (PR) proteins	201
5.3 Scope and objective	202
5.4 Materials and Methods	202
5.4.1 General comments	202
5.4.2 Measurements	202
5.4.3 Synthesis and characterization of di and triorganotin(IV) complexes of Schiff bases	203
5.4.3 Synthesis and characterization of di and triorganotin(IV) complexes of 2-mercapto isothiocyanate	204
5.4.4 Location	204
5.4.5 Weather	204
5.4.6 Soil Characteristics	205
5.4.7 Media	205
5.4.8 Planting material	206
5.4.9 Isolation of pathogens	207
5.4.10 Fungal culture	207

4.5.3 Spectral characterization and X-ray structure determination of diorganotin(IV) complexes	153
4.5.3.1 IR spectra	154
4.5.3.2 NMR spectra	155
4.5.3.3 Electronic spectra	162
4.5.3.4 X-ray Crystal Structures	163
4.5.3.4.1 Crystal structure of Me_2SnL^3 (5) and Me_2SnL^4 (9)	163
4.5.3.4.2 Crystal structure of $\text{n-Bu}_2\text{SnL}^3$ (6) and $\text{n-Bu}_2\text{SnL}^4$ (10)	169
4.5.3.4.3 Crystal structure of Ph_2SnL^3 (7)	173
4.5.3.5 Differential calorimetric analysis	176
4.5.4. Biological properties of diorganotin(IV) complexes of substituted salicylaldehyde thiosemicarbazone.	177
4.5.4.1 Anti-fungal activities	177
4.5.4.2 Phytotoxic properties	179
4.6 References	181

CHAPTER 5

BIOCIDAL ACTIVITY OF ORGANOTIN(IV) COMPLEXES ON FOLIAR BLIGHT DISEASES OF WHEAT (*Triticum aestivum* L.)

5.1 Introduction	187
5.2 Literature	188
5.2.1 Use of organotin as biocide	188
5.2.2 Economic importance of <i>B. sorokiniana</i>	190
5.2.3 Symptoms of <i>B. sorokiniana</i> infection	193
5.2.4 Management of foliar blight	193
5.2.4.1 Seed treatment	193
5.2.4.2 Chemical Management	194
5.2.4.3 Induced resistance	196
5.2.5 Biochemical changes due to infection	197
5.2.5.1 Phenol	198
5.2.5.2 Ortho-dihydroxyphenol	199
5.2.5.3 Protein	199
5.2.5.4 Polyphenoloxidase	200
5.2.5.5 Peroxidase	200
5.2.5.6 Phenylalanine ammonia-lyase	201
5.2.5.7 Pathogenesis Related (PR) proteins	201
5.3 Scope and objective	202
5.4 Materials and Methods	202
5.4.1 General comments	202
5.4.2 Measurements	202
5.4.3 Synthesis and characterization of di and triorganotin(IV) complexes of Schiff bases	203
5.4.3 Synthesis and characterization of di and triorganotin(IV) complexes of 2-mercapto isothiocyanate	204
5.4.4 Location	204
5.4.5 Weather	204
5.4.6 Soil Characteristics	205
5.4.7 Media	205
5.4.8 Planting material	206
5.4.9 Isolation of pathogens	207
5.4.10 Fungal culture	207

5.4.10.1 Source	207
5.4.10.2 Completion of Koch's postulate	207
5.4.10.3 Maintenance of stock	207
5.4.11 Definition of field experiments parameters	208
5.4.12 Disease Assessment	208
5.4.13 Parameters of laboratory experiment	209
5.4.13.1 Detached leaf assay	209
5.4.13.2 Phenol	209
5.4.13.3 Ortho dihydroxy phenol (OD Phenol)	210
5.4.13.4 Protein	210
5.4.13.5 Polyphenol oxidase (PPO)	211
5.4.13.6 Peroxidase (PO)	211
5.4.13.7 Phenylalanine ammonia-lyase (PAL)	212
5.4.13.8 SDS-polyacrylamide gel electrophoresis of total soluble protein	213
5.5 Result and Discussion	216
5.5.1 Set I	217
5.5.1.1 Effect of organotin compounds on spore germination and growth	217
5.5.1.2 Effect of organotin compounds on symptom expression and yield attributes in wheat plants	219
5.5.1.3 Studies on the biochemical changes associated with resistance in wheat plants	221
5.5.1.3.1 Total phenols	222
5.5.1.3.2 Ortho-dihydroxy phenols	222
5.5.1.3.3 Total protein	223
5.5.1.3.4 Peroxidase activity	224
5.5.1.3.5 Polyphenoloxidase activity	224
5.5.2 Set II	225
5.5.2.1 Effect of chemicals on <i>B. sorokiniana</i> in wheat	226
5.5.2.2 Biochemical changes associated with resistance in the wheat plant (cv Sonalika) after infection.	227
5.5.2.2.1 Total phenol	228
5.5.2.2.2 Ortho-dihydroxyphenol	229
5.5.2.2.3 Peroxidase activity	229
5.5.2.2.4 Polyphenoloxidase activity	230
5.5.2.2.5 Total protein	230
5.5.3 Phenylalanine ammonia lyase activity	231
5.5.4 Effect of organotin compounds on seedling growth of wheat	232
5.5.5 Effect of organotin compounds on <i>Alternaria titricina</i> and <i>Fusarium solani</i>	234
5.6 References	238

Corrigendum

245

Acknowledgement

I wish to express my deep sense of gratitude to Prof. Abhijit Roy (Supervisor, PI), Department of Chemistry, University of North Bengal, Darjeeling and Prof. Apurba Kumar Chowdhury (Co-supervisor), Department of Plant Pathology, Uttar Banga Krishi Viswavidalaya, Cooch Behar for their intensive and constant supervision throughout the course of this investigation.

I express my sincere gratitude to Prof. Edward R.T. Tiekink, Department of Chemistry, University of Malaya, 50603 Kuala Lumpur, Malaysia and Prof. C. J. Cardin, Department of chemistry, University of Reading, Whitenights RG6 6AD U.K. for their generous help in analyzing and interpreting the crystallographic data included in this thesis.

Prof Rudolph Willem and Prof Monique Biesemans High Resolution NMR Centre, Department of Materials and Chemistry, Vrije Universiteit Brussel, Pleinlaan 2, B-1050 Brussels, Belgium are thanked for their kind help in NMR spectroscopic analyses.

I take this opportunity to thank Prof. A. K. Saha, Ex-Dean, Faculty of Technology, Uttar Banga Krishi Viswavidalaya, Cooch Behar for providing me the research facilities at UBKV.

I am grateful to Prof. N. Chattopadhyay, Department of Chemistry, Jadavpur University, Kolkata for providing the fluorescence spectroscopic data.

I record my sincere gratitude for Dr. A. Saha, Department of Botany, University of North Bengal, Darjeeling for gifting a few fungal cultures.

I am indebted to my friends (juniors or seniors) and hostel mates Soma, Moumita, Babita, Gopalda, Aneamika, Ali, Uttam, Amitabha, Samik, Kaushik, Sujoy, Suranjan, Madhumita and Manisha in particular for their kind help during my stay at the North Bengal University campus. I also thank all the past and present research scholars of the Department of Chemistry, University of North Bengal for their pleasant association.

I wish to record my appreciation to the teaching as well as the non-teaching staff members, Department of Chemistry, University of North Bengal, Darjeeling and Department of Plant Pathology, Uttar Banga Krishi Viswavidalaya, Cooch Behar for their kind support and co-operation during the course of my work. I also would like to

thank Dr. A. Nanda and Dr. A. Majumder of the Department of Chemistry, University of North Bengal for kindly recording some of the spectra.

I express my special thanks for friendly support, collection of reprints and technical help to Dr Arindam Sarkar, Research associate, UCR, California, Dr. Biswajit Sinha, Department of Chemistry, University of North Bengal, Darjeeling and Dr. Jyotsna Das, Lecturer, Alipurduar College, Alipurduar.

Words are inadequate to express the constant kind and loving encouragements received from my Ma and Baba. They have been the pillar of strength in my life and I really owe it all to them.

My thanks are also due to Duke, Swati, Bapi, Dada, Simadi, Joy, Shymal, Tia, Priya, Pisimani, Arupda and Aishi. Without their inspiration, this study would not have seen the dawn of this day.

Vaibhav and Tapan deserve very special appreciation for their tremendous sacrifice during the entire period of my doing research for the degree.

‘GOD WHO HAS PROVIDED ME WITH POWER TO TAKE UP AND FINISH MY THESIS’

(Bipasa Sarkar)

PREFACE

The thesis entitled, “synthesis of new organotin (IV) derivatives of thio-semicarbazides and S, N, O containing related ligands: characterization and studies on the biocidal properties of the new compounds with special reference to their agricultural applications” has aimed to explore the chemistry of simple organotin(IV) thio-semicarbazides and other related compounds. The work has been divided into five chapters.

Chapter 1

This chapter describes a brief review on the nature of bonding, other related properties including biocidal properties of the organotin compounds.

Chapter 2

This chapter describes the synthesis and characterization of Mn(II), Fe(II), Co(II), Cu(II) and Zn(II) complexes 3-5, dinitrobenzoic acid. The complexes were characterized by UV-Vis, IR and elemental analysis. Magnetic moments studies and differential scanning calorimetric measurements were carried out for these complexes. The X-ray crystallography studies were carried for Co(II) and Cu(II) complexes. The biological activity of some of the compounds against two fungal pathogens namely (*Lasiodiplodia theobromae* and *Crucularia eragrostidis*) which were isolated from two different crops (a pathogen of mango, *Magnifera indica* and a pathogen of tea, *Camellia sinensis*) respectively were undertaken to demonstrate their fungicidal activity. The phytotoxic effects of these compounds were also investigated against *Oryzae sativa* cultivar Khitish.

Chapter 3

In this chapter, the synthesis and characterization of tri- and di-organotin(IV) complexes of the ligand 2-mercapto isothiocyanate are described. All the compounds were characterized by IR, (¹H and ¹³C) NMR spectroscopy along with the elemental analysis. Further differential scanning calorimetric measurements were also carried out. Biological studies for some selected complexes were carried out and summarized in chapter 5.

Chapter 4

This chapter describes the synthesis, characterization, fluorescence and biological properties of diorgano tin(IV) compound of Schiff bases derived from salicylaldehyde/substituted salicylaldehyde and thiosemicarbazide/ substituted thiosemicarbazide. The complexes were characterized by UV-Vis, Fluorescence, IR, (^1H , ^{13}C and ^{119}Sn) NMR spectroscopy and elemental analysis. The solid state structures of some of these complexes were studied by X-ray crystallography. Differential scanning calorimetric measurements were carried out for some of these complexes. The biological activity of some of the compounds against six fungal pathogens namely (*Bipolaris sorokiniana*, *Helminthosporium oryzae*, *Alternaria brassicae*, *Alternaria kikuchiana*, *Stemphylium pori* and *Colletotrichum capsici*) isolated from six different crops (*Triticum aestivum*, *Oryzae sativa*, *Brassica nigra*, *Brassica oleracea*, *Allium cepa* and *Capcicum annum*) were examined to demonstrate their fungicidal activity. The phytotoxic effects of these compounds were also investigated against five economically important crops such as (*Triticum aestivum*, *Oryzae sativa*, *Brassica nigra*, *Brassica oleracea* and *Capcicum annum*).

Chapter 5

This chapter deals with the biocidal properties of tri- and di-organotin(IV) compounds of 2-mercapto isothiocyanate and di-organotin(IV) compounds of Schiff bases derived from salicylaldehyde /substituted salicylaldehyde and thiosemicarbazide/ substituted thiosemicarbazide. Also some reported compounds were studied for effective control of *Bipolaris sorokiniana* the casual agents of foliar blight disease of wheat was reported in the cultivar of Sonalika. Further, the mechanism of action of these compounds on host physiology in respect of phenolics pathogenesis-related protein, enzyme such as polyphenol oxydase, peroxidase and phenyl alanine ammonia lyase and other biochemical parameters commonly associated with diseases resistance was registered. Finally the effect of these compounds on seedling growth and yield parameters were described. Additionally the fungitoxic effects of these compounds were also reported against two important fungi of wheat such as *Alternaria titricina* and *Fusarium solani*.

CHAPTER 1

**A SHORT REVIEW ON THE ORGANOTIN(IV)
COMPOUNDS**

1.1 Introduction

Tin (atomic number, 50; relative atomic mass, 118.69; electronic configuration $5s^2p^2$) is an element of group 14 of the periodic table, along with C, Si, Ge, and Pb. Tin as a metal, either as such or in the form of alloys and in its chemical compound has an astonishing amount of usefulness. Characteristically, for majority of its applications, only a small amount of tin are needed to see its effect. Tin exists in three allotropic modifications and it can form a variety of inorganic and organometallic compounds. This is generally true for organotin chemistry which is a subject of interest for years due to not only of its rich structural chemistry but also for its versatile applications. The use of organotin(IV) compounds in industry has risen dramatically during the last few decades as a result of their wide range of biocidal and industrial applications such as stabilizer for polyvinyl chlorides, industrial catalysts, wood preservatives and anti-fouling agents that has led to their accumulation in the environment and in biological systems [1,2]. At the present time, the industrial uses of non-toxic organotin compounds (R_2SnX_2 and R_3SnX_3 types) account for almost two third of the total world consumption, although the other major uses for these derivatives as selective biocides and pesticides (R_3SnX type) has increased rapidly in recent years. The estimated consumption of tin metal for chemical industry was large, the reason for this growth in tin chemicals are the diversity of tin applications in many cases, with their generally low toxicity [3]. The tetra organotins R_4Sn have no commercial outlets, but are important as intermediates in the manufacture of R_nSnX_{4-n} compounds from $SnCl_4$. So far, monosubstituted organotin compounds (R_3SnX_3) have had a very limited application, but they are used as stabilizers in poly (vinyl chloride) films.

Organotin(IV) compounds are characterized by the presence of at least one covalent C-Sn bond. The compounds contain tetravalent Sn centres and are classified as mono-, di-, tri- and tetraorganotin(IV)s, depending on the number of alkyl (R) or aryl (Ar) moieties. The anion is usually chloride, fluoride, oxide, hydroxide, a carboxylate or a thiolate [2].

1.2 Literature

The first organotin compound was prepared over 150 years ago. Way back, in 1849, E. Frankland in his paper described the reaction which occurred when ethyl iodide and zinc were heated together in a sealed tube [4]. Frankland described, the behaviour of ethyl iodide in contact with metal like tin at elevated temperatures (150 - 200 °C). Later, he showed that the crystalline mass diethyltin diiodide was obtained in this reaction (Eq.1)[5-7].



In an independent work, Löwig established that ethyl iodide when reacted with a tin/sodium alloy produced a compound which is now recognized as oligomeric diethyltin [8]. As an alternative to this so-called direct method, an indirect route was devised by Buckton in 1859, who obtained tetraethyltin by treating tin tetrachloride with Frankland's diethylzinc (Eq.2) [9].



In 1886, Letts and Collie were attempting to prepare diethylzinc and instead isolated tetraethyltin which was formed from tin (was present as impurity in the zinc). So they established that tetraethyltin could be prepared by heating ethyl iodide with a mixture of Zn and Sn powder (Eq.3) [10].



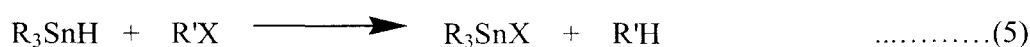
In (Eq.4), Frankland showed that the tin(IV) tetrachloride (which is used in Eq.2) could be replaced by tin(II) dichloride which is much more easier to handle and reacts in a more controllable fashion [11].



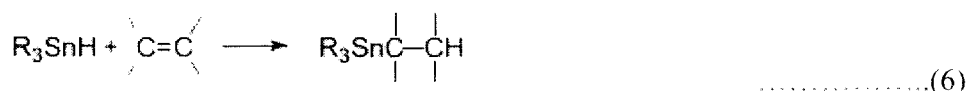
Up to 1900, some 37 papers were published on organotin compounds. In 1903, Pope and Peachey described the preparation of a number of simple as well as mixed tetraalkylstannanes and tetraphenyltin, from Grignard reagents and tin tetrachloride or alkyltin halides and reactions of this type soon became the standard route to alkyl- and aryl-tin compounds [12]. In 1937, Krause and von Grosse had summarized the early

work in *Organometallische Chemie* which is considered to be the first publication [13].

In 1962, Kuivila showed that the reaction of trialkyltin hydrides with alkyl halides (Eq.5) was a radical chain reaction involving short-lived trialkyltin radicals, $R_3Sn\cdot$ [14].



In 1964, Neumann showed that the reaction with non-polar alkenes and alkynes followed a similar mechanism and these reactions now provide the basis of a number of important organic synthetic methods (Eq.6) [15, 16].



A major development in recent years has been the increasing use of organotin reagents and intermediates in organic synthesis, exploiting both their homolytic and heterolytic reactivity [17].

In parallel with these developments, organotin compounds have found a variety of applications in industry, agriculture and medicine, though in recent years these have been circumscribed by environmental considerations. In industry, they are used for the stabilization of poly vinyl chloride, the catalysis of the formation of the polyurethanes and the cold vulcanization of silicone polymers and also as transesterification catalysts. Their biological properties are made use of in antifouling paints on ships, in wood preservatives, as agricultural fungicides as well as insecticides. Interestingly, in medicine, they are showing promise in cancer therapy and in the treatment of fungal infections [18].

In 1937, Krause and von Grosse published the first review of organotin chemistry [13]. In 1960, the field of organotin chemistry was reviewed by Ingham *et al.* with comprehensive tables of the known compounds [19]. In 1961, M. Dub compiled from Chemical Abstracts a non-critical compendium listing preparations, physical, chemical properties and literature surveyed from 1937 to 1959 [20]. Simultaneously, Weiss compiled an exhaustive list of organotin compounds which were reported between 1937 to 1964 [21]. A book namely, "Organotin Compounds:

New Chemistry and Applications", edited by J. J. Zuckermann (1976) was written based on lectures delivered at the centenary meeting of the ACS [22]. It is also noteworthy to mention that several famous books were written/edited describing the then progress of organotin research [1, 23-26]. A volume of Houben-Weyl deals particularly with preparative methods of organotin compounds [27]. In 1991, Guo Yushen reviewed the preparation, properties and applications of monoalkyltin compounds [28].

Structural aspects of organotin chemistry have been reviewed [29] and a comprehensive bibliography of X-ray diffraction studies is available from the International Tin Research Institute [30]. M.I. Bruce [31] who had written a comprehensive listing of organotin compounds (ca. 1500 entries) which have had their structure determined by electron diffraction or X-ray diffraction. The structural diversity of organotin compounds has been attracting the attention of a number of researchers and as a result a multitude of structural types have been discovered [32]. Gielen and Sprecher [33] included a discussion of organotin structure in which the coordination number of tin is greater than 4; the same topic was discussed in an article written by Okawara and Wada [34].

H. Ali and J. E. van Lier, have reviewed organotin compounds that react rapidly and chemo-, regio-, and stereo-selectively with a variety of reagents, and this have been exploited in the synthesis of pharmaceuticals with a radioactive label, particularly when the radioisotope has a short half-life [35]. A second review covering similar ground is included in Patai's volume [36].

J. J. Eisch and R. B. King have given tested experimental details for the synthesis of some 40 organotin compounds [37-39]. Synthesis, reactivity, structural aspects and applications of organotin(IV) complexes with phosphorous-based acids have been reviewed by V. K. Jain [40]. The applications of these complexes as catalysts, corrosion inhibitors and biocides were also discussed in this review. P.G. Harrison in 1989 has edited a multi-author book which has covered both inorganic and organic aspects of organotin chemistry [41].

S. J. de Mora in 1996 has edited a book in which chapters were written by various authors covering the different aspects of the problems associated with the use of tributyltin compounds in marine antifouling paints [42]. Nath *et al.* [43] have reviewed organotin (IV) complexes of the amino acids and peptides with special reference to their methods of synthesis, structural, thermal properties as well as their

solution studies and biological activity. The structures of these complexes were discussed on the basis of IR, electronic, multinuclear (^1H -, ^{13}C - and ^{119}Sn -) NMR, X-ray and ^{119}Sn Mössbauer spectral studies.

A review by Beckmann and Jurkschat [44] was given with 140 references on the recent progress in the chemistry of *cyclo*-stannasiloxanes of different ring size and their potential in ring-opening polymerization reactions is critically evaluated and compared with that of related *cyclo*-borasiloxanes, *cyclo*-germasiloxanes, and *cyclo*-siloxanes. Pellerito and Nagy [2] in 2002, have written a review which deals with the organotin(IV) cations forming complexes with ligands containing (O), (N), (S), or {phosphorus(O)} donor atoms with various composition and stability. The emergence of new experimental techniques (EXAFS, multinuclear ^1H -, ^{13}C -, ^{119}Sn -NMR, ^{119}Sn Mössbauer, etc., spectroscopic techniques) provided useful information about the structure and stabilities of the complexes formed. They also have reviewed the literature on these types of complexes taking into account the biological aspects of the complexes. Chandrasekhar *et al.* [45] have written this review which deals with the recent progress in the area of organotin assemblies that contain Sn—O bonds. Various kinds of tri-, di- and monoorganotin compounds are described in terms of their preparation by methods such as hydrolysis of organotin halides, reactions of suitable organotin compounds with various kinds of substrates such as carboxylic acids, sulfonic acids, oxide transfer reagents etc. The structural characterization of these compounds by the use of ^{119}Sn -NMR, ^{119}Sn Mössbauer and X-ray crystallography was presented in considerable detail. The amazing structural diversity present in this family of compounds was discussed. Organotin compounds can be assembled by using various synthetic methodologies. Although in most instances, organotin oxides and hydroxides are the preferred starting materials for preparing organotin compounds, Sn—C bond cleavage reactions involving organotin compounds also offer a rational route. This review deals with the recent progress in this area and examines various reactions, where Sn—C cleavage occurs. A wide range of products are accessible from this approach and these were presented in this article [46]. Roy and Roy have reviewed details about making and breaking of Sn-C and In-C Bonds in situ; the cases of Allyltins and Allylindiums [47].

In 1985, two independently published reviews have demonstrated the utility of organotin(IV) derivatives of poly alcohols in regioselective manipulations involving

indirect acylation, alkylation and oxidation [48,49], while a work by Grindley deals with the applications of organotin(IV)-containing intermediates in carbohydrate chemistry [50]. Strong sugar-organotin(IV) cation complexation have been discussed by Burger and Nagy [51], Gyurcsik and Nagy [52], Verchere *et al.* [53] while Barbieri *et al.* [54] dealt mainly with the interactions of organotin(IV) cations and complexes with DNA and their derivatives.

The agricultural applications of organotin compounds in 1950's and early in 1960's were first explored by G. J. M. Vander Kerk and his coworker. They were the pioneer in the discovery of the high fungicidal activity of triphenyl- and tributyl- tin compounds [55-58]. Crowe [59,60] has reviewed the applications of organotin compounds in agriculture upto 1980 and published it in two parts. In part I, he discussed about the fungicidal, bactericidal, and herbicidal aspects of those compounds and the part II covered acaricidal, antifeedant, chemosterilant and insecticidal properties of organotin compounds. In 1989, Molloy surveyed in the wild field of bio-organotin(IV) compounds [61]. Detailed discussion of organotin(IV) compounds as wood preservatives had been published [62,63]. In 2008, Basu Baul reported a comprehensive review on antimicrobial activity of organotin(IV) compounds. After the review of Pellerito and Nagy it was an off beating review of biocidal activity of organotin(IV) compounds [64].

In 1973, Atsushi *et al.* [65] reported a very important piece of work, it was the high affinity of tin for tumours which was the highest among the group 14 elements. This finding was further confirmed by various workers who prepared tin labeled technetium complexes and used them as imaging agents for tumour localization [66]. Subsequently, two important reviews covering the literature of anti cancer activity of organotin(IV) compounds had been published [67,68]. In 2006, Tabassum and Pettinari have published substantial information on the mode of action of organotins in cancer chemotherapy [69]. Tsangaris and Williams published a paper on tin including organotin(IV) compounds in pharmacy and nutrition [70].

1.3 Bonding in organotin compounds

Tin has the electronic configuration $5s^2p^2$ in its valence shell which result the occurrence of two oxidation states +2 and +4. Its principal valence state is Sn(IV), though Sn(II) inorganic compounds are common. 3P is the ground state which is

derived from s^2p^2 configuration. In the ground state, there are only two unpaired electrons. Therefore, two covalence bond could be expected [71]. The 5S state of the tin is the first excited state. The Sn(II) state uses mainly the 5p orbitals for bonding otherwise Sn(IV) oxidation state occurs readily, where the tin is sp^3 hybridized.

Tin(II) compounds are mostly bent, pyramidal or distorted due to the presence of an electron pair that does not participate in bonding and displays stereochemical activity, tin(IV) compounds adopt regular geometries as tetrahedral, bipyramidal and octahedral depending upon the coordination number, the electronegativity of tin change with its oxidation number. Tin(II) compounds are more ionic compared to corresponding tin(IV) derivatives. The marked increase in the stability of R_4Sn compounds over R_2Sn types demonstrates the effect of increased hybridization. So most of the organometallic tin compounds are of tin(IV) type [72]. The Sn-C bond should be polar since Sn is electropositive with respect to C. But the polarity is so low as in the tetraalkyls and aryl derivatives of tin so these are not hydrolysed by water. It is possible that the d orbital of tin are used for $(d\pi-p\pi)$ bonding.

1.4 Structure of organotin compounds

The principal valence state Sn(IV), is remarkable capacity to expand its coordination number from anywhere between four to seven. Therefore, the structure of organotin(IV) compounds are tetrahedral, trigonal bipyramidal and octahedral depending upon the coordination number. Tin(II) compounds are bent, pyramidal or distorted in structure [73-75].

Simple tetraalkyl- and tetraaryl-tin(IV) compounds exist under all conditions as tetrahedral monomers, but in derivatives R_nSnX_{4-n} ($n = 1$ to 3), where X is an electronegative group (halide, carboxylate *etc.*), the Lewis acid strength of the tin is increased, and Lewis bases form complexes with a higher coordination number. The compounds R_3SnX usually give five-coordinate complexes R_3SnXL which are approximately trigonal bipyramidal, and the compounds R_2SnX_2 and $RSnX_3$ usually form six-coordinate complexes $R_2SnX_2L_2$ and $RSnX_3L_2$ which are approximately octahedral. The groups X, however, usually carry unshared electron pairs, and can themselves act as Lewis bases, resulting in intermolecular self-association to give dimers, oligomers, or polymers. This self-association is governed by the nature of the ligands L and also by the steric demands of R, X, and L, and it is common for the

degree of association to increase in the sequence gas < solution < solid. If R or X carries a functional substituent Y beyond the α -position, the alternative of intramolecular coordination can occur leading to the formation of monomers with 5-, 6-, 7-, or 8-coordinated tin [11]. The structures of these intramolecularly self-associated monomers, oligomers, and polymers are seldom those of regular polyhedra, and the determination of their structures, and the steric and electronic factors which govern them, has been an important feature of organotin chemistry since the early 1960s [23,24,76].

1.5 Reactivity of organotin compounds

In the periodic table group 14 elements are Si, Ge, Sn, Pb. In Sn-C bond, Sn is electropositive with respect to C and it is represented by $C^{\delta-}-Sn^{\delta+}$. Therefore, it should be polar. The polarization of Sn-C bond makes tin atom more electrophilic and carbon atom which is attached to tin more nucleophilic. So the reactivity of organotin compounds towards nucleophilic and electrophilic both. But the polarity of tetraalkyl and aryl derivatives of tin is low that is why these are not actually hydrolyzed by water. In group 14 elements, reactivity of M-C bond in tetra-alkyl and aryl increases progressively from Si to Pb [77]. A bond between M-C, where M is C, there is possibility of forming double bond ($p\pi-p\pi$). When M substitutes other element of group 14 of the periodic table, there is enough evidence that the d orbitals of these elements are used for bonding ($d\pi-p\pi$). In bonding, the tendency for using d orbital decreases from Si to Sn. In $(GeH_3)_2S$ and $(GeH_3)_2O$, the Ge-S-Ge and Ge-O-Ge appears to be highly bent [78] whereas in $(SiH_3)_2O$, the Si-O-Si bond angle is around 150° [79]. Bond energy and thermal stability decreases in the same sequence Si to Pb. Expanding of the coordination number of the metal, it becomes easier with the increasing atomic size [80].

The alkyl groups are usually introduced to tin by complete alkylation of tin tetrachloride with an organometallic reagent, then the various alkyltin chlorides, R_nSnCl_{4-n} , are prepared. Other functional groups are then introduced by nucleophilic substitution of the chloride. Reaction of the alkyltin chlorides with the appropriate nucleophiles gives the alkyltin alkoxides, amides, thioalkoxides, carboxylates etc. The presence of these electronegative groups on the tin renders the metal susceptible to coordination by Lewis bases and simple tetrahedral four-coordination is the

exception rather than the rule. Hydrolysis of the organotin halides gives the organotin oxides, and in the case of the dihalides and trihalides, the reaction proceeds through a series of well-characterized intermediate hydrolysis products [26, 81].

Cleavage of the carbon-tin bond by heterolytic reaction is usually dominated by electrophilic attack at carbon, although nucleophilic assistance may be provided at the centre and this can sometimes predominate (Eq. 7) [82-84].



The most important electrophiles which are involved are protic acids, particularly carboxylic acids, metallic halides such as tin chlorides, and the halogens, particularly bromine. The cleavage of the alkyl-tin bond by sulphur dioxide is similar. Homolytic attack at carbon to break the carbon-tin bond has not yet been identified, but attack at hydrogen on the β -carbon may sometimes result in cleavage of the carbon-tin bond through a subsequent fragmentation process [85].

1.6 Analytical techniques applied to determination the structure of organotin compounds

The basic studies in the field of organotin compounds have been developed due to the success of a large number of modern analytical techniques applied to organotin compounds. Investigations can be performed by general techniques such as UV-Vis [24], IR [24, 81], 1H -NMR [86], ^{13}C -NMR [87], mass spectroscopy [88] and also by specialized techniques such as ^{119}Sn Mössbauer spectroscopy [24,26] and ^{119}Sn -NMR spectroscopy [89]. The ^{119}Sn Mössbauer and ^{119}Sn -NMR spectroscopy provide complementary information on the structure of the organotin molecules in the solid state and in solution respectively.

1.7 Applications of organotin compounds

Organotins are currently one of the most studied groups of organometallic compounds; their novel and often unique chemical properties have intrigued chemists for over 100 years and, today, many of these compounds find extensive use in

agriculture and industry [90]. As the world of organotin chemicals is quite extensive and diverse which are discussed briefly here. The majority of organotin uses are comprised of five major commercial applications: PVC Heat Stabilizers, Biocides, Catalysts, Agrochemicals, and Glass Coatings. These applications divided into two groups: biological applications and non biological application.

1.7.1 Biological applications

At the Institute for Organic Chemistry TNO, Utrecht, Holland, in early 1950s, Vander Kerk and Lujten, systematically discovered the high fungicidal activity of tributyl- and triphenyl-tin compounds [55, 56, 57]. It was not until 1925 that the first commercial application of an organotin was recorded (as a mothproofing agent). Seven years later, tetra-alkyltins found to have an industrial application as hydrogen chloride scavengers in chlorinated hydrocarbons used as insulators in heavy-duty transformers and capacitors. This was taken to mark the beginning of the more generalized biological commercial applications of organotin compounds [90]. The first organotin compound to reach commercialization in agriculture in the early 1960s were triphenyltin acetate (Brestan*, Hoechst A.G) and triphenyltin hydroxide (Duter*, Philips Duphar N.V), both of which were widely used [91] to combat a number of fungal diseases in various crops, like potato blight, leaf spot on sugar beet and celery, rice blast as well as coffee leaf rust. A further interesting property of chemosterilant [92,93]. A third triphenyltin compound, the chloride (fentin chloride: Brestanol) which was also produced by Hoechst is now used, although to a lesser extent [94]. A few years later Dow introduced the tricyclohexyltin hydroxide (cyhexatin: Plictran) which was highly effective in the control of phytophagous mites. Subsequently, two further organotin miticides were introduced; bis(trineophyltin)oxide (fenbutatin oxide: Vendex or Torque) by Shell and tricyclohexyltin- 1,2,4-triazole (azocyclotin: Peropal) by Bayer [91]. Activity of fungi was also influenced by the nature of the organic group. The tributyl compounds Bu_3SnX , was shown fungicidal activity was largely independent of the group X [95]. The fungicidal activity of a group of these triphenyltin fungicides was that they were function as antifeedants in which they deterred insects from feeding, and they also acted as insect Ph_3SnX compounds were shown to be highest when $X = NCO$ or NCS [96]. The trimethyl- and triethyl-tin

derivatives had a high toxicity to insects and mammals, [97,98] the tripropyltins to gram-negative bacteria, and the tributyltins to the gram positive bacteria and fungi [99]. The tricyclohexyl- and trineophyl- tin compounds are effective acaricides [100,101]. The toxic triorgano-tin compounds are able to inhibit mitochondrial oxidative phosphorylation and their biological activity pattern is probably due to their ability to bind certain proteins. The exact nature of the binding sites on the proteins is not known. The biological effect of the tetra organotin compounds R_4Sn appear to be caused entirely by the R_3SnX derivative, which is produced by their fairly rapid dealkylation *in vivo* [102, 103]. The dialkyltin compounds show a toxic behavior which is quite different from that of the R_4Sn and R_3SnX compounds. They combine with co-enzymes or enzymes possessing dithiol groups, e.g. reduced lipoic acid and thereby inhibit α -ketoacid oxidation. As with trialkyltin compounds, the mammalian toxicity of the di-n-alkyltins decreases with increasing length of the alkyl chain [102,104]. A series of diorganotin complexes were modeled for the antitumour agent like cisplatin showed antitumour activity. These compounds exert a selective cytotoxic action on T- lymphocytes and therefore hold potential as anti-T-cell tumor agents [105]. Organotin compounds have been used as anthelmintic agents e.g. dibutyltin dilaurate which is one of the constituents of the commercial product that has been used as formulation for treating poultry in combination with piperazine and phenothiazine [101]. Tin(II) fluoride is used in toothpastes as an antidecaying agent and applied to children's teeth [106]. Di-n-butyltin dilaurate and tin(II) acetate have been used as catalyst in vulcanizing silicon rubbers used for the protection of the dental prosthetic devices.[107]. Trialkyltin compounds are used in organic solvent-based wood preservative formulations. Tributyltin oxide at concentration up to 3% in a solvent like kerosene has been used for the pretreatment of the wood to protect it from insect attacks [108]. In the early 1960s, triorganotin compounds were used for antifouling paint and regular consumption of these compounds increases with the time [109].

1.7.2 Non biological Applications

There is considerable industrial activity in organotin chemistry because of its large-scale applications in the fields of polymer stabilization, organic synthesis and

catalysis. The PVC is the second most plastic after polyethylene. Certain organotin compounds are amongst the most effective stabilizers for plastic. Carboxylates and mercaptide tin salts can replace labile chlorine atoms; with more thermally stable C-O or C-S bond ligands. Organotin-based stabilizers are the efficient and widely used PVC stabilizers [110]. Certain monobutyl- and mono-octyl-tin compounds, e.g. $[\text{BuSn}(\text{O})\text{O}]^- \text{Na}^+$, are active hydrophobic agents for cellulosic materials, such as cotton textiles, paper and wood but have not reached commercialization for this application. These have been tested on building materials (limestone) bricks and concrete and on cellulosic substrate (cotton, paper and wood) as well [111,112]. Tin(II) chloride, ammonium hydrogen fluoride isopropanol and polishing agents are used to protect the sheepskin wool in the spray treatment process. The K_2ZrF_6 , tin(II) chloride and hydrochloric acid have been used for protection purposes in treatment process [113]. The most commonly used compounds in electroplating are tin(IV) sulphate, tin(II) chloride, tin(II) fluoroborates and sodium/potassium stannates [114]. Thin coatings of tin(IV) oxide on glass have a number of applications. The precursor of these tin(IV) oxide films was originally tin(IV) chloride, which is applied in the vapour phase at 500-600°C to hot glass surface where it is pyrolysed to tin(IV) oxide [114]. Tin(IV)oxide electrodes are used in the manufacture of lead-containing crystal glass by electric melting. The tin(IV) oxide electrodes are more preferably used as compared to the conventional molybdenum or graphite rod, because the electrical conductivity of tin(IV) oxide increases with increasing temperature [115]. The most widely used catalysts are stannous octoate [tin(II)2-ethyl hexoate] and various mono- and diorganotin compounds. These catalysts play an important role in the formation of polyurethane foams in the production of polyesters and in the curing of certain types of silicone resins. Dibutyltin dilaurate, dibutyltin diacetate are used as homogeneous catalyst in the manufacture of polyfoams and cross linking agents at room temperature for olefinic polymerization [116].

1.8 References

1. Davies AG, Smith PJ. *Adv. Inorg. Chem. Radiochem.* 1980; **23**: 1.
2. Pellerito L, Nagy L. *Coord. Rev.* 2002; **224**: 111.
3. Frame PK, Proc. 5th Internat. Tinplate Conf., ITRI, London, (1992) (ITRI Publicn. No. 727) P. 10
4. Frankland E, *J. Chem. Soc.*, 1849; **2**: 263.
5. Frankland E, *Phil. Trans.*, 1852; **142**: 417.
6. Frankland E, *Liebigs Ann. Chem.*, 1853; **85**: 329.
7. Frankland E, *J. Chem. Soc.*, 1854; **6**: 57.
8. Löwig C, *Liebigs Ann. Chem.*, 1852; **84**: 308.
9. Buckton GB, *Phil. Trans.*, 1859; **149**: 417.
10. Letts EA, Collie JN. *Phil. Mag.*, 1886; **22**: 41.
11. Davies AG, *Organotin Chemistry*, Wiley-VCH, Verlag, GmbH & Co., KGaA, Weinheim, 2003.
12. Pope WJ, Peachey SJ, *Proc. Chem. Soc.*, 1903; **19**: 290.
13. Krause E, von Grosse A, *Die Chemie der Metal-organischen Verbindungen*, Borntraeger, Berlin, 1937.
14. Kuivila HG, Menapace LW, Warner CR. *J. Am. Chem. Soc.*, 1962; **84**: 3584.
15. Neumann WP, Sommer R. *Liebigs Ann. Chem.*, 1964; **675**: 10.
16. Kuivila HG, *Adv. Organomet. Chem.*, 1964; **1**: 47.
17. Pereyre M, Quintard JP, Rahm A. *Tin in Organic Synthesis*, Butterworth, London, 1987.
18. Evans CJ, Karpel S, *Organotin Compounds in Modern Technology*, Elsevier, Amsterdam, 1985.
19. Ingham RK, Rosenberg SD, Gilman H. *Chem. Rev.*, 1960; **60**: 459.
20. Dub M, *Organometallic Compounds, Literature Survey 1937-1959. Vol. II. Organic Compounds of Germanium, Tin and Lead*. Springer Verlag, Berlin, 1961.
21. Weiss RW (Ed.), *Organometallic compounds*, 2nd Ed., Vol.2, Springer-Verlag, New York, 1967, pp.158.
22. Zuckerman JJ (Ed.) *Organotin Compounds: New Chemistry and Applications*, American Chemical Society, Washington, 1976.
23. Neumann WP, *The Organic Chemistry of Tin*, Wiley, London, 1970.
24. Poller RC, *The Chemistry of Organotin Compounds*, Logos Press, London, 1970.
25. Sawyer AK (Ed.), *Organotin Compounds*, Vols.1&2; Vol.3, Marcel Dekker Inc., New York, 1971; 1972.
26. Davies AG, Smith PJ. 'Tin', in: *Comprehensive Organometallic Chemistry*, Wilkinson G, Stone FGA, Abel EW (Ed.), Vol. 2, Pergamon Press, Oxford, 1982; 519.
27. Bähr G, Pawlenko S. in *Houben Weyl, Methoden der Organische Chemie*, vol. 13/16, Vol. 13/6,, Thieme, Stuttgart, 1978, 181.
28. Yushen G, Huaxue Shiji. 1991; **13**: 43.
29. Zubieta JA, Zuckerman JJ. *Prog. Inorg. Chem.* 1978; **24**: 251.
30. Cusack PA, Smith PJ, Donaldson JD, Grimes SM. *A Bibliography of X-ray Crystal Structures Of Tin Compounds*, International Tin Research Institute, London, 1981(Publication 588).
31. Bruce MI, in *Comprehensive Organometallic Chemistry II*, Vol. 13, Abel EW, Stone FGA, Wilkinson G (Eds.), Pergamon, Oxford, 1995.
32. Holmes RR. *Acc. Chem. Res.* 1989; **22**: 190.

33. Gielen M, Sprecher N. *Organometallic Chem. Rev.* 1966; **1**: 455.
34. Okawara R, Wada M. *Advances in Organometallic Chemistry*, Vol. 5, Academic Press, New York and London, 1967; 137.
35. Ali H, van Lier JE. *Synthesis*, 1996; 423.
36. Patai S. (Ed.) *The Chemistry of Organic Germanium, Tin and Lead Compounds*, Wiley, Chichester, 1995.
37. King RB, Eisch JJ. (Ed.) *Organometallic Syntheses, Vol 2*, Academic Press, New York, 1981.
38. King RB, Eisch JJ. (Ed.), *Organometallic Syntheses Vol. 3*, Elsevier, Amsterdam, 1986.
39. King RB, Eisch JJ. (Ed.), *Organometallic Syntheses Vol. 4*, Elsevier, Amsterdam, 1988.
40. Jain VK. *Coord. Chem. Rev.* 1994; **135/136**: 809.
41. Harrison PG (Ed.) *Chemistry of Tin*, Blackie, Glasgow, 1989.
42. de Mora SJ (Ed.) *Tributyltin: Case Study of an Environmental Contaminant*, Cambridge University Press, Cambridge, 1996.
43. Nath M, Pokharia S, Yadav R. *Coord. Chem. Rev.* 2001; **215**: 99.
44. Beckman J, Jurkschat K. *Coord. Chem. Rev.* 2001; **215**: 267.
45. Chandrasekhar V, Nagendran S, Baskar V. *Coord. Chem. Rev.* 2002; **235**: 1.
46. Chandrasekhar V, Gopal K, Sasikumar P, Thirumoortii R. *Coord. Chem. Rev.* 2005; **249**: 1745.
47. Roy UK, Roy S. *Chem. Rev.* 2010; **110**: 2472.
48. David S, Hanessian S. *Tetrahedron*. 1985; **41**: 634.
49. Patel A, Polar RC. *Rev. Sil. Ger. Tin Lead Comps.* 1985; **8**: 263.
50. Grindley TB. *Adv. Carbohydr. Chem. Biochem.* 1998; **53**: 17.
51. Burger K, Nagy L. Chapter VI. in: Burger K (Ed.) *Biocordination Chemistry, Metal Complexes of Carbohydrates and Sugar-type Ligands*, Ellis Horwood, London, 1990; 236.
52. Gyurcsik B, Nagy L. *Coord. Chem. Rev.* 2000; **203**: 81.
53. Verchere JF, Chapelle S, Xin F, Crans DC. *Prog. Inorg. Chem.* 1998; **47**: 837.
54. Barbieri R, Pellerito L, Ruisi G, Silvestri A, Barbieri-Paulsen A, Barone G, Posante S, Rossi M. ¹¹⁹Sn Mössbauer spectroscopy studies on the interaction of organotin(IV) salts and complexes with biological systems and molecules. Chapter 12 in: Gianguzza A, Pelizetti E, Sammartano (Eds.), *Chemical Processes in Marine Environments*, Springer, Berlin, 2000; 229.
55. Vander Kerk GJM, Luijten JGA. *J. Appl. Chem.* 1954; **4**: 314.
56. Vander Kerk GJM, Luijten JGA. *J. Appl. Chem.* 1956; **6**: 56.
57. Vander Kerk GJM, Luijten JGA. *J. Appl. Chem.* 1961; **11**: 35.
58. Noltes JG, Luijten JGA, Vander Kerk GJM. *J. Appl. Chem.* 1961; **11**: 38.
59. Crowe AJ, *Appl. Organomet. Chem.* 1987; **1**: 143.
60. Crowe AJ, *Appl. Organomet. Chem.* 1987; **1**: 331.
61. Molloy KC. *Bioorganotin Compounds*, in: Hartley FR (ed.), *The Chemistry of Metal-Carbon bond*, John Wiley & Sons, London. 1989; **5**: 465.
62. Blunden SJ, Cusack PA, Hill R. *The Industrial Use of Tin Compounds*, Royal Society of Chemistry, London, 1985.
63. Crowe AJ, Hill R, Smith PJ. *Laboratory Evaluation of tributyltin(IV) Compounds as Wood-Preservatives*, Publication 559, International Tin Research Institute, London, 1979.
64. Basu Baul TS. *Appl. Organomet. Chem.* 2008; **22**: 195.
65. Atsushi A, Hisada K, Anda I, *Radioisotopes*. 1973; **22**: 7.

66. Yamaguchi M, Sugii K, Okada S. *J. Toxicol. Sci. Jpn.* 1981; **5**: 238.
67. Saxena AK, Huber F. *Coord. Chem. Rev.* 1989; **95**: 109.
68. Gielen M, *Coord. Chem. Rev.* 1996; **151**: 41.
69. Tabassum S, Pettinari C. *J. Organomet. Chem.* 2006; **691**: 1761.
70. Tsangaris JM, Williams DR. *Appl. Organomet. Chem.* 1992; **6**: 3.
71. Moore CE. *Atomic energy levels*, Circular 467 of the National Bureau of Standards, Vol.1, Government Printing Office, Washington, D.C. (1949).
72. Gynane MJS, Lappert MF, Miles SJ, Power PP. *J. Chem. Soc., Chem. Commun.* 1976; 256.
73. DeSousa GF, Filgueiras CAL, Abras A, Al-Juaid SS, Hitchcock PB, Nixon JF. *Inorg. Chim. Acta.* 1994; **218**: 593.
74. Moreno PC, Francisco RHP, do P. Gamberdella MT, de Sousa GF, Abras A. *Acta Cryst.* 1997; **C53**: 1411.
75. de Sousa GF, Filgueiras CAL, Darensbourg MY, Reibenspies JH. *Inorg. Chem.* 1992; **31**: 3044.
76. Poller RC. *J. Organomet. Chem.* 1965; **3**: 321.
77. Mehrotra RC, Singh A. *Organometallic Chemistry-A unified Approach*, 2nd Ed., New Age International (P) Ltd. Publishers, New Delhi, 2000.
78. Goldfrab TD, Sujishi S. *J. Am. Chem. Soc.* 1964; **86**: 1679.
79. Verma R, Mac Diarmid AG, Miller JG. *Inorg. Chem.* 1964; **3**: 1754.
80. Veith M, Recktenwald O, Gielen M, Rzaev ZMC. *Topics in Current Chemistry, Organotin compound*, Springer-Verlag, Berlin, Heidelberg, New York 1982: 104.
81. Tanaka T. *Organomet. Chem. Rev.* 1970; **5(A)**: 1.
82. Abraham MH. in: *Electrophilic Substitution at a saturated carbon Atom*, ed. Bamford CH, Tipper CFH, Elsevier, Amsterdam, 1973.
83. Eaborn C. *J. Organomet Chem.* 1975; **100**: 43.
84. Reutov OA. *J. Organomet Chem.* 1975; **100**: 219.
85. Davies AG. *Adv. Chem. Ser.* 1976; **157**: 26.
86. Maddox ML, Stafford SL, Koesz HD, *Applications of Nuclear Magnetic Resonance to the Study of Organometallic Compounds, in Advances in Organometallic Chemistry*, Stone FGA, West R (Ed.), Vol. 3, Academic Press, London and New York, 1965; 1.
87. Gansow OA, Vernon WD, in: Levy GC (Ed.), *Topics in Carbon-13 NMR Spectroscopy*, 1970; **2**: 270.
88. Limouzin Y, Maire JC, *Adv. Chem. Ser.* 1976; **157**: 227.
89. Wrackmeyer B, ¹¹⁹Sn NMR Parameters, in: *Annu. Rep. NMR Spectrosc.*, Webb GA (Ed.), Vol. 18, Academic Press, London, 1985; 73.
90. Nicklin S, Robson MW. *Appl. Organomet. Chem.* 1988; **2**: 487.
91. Sugavanam, B *Tin and its Uses.* 1980, **126**: 4.
92. Ascher KRS, Nissim S. *World Review Pest Control.* 1965; **7**: 21.
93. Kissam JB, Hays SB. *J. Econ. Entomol.* 1966; **59**: 748.
94. Blunden, SJ, Cusack, PA and Hill, R 'The Industrial Uses of' Tin Chemiculs, Royal Society of Chemistry, London, 1985.
95. Fuse G, Nishimoto K. *Mokuzai Kenkyu* 1964; **32**: 15.
96. Srivastava TN, Tandon SK. *Naturwissenschaften.* 1968; **55**: 391.
97. Barnes JM, Magos L. *Organomet. Chem. Rev.* 1968; **3**: 137.
98. Smith PJ, 'Toxicological Data on Organotin Compounds' International Tin Research Institute, London, 1978 (Publication538).

99. Sijpesteijn AK, Luijten JGA, Vander Kerk GJM. in: '*Fungicides, An Advanced Treatise*', Ed. Torgeson DC, Academic Press, New York, 1969; **2**: 331.
100. Evans CJ. *Tin and Its Uses*. 1970; **56**: 7.
101. Evans CJ. *Tin and Its Uses*. 1981; **5**: 130.
102. Aldridge WN. In '*Chemistry and Technology of Silicon and Tin*', Ed. Kumardas VG, Ng SW, Gielen M. Oxford University Press, Oxford, 1992; 78.
103. Hall WT, Zuckerman JJ. *Inorg. Chem.* 1977; **16**: 1239.
104. Aldridge WN. In '*Proc.2nd Internat. Conf. Si, Ge, Sn and Pb Compounds*', Ed. Gielen M, Harrison PG. *Rev. Si, Ge and Pb Compounds*, Special Issue, Freund, Tel Aviv, 1978; 9.
105. Crowe AJ. *ITRI pub.*1990; **709**: 69.
106. Horowitz MS. *J. Public Health Dent.* 1991; **5**: 20.
107. Evans CJ. *Tin and Its Uses*. 1972; **91**: 3.
108. Lay DE. *Plating and Surface Finishing*. 1991; **26**: 75.
109. Blunden SJ, Hill R. In *Surface Coating* (Eds. Nicholson JW Prosser HJ.), Elsevier Applied Science, London- New York 1986.
110. Kirk A. *Othmer Encyclopedia of Chemical Technology* (Ed. Howe-Grant M), 4th Edn., Vol. 12, Heat Stabilizers, Wiley, New York 1984.
111. Plum H. *Tin and Its Uses*. 1981; **7**: 127.
112. Hobbs LA. *Tin and Its Uses*. 1982; **10**: 134.
113. Cusack PA. *Fire and Materials*. 1993; **1**: 17.
114. Burkhardt W. *Galvantechnik*. 1993; **84**: 2922.
115. Riger W, Bull V. *Information. Space. Issue*, Jan. 1987;3.
116. Evans CJ. *Tin and Its Uses*. 1978; **1**: 118.

CHAPTER 2

SYNTHESIS AND CHARECTERIZATION OF Mn(II), Fe(II), Co(II), Cu(II), Zn(II) COMPLEXES OF 3,5-DI NITRO BENZOIC ACID, CRYSTAL STRUCTURES OF Co(II) AND Cu(II)

13904

2 MAY 2012



2.1 Introduction

The Mn, Fe, Co, Cu and Zn all are belonged in 1st transition metal series because the last electron in the atoms of these elements enters in d-sub-shell belonging to penultimate shell. Most of the transition metals show more than one oxidation states. Because of the presence of 'd' electron these transition metals display different oxidation states and sometimes form complexes with the same ligand in different oxidation state. This is generally true for the complex compounds of transition metal chemistry and is a subject of interest for years due to not only of its rich structural chemistry but also for its versatile applications. It is now well recognized that in the human body minute amount of many elements can be detected and estimated. Some of these elements have been shown to be essential for life. They are involved in all major metabolic pathways of life. They serve a variety of functions that include catalytic, structural and regulatory activities in which they interact with various enzymes and biological membranes [1]. Iron functions as a cofactor for enzymes involved in many metabolic processes, including oxygen transport, DNA synthesis, electron transport and are transformed into biologically available form in the mitochondrion by the iron-sulphur cluster and haeme synthesis pathway [2]. Zinc plays an important roles in nucleic acid metabolism, cell replication, tissue repair and growth, as well as zinc-containing nucleoproteins are involved in gene expression of multiple proteins [3,4]. The Cu is present in the oxygen carrying system in blood of many invertebrates and is a major constituent of many enzymes and proteins [5]. The Mn is an essential element to be found in all tissues. It is needed for metabolism of amino acids, lipids, proteins and carbohydrates as well as it takes part in the defense of red blood cells in the metabolism of iron [6]. It is well known that Co is an essential metal necessary for the formation of vitamin B₁₂ [7]. The important role of Mg in chlorophyll is well established in green plant system. But all the metals are essential in small amounts; in large amounts, however, these may endanger the life processes. Small amounts of Fe, Cu, Zn etc. are found as growth and development agents of fungi. Whereas, e.g, Cu and Zn when incorporated in some organic ligands act as important fungicide. The (more toxic metals) Hg and Pb compounds can also

act as fungicides [8]. Further many transition metal complexes are associated with biological and commercial applications [9-15].

2.2 Literature

Several cupric carboxylates are dimeric either in the crystalline state, in solution or in both [16]. Considerable controversy has been caused over the mode of bonding in the dimeric Cu(II) acetate monohydrate [17]. The main cause of the problem possibly arises from the method of preparation of the complexes. Frequently, they are isolated as hydrates or solvates followed by dehydration under vacuum. The application of heat to these complexes may cause slight decarboxylation of the compounds affording anhydrous materials contaminated with small amounts of copper oxide in insufficient quantities to affect the elemental analysis [18]. This contamination of the complex would significantly affect the magnetic properties. So the bonding mode of dimeric Cu(II) acetate is debatable [17]. Kumar and Suri [19] have reported that the adducts of copper (II) aryl carboxylates with morpholine can be prepared by interacting the reactants in 1:1 molar ratio or using a large excess of morpholin in acetone medium. Analytical results show that the adducts are either mono-morpholine or bis-morpholine of 1:1 or 1:2 stoichiometry formulated as $\text{Cu}(\text{O}_2\text{CC}_6\text{H}_4\text{R})_2(\text{morph})_n$ where R is H, CH₃-o, CH₃-m, Cl-o, Cl-m, Br-o, CH₃O-o, CH₃O-m, CH₃O-p, NO₂-o, NO₂-m, NO₂-p, OH-o, OH-m, and OCOCH₃-o; Morph is Morpholine and n is 1 or 2. Conductance measurements show that all these adduct are non-ionic. Magnetic and electronic spectral studies suggest that mono-morpholin adducts are dinuclear syn-syn carboxylate bridge species whilst bis-morpholin adducts are mononuclear distorted octahedral molecules. IR-spectra show that morpholin behaves as a N-bonded monodentate ligand [19-20]. J. Bickley and his coworkers [21] have described the synthesis and crystal structures of two new copper complexes with chelating dicarboxylic acids. Reaction of copper(II) acetate with diacid H₂L₂ (HO₂CC(Me)₂OArOC(Me)₂CO₂H, Ar=1,3-substituted phenyl) gave a bischelate complex (L₂)₂Cu₂ · 2MeOH (Fig. 2.1) with the normal paddlewheel structure and tilted, *trans*-oriented chelate rings with skewed conformations. The overall structure was reasonably well reproduced by density functional calculations on (L₂)₂Cu₂. Treatment of the product from reaction of Cu₂(OAc)₄ and diacid H₂L₃ (Ar=1,3-substituted 2,4-dibromophenyl) with pyridine gave a six-coordinate

mononuclear chelate (L3)Py₂Cu · H₂O (Fig. 2.2) in which one chelate carboxylate is monodentate, the other is unsymmetrically bidentate and the pyridines are *cis*-coordinated.

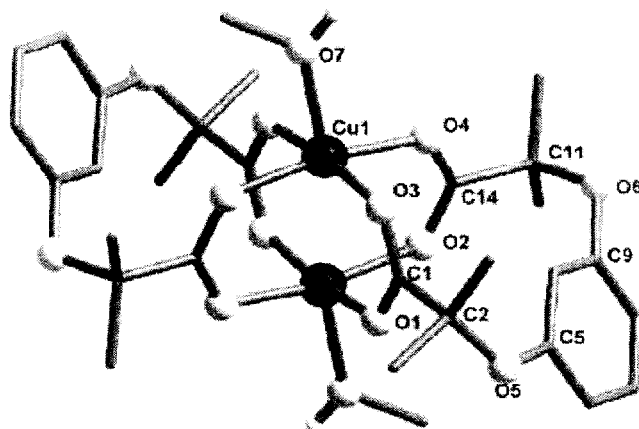


Fig. 2.1 Structure of (L2)₂Cu₂ · 2MeOH [21].

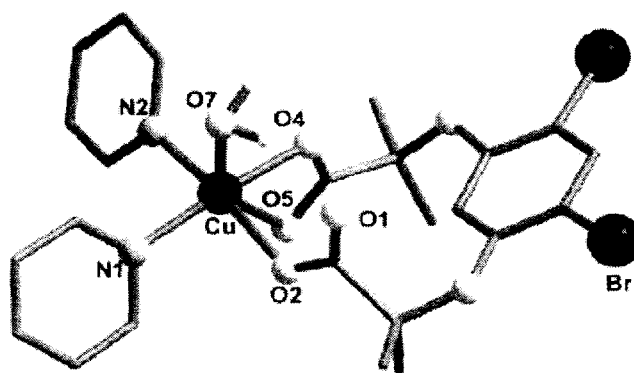


Fig. 2.2 Structure of (L3)Py₂Cu · H₂O [21].

In 1998, the dinucleating ligand *N,N'*-(2-hydroxy-5-methyl-1,3-xylylene)bis(*N*-(carboxymethyl)glycine) (CH₃HXTA) has been used to synthesize the dinuclear Cu(II) bis(pyridine) complex Na[Cu₂(CH₃HXTA)(Py)₂] · 1.5(1,4-dioxane) [Na(1)]: triclinic. The structure shows two distinct distorted square pyramidal Cu(II) centers with each Cu(II) ion bound by two carboxylate oxygen atoms, one amine nitrogen atom, a phenolate oxygen atom, and one pyridine nitrogen atom. The phenyl ring of the CH₃HXTA ligand is twisted relative to the Cu1-O1-Cu2 plane, and the resulting dihedral angle is 44.2°. The electronic absorption spectrum of **1** in aqueous solution at pH 3 suggests a shift toward trigonal bipyramidal Cu(II) coordination in

solution. Spectral titration of $\text{Na}[\text{Cu}_2(\text{CH}_3\text{HXTA})(\text{H}_2\text{O})_2]$ (Fig. 2.3) with L (where L= pyridine or sodium cyanide) results in complexes with terminal L groups. These exogenous ligands appear to bind in a positive cooperative stepwise fashion. Variable-temperature magnetic susceptibility data for **1** indicate that the Cu(II) ions are antiferromagnetically coupled ($-2J = 168 \text{ cm}^{-1}$). The ^1H NMR studies on a methanol solution of **1** are consistent with weak spin-coupling in solution [22].

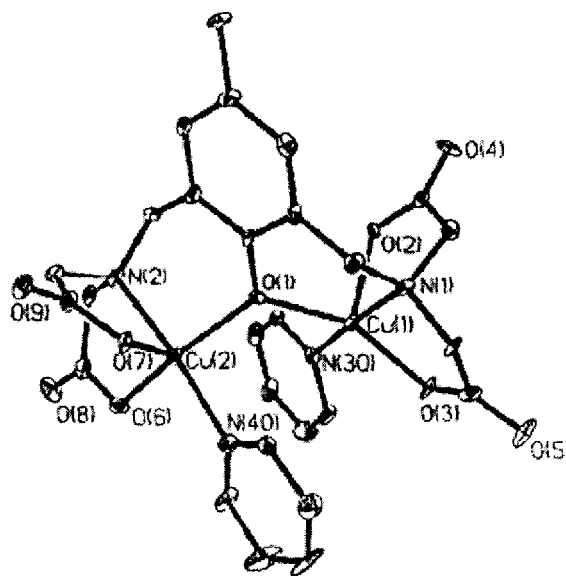
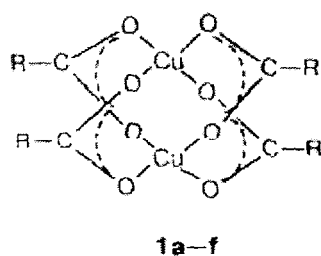


Fig. 2.3 Structure of $[\text{Cu}_2(\text{CH}_3\text{HXTA})(\text{Py})_2]^-$ anion [22].

Akopova *et al.* [23] described the synthesis, structure, and mesomorphism of a new series of copper carboxylates **1a-f** (Fig. 2.4). Compounds **1a,b,c,e** were obtained by fusing copper hydroxide with the corresponding acid, while compounds **1d,f** were obtained by the exchange reaction. The influence of periphery of the chelate node on the appearance of discophase was studied. A stacked hexagonal structure of copper erucate was proved. The effect of restructuring of the chelate node in this compound after its isothermic exposure, causing the loss of mesomorphism was revealed.



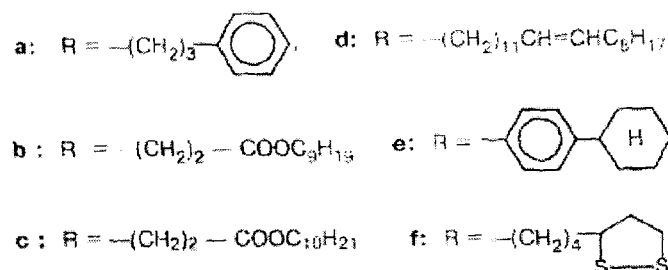


Fig. 2.4 Structure of copper carboxylate [23].

Kozlevčar *et al.* [24] during the investigations of fatty acid copper(II) carboxylates with biologically important ligands prepared several compounds of the composition $[Cu_2(O_2CC_nH_{2n+1})_4(urea)_2]$ ($n = 5$ to 11) and $[Cu_2(O_2CC_5H_{11})_4(urea)_2]$. The molecular structure of the compound $[Cu_2(O_2CC_5H_{11})_4(urea)_2]$ (Fig. 2.5) was determined by X-ray diffraction analysis. The compounds were characterized by standard physical and chemical methods and tested for their fungal mycelial growth inhibition activity with mycelia of two wood decay fungi *Trametes versicolor* and *Antrodia vaillantii*. The results of the characterization are in agreement with the values typical for dimeric copper(II) carboxylates. In the electronic spectra the difference between both types of hexanoate compounds was observed, however in vibrational spectra also the differences among the compounds where one molecule of urea is bonded on each dimer were noticed. Significantly higher growth inhibition for the whole series for *Antrodia vaillantii* was observed.

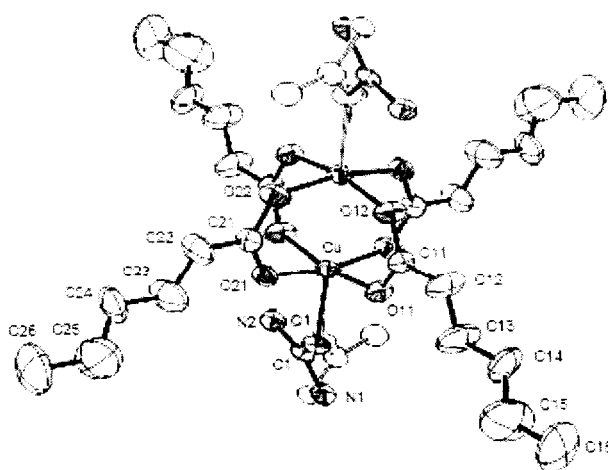


Fig. 2.5 Structure of $[Cu_2(O_2CC_5H_{11})_4(OCN_2H_4)_2]$ [24].

Waizump *et al.* [25] have reported the synthesis and crystal structures of $[\text{Co}(\text{nic})_2(\text{H}_2\text{O})_4]$ (1), $[\text{Co}(\text{iso})_2(\text{H}_2\text{O})_4]$ (2), $[\text{Cu}(\text{nic})_2(\text{H}_2\text{O})_4]$ (3), and $[\text{Cu}(\text{iso})_2(\text{H}_2\text{O})_4]$ (4) (nic = nicotinate; iso = isonicotinate) (Fig. 2.6). The crystal of complex 1 is monoclinic, space group $C2/m$ and the other crystals 2 3 and 4 are all triclinic. The arrangements around the metal ions are *trans*-octahedra with two pyridyl nitrogen and two aqua oxygen in the equatorial positions and two aqua oxygen in the axial positions, although the Cu(II) complexes show a larger Jahn-Teller distortion.

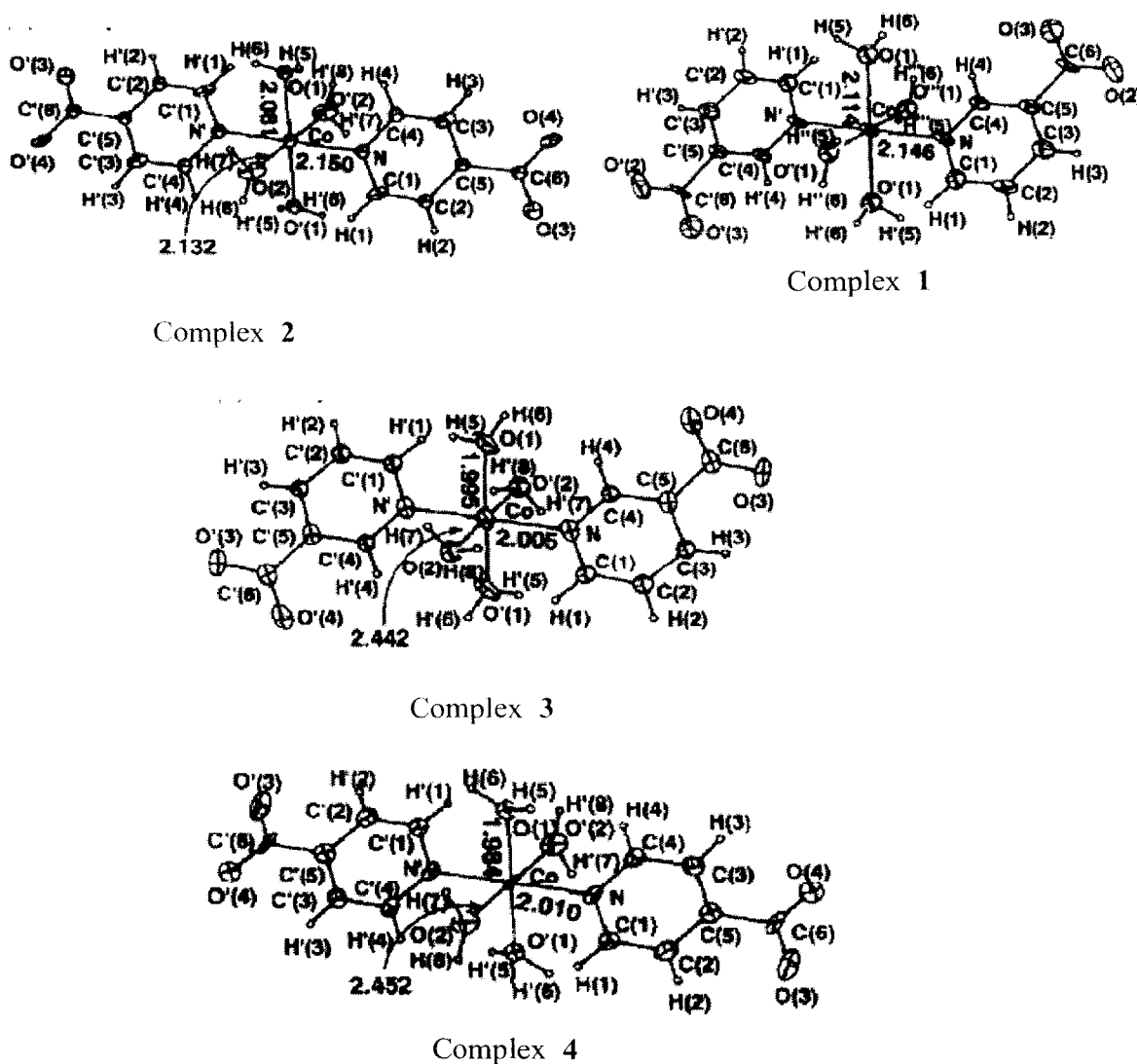


Fig. 2.6 Crystal structures of $[\text{Co}(\text{nic})_2(\text{H}_2\text{O})_4]$ (1), $[\text{Co}(\text{iso})_2(\text{H}_2\text{O})_4]$ (2), $[\text{Cu}(\text{nic})_2(\text{H}_2\text{O})_4]$ (3) and $[\text{Cu}(\text{iso})_2(\text{H}_2\text{O})_4]$ (4) (nic = nicotinate; iso = isonicotinate) [25].

Very recently, a Chinese group has synthesized a new complex, $\text{Co}(\text{MBTC})_2(\text{DMF})_2$ (MBTC = 6-methoxybenzothiazole-2-carboxylate, DMF = *N,N*-dimethylformamide), in DMF solution and characterized by single crystal X-ray diffraction analysis. Using the cobalt complex as catalyst, phenylacetic acid was prepared by the carbonylation of benzyl chloride with carbon monoxide (0.1 MPa). The effects of solvents, phase transfer catalysts and temperature on the reactions were investigated. The yield of phenylacetic acid was higher than 90% in optimized conditions [26]. Vučković *et al.* [27] reported novel binuclear Co(II) complexes with *N*-functionalized cyclam, *N,N',N'',N'''*-tetrakis (2-pyridylmethyl) tetraazacyclotetradecane (tpmc) and one of the aromatic mono or dicarboxylate ligands (benzoate, phthalate or isophthalate ions). The compounds were analyzed and studied by elemental analyses (C, H, N), electrical conductivities, VIS and IR spectroscopy and magnetic as well as cyclic voltammetric measurements. In $[\text{Co}_2(\text{C}_6\text{H}_5\text{COO})_2\text{tpmc}](\text{ClO}_4)_2 \cdot 3\text{H}_2\text{O}$ (Fig. 2.7), the benzoate ligands are most probably coordinated as chelates in the *trans*-position to each Co(II) and the macrocycle adopts a *chair* conformation. In the complexes $[\text{Co}_2(\text{Y})\text{tpmc}](\text{ClO}_4)_2 \cdot z\text{H}_2\text{O}$, (Y = phthalate or *i*-phthalate dianion, $z = 2; 4$), it is proposed that the isomeric dicarboxylates are bonded combined as bridges and chelates. The composition and the assumed geometries of the complexes are compared with the, earlier reported, corresponding Cu(II) complexes. Cyclic voltammetry measurements showed that the compounds are electrochemically stable.

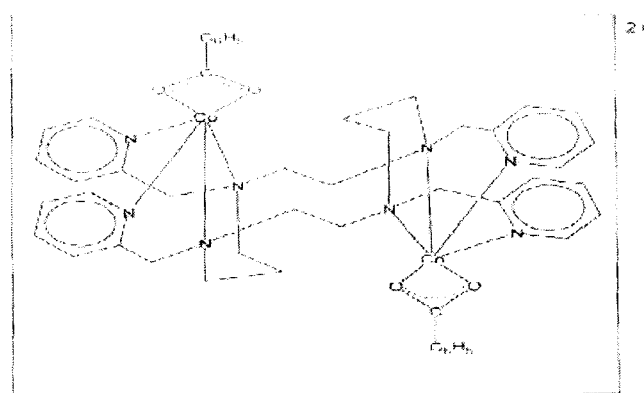


Fig. 2.7 Suggested structure of the $[\text{Co}_2(\text{C}_6\text{H}_5\text{COO})_2\text{tpmc}]^{2+}$ from complex (1) in a *chair* conformation [27].

T. A. Zevaco and his coworkers [28] in 1998, have published a paper covering the synthesis, spectral characterization and X-ray structure determination of the zinc(II) norbornen-2,3 dicarboxylate $[\text{Zn}(\text{cis-2,3-ndc})\text{-(1-methylimidazole)}_2(\text{H}_2\text{O})]_n$ (**1**) (*cis*-2,3-ndc = bicyclo[2,2,1]-hept-5-ene-2,3-*cis*-dicarboxylic acid). It crystallizes in the monoclinic space group $P2_1/c$. The crystal structure of **1** consists of polymeric chains which propagate along the *c* axis. The structure is stabilized by extended hydrogen bonds involving adjacent chains and water molecules. The metal centers display a slightly distorted tetrahedral geometry. The norbornenedicarboxylic acid acts as a *syn*-bound O,O'-bridging ligand. In the same year they also published another paper which was covering the reaction of an aqueous suspension of zinc oxide with 2-quinolinecarboxylic acid afforded, after recrystallization from a 1-methylimidazole/ acetonitrile solution, crystals of the anhydrous carboxylate $[\text{Zn}(\text{2-quinolinecarboxylato})_2 \text{ (1-methylimidazole)}_2]$. **1** $[\text{Zn}(\text{C}_{10}\text{H}_6\text{NO}_2)_2 (\text{C}_4\text{H}_6\text{N}_2)_2]$, monoclinic, space group $P2_1/n$. The zinc atom is hexacoordinated, located at an inversion center and exhibits a slightly distorted octahedral geometry. The Zn-equatorial ligand distances are 2.057(2) Å for Zn---O and 2.244(2) Å for Zn---N. The Zn---N distance for the apical imidazole ligands is 2.144(2) Å [29].

Hamed *et al.* [30] have reported that the compounds having the general formula: $\text{K}_n[\text{M}(\text{FO})_2(\text{H}_2\text{O})_2] \cdot x\text{H}_2\text{O}$, where (M = Cu(II) or Fe(III), n = 2 or 1, FO = folate anion, x = 2 or 3 with respect) (Fig. 2.8), could be prepared and their absorption efficiency in rodent's blood was determined. The obtained compounds were characterized by elemental analysis, infrared as well as thermogravimetric analysis and polarization of light. The results suggest that the two folate complexes were formed in 1:2 molar ratio (metal:folic acid) which acted as a bidentate ligand through both carboxylic groups. Polarization of light proved that the folate complexes have symmetric geometry.

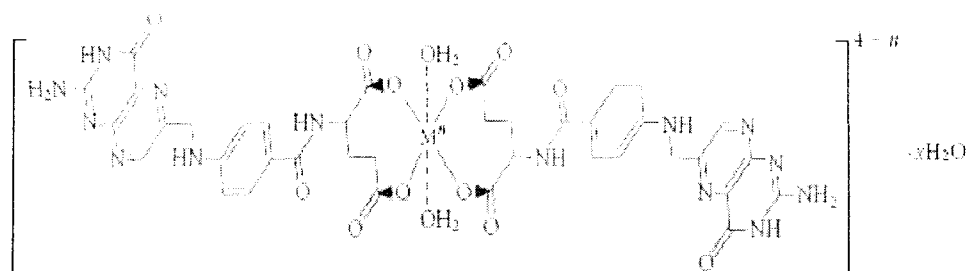


Fig. 2.8 Structure of $K_n[M(FO)_2(H_2O)_2] \cdot xH_2O$ [30].

V. M. Trukhan and his coworkers [31] have reported that the reaction of the new polydentate ligand 2,6-bis{3-[*N,N*-di(2-pyridylmethyl)amino]propoxy}benzoic acid (LH) with $Fe(ClO_4)_3$ followed by addition of chloroacetic acid leads to the formation of the tetranuclear complex $[\{Fe_2OL(ClCH_2CO_2)_2\}_2](ClO_4)_4$ (Fig. 2.9), the crystal structure of which reveals that it consists of two $Fe^{II}_2(\mu-O)(\mu-RCO_2)_2$ cores linked *via* the two L ligands in a helical structure, with the carboxylate moieties of the two ligands forming a hydrogen-bonded pair at the center of the helix.

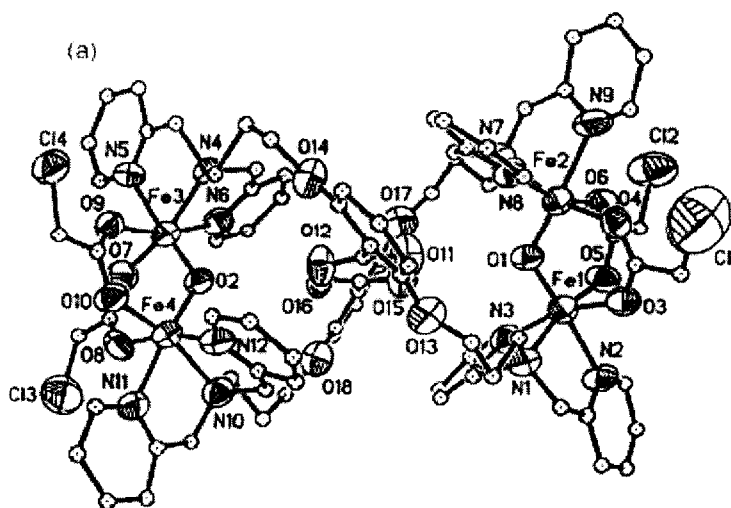


Fig. 2.9 Structure of $[\{Fe_2OL(ClCH_2CO_2)_2\}_2](ClO_4)_4$ [31].

Ghatts *et al.* [32] prepared a μ -oxo-diiron(III) complex bridged by two molecules of 1-aminocyclopropane-1-carboxylic acid (ACCH) that was prepared with the ligand 1,4,7-triazacyclononane (TACN): $[(TACN)Fe_2(\mu-O)(\mu-ACCH)_2](ClO_4)_4 \cdot 2H_2O$ (**1**) (Fig. 2.10). This complex was characterized, and its crystal structure was

solved. The bridging amino acid moieties were found in their zwitterionic forms (noted as ACCH). Reactivity assays were performed in the presence of hydrogen peroxide and **1** turned out to be the first example of a well-characterized iron-ACCH complex able to produce ethylene from the bound ACCH moiety.

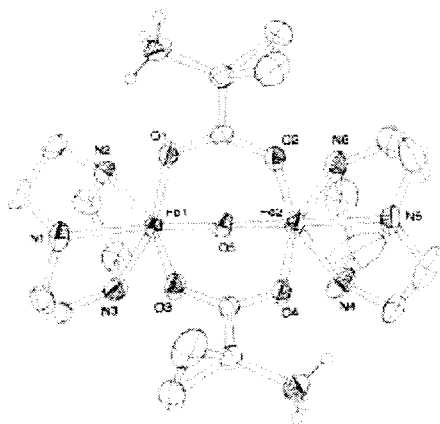


Fig. 2.10 Structure of the cation $[\text{Fe}_2(\text{TACN})_2(\mu\text{-O})(\mu\text{-ACCH})_2]^{4+}$ [32].

C. M. Grant and his coworker [33] have carried out a reaction between FeCl_3 , NaO_2CPh and L [L = 1,2-bis(2,2'-bipyridyl-6-yl)ethane] in MeCN that gave the complex $[\text{Fe}_6\text{O}_4\text{Cl}_4(\text{O}_2\text{CPh})_4\text{L}_2][\text{FeCl}_4]_2$ **1** whose cation contains an unusual $[\text{Fe}_6(\mu_3\text{-O})_4]^{10+}$ core, whereas in MeOH the dinuclear complex $[\text{Fe}_2(\text{OMe})_2\text{Cl}_2(\text{O}_2\text{CPh})\text{L}][\text{FeCl}_4]$ **2** was obtained; magnetic studies indicate that the cations of **1** (Fig. 2.11) and **2** (Fig. 2.12) both have $S = 0$ ground states, consistent with the expected antiferromagnetic exchange interactions.

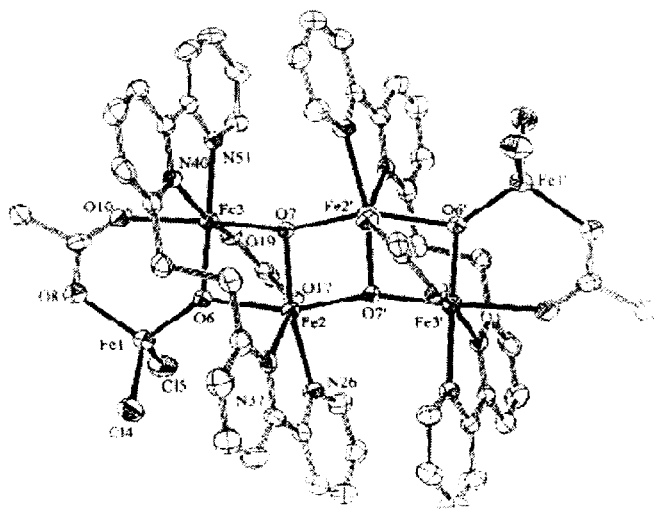


Fig. 2.11 Structure of the cation of **1** [33].

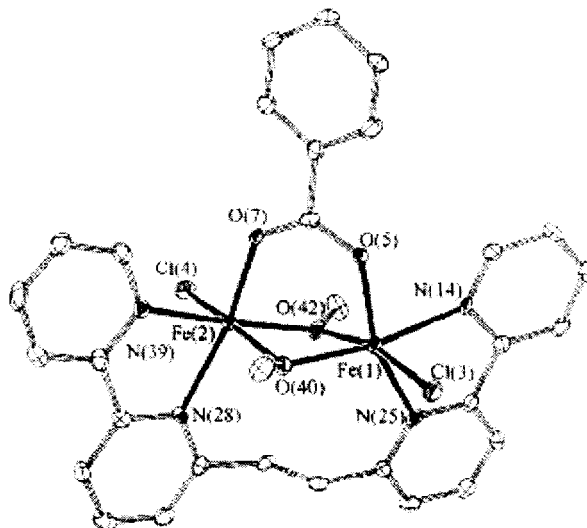


Fig. 2.12 Structure of the cation of **2** [33].

Moon *et al.* [34] have prepared the dinuclear Mn(II) complex, $[\text{Mn}_2(\text{Hbida})_2(\text{H}_2\text{O})_2]$ (Fig. 2.13), using a tetradentate tripodal ligand, *N*-(benzimidazol-2-ylmethyl)iminodiacetic acid (H_3bida) which has two carboxylate and one benzimidazole groups. The manganese ions are doubly bridged using μ, η^1 -bridging monodentate carboxylate oxygen atoms. The Mn–Mn bond distance of 3.446 Å in this complex. The geometry of the complex is with four carboxylates in two different types of binding modes, non-bridging monodentate and μ, η^1 -type bridging monodentate. The magnetic properties of the complex show a coupling constant of $J = -0.471(1) \text{ cm}^{-1}$, which is consistent with weakly coupled antiferromagnetic Mn^{II} ($S = 5/2$) centers.

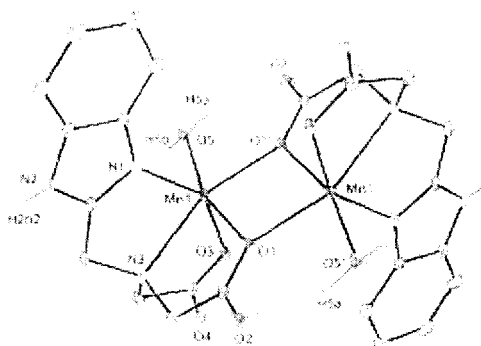


Fig. 2.13 The graphical structure of $[\text{Mn}_2(\text{Hbida})_2(\text{H}_2\text{O})_2]$ [34].

Maryudi *et al.* [35] have reported a method of synthesis of manganese carboxylates and their characterization. The new method involves reaction between molten carboxylic acid with sodium hydroxide in alcoholic solution to produce sodium carboxylates and continued by reacting sodium carboxylate with chloride salt of manganese. 1st and 2nd both step of reactions were conducted at 80-85°C and under perfect agitation. 2nd step of reaction took place well in the low concentration of manganese chloride, about 0.25 M or less. Thermogravimetric Analyzer test have been done and the results obtained in this study have exposed the capacity of manganese carboxylates stability at processing temperature of polyethylene.

Reaction of $\text{Fe}(\text{O}_2\text{CCH}_3)_2$ or $\text{Mn}(\text{O}_2\text{CCH}_3)_2 \cdot 4\text{H}_2\text{O}$ with bidentate nitrogen donor ligands affords the trinuclear complexes $[\text{M}_3(\text{O}_2\text{CCH}_3)_6\text{L}_2]$ [$\text{M}=\text{Fe}$, $\text{L}=\text{BIPhMe}$ (**1**) (Fig. 2.14); $\text{M}=\text{Mn}$, $\text{L}=\text{BIPhMe}$ (**2**) (Fig. 2.15) or 1,10-phenanthroline (**3**)] in high yields. As judged from X-ray diffraction studies, these complexes adopt a novel linear structure, with one monodentate and two bidentate bridging carboxylates spanning each pair of metal atoms. Within this motif there are two geometric isomers that exist, designated “syn” or “anti” depending upon the orientation of the bidentate nitrogen donor ligands with respect to one another across the plane defined by the three metal atoms and the two monodentate bridging oxygen atoms. Structural characterization of three isomers of compound **2** revealed a considerable degree of flexibility in the tricarboxylate-bridged dimetallic unit, with M-M distances ranging from 3.370 (**3**) to 3.715 (**2**) Å [36].

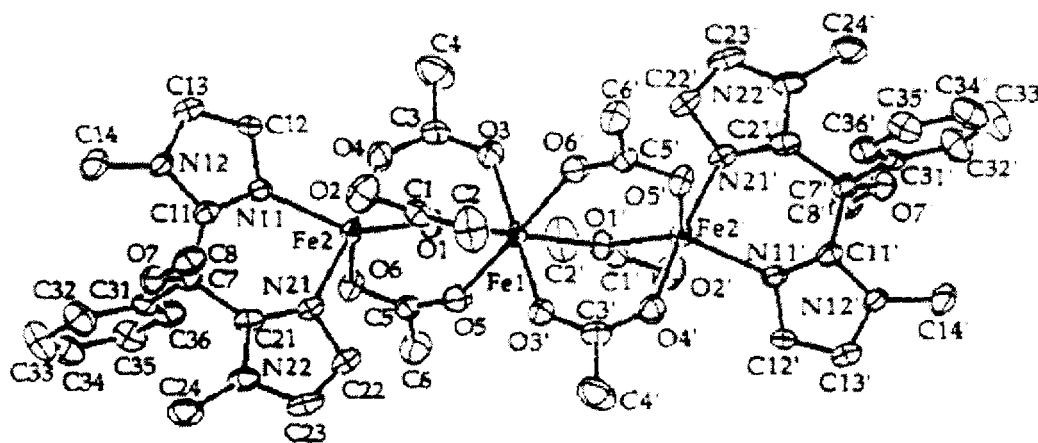


Fig. 2.14 Structure of $[\text{Fe}_3(\text{O}_2\text{CCH}_3)_6(\text{BIPhMe})_2] \cdot 2\text{THF}$, *anti*-1 [36].

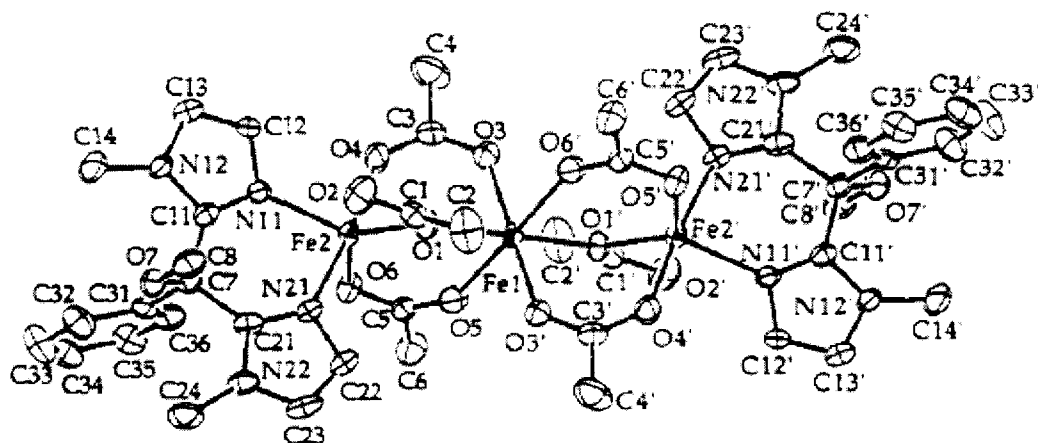


Fig. 2.15 Structure of $[\text{Mn}_3(\text{O}_2\text{CCH}_3)_6(\text{BIPhMe})_2] \cdot 2\text{CH}_2\text{Cl}_2$, *anti*-2A [36].

Thermal decomposition of transition metal malonates, $\text{MCH}_2\text{C}_2\text{O}_4 \cdot x\text{H}_2\text{O}$ and transition metal succinates, $\text{M}(\text{CH}_2)_2\text{C}_2\text{O}_4 \cdot x\text{H}_2\text{O}$ ($\text{M}=\text{Mn, Fe, Co, Ni, Cu \& Zn}$) have been studied employing TG, DTG, DTA, XRD, SEM, IR and Mössbauer spectroscopic techniques by Randhawa *et al.* [37]. After dehydration, the anhydrous metal malonates and succinates decomposed directly to their respective metal oxides in the temperature ranges 310-400°C and 400-525°C respectively. The oxides obtained have been found to be nanosized. The thermal stability of succinates was observed to be higher than that of the respective malonates [37].

Few complexes of Fe (III), Co (II), Ni (II) and Cu (II) with uracil, 6-amino uracil and those with substituted phenyl azo-6-amino uracils containing *o*-methyl,*p*-carboxy and *o*-carboxy substituents and 5,5'-diethyl barbituric acid sodium salt have been synthesized and characterized by elemental analysis, magnetic moment and spectral measurements (IR, UV-Vis, ESR). The IR spectra showed that uracil existed in keto-enol tautomerism but 6-amino uracil possessed the keto amino-imine structure with some enol form. The iron complexes were with octahedral geometries. The square planar copper complexes existed in ligand bridged structures. The nickel complexes were of tetrahedral configuration. In general, the azo group was involved in the structural chemistry of the complexes. The coordination bond length was calculated. The thermal properties (TG and DTA) of the complexes were measured and discussed and thermodynamic parameters were also evaluated [38].

A. Golobič and his coworkers [39] applied different synthetic routes for preparation of some copper(II) carboxylates with 3-hydroxypyridine (3-pyOH). The monomeric and dimeric complex of copper(II) acetate were isolated, $[\text{Cu}(\text{O}_2\text{CCH}_3)_2(3\text{-pyOH})_2]$, **1**, and $[\text{Cu}_2(\text{O}_2\text{CCH}_3)_4(3\text{-pyOH})_2]$, **2**, respectively. A covalently linked 2D CuII compounds of general formula $[\text{Cu}(\text{O}_2\text{CR})_2(3\text{-pyOH})_2]_n$, were prepared with benzoate ($\text{R}=\text{C}_6\text{H}_5$, **3**), hexanoate ($\text{R}=\text{CH}_3(\text{CH}_2)_4$, **4**), and heptanoate ($\text{R}=\text{CH}_3(\text{CH}_2)_5$, **5**) ligands. The crystal structures of all five compounds were determined by X-ray structure analysis. The compounds were tested for fungicidal activity against two fungal species *Trametes versicolor* and *Antrodia vaillantii*. Complete growth retardation for *Antrodia vaillantii* was noticed for compounds **3**, **4**, and **5** at concentrations of $5 \cdot 10^{-3} \text{ mol L}^{-1}$, $1 \cdot 10^{-3} \text{ mol L}^{-1}$, and $5 \cdot 10^{-4} \text{ mol L}^{-1}$, while in the case of *Trametes versicolor* complete growth retardation was observed for the same three compounds only at the highest tested concentration.

Kozlevčar *et al.* [40] synthesized and characterized a series of compounds of the composition $[\text{Cu}_2(\text{OOCCH}_n\text{H}_{2n+1})_4(\text{nia})_2]$ (nia = nicotinamide; $n = 6$ to 11) and also tested for fungicidal activity. Crystal structure determinations revealed dinuclear structures of the copper(II) acetate hydrate type for compounds $[\text{Cu}_2(\text{OOCCH}_6\text{H}_{13})_4(\text{nia})_2]\text{-A}$ (1A), $[\text{Cu}_2(\text{OOCCH}_6\text{H}_{13})_4(\text{nia})_2]\text{-B}$ (1B) and $[\text{Cu}_2(\text{OOCCH}_8\text{H}_{17})_4(\text{nia})_2]$ (3). Other applied characterization methods indicate dimeric structures for all synthesized compounds [μ_{eff} (298 K) = 1.43–1.50 BM; characteristic band in UV-Vis spectra in the region $\lambda = 350\text{--}400 \text{ nm}$]. The same conclusion may also be deduced from the IR ($\Delta \nu_{\text{asym}}(\text{COO}^-) - \nu_{\text{sym}}(\text{COO}^-) = 183\text{--}189 \text{ cm}^{-1}$) and EPR spectra, though some differences were observed for heptanoate modification 1A, probably due to a different hydrogen bonding scheme. Screening for fungicidal activity against the wood-rotting fungus *Trametes versicolor* (L. ex Fr.) Pilat shows that the compounds dissolved in DMSO completely stop mycelium growth at a concentration of $1.0 \times 10^{-3} \text{ mol L}^{-1}$. Some of them ($n = 8, 9, 10$) show strong activity also in more diluted solutions ($1.0 \times 10^{-4} \text{ mol L}^{-1}$).

S. Shahzadi and his coworkers [41] synthesized transition metal carboxylates, i.e., 3-[(2,4,6-trichloroanilino)carbonyl]prop-2-enoic acid and 3-[(4-bromoanilino)carbonyl] prop-2-enoic acid. The unimolar and bimolar substituted products have been characterized by elemental analysis, IR, UV-Vis spectroscopy, ^1H NMR, and

atomic absorption. IR data show the bidentate nature of the carboxylate group. The transition metal complexes were tested *in vitro* against a number of microorganisms to assess their biocidal properties.

2.3 Scope and objective

Carboxylates are ligands which contain O atoms as donors. In case of the dinitrobenzoic acid the nitro groups may also act as donors through the O and N atoms. Hence the acid as a ligand might be useful for complex formation. Therefore, the ligand was chosen to examine its complex forming ability with transition metals as a model and then to examine their fungitoxicity. Many transition metal compounds [39-43] are known to be potential fungicides.

2.4 Experimental

2.4.1 General Comments

The solvents used in reactions were of AR grade and were obtained from commercial sources (Merck, India). The solvents were dried using standard literature procedures. Water were distilled with sodium hydroxide and potassium permanganate where as methanol was distilled after reacting it with solid iodine and magnesium.

2.4.2 Materials

The 3,5-di nitro benzoic acid (s.d.fine-chem limited, India), $\text{CuSO}_4 \cdot 5\text{H}_2\text{O}$ (s.d.fine-chem limited, India), $\text{CoCl}_2 \cdot 6\text{H}_2\text{O}$ (Merck, India), $\text{FeSO}_4 \cdot 7\text{H}_2\text{O}$ (s.d.fine-chem limited, India), $\text{ZnSO}_4 \cdot 7\text{H}_2\text{O}$ (s.d.fine-chem limited, India), $\text{MnCl}_2 \cdot 4\text{H}_2\text{O}$ (Merck, India) of AR quality were used as received from commercial sources. Methanol (Merck, India) used in the reaction was of AR grade.

2.4.3 Measurements

The IR spectra in the range $4000\text{-}400\text{ cm}^{-1}$ were recorded on FTIR-8300 Shimadzu spectrophotometer with samples investigated with KBr on CsI window. UV/VIS spectra were recorded on JASCO V-530. Microanalyses were performed at

the ICAS, Kolkata, India. Magnetic susceptibility was measured at room temperature on a PAR 155 sample vibrating magnetometer using $\text{Hg}[\text{Co}(\text{SCN})_4]$ as the calibrate. Differential calorimetric analyses were carried out on a Perkin-Elmer Thermal analyzer from 100-230°C at a heating rate of 10°C/min. Metals were estimated using standard methods in our laboratory.

2.4.4 Synthetic procedures

2.4.4.1 Preparation of sodium salt of 3,5-dinitro benzoic acid (LNa)

To a solution (40 ml) of 3,5-dinitro benzoic acid (4.0g, 18.85 mmol) was added drop wise with continuous stirring NaOH (0.75g, 18.85 mmol) solution in water (20 ml) in the presence of phenolphthalein as an indicator. The reaction system was stirred for half an hour. Solvents removed by evaporation, leaving behind the crystallized product of sodium salt of 3,5-dinitro benzoic acid. Then the sodium salt was further recrystallized in methanol and dried *in vacuo*.

LNa: Yield: 3.15 g; 78.75 %; M.P.: >240°C (dec).

Elemental analysis (Calcd. For $\text{C}_7\text{H}_3\text{N}_2\text{O}_6\text{Na}$):

Calcd.: C, 35.91; H, 1.29; N, 11.97 %.

Found: C, 35.82; H, 1.20; N, 11.94%.

IR (cm^{-1}): $\nu(\text{OCO})_{\text{asym}}$, 1620(m); $\nu(\text{OCO})_{\text{sym}}$, 1459 (s); $\nu(\text{NO}_2)_{\text{asym}}$, 1534(m); $\nu(\text{NO}_2)_{\text{sym}}$, 1345(m).

2.4.4.2 Preparation of Mn(II) complex of 3,5-dinitro benzoic acid (1)

Sodium salt of 3,5-dinitro benzoic acid (1.18g, 5.05 mmol) was dissolved in water (4 ml) methanol (120 ml) mixture and the solution was taken in 250 ml round bottomed flask. The $\text{MnCl}_2 \cdot 4\text{H}_2\text{O}$ (0.5g, 2.52 mmol) was dissolved in methanol (10 ml) and added drop wise to the sodium salt of the acid. The mixture was then heated under reflux for 10h. The brown volatiles were removed from reaction mixture and

the dry mass washed with hot methanol and the brownish solid of desired product was obtained by filtration which was dried *in vacuo*.

2.4.4.3 Preparation of Fe(II) complex of 3,5-dinitro benzoic acid (2)

Sodium salt of 3,5-dinitro benzoic acid (1.68g, 7.19 mmol) was dissolved in water (4 ml) methanol (130 ml) mixture and the solution was placed in 250 ml round bottomed flask. The $\text{FeSO}_4 \cdot 7\text{H}_2\text{O}$ (1.0g, 3.59 mmol) was dissolved in methanol (15 ml) and added drop wise to the sodium salt of the acid. The colour of the mixture turned to deep chocolate and a precipitate appeared. The mixture was heated under reflux for 6h. Desired product as a reddish brown precipitate was obtained by filtration. The product was washed with hot methanol and dried *in vacuo*.

2.4.4.4 Preparation of Co(II) complex of 3,5-dinitro benzoic acid (3)

Sodium salt of 3,5-dinitro benzoic acid (0.98g, 4.20 mmol) was dissolved in water (3 ml) methanol (140 ml) mixture and the solution was placed in 250 ml round bottomed flask. The $\text{CoCl}_2 \cdot 6\text{H}_2\text{O}$ (0.5g, 2.10 mmol) was dissolved in methanol (15 ml) and purple solution was added drop wise to the sodium salt of the acid. The colour of the mixture turned pink after addition was complete. The solution was then heated under reflux for 6h. Pink crystals of the desired product was obtained from the filtrate after 25 days on slow evaporation, at room temperature.

2.4.4.5 Preparation of Cu(II) complex of 3,5-dinitro benzoic acid (4)

Sodium salt of 3,5-dinitro benzoic acid (0.94g, 4.00 mmol) was dissolved in water (3 ml) methanol (130 ml) mixture and the solution was placed in 250 ml round bottomed flask. The $\text{CuSO}_4 \cdot 5\text{H}_2\text{O}$ (0.5g, 2.00 mmol) was dissolved in methanol (20 ml) and the blue solution was added drop wise to the sodium salt of the acid. After addition the colour of the mixture became intense blue. The solution was then heated under reflux for 6 h and then filtered. The filtrate was concentrated to a volume of 40 ml. Deep blue crystals of the desired product were obtained by slow cooling of the solution.

2.4.4.6 Preparation of Zn(II) complex of 3,5-dinitro benzoic acid (5)

Sodium salt of 3,5-dinitro benzoic acid (0.81g, 3.47 mmol) was dissolved in water (3 ml) methanol (120 ml) mixture and the solution was placed in a 250 ml round bottomed flask. The ZnSO₄·7H₂O (0.5g, 1.73 mmol) dissolved in methanol (15 ml) was added drop wise to the sodium salt of the acid. Then little amount of white precipitate was appeared. The mixture was the heated under reflux for 6h and then filtered. The filtrate was concentrated to a volume of 40 ml. White crystals of the desired product were obtained by slow cooling of the solution.

2.4.5 Crystal structure determinations

The crystals of **3** and **4** suitable for the X-ray diffraction study were prepared by slow crystallization of methanol solution of the respective compounds, the crystallographic analysis of compounds showed the sample had crystallized as methanol solvate. Intensity data were measured for selected crystals of **3** and **4** at 293 K on a Bruker SMART APEX diffractometer with fine-focus sealed graphite tube with MoK α radiation, $\lambda = 0.71073 \text{ \AA}$ so that $\theta_{\max} = 27.5^\circ$. The data set was corrected for absorption based on multiple scans [44]. Each structure was solved by SHELXS-97 [45] and refined by a full-matrix least-squares procedure SHELXL-97 [45] on F^2 with primary atom site location: structure- invariant direct methods, with hydrogen atoms treated by a mixture of independent and constrained refinement and using a weighting scheme of the form $w = 1/[\sigma^2(F_o^2) + (0.0522P)^2 + 0.1427P]$ where $P = (F_o^2 + 2F_c^2)/3$. For compound **3** carbon-bound H-atoms were placed in calculated positions (C–H 0.93 to 0.96 \AA) and were included in the refinement in the riding model approximation, with $U_{\text{iso}}(\text{H})$ set to 1.2 to 1.5 $U_{\text{equiv}}(\text{C})$. The methanol H-atoms were located in a difference Fourier map, and were refined with a distance restraint of O–H 0.85 \pm 0.01 \AA ; their U_{iso} values were freely refined. The molecular structures showing crystallographic numbering schemes were drawn with 50% displacement ellipsoids using ORTEP-3 [46] and diagrams were generated with the aid of the DIAMOND programmer [47].

2.4.6 Crystallographic data and refinement details for 3 and 4

Crystallographic data and refinement details for 3

Formula	[Co (C ₇ H ₃ N ₂ O ₆) ₂ (CH ₃ OH) ₄]
Formula weight	609.33
Crystal habit, colour	Prism, pink
Crystal system	Triclinic
Space group	$P\bar{1}$
a (Å)	6.4068(8)
b (Å)	8.7660(11)
c (Å)	12.1603(16)
α (°)	90.411(2)
β (°)	100.407(2)
γ (°)	102.214(2)
V (Å ³)	655.77(14)
Z	1
D _x (Mg m ⁻³)	1.543
λ (MoK α , Å)	0.71073
F(000)	313
Crystal size (mm)	0.35 × 0.30 × 0.05
Absorption coefficient μ (mm ⁻¹)	0.74
θ range for data collection (°)	2.4-22.8
Reflection collected	6372
Independent reflection	2999
R _{int}	0.028
Reflection with $I > 2\sigma(I)$	2388
Number of parameters	188
R[F ² > 2 σ (F ²)]	0.043
wR(F ²)	0.110
S	1.03
Largest difference peak and hole (Å ⁻³)	0.001,0.38

2.4.7 Biological studies

2.4.7.1 Antifungal activity

The virulent fungal strains of *Lasiodiplodia theobromae* and *Crucularia eragrostidis* were collected from the type culture collection, Dr. A. Saha, Department of Botany, University of North Bengal. The strains were isolated from *L. theobromae* (a pathogen of mango, *Magnifera indica*) and *C. eragrostidis* (a pathogen of tea, *Camellia sinensis*). These strains were grown on potato- dextrose agar (PDA, HiMedia, India) medium at 27°C. The fungicidal activities were determined following spore germination bioassay as described by Rouxel *et al.*[48]. Purified eluants (15µl) were placed on two spots 3 cm apart on a clean grooved slide. One drop of spore suspension (15µl), which was prepared from 15 day old cultures of the fungi, was added to the treated spots. The slides were incubated in trays at 27°C for 24h under humid conditions. After incubation, one drop of Lactophenol mixture was added to each spot to fix the germinated spores. The number of spore germination events was compared with the spore germination of the control.

2.4.7.2 Phytotoxic effect

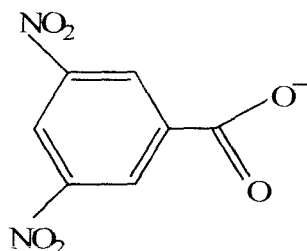
Seeds of Indian rice (*Oryzae sativa*), cultivar *Khitish* were collected from the Directorate of Farm, Uttar Banga Krishi Viswavidyalaya, Cooch Behar, West Bengal, India. Seeds were first surface sterilized with 0.1% mercuric chloride for 3 min, washed with distilled water and then the phytotoxic effects of the transition metal carboxylates (dissolved in 2 ml methanol then diluted with 10 ml water) were determined [49]. Seeds were incubated with different concentration of transition metal carboxylates for different time periods. After incubation, the seeds were washed with distilled water and incubated in a B.O.D. incubator for 48h at 27°C. The percentage of seed germination was calculated and compared with the control.

2.5 Result and discussion

2.5.1 Preparation of sodium salt of 3,5-dinitrobenzoic acid

Sodium salt of the 3,5-dinitrobenzoic acid was prepared by neutralization with equimolar aqueous solution of sodium hydroxide. The sodium salt of the 3,5-

dinitrobenzoic acid was obtained in good yield. The product was recrystallized from water/ethanol mixture. The ligand was soluble in water, water/ethanol and water/methanol mixture. The ligand had a decomposition temperature at > 240°C. The synthetic detail and characterization data for LH and LNa are described in section 2.4.4.1. The formula of the ligand and the abbreviations of the complexes are presented in scheme 2.1.



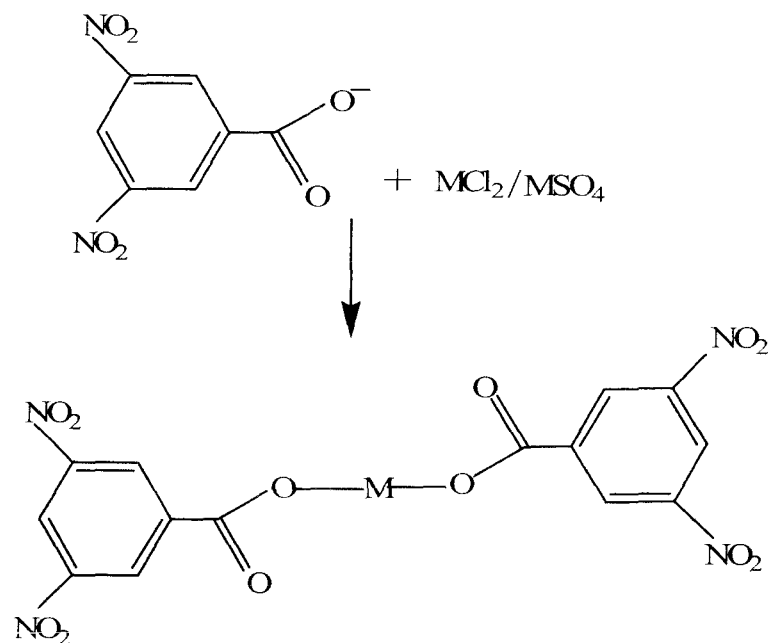
1. $[\text{Mn}(\text{L})_2 \cdot (\text{CH}_3\text{OH})_4]$; 2. $[\text{Fe}(\text{L})_2 \cdot (\text{CH}_3\text{OH})_4]$; 3. $[\text{Co}(\text{L})_2 \cdot (\text{CH}_3\text{OH})_4]$;
4. $[\text{Cu}_2(\text{L})_4 \cdot \text{Cu}(\text{L})_2 \cdot (\text{CH}_3\text{OH})_4]$; 5. $[\text{Zn}(\text{L})_2 \cdot (\text{CH}_3\text{OH})_4]$

Scheme 2.1

2.5.2. Synthesis of transition metal(II) complexes of 3,5-dinitrobenzoic acid (LH)

The transition metal carboxylates of 3,5-dinitrobenzoic acid (M=Mn, Fe, Co, Cu and Zn) were obtained in moderate yields (except for Mn-carboxylate) by the 1:2 reaction of transition metal sulfates/chlorides with the sodium salt of the ligand in water/methanol mixture as solvent for refluxation (Eq. 1 and Eq. 2). The sodium salt of the ligand was generated by the addition of aqua's solution of NaOH to the aqueous solution of 3,5-dinitrobenzoic acid. The reactions were completed in 10h time. The complexes produced are neutral chelated types. These are air stable for 48h because bonding solvents are released. The synthetic methodologies are described in scheme 2.2.





1. [Mn(L)₂(CH₃OH)₄]; 2. [Fe(L)₂(CH₃OH)₄]; 3. [Co(L)₂(CH₃OH)₄];
 4. [Cu₂(L)₄ · Cu(L)₂ · (CH₃OH)]; 5. [Zn(L)₂(CH₃OH)₄].

Scheme 2.2

2.5.3 Spectroscopic characterization and X-ray crystal structure determination of transition metal carboxylates, M(L)₂ [where M= Mn, Fe, Co, Cu and Zn; L=3,5-dinitrobenzoic acid]

The complexes were characterized by UV, IR and elemental analysis. Magnetic moment data further suggested the composition of the complexes as proposed. The composition of the complexes, however, are mainly based upon the elemental analyses supported by the spectroscopic and other data where available as far as practicable in our laboratory conditions. In general, the X-ray crystallographic data of the complexes (*e.g.*, 3 and 4) supports the observed spectral and magnetic moment data. Table 2.1 contains the relevant physical data of the compounds.

Table 2.1. Physical and analytical data for 1-5.

Composition	Yield(%)	M.P.(°C)	Colour	Elemental composition found (calcd) (%)			
				C	H	N	M
1. [Mn(C ₇ H ₃ N ₂ O ₆) ₂ · (CH ₃ OH) ₄]	30	Started decomposing at >230°C	Pale- brown	35.48 (35.72)	3.62 (3.66)	9.22 (9.26)	8.99 (9.08)
2. [Fe(C ₇ H ₃ N ₂ O ₆) ₂ · (CH ₃ OH) ₄]	87	172-174	Brown	35.75 (35.66)	3.58 (3.66)	9.20 (9.24)	9.11 (9.21)
3. [Co(C ₇ H ₃ N ₂ O ₆) ₂ · (CH ₃ OH) ₄]	85	Started decomposing at 129°C	Pink	35.31 (35.48)	3.72 (3.63)	9.11 (9.19)	9.73 (9.67)
4. [Cu ₂ (C ₇ H ₃ N ₂ O ₆) ₄ · Cu(C ₇ H ₃ N ₂ O ₆) ₂ · (CH ₃ OH)]	80	Started decomposing at 218°C	Deep blue	34.68 (34.50)	1.49 (1.38)	11.29 (11.15)	12.80 (12.69)
5. [Zn(C ₇ H ₃ N ₂ O ₆) ₂ · (CH ₃ OH) ₄]	75	165-167	White	35.01 (35.11)	3.48 (3.60)	9.05 (9.10)	10.45 (10.62)

2.5.3.1 IR spectra

Selected IR spectra and their assignment for the transition metal carboxylates have been presented in Table 2.2. A broad band in the 3500-3200cm⁻¹ region is assigned to -OH stretching modes. The carboxylate group displayed two absorbance bands one at $\nu(\text{OCO})_{\text{asym}}$ 1630-1660 cm⁻¹ region and other at $\nu(\text{OCO})_{\text{sym}}$ 1400-1470 cm⁻¹ region in the complexes [50]. The nitro group also displayed two absorbance bands. The $\nu(\text{NO}_2)_{\text{asym}}$ and $\nu(\text{NO}_2)_{\text{sym}}$ bands appeared at 1527-1545 cm⁻¹ and at 1340-1357 cm⁻¹ respectively in the transition metal complexes [50]. The broad band at 3500-3200 cm⁻¹ due to $\nu(\text{OH})$ attributable to the coordinated methanol (solvent) molecules slowly disappeared as the solvent molecules were lost during standing the complexes at room temperature on bench for ~ 48h. This indicated that the solvent molecules are loosely bound to the central metal atom. The carboxylate stretching

frequency indicated it to be a bridging bidentate type rather than a monodentate type. The difference between $\nu(\text{OCO})_{\text{asym}}$ and $\nu(\text{OCO})_{\text{sym}}$ ($\Delta\nu= 153\text{-}166$) is an indication of the bridging nature of the ligand [51]. Crystallographic data also confirmed the IR spectral interpretation at least for two complexes (**3** and **4**). The IR of the Cu-carboxylate compound (**4**) attracts special interest. The structure has a dimeric Cu_2 unit as well as a monomeric carboxylate molecule in its molecule joined via a $\text{NO}_2\cdots\text{O}$ (Fig. 2.18). The IR stretching vibrations for the $-\text{OCO}$ group, therefore, show two types of absorptions both are in the same frequency range but identifiably separate. The one binding the single Cu(II) units as a bridging bidentate group, the other also as the bridging bidentate group but bridging the Cu atoms in the Cu_2 dimeric moiety.

The complexation of the carboxylate moiety to the metal atom is indicated in the new compounds not only by the x-ray crystal structure determinations (for Co^{2+} and Cu^{2+}) but also by the shift of νCO of the (free) carboxylic acid group ($-\text{COOH}$) at 1699cm^{-1} to the $\sim 1622\text{-}1629\text{ cm}^{-1}$ $\nu(\text{OCO})_{\text{asym}}$ and $\sim 1458\text{-}1469\text{cm}^{-1}$ $\nu(\text{OCO})_{\text{sym}}$. In addition, the $\nu(\text{NO}_2)_{\text{asym}}$ and $\nu(\text{NO}_2)_{\text{sym}}$ of the ligand molecule could be assigned unequivocally.

The shape of the $\nu(\text{NO}_2)$ band in the spectra merits a point to be mentioned. The band is strong and slightly broad which on closer inspection indicates that an additional stretching frequency is present almost superimposed on it. This additional band is most likely due to the $\nu(\text{NO}_2)$ of the coordinated $-\text{NO}_2$ group. The $-\text{NO}_2$ group is connected to form the molecule of the complex with a “Cu-carboxylate dimer” and a mononuclear species... which are not connected via bridging carboxylate ligands but via the nitro-O atoms... as has been demonstrated by the X-ray crystallography (Fig. 2.18). In all other compounds of this series $-\text{NO}_2$ group stretching frequency did not show this characteristic indicating its noninvolvement in further coordination.

2.5.3.2 Magnetic moment

The magnetic moment data are in table 2.3. The magnetic moment data indicate an octahedral geometry for Mn(II), Fe(II) and Co(II) complexes. The magnetic moment data correspond satisfactorily to the required values for unpaired electrons in the compounds for an octahedral disposition around the central metal ion

[52]. The subnormal value of μ_{eff} for Cu(II) complex indicates that the coordination is possibly octahedral around the metal atom and suggesting an antiferromagnetic spin-exchange interaction within each molecule [53]. The magnetic moment data thus indicates in the complex a dimeric Cu_2 unit is present. The magnetic moment value of 1.49 B.M. per copper appears to be low for a d^9 configuration. This suggests the presence of a strong spin-spin interaction through the bridging ligand in the dimeric unit [54-58] as also identified by the preliminary X-ray crystallography study.

Table 2.2 IR spectral data (cm^{-1}) for compounds 1-5

Compound	$\nu(\text{OCO})_{\text{asym}}$	$\nu(\text{OCO})_{\text{sym}}$	$\Delta\nu =$ $[\nu(\text{OCO})_{\text{asym}} - \nu(\text{OCO})_{\text{sym}}]$	$\nu(\text{OH})$	$\nu(\text{NO}_2)_{\text{asym}}$	$\nu(\text{NO}_2)_{\text{sym}}$
1.	1624(s)	1460(s)	164	3446(v,b)	1541(s)	1350(s)
2.	1624(m)	1458(s)	166	3421(m,b)	1541(s)	1352(s)
3.	1627(w)	1462(m)	165	3386(m,b)	1527(w)	1357(s)
4.	1629(m) ^a 1655(s)	1467(s) ^a 1400(s)	162	3356(w,b)	1536(m) ^b 1545(s)	1355(s) ^b 1340(s)
5.	1622(m)	1469(m)	153	3421(v,b)	1542(m)	1344(s)

s, strong; m, medium; w, weak; b, broad; v, very

a= weak bridging bidentate type $\nu(\text{OCO})$, b=For uncoordinated free $\nu(\text{NO}_2)$

2.5.3.3 Differential calorimetric analysis

The Differential calorimetric analysis of **2** exhibited a peak at 171.56°C . It shows that the enthalpy at 171.56°C is $\Delta H = 14.11 \text{ J/g}$. The complexes **3** and **4** on heating from $100\text{-}230^\circ\text{C}$ underwent decomposition. The compound **3** displayed a peak at 128.64°C corresponding to the melting of the compound ($\Delta H = 10.38 \text{ J/g}$). Compound **3** after melting yielded a compound which underwent further decomposition between $130\text{-}150^\circ\text{C}$. Compound **3** decomposes further beyond 150°C finally to decompose at 163.93°C ($\Delta H = 74.12 \text{ J/g}$). The compound **4** also underwent decomposition at a temperature between 148.07°C to 218.56°C . At 218.56°C the enthalpy of **4** was ($\Delta H = 50.31 \text{ J/g}$). But no information of phase change could be

obtained during the cooling of the compounds as because the compounds were decomposed by then. It is likely that the compounds decomposed by giving off CO₂. However, investigations on the decomposed products were not carried out in this investigation.

2.5.3.4 Electronic Spectra

The spectral data for 1–5 are summarized in Table 2.4. Towards the visible region, the electronic spectra showed absorptions for 3 and 4 attributable to an $n \rightarrow \pi^*$ transition within the nitro group and benzene ring chromophore owing to extensive conjugation, which is most likely the reason for the observed spectra in methanol solution.

Table 2.3 Magnetic moment data for compounds 1-4^a

Complex	Magnetic moment (B.M.)	No. of unpaired spins	Hybridization	Stereochemistry
1.	5.88	5	d ² sp ³	Octahedral
2.	4.99	4	d ² sp ³	Octahedral
3.	4.48	3	d ² sp ³	Octahedral
4.	1.49	1	sp ³ d ²	Octahedral

^a Hg[Co(SCN)₄] as standard

Table 2.4 Electronic absorption spectra of compounds 1-5 recorded in methanol

Compounds	λ_{\max} (nm)
1.	234,209
2.	229,214
3.	236,222, 515
4.	234, 214, 458
5.	232,213

2.5.3.5 X-ray Crystal Structure

This section deals with the X-ray crystallographic studies of transition metal carboxylates of 3,5-dinitrobenzoic acid Co(II) and Cu(II). Compounds **3** and **4** provided single crystals suitable for the X-ray crystal structure determination. The crystal structures of these complexes are described below.

2.5.3.5.1 Crystal Structure of Co(II) complex of 3,5-dinitrobenzoic acid (**3**)

The author was able to successfully isolate suitable single crystal of **3** for X-ray crystallography. The Co^{II} atom (site symmetry $\bar{1}$) in the title complex, [Co(C₇H₃N₂O₆)₂(CH₃OH)₄], exists within an octahedral O₆ donor set defined by two O-monodentate 3,5-dinitrobenzoate anions and four methanol O atoms. An intramolecular O_m-H ··· O_c (m = methanol and c = carbonyl) hydrogen bond leads to the formation of an S(6) ring. In the crystal, centrosymmetrically related molecules associate via further O_m-H ··· O_c hydrogen bonds, leading to linear supramolecular chains propagating along the a-axis direction. The Co(II) atom in (I), (Fig. 2.16), is located on a crystallographic centre of inversion and exists within an octahedral O₆ donor set defined by two carboxylate-O1 atoms and four methanol-O atoms. The Co-O1 bond distance [Co-O1 = 2.0666 (17) Å] is comparable to those, *i.e.* 2.0525 (20) and 2.0587 (19) Å, found in the related tetra-aqua-bis(3,5-dinitrobenzoato-O)cobalt(II) tetrahydrate structure [59-61]. A small disparity in the Co—O_{methanol} bond distances in (I) [Co-O7 = 2.1094 (16) and Co-O8 = 2.0645 (18) Å] is noted. The methanol-O7-H hydrogen forms an intramolecular O-H···O hydrogen bond with the carbonyl-O2 atom to close an almost planar {Co-O-C-O···H-O} S(6) ring, Table 2.5. The methanol-O8-H also forms a hydrogen bond to the carbonyl-O2 atom on a centrosymmetrically related complex, Table 2.5. This results in the formation of 12-membered {Co-O-H···O-C-O}₂ synthons and linear supramolecular chains along the *a* axis, (Fig. 2.17). It is noted that the packing of molecules brings into close proximity two nitro-O atoms, *i.e.* O4···O4ⁱⁱ = 2.756 (3) Å for 3-*x*, -*y*, 2-*z*. While the nature of this interaction is not obvious, there are approximately 50 precedents for such O_{nitro}···O_{nitro} contacts < 2.70 Å in the crystallographic literature [62]. Table 2.6 describes the Hydrogen-bond geometry in (Å, °) and Geometric parameters (Å, °) is presented below.

Table 2.5 Selected bond lengths (Å).

Compound	3
Co—O7	2.1094 (16)
Co—O8	2.0666 (17)
Co—O1	2.0666 (17)

Table 2.6 Hydrogen-bond geometry (Å, °) of compound 3.

<i>D</i> —H... <i>A</i>	<i>D</i> —H	H... <i>A</i>	<i>D</i> ... <i>A</i>	<i>D</i> —H... <i>A</i>
O7—H7o...O2 ⁱ	0.85 (3)	1.840 (15)	2.645 (2)	158 (3)
O8—H8o...O2 ⁱⁱ	0.85 (3)	1.817 (10)	2.662 (2)	179 (3)

Symmetry codes: (i) $-x+1, -y+1, -z+1$; (ii) $x-1, y, z$.

Geometric parameters (Å, °) of compound 3.

Co—O8	2.0645 (18)	N2—C6	1.476 (4)
Co—O8 ⁱ	2.0645 (18)	C1—C2	1.511 (3)
Co—O1	2.0666 (17)	C2—C7	1.380 (3)
Co—O1 ⁱ	2.0666 (16)	C2—C3	1.385 (3)
Co—O7	2.1094 (16)	C3—C4	1.373 (3)
Co—O7 ⁱ	2.1094 (16)	C3—H3	0.9300
O1—C1	1.250 (3)	C4—C5	1.371 (4)
O2—C1	1.247 (3)	C5—C6	1.378 (4)
O3—N1	1.179 (4)	C5—H5	0.9300
O4—N1	1.190 (3)	C6—C7	1.379 (4)
O5—N2	1.220 (4)	C7—H7	0.9300
O6—N2	1.209 (4)	C8—H8A	0.9600
O7—C8	1.418 (3)	C8—H8B	0.9600
O7—H7O	0.85 (3)	C8—H8C	0.9600
O8—C9	1.408 (3)	C9—H9A	0.9600
O8—H8O	0.85 (3)	C9—H9B	0.9600
N1—C4	1.482 (3)	C9—H9C	0.9600
O8—Co—O1	91.36 (8)	C7—C2—C3	119.3 (2)
O8 ⁱ —Co—O1	88.64 (8)	C7—C2—C1	120.5 (2)
O8—Co—O1 ⁱ	88.64 (8)	C3—C2—C1	120.2 (2)
O8 ⁱ —Co—O1 ⁱ	91.36 (8)	C4—C3—C2	119.1 (2)
O8—Co—O7	88.14 (7)	C4—C3—H3	120.5
O8 ⁱ —Co—O7	91.86 (7)	C2—C3—H3	120.5
O1—Co—O7	89.22 (7)	C5—C4—C3	123.3 (2)
O1 ⁱ —Co—O7	90.78 (7)	C5—C4—N1	119.3 (2)
O8—Co—O7 ⁱ	91.86 (7)	C3—C4—N1	117.4 (2)
O8 ⁱ —Co—O7 ⁱ	88.14 (7)	C4—C5—C6	116.3 (2)
O1—Co—O7 ⁱ	90.78 (7)	C4—C5—H5	121.9
O1 ⁱ —Co—O7 ⁱ	89.22 (7)	C6—C5—H5	121.9
O1—Co—O1 ⁱ	180.0	C5—C6—C7	122.6 (2)
O7—Co—O7 ⁱ	180.0	C5—C6—N2	119.1 (3)
O8—Co—O8 ⁱ	180.0	C7—C6—N2	118.3 (3)
C1—O1—Co	130.70 (16)	C6—C7—C2	119.4 (2)
C8—O7—Co	128.82 (16)	C6—C7—H7	120.3

C8—O7—H7O	113 (2)	C2—C7—H7	120.3
Co—O7—H7O	105 (2)	O7—C8—H8A	109.5
C9—O8—Co	131.57 (18)	O7—C8—H8B	109.5
C9—O8—H8O	110 (2)	H8A—C8—H8B	109.5
Co—O8—H8O	118 (2)	O7—C8—H8C	109.5
O3—N1—O4	122.3 (3)	H8A—C8—H8C	109.5
O3—N1—C4	118.6 (3)	H8B—C8—H8C	109.5
O4—N1—C4	119.1 (3)	O8—C9—H9A	109.5
O6—N2—O5	123.7 (3)	O8—C9—H9B	109.5
O6—N2—C6	118.5 (3)	H9A—C9—H9B	109.5
O5—N2—C6	117.8 (3)	O8—C9—H9C	109.5
O2—C1—O1	126.1 (2)	H9A—C9—H9C	109.5
O2—C1—C2	118.0 (2)	H9B—C9—H9C	109.5
O1—C1—C2	115.9 (2)		
O8—Co—O1—C1	87.5 (2)	C1—C2—C3—C4	-179.8 (2)
O8i—Co—O1—C1	-92.5 (2)	C2—C3—C4—C	5 0.0 (4)
O7—Co—O1—C1	175.6 (2)	C2—C3—C4—N1	179.5 (2)
O7i—Co—O1—C1	-4.4 (2)	O3—N1—C4—C5	173.0 (3)
O8—Co—O7—C8	125.9 (2)	O4—N1—C4—C5	-9.2 (5)
O8i—Co—O7—C8	-54.1 (2)	O3—N1—C4—C3	-6.5 (5)
O1—Co—O7—C8	34.5 (2)	O4—N1—C4—C3	171.2 (3)
O1i—Co—O7—C8	-145.5 (2)	C3—C4—C5—C6	0.2 (4)
O1—Co—O8—C9	-58.0 (3)	N1—C4—C5—C6	-179.3 (3)
O1i—Co—O8—C9	122.0 (3)	C4—C5—C6—C7	-0.5 (4)
O7—Co—O8—C9	-147.1 (3)	C4—C5—C6—N2	178.2 (3)
O7i—Co—O8—C9	32.9 (3)	O6—N2—C6—C5	177.2 (3)
Co—O1—C1—O2	-6.2 (4)	O5—N2—C6—C5	-3.4 (5)
Co—O1—C1—C2	175.42 (15)	O6—N2—C6—C7	-4.0 (5)
O2—C1—C2—C7	-178.2 (2)	O5—N2—C6—C7	175.4 (3)
O1—C1—C2—C7	0.3 (4)	C5—C6—C7—C2	0.6 (4)
O2—C1—C2—C3	1.6 (4)	N2—C6—C7—C2	-178.1 (3)
O1—C1—C2—C3	-179.9 (2)	C3—C2—C7—C6	-0.3 (4)
C7—C2—C3—C4	0.0 (4)	C1—C2—C7—C6	179.5 (2)

Symmetry codes: (i) $-x+1, -y+1, -z+1$.

Supplementary data and figures for this paper are available from the IUCr electronic archives (Reference: HB5347).

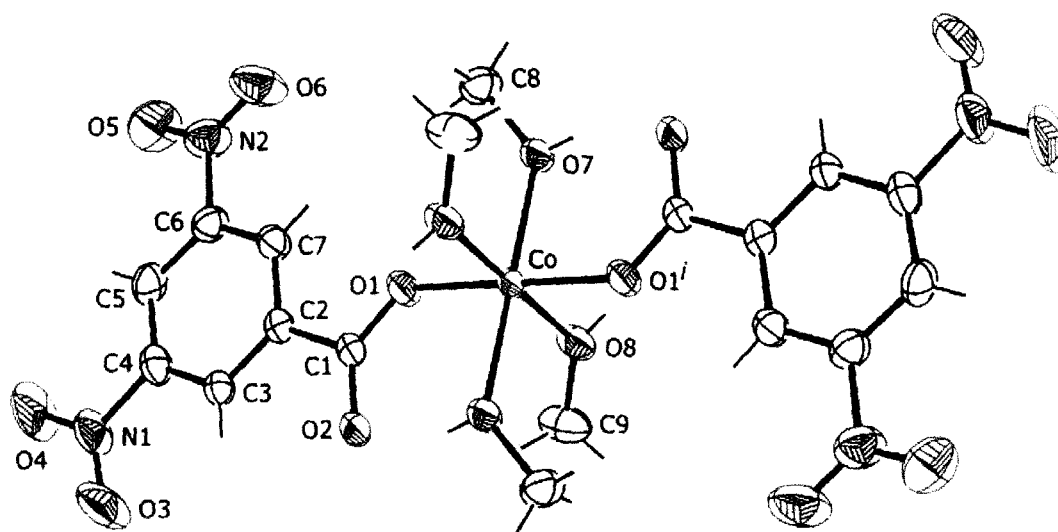


Fig. 2.16 The molecular structure of (**3**) extended to show the coordination geometry for the Co(II) atom, showing displacement ellipsoids at the 50% probability level. Symmetry operation: $i: 1-x, 1-y, 1-z$.

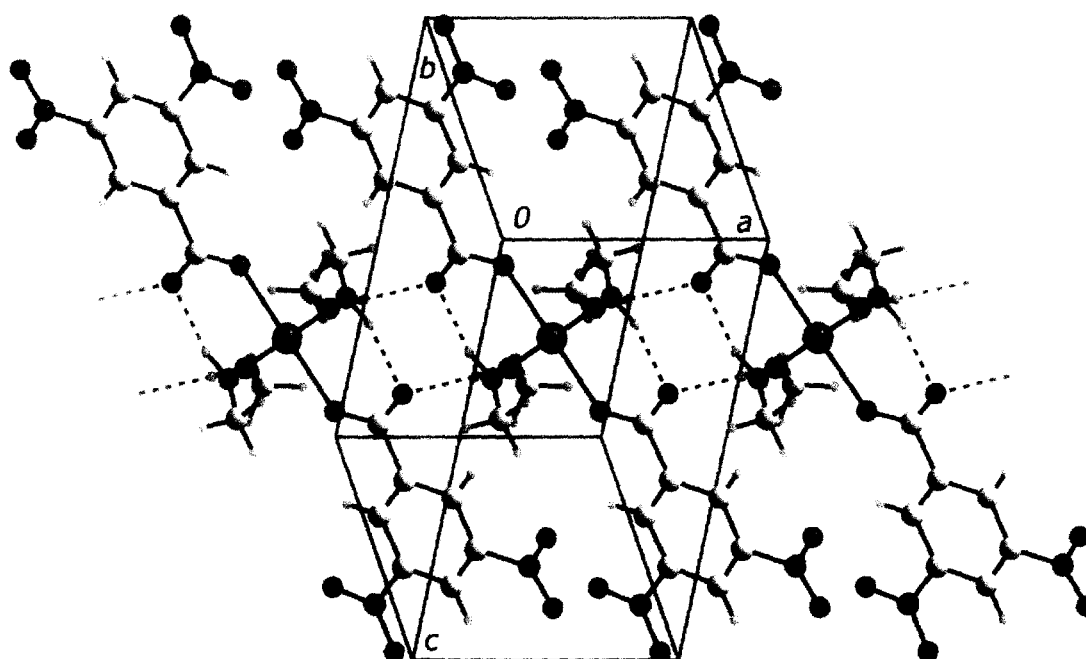


Fig. 2.17 Linear supramolecular chain along the a axis in (**3**) mediated by O—H...O hydrogen bonding. These and the intramolecular O—H...O hydrogen bonds are shown as blue dashed lines.

2.5.3.5.1 Crystal Structure of Cu(II) complex of 3,5-dinitrobenzoic acid (**4**)

The author was able to successfully isolate suitable single crystals of **4** for X-ray crystallography. The preliminary analysis of the X-ray crystallography studies of **4** reveals that the complex contains the asymmetric unit comprises two Cu centers, three carboxylates, a coordinated methanol molecule and half a solvent methanol molecule. These connect to form a “Cu carboxylate dimer” and a mononuclear species which are connected via bridging carboxylate ligands but via the nitro-O atoms (Fig. 2.18) and overall, a 2-D array is formed (Fig. 2.19). The details of the bond angles and bond distances are not available at the moment.

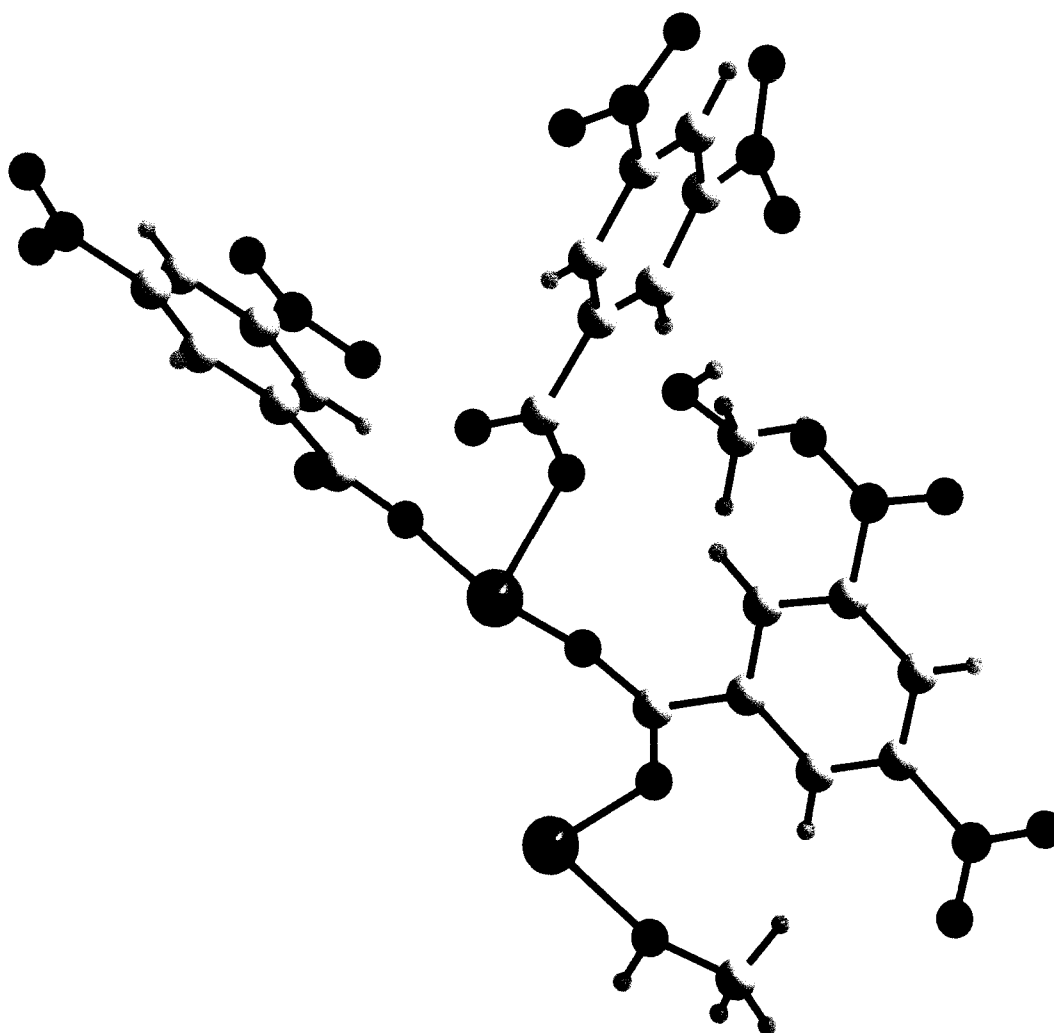


Fig. 2.18 X-ray crystallography structure of the asymmetric unit of compound **4**.

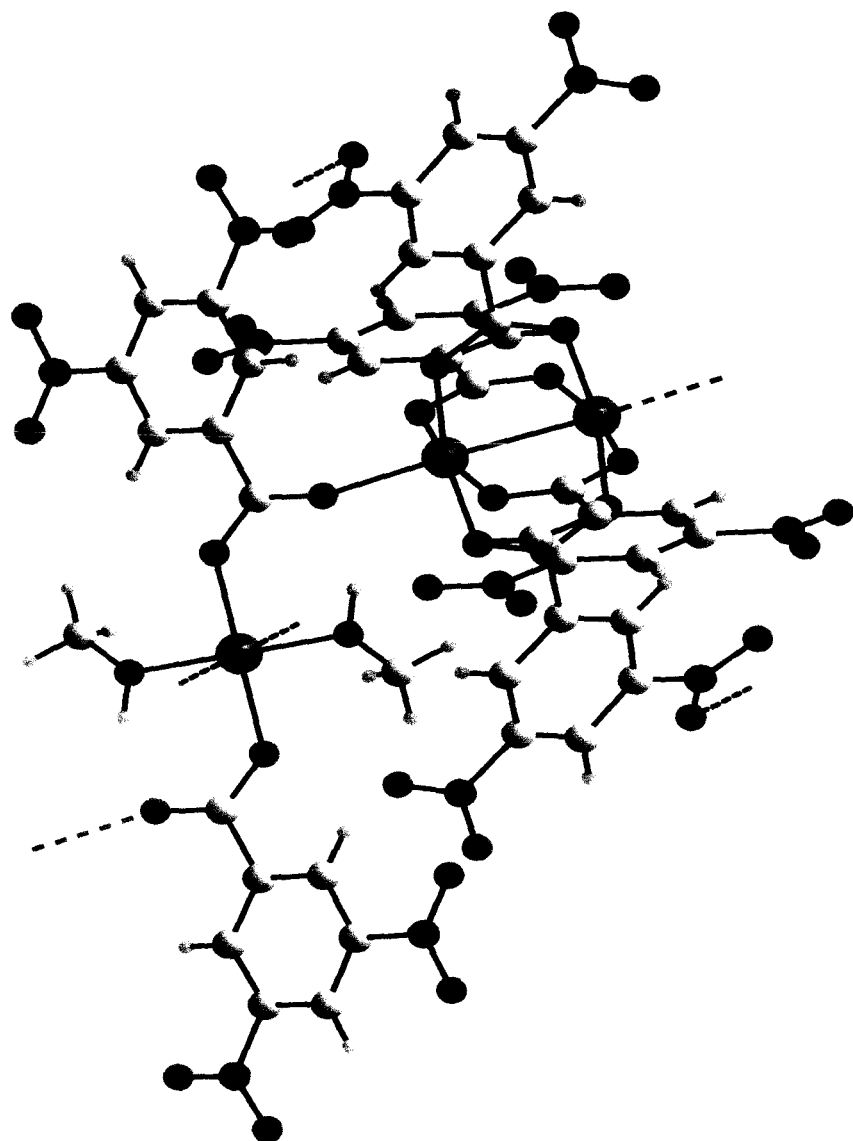


Fig. 2.19 A 2-D array of compound 4.

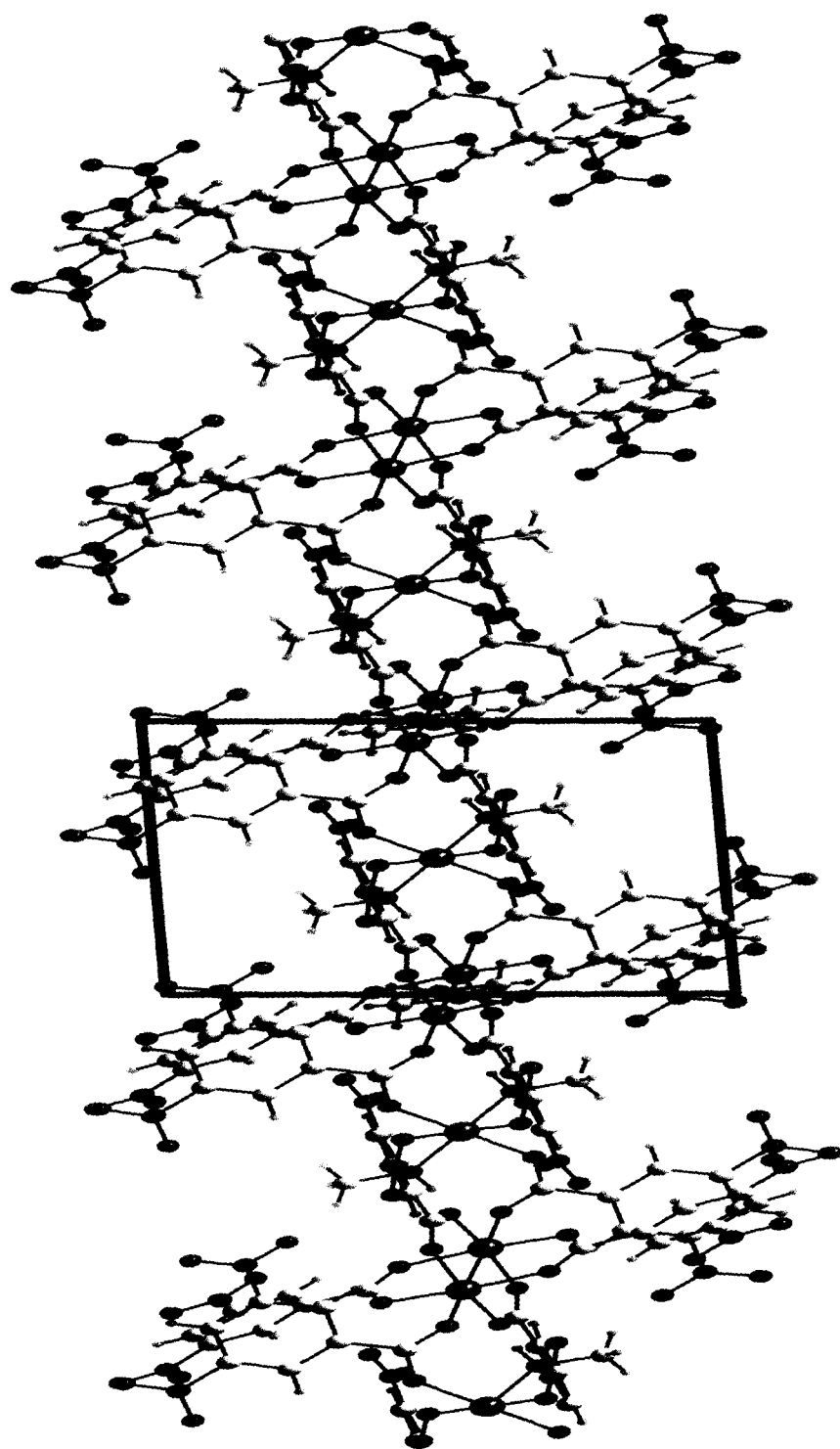


Fig. 2.20 Crystal packing structure of compound 4.

2.5.4 Biological properties of transition metal carboxylates of 3,5-dinitrobenzoic acid.

2.5.4.1 Anti-fungal activities

The antifungal properties of the transition metal carboxylates **2-4** are summarized in table 2.5. The fungitoxic effect of the transition metal carboxylates were screened at three concentrations 25, 50 and 100 ppm, on spore germination of two different pathogens of mango (*L. theobromae*) and tea (*C. eragrostidis*). The results showed that **4** was most active followed by **3** against the tested fungal strains. Copper fungicides in potentiality are comparable to organotin compounds, such as triphenyltin acetate and triphenyltin hydroxide [63]. The compound **4** markedly inhibit the spore germination of each of the above fungi at concentrations above 50 ppm. At 100 ppm, almost complete inhibition of spore germination ensued, irrespective of the pathogen, which indicates high fungitoxicity against different groups of pathogen.

Table 2.5. Spore germination (%) of *L. theobromae* and *C. eragrostidis* in the presence of compounds **2-4**.

Chemicals	Spore germination % of <i>L. theobromae.</i>			Spore germination % of <i>C. eragrostidis.</i>		
	Conc (ppm)			Conc (ppm)		
	25	50	100	25	50	100
2.	84.0	78.5	68.3	86.6	79.2	67.1
3.	81.2	49.3	23.4	79.3	48.3	21.4
4.	14.1	5.1	2.2	12.2	5.7	2.5
Control (water)	87			92		

2.5.4.2 Phytotoxic properties

The phytotoxic effects of transition metal carboxylates were studied on economically important crop *Oryzae sativa* (Khitish). The phytotoxic effects of compounds 2–4 as a function of the concentration are summarized in Table 2.6. The results indicate that none of the transition metal carboxylates displays any inhibitory effect on seed germination.

Table 2.6 Phytotoxicity of compounds 2–4, after seed treatment of Indian rice (*Oryzae sativa*), cultivar Khitish.

Compound	Percentage (%) of seed germination after 4h treatment			Percentage (%) of seed germination after 8h treatment			Percentage (%) of seed germination after 12h treatment		
	Conc. (ppm)			Conc. (ppm)			Conc. (ppm)		
	25	50	100	25	50	100	25	50	100
2.	94	95	96	95	94	93	95	93	95
3.	95	96	94	93	94	94	94	93	94
4.	95	92	92	92	93	92	91	92	92
Control ^a	95			94			95		

^a The control seeds were incubated in methanol/water (1:5) for the indicated period.

2.6 References

1. Hambidge M. *J. Nutr.* 2003; **133**: 948S.
2. Lieu PT, Heiskala M, Peterson PA, Yang Y. *Mol. Aspects. Med.* 2001; **22**: 1.
3. Murakami M, Hirano T. *Cancer. Sci.* 2008; **99**: 15.
4. Cole CR, Lifshitz F. *Pediatr. Endocrinol. Rev.* 2008; **5**: 889.
5. Schümann K, Classen HG, Dieter HH, König J, Multhaup G, Rückgauer M, Summer KH, Bernhardt J, Biesalski HK. *Eur. J. Clin. Nutr.* 2002; **56**: 469.
6. Szentmihalyi K, Vinkler P, Fodor J, Balla J, Lakatos B. *Orv. Hetil.* 2006; **147**: 2027.
7. Barceloux DG. *J. Toxicol. Clin. Toxicol.* 1999; **37**: 201.
8. Pandit T. *Ph.D. Thesis*, University of North Bengal, West Bengal, India, 1989.
9. Jorgenson CK. *Inorg. Chim. Acta Rev.* 1968; **2**: 65.
10. Coucouvanis D. *Progr. Inorg. Chem.* 1970; **11**: 233.
11. Bloodworth BC, Demetrio B, Grezeskoviak R. *Inorg. Chim. Acta.* 1981; **53**: L85.
12. Natarajan C, Tharindiraj P. *Ind. J. Chem.* 1990; **29A**: 666.
13. Singh H, Srivastava VK, Shukla SN, Upadhyaya MK. *Ind. J. Chem.* 1992; **31A**: 472.
14. Nair MS, Joseyphus RS. *Ind. Chem. Soc.* 2007; **84**: 323.
15. Rosu T, Gulea A, Nicolae A, Georgescu R. *Molecules* 2007; **84**: 782.
16. Cotton FA, Wilkinson G, *Advanced Inorganic Chemistry*, 2nd Ed. Wiley-Inter Science Publishers, New York. 1970.
17. Carlin RL. *Transition Metal Chemistry*, New York and London, 1969, Vol. **5**, pp. 105.
18. Fountain CS, Hatfield WE, *Inorg. Chem.* 1965; **4**: 1366.
19. Kumar N, Suri AK. *Proc. Indian natn. Sci. Acad.* 1980; **46A**: 565.
20. Kumar N, Kalsotra BL, Suri AK. *J. Chinese Chem. Soc.* 1975; **23**: 359.
21. Bickley J, Bonar-Law RP, Borrero Martinez MA, Steiner A. *Inorg. Chim. Acta*, 2004; **357**: 891.
22. Holz RC, Bradshaw JM, Bennett B. *Inorg. Chem.* 1998; **37**: 1219.
23. Akopova OB, Shabyshev LS, Bobrov VL. *Russian Chemical Bulletin*, 1995; **44**: 1210.

24. Kozlevčar B, Lah N, Makuc S, Šegedin P, Pohleven F. *Acta Chim. Slov.* 2000; **47**: 421.
25. Waizump k, Takuno M, Fukushima N, Masuda H. *J. Coord. Chem.* 1998; **44**: 269.
26. Bin Z, Jianli L, Wei C, Yunxia W, Zhen S. *Chinese J. Chem.* 2010; **28**: 111.
27. Vučković G, Stanić V, Sovilj Sp, Antonijević-Nikolić M, Mroziński J. *J. Serb. Chem. Soc.* 2005; **70**: 1121.
28. Zevaco TA, Görls H, Dinjus E. *Inorg. Chem Com.* 1998; **1**: 170.
29. Zevaco TA, Görls H, Dinjus E. *Inorg. Chim. Acta.* 1998; **269**: 283.
30. Hamed E, Attia MS, Bassiouny K. *Bioinorg. Chem. Appl.* 2009; **2009**:1.
31. Trukhan VM, Pierpont CG, Jensen KB, Nordlander E, Shteinman AA. *Chem. Commun.* 1999; 1193.
32. Ghattas W, Serhan Z, Bakkali-Taheri NE, Réglie M, Kodera M, Hitomi Y, Simaan AJ. *Inorg. Chem.* 2009; **48**: 3910.
33. Grant CM, Knapp MJ, Huffman JC, Hendrickson DN, Christou G. *Chem. Commun.* 1998; 1753.
34. Moon D, Kim J, Oh M, Suh BJ, Lah MS. *Polyhedron.* 2008; **27**: 447.
35. Maryudi, Yunus RM, Nour AH, Abidin MH. *J. Appl. Sci.* 2009; **9**: 3156.
36. Rardin RL, Poganiuch P, Bino A, Goldberg DP, Tolman WB, Liu S, Lippard JS. *J. Am. Chem. Soc.* 1992; **114**: 5240.
37. Randhawa B, Gandotra K, *Thermal Analysis and Calorimetry.* 2006; **85**: 417.
38. Masoud MS, Abou El Enien SA, Kamel HM. *Ind. J. Chem.* 2002; **41A**: 297.
39. Golobič A, Ožbolt L, Pohleven F, Leban I, Šegedin P. *Acta Chim. Slov.* 2006; **53**: 238.
40. Kozlevčar B, Lah N, Leban I, Turel I, Šegedin P, Petrič M, Pohleven F, White AJP, Williams DJ, Giester G. *Croatica Chim. Acta.* 1999; **72** (2–3): 427.
41. Shahzadi S, Ali S, Jabeen S, Kanwal N, Rafique U, Khan AN. *Russian J. Coord. Chem.* 2008; **34**: 38.
42. Chandra S, Sharma AK. *Research Letters in Inorganic Chemistry.* Volume 2009(2009), Article ID 945670, DOI:10.1155/2009/945670.
43. Petrič M, Pohleven F, Turel I, Egedin PŠ, White AJP, Williams DJ. *Polyhedron.* 1998; **17**: 255.
44. Sheldric GM. *Acta Cryst.* 2008; **A64**: 112.

45. Sheldrick GM. *SADABS*. University of Göttingen. Germany, 1996.
46. Farrugia LJ. *J. Appl. Cryst.* 1997; **30**: 565.
47. Brandenburg K. *DIAMOND*. Crystal Impact GbR, Bonn, Germany, 2006.
48. Rouxel T, Sarniget A, Kollmann A, Bousquet JF. *Physiol. Mol. Plant Pathol.* 1989; **34**: 507.
49. Kamruddin Sk. Ph.D Thesis, University of North Bengal, West Bengal, India, 1996.
50. Chantrapromma S, Usman A, Fun HK, Poh BL, Karalai C. *J. Mol. Str.* 2004; **688**: 59.
51. Sandhu GK, Boparoy NS. *J. Organomet. Chem.* 1992; **423**: 183.
52. Dutta RL, Saymal A. *Elements of Magnetochemistry*. S. Chand and Company Ltd., 1982.
53. Hasanvand F, Nosrollahi N, Vajed A, Amani S. *Malays. J. Chem.* 2010; **12(1)**: 27.
54. Selwood PW. "Magnetochemistry" 2nd Ed., *Interscience*, New York 1956.
55. Kato M, Jomassen HB, Fanning JC. *Chem. Rev.* 1964; **64(2)**: 99.
56. Patel RN, Pandey HC, Pandeya KB. *Transition Met. Chem.* 1999; **24**: 35.
57. Asefa W, Raju VJT, Chebude Y, Retta N. *Bull. Chem. Soc. Ethiop.* 2009; **23(2)**: 187.
58. Venkatswara Rao B. *J. Therm. Anal. Calorim.* 2010; **100**: 577.
59. Tahir MN, Ülkü D, Mövsümov EM. *Acta Cryst.* 1996; **C52**: 1392.
60. Yang G, Zhu H-G, Zhang L-Z, Cai Z-G, Chen X-M. *J. Chem.* 2000; **53**: 601.
61. Jin Y, Che YX, Zheng JM. *Inorg. Chim. Acta.* 2008; **361**: 2799.
62. Allen FH. *Acta Cryst.* 2002; **B58**: 380.
63. Sugavanam B. *Tin and its Uses*. 1980; **126**: 4.

CHAPTER 3

SYNTHESES AND CHARACTERIZATION OF ORGANOTIN (IV) COMPLEXES OF 2-MARCAPTO ISOTHIOCYANATE

3.1 Introduction

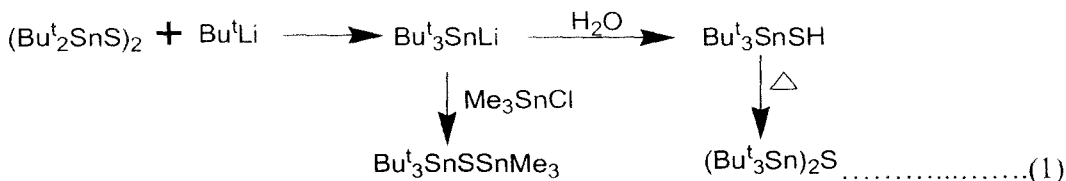
In about 3500 BC, tin has been discovered as a hard alloy with copper. The abundance of tin in the Earth's surface is less than that of Zn, Cu, Pb etc. During 2005-06, the total annual production of refined tin was about 350000 tones globally [1]. It is in group 14 element and its principal valence state is Sn(IV), though Sn(II) inorganic compounds are common and many stannous organic compounds, in recent years. Metallic tin has two allotropes namely white tin or β -tin and grey tin or α -tin. Below 10°C, white tin slowly converts into grey tin, with a 26% increase in volume [2]. Both the Sn (II) and Sn(IV) states are stable. The Sn(II) state uses mainly the 5p orbitals for bonding otherwise Sn(IV) state occurs oxidation readily, where the tin is sp^3 hybridized. In 1849, the first organotin compound, diethyltin dichloride, was prepared by Frankland by heating ethyl chloride, with metallic tin. This is taken to mark the beginning of organometallic chemistry. In 1943, the first application of organotin compounds came for the stabilization of PVC against heat during processing and a variety of industrial and biological applications were slowly developed. The thio-organotin was introduced in the early 1950s as a considerable improvement in clarity and heat stability. Tin mercaptides gained acceptance for the stabilization of rigid PVC than structurally equivalent tin carboxylates. A possible explanation lies in the ability of sulphur to internally satisfy the secondary bonding capabilities of tin to a greater extent than oxygen [3]. Thio-organotin compound means at least one Sn-S bond is present in complexes. Recently, organotin(IV) complexes of sulphur-containing ligands have received considerable attention for their antibacterial and antifungal activities to study their biological significance [4,5]. So the current interest in metal-sulfur chromophores in biological molecules requires a detailed study which have not been adequately investigated in the past.

3.2 Literature

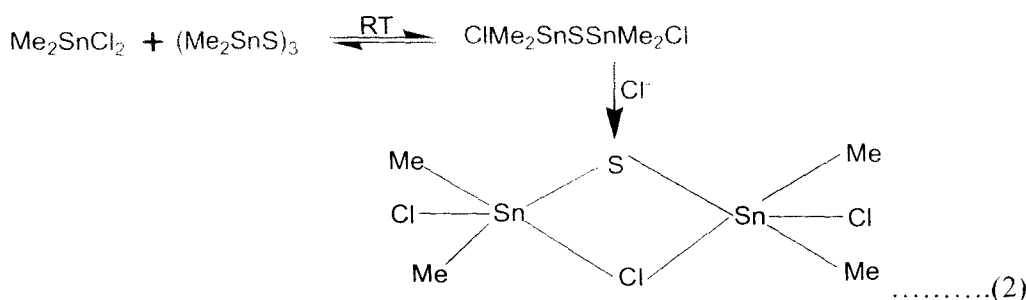
There are many parallels between the chemistry of compounds containing Sn-S bonds and compounds of structures R_3SnSR' , $R_2Sn(SR')_2$, $RSn(SR')_3$, $(R_3Sn)_2S$ and $(R_2SnS)_n$ can be prepared by substitution of tin by a sulphur nucleophile. The Sn-O bonded compounds often self-associate to give oligomers or polymers with five coordinate tin, where as the sulphur compounds show less tendency to associate. For

example the compounds like $(R_2SnX)_n$ when $X=O$ are usually cross-linked insoluble polymers whereas when $X=S$, there are usually unassociated, soluble compounds. The Sn-S bonds are also less easily cleaved in substitution like hydrolysis and addition reactions. The Sn-S bond is often formed in an elimination process [6].

The tin thiols like R_3SnSH are usually unstable. But Hännsgen and his co-workers [7] showed that tri-*t*-butyltin hydrosulphide which has been prepared by the reaction shown in the (Eq.1)



So many organotin-thiolate compounds have found industrial application and therefore, are published in patent work. Organotin sulphide compounds are shown little tendency towards self-association. Thus $(Ph_3Sn)_2S$ is a monomer in the crystal, with slightly distorted tetrahedral tin and $SnSSn$ 107.4° [8]. Similarly $[(PhCH_2)_3Sn]_2S$ is bent [$SnSSn$ $105.52(14)^\circ$] [9], but $(Bu^t_3Sn)_2S$, for steric reason is linear [10]. Most dialkyltin sulphides are cyclic trimer, with the structure of a twisted boat [11, 12]. But Puff *et al.* [13] showed di-*t*-butyltin sulphide is a dimer with planer ring. The compounds $(Ph_2SnX)_3$ when $X=S$, all have twist boat structure [14]. Another compound $ClR_2SnSSnR_2Cl$ is monomeric in solution, with tetra-coordinated tin. They are in equilibrium with $(R_2SnS)_3$ and R_2SnX_2 . With Cl ion, they form the penta-coordinate dinuclear complex as in (Eq.2) [15,16].



The tin-sulphur bonds are usually stable towards air and water but react with acids like HCl to liberate H_2S and give corresponding tin halides. Bis(trimethyltin) sulphide can be reduced with sodium [17]. The Sn-S and M-X where M= tin or some other metal and X= S or some other electronegative ligand, the exchange readily occurs. With the Sn-S bond in dialkyltin sulphides and the Sn-X bond in the organotin

the compound is proposed on the basis of results from mass spectrometry, infrared spectroscopy, thermal analysis and vapour pressure osmometry. Xanthopoulou *et al.* [22] reported five new organotin (IV) molecules with the heterocyclic thioamides; 2-mercaptobenzothiazole (Hmbzt), 5-chloro-2-mercaptobenzothiazole (Hcmbzt), 3-methyl-2-mercaptobenzothiazole (mmbzt) and 2-mercaptonicotinic acid (H₂mna) of formulae $[(n\text{-C}_4\text{H}_9)_2\text{Sn}(\text{mbzt})_2]$ (1), $[(\text{C}_6\text{H}_5)_2\text{Sn}(\text{mbzt})_2]$ (2), $\{(\text{CH}_3)_2\text{Sn}(\text{cmbzt})_2\cdot 1.7(\text{H}_2\text{O})\}$ (3), $[(n\text{-C}_4\text{H}_9)_2\text{SnCl}_2(\text{mmbzt})_2\cdot (\text{CH}_2\text{Cl}_2)]$ (4) and $\{[(\text{C}_6\text{H}_5)_3\text{Sn}]_2(\text{mna})\cdot [(\text{CH}_3)_2\text{CO}]\}$ (5) (Fig. 3.1) who synthesized and characterized the compounds by elemental analysis, ¹H-, ¹³C-NMR, FT-IR and Mössbauer spectroscopic techniques. Crystal structures of molecules 1, 3 and 5 have been determined by X-ray diffraction at 173K (1 and 5) and 293K (3). 1, 3 and 5 are monoclinic. In both molecules 1 and 3, two carbon atoms from aryl groups, two sulfur and two nitrogen atoms from thione ligands form a distorted octahedral geometry around tin(IV) with *trans*-C₂, *cis*-N₂, *cis*-S₂ configurations. The compound 5 contains two triphenyltin moieties linked by a doubly de-protonated 2,mercaptonicotinic acid (H₂mna). It is an example of a pentacoordinated Ph₃SnXY system with an axial-equatorial arrangement of the phenyl groups at Sn(1). Compounds 1, 3 and 5 were tested for in vitro cytotoxicity against the cancer cell line.

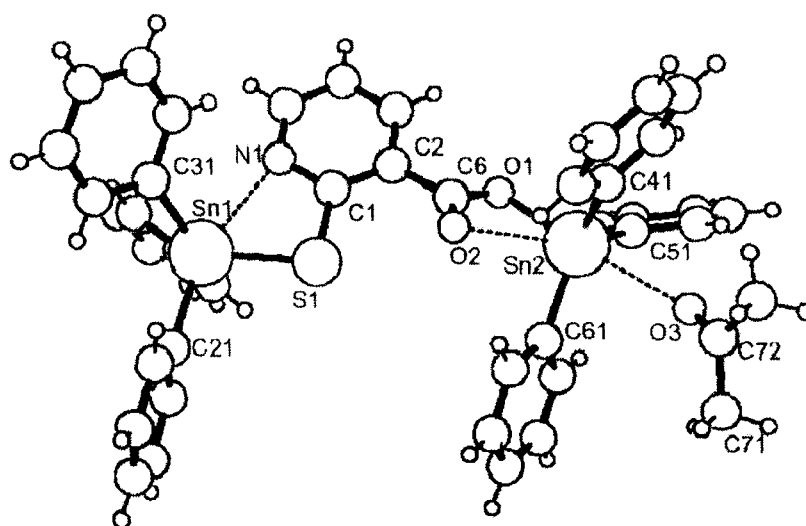


Fig. 3.1 Structure of the compound (5) $\{[(\text{C}_6\text{H}_5)_3\text{Sn}]_2(\text{mna})\cdot [(\text{CH}_3)_2\text{CO}]\}$ [22].

In 2007, Rehaman *et al.* [23] characterized and reported dimethyl bis(4-methylpiperidine dithiocarbamato-S,S')-tin(IV) (Fig. 3.2) by elemental analysis, IR and mass spectrometry, multinuclear NMR (¹H- and ¹³C-NMR), and X-ray single

crystal analysis. IR data showed that the ligand acts as a bidentate in the solid state. X-ray data showed the unsymmetrical nature of the ligand towards coordination to tin. It crystallized in the monoclinic $P2_1/n$ space group. Its geometry is distorted octahedral. Antimicrobial activity data shows that the complex exhibits significantly more activity than the free ligand.

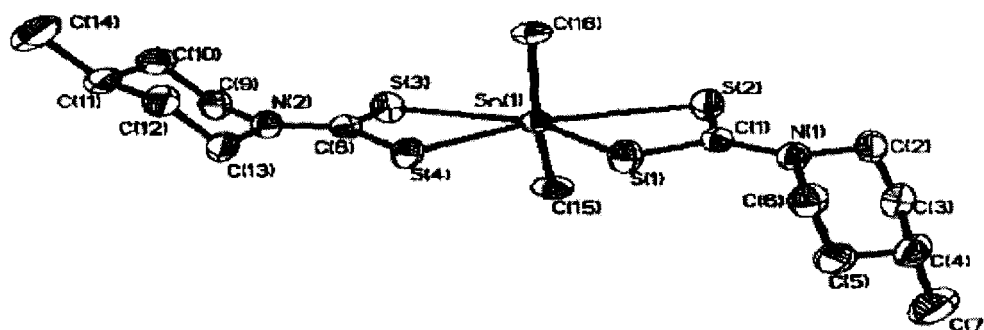
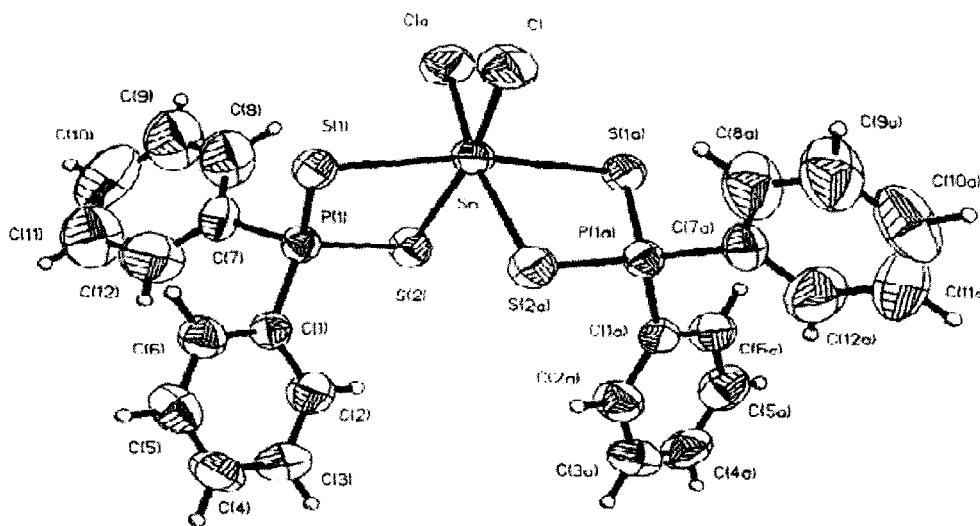


Fig. 3.2 The structure of dimethyl bis(4-methylpiperidine dithiocarbamate-S,S')-tin(IV) [23].

Lewis acid interactions of tin are of interest because it is often through intermolecular hypervalent mechanisms that organotin compounds interact with biological materials, resulting in their characteristic biocidal capabilities. They [24] investigate the nature of the Sn---S intramolecular interactions in previously known and new organotin sulfides that may prove to be useful in modifying biocidal activity due to competition with intermolecular Sn---S biological interactions. G. Engel and G. Z. Mattern [25] described the crystal structure of bis(trimethyltin)-1,3,4-thiadiazole-2,5-dithiolate) is monoclinic, space group $P21/c$, $a = 10.492(5)$, $b = 12.257(6)$, $c = 12.691(6)$ Å, $\beta = 95.86(1)^\circ$. The zigzag chain structure of the coordination polymer can be derived by the structure correlation method. The starting point is a monomolecular symmetric bis(trimethyltin)-1,3,4-thiadiazole-2,5-dithiolate (Me_3SnS)₂ ($\text{C}_2\text{N}_2\text{S}$): The first of the Me_3SnS moieties, bound to the atom C5 of the heterocyclus, remains tetrahedral, whereas the other, bound to C2, is transformed through the N3 atom of the neighbouring ring to a trigonal bipyramid $\text{S}\cdots(\text{Me}_3\text{Sn})\cdots\text{N}$. In 2003, the new organotin compound, $\text{Ph}_2\text{Sn}(\text{Cl})[\text{S}(\text{C}_7\text{H}_3\text{N}_2\text{O}_2\text{S})]\cdot[(\text{C}_7\text{H}_3\text{N}_2\text{O}_2\text{S})\text{OEt}]$, has been synthesized by the reaction of diphenyltin dichloride with 2-mercapto-6-nitrobenzothiazole. The compound was characterized by elemental, IR, ^1H NMR, and X-ray crystallography analyses. Interestingly, single-

crystal X-ray diffraction data reveals that the compound has two different molecular components and the component $\text{Ph}_2\text{Sn}(\text{Cl})[\text{S}(\text{C}_7\text{H}_3\text{N}_2\text{O}_2\text{S})]$ has a pentacoordinate tin [26].

In 1993, Haiduc *et al.* [27] are reported that a new inorganic heterocycle is obtained by reacting potassium tetraphenyldithioimidodiphosphinate with trimethyltin and dimethyltin chlorides, in benzene. X-ray diffraction analysis reveals a spirocyclic structure with the dimethyltin moiety as the coordination centre with non-planar six-membered $\text{SnS}_2\text{P}_2\text{N}$ rings. The coordination at tin is nearly perfectly octahedral, with equal Sn---S [273.3(2) and 273.7(2) pm] and P---S bonds [200.9(3) and 201.9(3) pm]. Cristian Silvestru and his coworkers [28] reported that Bis(diethyldithiophosphinato)diorganotin(IV), $\text{R}_2\text{Sn}(\text{S}_2\text{PET}_2)_2$ (R = Me, n-Bu, CH_2Ph , Ph) and diethyldithiophosphinatotriorganotin(IV), $\text{R}_3\text{SnS}_2\text{PET}_2$ (R = Me, cyclo- C_6H_{11} , CH_2Ph , Ph) were synthesized in nearly quantitative yield by reaction of organotin chlorides with sodium diethyldithiophosphinate. The compounds were characterized by infrared and ^1H NMR spectra and, in part, by mass and $^{119\text{m}}\text{Sn}$ Mössbauer spectroscopy. The probable structure of the new compounds was inferred from the spectral data. The crystal and molecular structure of $\text{Me}_2\text{Sn}(\text{S}_2\text{PET}_2)_2$ has been determined by X-ray diffraction. The compound is monoclinic structure and the molecule exhibits a distorted tetrahedral environment around tin. In 1996 Ramirez *et al.* [29] also reported the crystal and molecular structure of *cis*-dichlorobis(diphenyldithiophosphinato)tin(IV) (Fig. 3.3). The compound was isolated as $\text{Cl}_2\text{Sn}(\text{S}_2\text{PPh}_2)_2 \cdot 0.5(\text{CH}_3)_2\text{CO}$ and its crystal structure was determined by X-ray diffractometry. The dithiophosphinato groups are isobidentate coordinated through both sulfur atoms. The chlorine atoms are in *cis* positions in a distorted octahedral tin complex.



ORTEP-like view of the $C_{12}Sn(S_2PPh_2)_2$ molecule.

Fig. 3.3 Molecular structure of cis-dichlorobis(diphenyldithiophosphinato)tin(IV) [29].

In 1997, Silvestru *et al.* [30] reported the crystal structure of (diphenylmonothio phosphinato)triphenyltin(IV) (Fig. 3.4) by X-ray diffractometry. The diphenylmonothio phosphinato ligand is bimetallic biconnective leading to a polymeric $[SnSPO]_n$ chain. The coordination geometry about tin is trigonal bipyramidal with chalcogen atoms in apical positions and carbon atoms of the phenyl groups attached to the metal in equatorial positions. The bridging pattern of the ambident monothio ligand is discussed in terms of partial bond orders.

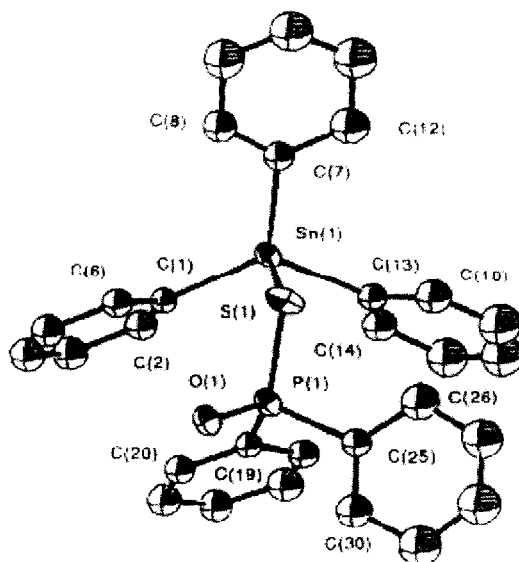


Fig. 3.4 The molecular structure of $Ph_3SnOSPPH_2$ [30].

Alkyl- and aryl-tin(IV) diphenyldithioarsinates, $R_n\text{Sn}[\text{S}_2\text{As}(\text{C}_6\text{H}_5)_2]_{4-n}$, where $n = 2$, $R = \text{CH}_3, \text{C}_4\text{H}_9, \text{C}_6\text{H}_5$; $n = 3$, $R = \text{CH}_3, \text{C}_6\text{H}_{11}, \text{C}_6\text{H}_5$ were prepared in good yields by the reaction of the appropriate organotin halides and the sodium salt of diphenyldithioarsinic acid. The IR spectra of the dialkyl- and trialkyl-tin species, are consistent with four coordination, while the phenyltin derivatives seem to be six coordinate. The molecular structure of $(\text{CH}_3)_2\text{Sn}[\text{S}_2\text{As}(\text{CH}_3)_2]_2$ was determined by X-ray diffraction. The dimethyldithioarsinate ligand is monodentate, with single ($\text{As}\cdots\text{S}$ 2.171 Å) and double ($\text{As}=\text{S}$ 2.089 Å) arsenic-sulphur bonds. In it the tin atom is four coordinate and nearly tetrahedral [31].

In 1995, the compound spiro-bis(trithiastannocane), $\text{Sn}(\text{SCH}_2\text{CH}_2\text{SCH}_2\text{CH}_2\text{S})_2$ (Fig. 3.5) was prepared from $\text{S}(\text{CH}_2\text{CH}_2\text{SNa})_2$ and SnCl_4 as well as the compound was investigated by X-ray diffraction. In the compound π - π annular secondary $\text{Sn}\cdots\text{S}$ interactions in the eight-membered rings produce a distortion of the SnS_4 tetrahedron. This consists of an enlargement of $\text{S}\cdots\text{Sn}\cdots\text{S}$ angle to 126.1° with simultaneous decrease of the opposite tetrahedral angle to 93.2° . The coordination geometry can be described as based upon a bicapped tetrahedron [32].

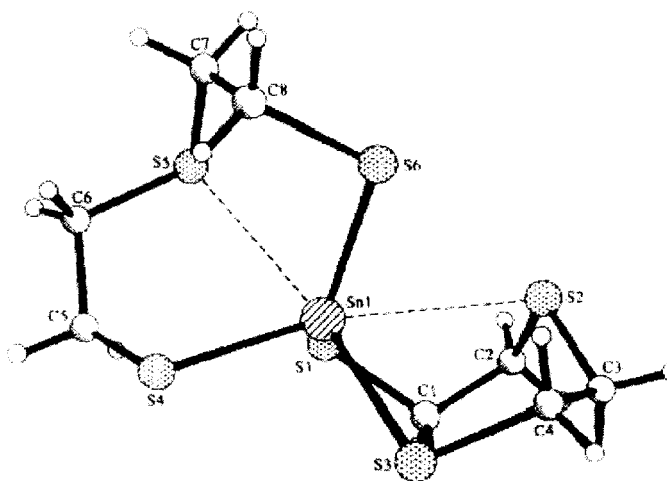


Fig. 3.5 The structure of cyclic tin-sulphur compound, $\text{Sn}(\text{SCH}_2\text{CH}_2\text{SCH}_2\text{CH}_2\text{S})_2$ [32]

In 2000, P.O. Dunstan [33] reported the compounds $[\text{SnCl}_4(\text{L})_2]$ (where L is thiourea (tu), tetramethylthiourea (tmtu) or 1-allyl-2-thiourea (atu) which were synthesized and characterized by melting points, elemental analysis, thermal studies and IR spectroscopy. The enthalpies of dissolution of the adducts, tin(IV) chloride and ligands in methanol were measured and by using thermochemical cycles. The mean

standard enthalpies of the tin-sulphur (\bar{D} (Sn-S)) bonds have been estimated. He also reported the compounds $\text{SnBr}_4 \cdot n\text{L}$ (where L is thiourea (tu), tetramethylthiourea (tmu) or 1-allyl-2-thiourea (atu) and $n=2, 3$ or 4) which were synthesized and characterized by melting points, elemental analysis, thermal analysis and IR spectroscopy. He then estimated the enthalpies of dissolution and mean standard enthalpies of the tin-sulphur (\bar{D} (Sn-S)) bonds [34].

F. E. Smith and K. I. Ee [35] investigated and described the complexes of pyridine-2-carbothioamide with diethyltin dichloride, dibenzyltin dichloride and phenyltin trichloride. In each case, the chelating agent is bound to the tin(IV) atom by the pyridine nitrogen and the carbothioamide sulphur, giving support to proposals that certain organotin compounds cause enzyme deactivation via the formation of tin-sulphur bonds. This was first reported by Lozano-Lewis *et al.* [36] in 2007 that the bis(thioether)silanes $\text{Me}_2\text{Si}(\text{CH}_2\text{SR})_2$ (abbreviated Bts^{R} , where $\text{R} = \text{Me}$ or Pr^{j}), the first two members of a new family of bidentate thioether ligands, have been readily prepared and fully characterized. The tin(IV) tetrahalide derivatives $(\text{Bts}^{\text{R}})\text{SnX}_4$ ($\text{X} = \text{Cl}, \text{Br}$), which comprise the first four metal coordination complexes of these new sulfur-donor ligands, have also been isolated, and the X-ray structure of the tetrabromide derivative $(\text{Bts}^{\text{Me}})\text{SnBr}_4$ confirms the chelating nature of the dithioether. Teoh *et al.* [37] reported the reaction of triphenyltin(IV) chloride with monothiobenzoic acid results in the formation of triphenyl (monothiobenzoato) tin (IV), $\text{C}_{25}\text{H}_{20}\text{OSSn}$, which crystallizes in the orthorhombic system. The ligand functions as a monodentate anion coordinating to the tin atom through its sulphur atom and conferring a tetrahedral geometry about the tin atom. The average bond length between tin and sulphur is 2.430(5)Å. R. Singh and N.K. Kaushik [38] in 2006, have reported organotin(IV) complexes of tribenzyltin(IV) chloride and di(*para*-chlorobenzyl)tin(IV) dichloride with thiohydrazides. The synthesized ligands were bidentate coordinating through sulphur and terminal nitrogen atoms. These form 1:1 metal–ligand complexes. The following organotin(IV) complexes have been synthesized: $(\text{C}_6\text{H}_5\text{CH}_2)_3\text{Sn}(\text{L}^1)\text{Cl}$, $(p\text{-ClC}_6\text{H}_4\text{CH}_2)_2\text{Sn}(\text{L}^1)\text{Cl}_2$, $(\text{C}_6\text{H}_5\text{CH}_2)_3\text{Sn}(\text{L}^1)\text{Cl}$, $(p\text{-ClC}_6\text{H}_4\text{CH}_2)_2\text{Sn}(\text{L}^2)\text{Cl}_2$, $(\text{C}_6\text{H}_5\text{CH}_2)_3\text{Sn}(\text{L}^3)\text{Cl}$, $(p\text{-ClC}_6\text{H}_4\text{CH}_2)_2\text{Sn}(\text{L}^3)\text{Cl}_2$, where (L^1) : 2-phenylethyl *N*-thiohydrazide, (L^2) : *N*-(2-phenylethyl-*N*-thio)-1,3-propane diamine, (L^3) : *N*-(2-phenylethyl-*N*-thio)-1,2-ethane diamine. The complexes were synthesized by directly mixing, refluxing and stirring the ligands with organotin(IV)

chlorides in a suitable solvent and were characterized by elemental analysis, electronic, infrared, ^1H and ^{13}C NMR spectroscopy. They also reported [39] complexes of 2-phenylethyl dithiocarbamate, thiohydrazides and thiodiamines with dibenzyltin(IV) chloride, tribenzyltin(IV) chloride and di(*para*-chlorobenzyl)tin(IV) dichloride have been synthesized in 1:2 and 1:1 molar ratio (Fig. 3.6). The dithiocarbamate ligand act as monoanionic bidentate and thiohydrazide, thiodiamines act as neutral bidentate ligand. The synthesized complexes have been characterized by elemental analysis and molecular weight determination studies and their bonding pattern suggested on the basis of electronic, infrared, ^1H and ^{13}C NMR spectroscopy. Using thermogravimetric (TG) and differential thermal analysis (DTA) various thermodynamic and kinetic parameters have been calculated and correlated with the structural aspects for solid-state decomposition of complexes. The ligands and their tin complexes have also been screened for their fungitoxicity activity against *Rhizoctonia solanii* and *Sclerotium rolfsii* and their ED_{50} values calculated.

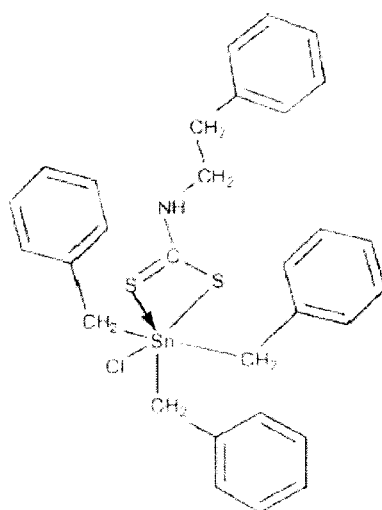


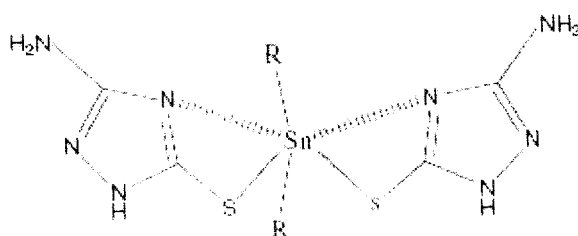
Fig. 3.6 Dithiocarbamate complexe [39]

In 2002, Shing *et al.* [40] investigated a new class of coordination compounds of organotin(VI) with a sulphur-containing ligand moiety derived by the condensation of 1-acetylferrocene and thiosemicarbazide, R_3SnL and $\text{R}_2\text{SnCl}_{2-n}(\text{L}_n)$ when $\text{R} = \text{Me}$ and Ph , $n = 1$ or 2 , $\text{L} =$ anion of 1-acetylferrocenethiosemicarbazone. Then attempts have been made to establish a correlation between a variety of biointeraction

activities, including antimicrobial activity and antifertility activity of the condensation products.

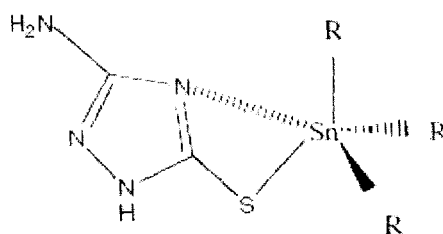
Nath *et al.* [41] reported organotin(IV) triazolates of general formula $R_nSn(L)_{4-n}$ (where $R = Me, n-Bu$ and Ph for $n = 2$; $R=Me, n-Pr$ and $n-Bu$ for $n = 3$ and $HL = 3-amino-5-mercapto-1,2,4-triazole$) (Fig. 3.7a and Fig. 3.7b) which were synthesized by the reaction of R_2SnCl_2/R_3SnCl with NaL in 1:2/1:1 molar ratio. Among these compounds, Oct_2SnL_2 was synthesized azeotropically by the reaction of Oct_2SnO and HL in 1:2 molar ratio. Physical measurements, viz. UV/Vis, IR, far-IR, multinuclear (1H , ^{13}C and ^{119}Sn) NMR and ^{119}Sn Mössbauer spectroscopic studies were used to accomplish a definitive characterization and determination of their most probable structures. In these compounds triazole acts as a monoanionic bidentate ligand, coordinating through S_{exo} and $N(4)$.

a)



Proposed structure for R_2SnL_2 (where $R = Me, n-Bu, Oct$ and Ph).

b)



Proposed structure for R_3SnL (where $R = Me, n-Pr$ and $n-Bu$).

Fig. 3.7 a) Proposed structure for R_2SnL_2 (where $R=Me, n-Bu, Oct$ and Ph) and b) R_3SnL (where $R= Me, N-Pr$ and $n-Bu$) [41].

In the same year, they also reported some tri- and diorganotin(IV) compounds of the general formula, R_nSnL_{4-n} (where $n=2, R=Me, n-Bu$ and Ph ; $n=3, R=Me, n-Bu,$

n-Pr and Ph; HL= 5-amino-3H-1,3,4-thiadiazole-2-thione) (Fig. 3.8) which were synthesized by the reaction of $R_n\text{SnCl}_{4-n}$ (where $n = 2$ or 3 , $R = \text{Me}$, *n*-Bu, *n*-Pr and Ph) and the sodium salt of the ligand. Oct_2SnL_2 was obtained by the reaction of Oct_2SnO with HL in a 1:2 molar ratio under azeotropic removal of water. The bonding and coordination behavior in these derivatives are discussed on the basis of IR, Far-IR, multinuclear (^1H , ^{13}C and ^{119}Sn) NMR and ^{119}Sn Mössbauer spectroscopic studies. These investigations suggest that in all the compounds the ligand acts as monoanionic bidentate coordinating through ring N(3) and exocyclic S [42].

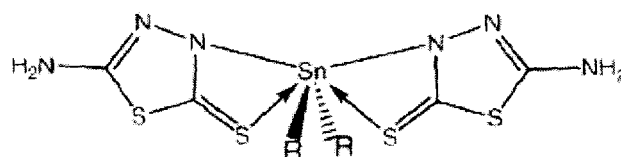
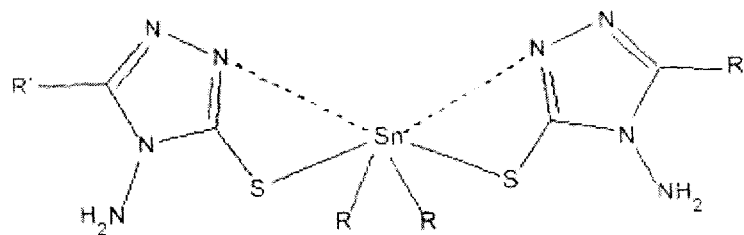


Fig. 3.8 Proposed structure of $R_2\text{Sn(IV)}$ derivatives of 5-amino-3H-1,3,4-thiadiazole-2-thione, where $R = \text{Me}$ and *n*-Bu [42].

In 2008, Nath *et al.* [43] have also reported that some di- and triorganotin(IV) triazolates of general formula, $R_{(4-n)}\text{SnL}_n$ (where $n=2$; $R = \text{Me}$, *n*-Bu and Ph; $n=1$; $R = \text{Me}$, *n*-Pr, *n*-Bu and Ph and HL= 4-amino-3-methyl-1,2,4-triazole-5-thiol (HL-1); and 4-amino-3-ethyl-1,2,4-triazole-5-thiol (HL-2)) (Fig. 3.9 and Fig. 3.10) were synthesized by the reaction of $R_{(4-n)}\text{SnCl}_n$ with sodium salt of HL-1 and HL-2. The bonding and coordination behavior in these derivatives have been discussed on the basis of IR and ^{119}Sn Mössbauer spectroscopic studies in the solid state. Their coordination behavior in solution is discussed by multinuclear (^1H , ^{13}C and ^{119}Sn) NMR spectral studies. The IR and ^{119}Sn Mössbauer spectroscopic studies indicate that the ligands, HL-1 and HL-2 act as a monoanionic bidentate ligand, coordinating through S_{exo} and N_{ring} . The distorted skew trapezoidal-bipyramidal and distorted trigonal bipyramidal geometries have been proposed for $R_2\text{SnL}_2$ and $R_3\text{SnL}$, respectively, in the solid state. They are *in vitro* antimicrobial screening of some of the newly synthesized derivatives.



Proposed structure for R_2SnL_2 (where $R = \text{Me}, n\text{-Bu}$ and Ph).

Fig. 3.9 Proposed structure for R_2SnL_2 [43].

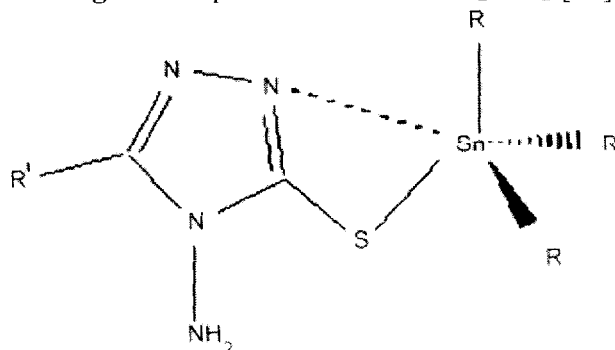


Fig. 3.10 Proposed structure for R_3SnL (where, $R = \text{Me}, n\text{-Pr}, n\text{-Bu}$ and Ph ; $R' = \text{Me}$ or Et) [43]

Shahzadi *et al.* [44] reported the synthesis of (4-Methylpiperidine-dithiocarbamate-*S,S'*) triphenyltin(IV) (Fig. 3.11) derivative of 4-methyl-1-piperidine carbodithioic acid (4-MePCDTA) and characterized it by elemental, IR, multinuclear NMR (^1H and ^{13}C) and mass spectrometric studies. The crystal structure of the complex has been determined by X-ray single crystal analysis, which shows unsymmetrical nature of the ligand towards coordination to tin. It crystallizes in monoclinic structure. The tin atom is coordinated to the two sulfur atoms of the dithiocarbamate ligand and three carbon atoms of the phenyl groups are in distorted trigonal bipyramid geometry. This complex was tested for its antimicrobial activity against six different plant and human pathogens. The screening results show that the complex exhibit higher antibacterial and antifungal activity than the free ligand.

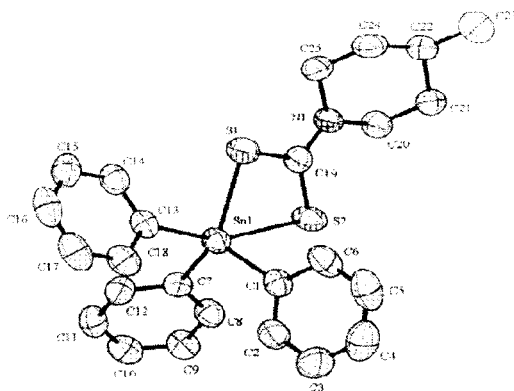


Fig. 3.11 Molecular structure of (4-methylpiperidinedithiocarbamato-S,S') triphenyltin(IV) [44].

The 1,3-dithia-2-stannacyclopentane derivatives with dialkyldithiocarbamates of the types $\text{SCH}_2\text{CH}_2\text{SSn}[\text{S}_2\text{CNR}_2]\text{Cl}$ (I) and $\text{SCH}_2\text{CH}_2\text{SSn}[\text{S}_2\text{CNR}_2]_2$ (II) (where R = CH_3 , C_2H_5 and $-\text{CH}_2-\text{CH}_2-$) have been synthesized by the reaction of 2,2-dichloro-1,3-dithia-2-stannacyclopentane and sodium/ammonium salts of dialkyldithiocarbamates in 1:1 and 1:2 molar ratios, respectively, in anhydrous benzene. These newly synthesized derivatives have been characterized by elemental analyses (C, H, N, S and Sn), thermal [thermogravimetry (TG) and differential thermal analyses (DTA)] as well as spectral [UV, IR and multinuclear NMR (^1H , ^{13}C and ^{119}Sn)] studies. The monodentate behaviour of the dialkyldithiocarbamate ligands was confirmed by IR and ^{119}Sn NMR spectral data and distorted tetrahedral structures have been suggested for both type (I) and (II) compounds. The free ligands and their tin complexes have also been screened for their antibacterial and antifungal activities. These results made it desirable to delineate a comparison between free ligands and their tin complexes. These exhibit higher antibacterial effect than some of the previously investigated antibiotics [45].

R. R. Holmes [46] has written a review about the cluster chemistry of organotin (IV) compounds based on Sn-O-Sn and Sn-S-Sn bonding formed in reactions of stannonic acids with carboxylic and phosphorus-based acids as participating ligands. Introduction of sulfur in the organotin framework leads to additional varieties of cluster molecules. An interesting sulfur-capped cluster, $[\{n\text{-BuSn}-(\text{S})\text{OP}(\text{OH})(\text{O}-t\text{-Bu})_2\}_3\text{S}][\text{O}_2\text{P}(\text{O}-t\text{-Bu})_2] \cdot \text{H}_2\text{S} \cdot \text{H}_2\text{O}$ (Fig. 3.12), was prepared by passing H_2S through a benzene solution of the triphosphate $n\text{-BuSn}[\text{O}_2\text{P}(\text{O}-t\text{-$

Bu)₂]₃ at room temperature. In the structure, it is clear that the tin atoms are pentacoordinate and the ligands are monodentate as well as contain dangling P-O-H units. In the oxygen-capped clusters, oxygen atoms other than the capping oxygen are present as OH groups, whereas in the sulfur-capped derivative, sulfur atoms occupy both types of framework sites. Because the presence of larger sulfur atoms producing a greater tin-tin distance that the phosphates need to span to act as bidentate ligands and the tin centers should be less acid with framework Sn-S bonding, resulting in weaker tin-phosphate coordination [47,48].

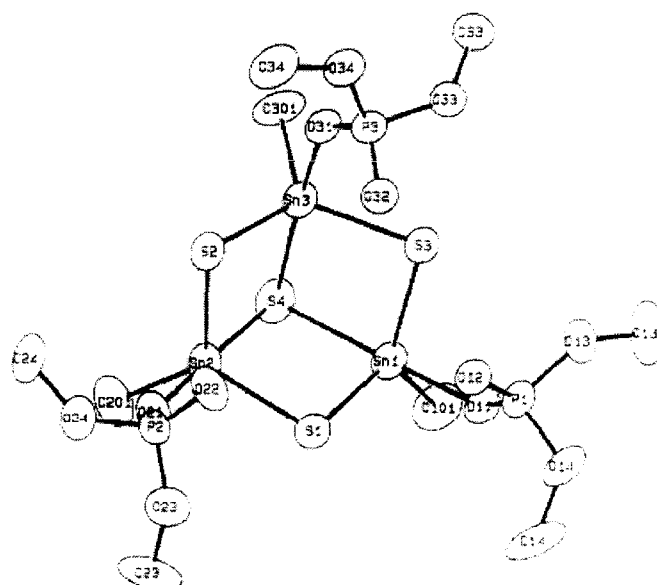


Fig. 3.12 Structure of $[\{n\text{-BuSn}-(\text{S})\text{OP}(\text{OH})(\text{O}\text{-t}\text{-Bu})_2\}_3\text{S}][\text{O}_2\text{P}(\text{O}\text{-t}\text{-Bu})_2]\cdot\text{H}_2\text{S}\cdot\text{H}_2\text{O}$ [47]

The first heptanuclear tin-sulfur cluster, $[\{n\text{-BuSnS}(\text{O}_2\text{PPh}_2)\}_3\text{O}]_2\text{Sn}$ (Fig. 3.13) was obtained by the refluxing $\text{Ph}_2\text{P}(\text{OH})$, sulphur and $n\text{-BuSn}(\text{O})\text{OH}$ in toluene. X-ray analysis revealed a unique double cube arrangement [49,50]. The geometry at each cube center is depicted on the top and the core structure on the bottom [48,49].

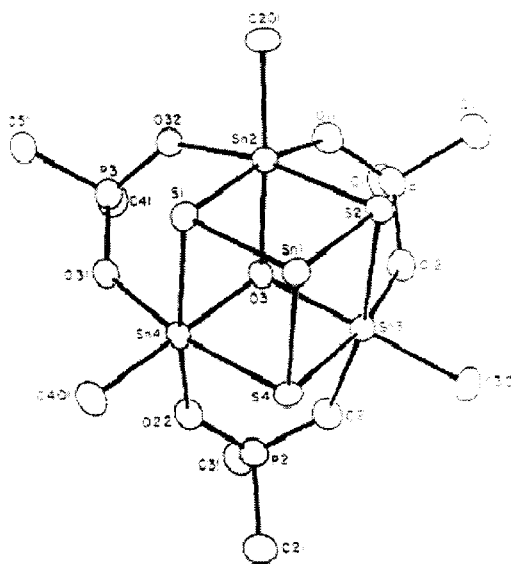


Fig. 3.13 Structure of $[\{n\text{-BuSnS}(\text{O}_2\text{PPh}_2)\}_3\text{O}]_2\text{Sn}$ [49]

A trinuclear tin cluster $[(n\text{-BuSn})_3(\text{S})(\text{O})(\text{O}_2\text{CPh})_5]$ (Fig. 3.14), with carboxylate ligands, containing a Sn-S-Sn bridge which was prepared by passing hydrogen sulfide through a CCl_4 solution of *n*-butyltin tribenzoate at room temperature in the presence of atmospheric moisture. X-ray analysis showed an almost planar Sn_3O system [47,48].

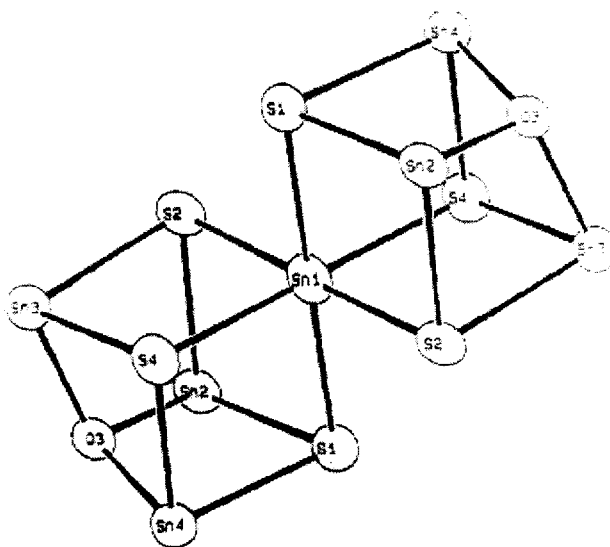


Fig. 3.14 Structure of $[(n\text{-BuSn})_3(\text{S})(\text{O})(\text{O}_2\text{CPh})_5]$ [47]

In 2006, Wang *et al.* [51] attempted to prepare cubane-like clusters from the precursor $(\text{Bu}_4\text{N})_2[\text{Sn}_3\text{S}_4(\text{edt})_3]$ (edt = 1,2-ethanedithiolate). But two new tetranuclear

tin(IV) oxysulfide clusters, $(\text{Bu}_4\text{N})_2 [\text{Sn}_4(\mu_4\text{-O})\text{S}_5(\text{edt})_2\text{Cl}_2]$ and $(\text{Bu}_4\text{N})_2[\text{Sn}_4(\mu_4\text{-O})\text{S}_5(\text{edt})_2\text{Br}_2]$ were unexpectedly obtained by reaction of $(\text{Bu}_4\text{N})_2[\text{Sn}_3\text{S}_4(\text{edt})_3]$ with SnX_2 ($\text{X} = \text{Cl}, \text{Br}$). X-ray crystal structure analyses show that the two compounds possess an isostructural anionic cluster with a highly distorted tetrahedral metal skeleton and the two compounds have been characterized spectroscopically.

3.3 Scope and Objective

As has been mentioned the organotin sulphur compounds have very important industrial applications not only as the PVC stabilisers but also for the inherent activity of the ligands used containing sulphur atoms as biomolecules [52, 53]. In addition the presence of nitrogen atom in the ligand is expected to increase the bioactivity of the organotin compounds after the incorporation of such ligand moieties to tin atom(s). The scope for the syntheses of these sulphur tin compounds, therefore, is unlimited. The ligand bonding to tin atom should result into interesting structural (with or without X ray crystal structure data) diversity. Additionally, systematic investigation on the activities of these compounds as agricultural biocides could also be undertaken to study the biocidal properties. Our interest in the investigations on the syntheses, structures and biocidal properties of different types of organotin compounds [54,55] led the author to undertake the syntheses, structures and biocidal properties of such organotin sulphur compounds as 2-mercapto isothiocyanate derivatives of organotins. As far as the knowledge of the author is concerned limited work is available in the literature [56] on the organotin isothiocyanates.

Hence the objective of this work is to:

- (a) syntheses of new organotin isothiocyanates
- (b) characterisation of the new compounds and
- (c) determination of the biocidal activities of these and related compounds.

3.4 Experimental

3.4.1 General comments

The solvents used in reactions were of AR grade and were obtained from commercial sources (Merck, India). The solvents were dried using standard literature procedures. Petroleum ether (60-80°C) and benzene were distilled from sodium where

as methanol was distilled after reacting it with solid iodine and magnesium. While working with benzene as a solvent proper health precaution was undertaken.

In this chapter the author wishes to describe the result of a crystal structure determination of a selected compound of an interesting class of compounds containing Sn-S bond for its similarity with the 2-mercapto isothiocyanates of organotins (*i.e.*, having Sn-S bond).

It was reported that a series of compounds [57] formed by an unusual transformation (or rearrangement) that took place during the reaction between the triorganotin hydroxides and phenylthiohydantoic acid produce unexpected $R_3SnSCH_2CONHPh$ following the reaction as follows:



(Ligand **A** = $C_6H_5-NC(NH_2)-SCH_2COOH$, compound

B = $(C_6H_5CH_2)_3SnSCH_2COPh$) and (where R = $-C_6H_5; Ph, -C_6H_{11}; Cy-hex$ and $-CH_2C_6H_5; Bz$)

The biocidal activities of these tin compounds where R = Ph and Cy-hex on *Bipolaris sorokiniana* are detailed in Chapter 5 of this thesis. However, the structure of the compound (a compound similar to triphenyl- and tricyclohexyltin derivatives), *namely*, $(C_6H_5CH_2)_3SnSCH_2COPh$ not established earlier is now established by X-ray crystal structure determinations and is described herein.

3.4.2 Materials

2-aminothiophenol (s.d.fine-chem, India), NH_4OH (Merck, India), carbon disulphide (s.d.fine-chem, India), ethanol (Bengal Chemical, India), chloroacetic acid (BDH Lab Chem Glaxo, India), hydrazine hydrate (s.d.fine-chem, India), n-dibutyltin oxide (Alfa, USA), Me_2SnCl_2 (Fluka, Switzerland), Ph_2SnCl_2 (Aldrich, USA), and n-Bu₂SnCl₂ (Merck, Germany), Ph_3SnCl (Merck, Germany), Ph_3SnOH (M&T CHEMICALS INC., USA) c-Hex₃SnCl (Aldrich, USA), n-Bu₃SnCl (Fluck, Germany), Bis(tri-n-butyltin) Oxide (HIMEDIA, India), Me_3SnCl (Aldrich, USA), were used as received from commercial sources. Bz_2SnCl_2 , Bz_3SnCl was prepared using the method of Sisido *et al.* [58]. Me_2SnO , Ph_2SnO , Bz_2SnO and Bz_3SnOH were prepared by the alkaline hydrolysis of respective diorganotin dichlorides/triorganotinchloride in water/ether mixtures.

3.4.3 Measurements

The ^1H , and ^{13}C NMR spectra were recorded in CDCl_3 solution using TMS as an internal standard on a Bruker DPX 300 spectrophotometer. The IR spectra in the range $4000\text{-}400\text{ cm}^{-1}$ were recorded on FTIR-8300 Shimadzu spectrophotometer with samples investigated on CsI window. Differential scanning calorimetric analyses were recorded on Pyris 6 DSC Perkin Elmer from $100\text{-}230^\circ\text{C}$ at a heating rate of $5^\circ\text{C}/\text{min}$. Microanalyses were performed at Indian Association of Cultivation of Science, Kolkata, India. Tin was estimated as SnO_2 gravimetrically using standard procedure in our laboratory.

3.4.4 Crystallography

A crystal of $(\text{C}_6\text{H}_5\text{CH}_2)_3\text{SnSCH}_2\text{COPh}$ of approximate size $0.2\times 0.2\times 0.2\text{ mm}^3$ was mounted on an Mar Research image plate scanner and graphite monochromatized $\text{MoK}\alpha$ radiation was used to measure $95\ 2^\circ$ frames with an exposure time of 120 sec per frame. The data were corrected using the XDS package to give 4244 unique reflections ($R\ \sigma = 0.045$).

Structure solution and refinement

The structure was solved by the direct method SHELX 86 [59] and refined using SHELXL (courtesy of Prof. G.M. Sheldrick, University of Gottingen), by full-matrix least squares of 557 variables, to a final R-factor of 0.045 for 4244 reflections with $[\text{Fo}] > 4\sigma(\text{F})$. All atoms (including hydrogens) were revealed by difference Fourier maps. Non-hydrogen atoms were refined anisotropically. Hydrogen atoms were placed geometrically and refined with a fixed temperature factor of 0.05. The final difference Fourier map had a largest peak of $1.280\ \text{A}^{-3}$. The structure of (**B**) are shown in (Fig.3.15) drawn with ORTEP [60], crystal data, positional parameters, bond distances and bond angles are summarised in Table 3.1-3.4 for **B** (Crystallographic data have been deposited at the Cambridge Crystallographic Data centre as supplementary publication number CCDC 714149). It should be pointed out that the ligand (**A**) has undergone rearrangement to $-\text{SCH}_2\text{CONHC}_6\text{H}_5$ during the reaction which is confirmed by the crystallographic analyses.



Fig. 3.15 The molecular structure and crystallographic numbering scheme for tribenzyltin (N-phenylamido methyl mercaptide)

Table 3.1 Crystallographic data for $(C_6H_5CH_2)_3SnSCH_2CONHC_6H_5$

Empirical Formula	$C_{29}H_{28}NOSSn$
Formula weight	557.27
Temperature	293(2) K
Wave length	0.71069 Å
Crystal system	Monoclinic
Space group	P 21/c
Unit cell dimension	a=14.746Å alpha = 90deg b=7.827Å beta=92.43deg c=22.573Å gamma = 90deg
Volume	2603.0 Å ³
Z	4

Density (calculated)	1.422 Mg/m ³
Absorption coefficient	1.083 mm ⁻¹
F(000)	1132
Crystal size	0.2x0.2x0.2mm
Theta range for data collection	2.23 to 24.72 deg
Index ranges	0≤h≤17,0≤k≤9,-26≤l≤26
Reflections collected	15717
Independent reflections	4244 [R(σ) = 0.045]
Refinement method	Full-matrix least squares on F ²
Data/restraints/parameters	4244 / 0 / 299
Goodness –of-fit on F ²	2.598
Final R indices [I>2σ (I)]	R1 = 0.0651, wR2 = 0.2693
R indices (all data)	R1 = 0.0739, wR2 = 0.2812
Extinction coefficient	0.010 (2)
Largest diff. Peak and hole	1.184 and –0.752 e. Å ⁻³

Table 3.2 Bond lengths [Å] and angles (deg) for (C₆H₅CH₂)₃SnSCH₂CONHC₆H₅

Atoms	Lengths/angles
Sn(1) - C(7)	2.136(7)
Sn(1) - C(17)	2.142(7)
Sn(1) - C(14)	2.155(9)
Sn(1) - S(1)	2.430(2)
S(1)-C(21)	1.798(8)
N(1)-C(5)	1.309(10)
N(1)-C(10)	1.410(10)
C(5)-O(1)	1.221(9)
C(5)-C(21)	1.506(11)
C(7)-C(8)	1.487(11)
C(8)- C(22)	1.34(2)
C(8)-C(28)	1.385(13)
C(10)-C(15)	1.376(13)

C(10)-C(25)	1.398(11)
C(11)-C(16)	1.359(13)
C(11)-C(20)	1.359(13)
C(11)-C(14)	1.516(11)
C(12)-C(24)	1.374(11)
C(12)-C(18)	1.401(11)
C(12)-C(17)	1.497(10)
C(15)-C(27)	1.343(14)
C(16)-C(35)	1.35(2)
C(18)-C(26)	1.332(14)
C(19)-C(24)	1.356(14)
C(19)-C(23)	1.374(14)
C(20)-C(35)	1.39(2)
C(22)-C(36)	1.41(2)
C(23)-C(26)	1.396(14)
C(25)-C(29) # 1	1.36(2)
C(27)-C(30)	1.38(2)
C(23)-C(33)	1.36(2)
C(29)-C(25) # 1	1.36(2)
C(29)-C(30) # 1	1.38(2)
C(30)-C(29) # 1	1.38(2)
C(31)-C(32)	1.43(2)
C(32)-C(35)	1.36(2)
C(33)-C(34)	1.33(2)
C(34)-C(36)	1.47(2)
C(7)-Sn(1)-C(17)	111.2(3)
C(7)-Sn(1)-C(14)	110.5(3)
C(17)-Sn(1)-C(14)	112.7(3)
C(7)-Sn(1)-S(1)	113.7(2)
C(17)-Sn(1)-S(1)	111.1(2)
C(14)-Sn(1)-S(1)	96.9(2)
C(21)-S(1)-Sn(1)	101.2(3)
C(5)-N(1)-C(10)	126.7(6)
O(1)-C(5)-N(1)	124.5(7)
O(1)-C(5)-C(21)	121.1(7)
N(1)-C(5)-C(21)	114.4(6)
C(8)-C(7)-Sn(1)	111.6(5)
C(22)-C(8)-C(28)	119.4(9)
C(22)-C(8)-C(7)	118.6(9)
C(28)-C(8)-C(7)	122.0(9)
C(15)-C(10)-C(25)	118.0(8)
C(15)-C(10)-N(1)	124.5(7)
C(25)-C(10)-N(1)	117.3(8)
C(16)-C(11)-C(20)	118.3(8)
C(16)-C(11)-C(14)	121.2(8)
C(20)-C(11)-C(14)	120.5(8)
C(24)-C(12)-C(18)	116.5(8)
C(24)-C(12)-C(17)	122.8(7)
C(18)-C(12)-C(17)	120.6(7)
C(11)-C(14)-Sn(1)	114.4(5)

C(27)-C(15)-C(10)	132.0(9)
C(31)-C(16)-C(11)	122.2(12)
C(12)-C(17)-Sn(1)	111.3(5)
C(26)-C(18)-C(12)	122.2(8)
C(24)-C(19)-C(23)	120.9(9)
C(11)-C(20)-C(35)	123.5(12)
C(5)-C(21)-S(1)	113.6(5)
C(8)-C(22)-C(36)	120.9(13)
C(19)-C(23)-C(26)	118.1(8)
C(19)-C(24)-C(12)	121.9(8)
C(29) # 1-C(25)-C(10)	120.6(11)
C(18)-C(26)-C(23)	120.4(8)
C(15)-C(27)-C(30)	119.2(12)
C(33)-C(28)-C(8)	122.8(12)
C(25) # 1-C(29)-C(30) # 1	119.7(9)
C(29) # 1-C(30)-C(27)	120.4(11)
C(16)-C(31)-C(32)	118.1(12)
C(35)-C(32)-C(31)	121.3(10)
C(34)-C(33)-C(28)	119.6(13)
C(33)-C(34)-C(36)	120.2(12)
C(32)-C(35)-C(20)	116.6(12)
C(22)-C(36)-C(34)	116.7(14)

Symmetry transformations used to generate equivalent atoms :

1 -x, -y, -z

Table 3.3 Atomic coordinates ($\times 10^4$) and equivalent isotropic displacement parameters ($\text{Å}^2 \times 10^3$) for $(\text{C}_6\text{H}_5\text{CH}_2)_3\text{SnSCH}_2\text{CONHC}_6\text{H}_5$. $U(\text{eq})$ is defined as one third of the trace of the orthogonalized U_{ij} tensor.

	x	y	z	U(eq)
Sn(1)	1997 (1)	1498 (1)	1814 (1)	38(1)
S(1)	1505 (2)	3490 (2)	2561 (1)	49(1)
N(1)	-765 (4)	4703 (7)	1704 (3)	42 (1)
C(5)	- 21 (5)	3825 (9)	1813 (3)	39 (2)
O(1)	79 (4)	2328 (7)	1678 (3)	57 (2)
C(7)	1334 (6)	- 926 (9)	1837(3)	45 (2)
C(8)	1100 (7)	-1573 (9)	1231 (3)	47 (2)
C(10)	-1581 (6)	4098 (11)	1432 (3)	47 (2)
C(11)	3817 (5)	-444 (10)	2032 (3)	44 (2)
C(12)	2767 (5)	2564 (10)	648 (3)	38 (2)
C(14)	3386 (6)	1278 (11)	2142 (4)	53 (2)
C(15)	-1850 (6)	2414 (12)	1425 (4)	55 (2)
C(16)	3659 (7)	-1808 (13)	2386 (5)	61 (2)
C(17)	1879 (5)	2604 (11)	946 (3)	45 (2)

C(18)	2951 (7)	1279 (10)	237 (4)	51 (2)
C(19)	4247 (7)	3667 (12)	494 (4)	61 (2)
C(20)	4386 (7)	- 653 (15)	1579 (4)	69 (3)
C(21)	730 (5)	4812 (9)	2130 (4)	45 (2)
C(22)	245 (9)	- 1402 (14)	1015 (6)	79 (4)
C(23)	4424 (6)	2379 (13)	102 (4)	58 (2)
C(24)	3439 (6)	3752 (11)	758 (4)	51 (2)
C(25)	-2183 (7)	5312 (14)	1186 (4)	70 (3)
C(26)	3749 (7)	1157 (12)	- 14 (4)	57 (2)
C(27)	-2653 (7)	1915 (17)	1181 (5)	76 (3)
C(28)	1732 (8)	-2391 (12)	893 (4)	70 (3)
C(29)	2989 (8)	5175 (18)	- 929 (5)	85 (4)
C(30)	-3231 (9)	3128 (18)	927 (6)	91 (4)
C(31)	4066 (10)	-3330 (14)	2311 (7)	89 (4)
C(32)	4672 (10)	-3498 (16)	1838 (7)	93 (5)
C(33)	1528 (12)	-3012 (15)	341 (6)	85 (4)
C(34)	699 (17)	-2797 (18)	101 (6)	129 (7)
C(35)	4824 (9)	-2176 (25)	1464 (6)	99 (4)
C(36)	-20 (11)	-2047 (18)	452 (5)	97 (4)

Table 3.4 Anisotropic displacement parameters ($\text{Å}^2 \times 10^3$) for $(\text{C}_6\text{H}_5\text{CH}_2)_3\text{SnSCH}_2\text{CONHC}_6\text{H}_5$. The anisotropic displacement factor exponent takes the form: $-2 \pi^2 [h^2 a^{*2} U_{11} + \dots + 2 h k a^* b^* U_{12}]$

	U11	U22	U33	U23	U13	U12
Sn(1)	40(1)	30(1)	44(1)	0(1)	2(1)	-1(1)
S(1)	58(1)	40(1)	49(1)	-9(1)	-2(1)	1(1)
N(1)	50(4)	29(3)	44(3)	4(2)	-5(3)	12(3)
C(5)	42(4)	27(4)	48(4)	1(3)	9(3)	0(3)
O(1)	50(34)	42(3)	80(4)	-26(3)	-5(3)	13(3)
C(7)	74(5)	23(4)	38(4)	-1(3)	0(3)	-8(3)
C(8)	71(6)	35(5)	33(4)	8(3)	4(4)	-16(3)
C(10)	57(5)	49(5)	35(4)	2(3)	1(3)	14(4)
C(11)	41(4)	41(4)	50(4)	-4(3)	-15(3)	6(3)
C(12)	35(3)	40(4)	38(4)	6(3)	-1(3)	-1(3)
C(14)	44(5)	48(5)	66(5)	-9(4)	-5(4)	10(3)
C(15)	56(5)	48(5)	62(5)	-4(4)	-6(4)	2(4)
C(16)	60(6)	53(5)	71(6)	2(4)	-6(5)	7(4)
C(17)	49(4)	45(5)	42(4)	9(3)	4(3)	- 5(3)
C(18)	65(6)	41(1)	46(4)	-6(3)	-8(4)	-9(4)
C(19)	51(5)	73(7)	58(5)	4(4)	0(4)	-10(4)
C(20)	55(5)	83(8)	68(6)	0(5)	-2(4)	21(5)
C(21)	50(4)	18(3)	66(5)	-1(3)	3(4)	2(3)
C(22)	74(8)	81(9)	81(8)	-21(5)	-19(6)	-18(5)
C(23)	56(5)	66(6)	53(5)	3(4)	6(4)	11(4)
C(24)	50(5)	39(4)	66(6)	-1(4)	16(4)	2(3)
C(25)	67(6)	76(7)	65(6)	3(5)	-11(5)	37(5)

C(26)	70(6)	53(5)	47(5)	1(4)	9(4)	8(4)
C(27)	59(6)	90(8)	78(7)	-23(6)	35(5)	9(5)
C(29)	82(8)	99(10)	71(6)	-6(6)	-25(6)	51(7)
C(30)	70(7)	103(10)	96(9)	-18(7)	-29(6)	14(7)
C(31)	86(9)	67(8)	110(10)	13(6)	-41(8)	9(6)
C(32)	87(9)	98(11)	90(9)	-39(7)	-37(7)	47(7)
C(33)	138(12)	56(6)	64(7)	-21(5)	40(7)	18(7)
C(34)	274(24)	49(8)	65(8)	-21(6)	20(12)	38(11)
C(35)	74(8)	152(13)	69(7)	-21(9)	-16(6)	39(9)
C(36)	137(12)	79(8)	74(7)	-10(6)	-14(8)	39(8)

3.4.5 Synthetic Procedure

The method employed for the preparation of the ligand 2-mercapto isothiocyanate is described along with analytical and spectral data in section 3.4.4.1-3.4.4.2. The synthesis of organotin complexes of the 2-mercapto isothiocyanate are described in section 3.4.4.2- 3.4.4.11. Their characterization, analytical and spectroscopic data are given in section 3.5.

3.4.5.1 Preparation of 2-mercapto isothiocyanate (LH)

2-aminothiophenol (100 mmol, 10.68 ml, 12.5g) was dissolved in ammonia solution (20 ml, d 0.88) and CS₂ (8 ml) was added to it gradually with stirring and cooling below 30°C. Ethanol 25 ml was then added by continued stirring till CS₂ had completely dissolved. The reaction mixture was allowed to stand for 2h and a solution of sodium chloroacetate (100 mmol, 11.69g) was added, followed by hydrazine hydrate (10 ml, 50%). The mixture was then warmed and cooled to room temperature and filtered. The filtrate was concentrated to half its volume and left to stand overnight. The crystals separated were filtered and recrystallized from ethanol.

LH: yield: 9.2 g, 73.6%, M.P.: 178°C

Elemental analysis (Caled. For C₇H₅NS₂)

Calcd.: C, 50.27; H, 3.01; N, 8.37%

Found: C, 50.40; H, 2.96; N, 8.35%

IR (cm⁻¹): ν(-N=C), 2095(m); ν(C-S), 748(m); ν(SH), 2680(w); ν(C=S), 1246(w);

NMR ¹H : δ SH: 1.78, H-4=7.46, H-5=7.38, H-6=7.26, H-7=7.50.

NMR ¹³C : C-1=190, C-2 = 112, C-3= 121, C-4=130, C-5=127, C-6=140, C-7=124.

Numbering scheme shows at table 3.4.

3.4.5.2 Preparation of sodium salt of 2-marcapton isothiocyanate (LNa)

To a methanolic solution (50 ml) of 2-marcapto isothiocyanate (LH) (5g, 29.94 mmol) was added drop wise with continuous stirring, 0.5 N methanolic NaOH (1.2g, 60.87 ml, 29.94 mmol) in the presence of phenolphthalein as an indicator. The reaction system was stirred for 5h. The solvents removed in vacuum which left behind the crude product of sodium salt of 2-marcapto isothiocyanate. The sodium salt thus prepared was recrystallized from methanol and then dried in an air oven at 100°C for 24h.

LNa: yield: 5.1g, 82.2%, M.P.: 225°C(dec.).

Elemental analysis (Caled. For C₇H₄NS₂Na)

Calcd.: C, 44.43; H, 2.13; N, 7.40%

Found: C, 44.20; H, 2.10; N, 7.44%

IR (cm⁻¹): ν(-N=C), 2082(m); ν(C-S), 725(m); ν(C=S), 1240(w);

¹H and ¹³C NMR could not be recorded because of poor solubility reasons.

3.4.5.3 Synthesis of trimethyltin(IV) 2-marcapto isothiocyanate, Me₃SnL (1)

To a solution of sodium salt of 2-marcapto isothiocyanate (0.95g, 5.02 mmol) in methanol was added to a methanolic solution of Me₃SnCl (1g, 5.02 mmol). The mixture was continued to stir for 3h. The reaction mixture was then heated under reflux for 6h under inert conditions. The volatiles were removed and the dry mass extracted with hot petroleum ether (60-80°C, 50 ml). Colourless liquid of the desired product were obtained by cooling the solution at room temperature and then removing the solvent under vacuum at room temperature.

3.4.5.4 Synthesis of n-tributyltin(IV) 2-marcapto isothiocyanate, n-Bu₃SnL (2)

(A) A mixture of (n-Bu₃Sn)₂O (1.78g, 1.52 ml, 2.99 mmol) and 2-marcapto isothiocyanate (1g, 5.98 mmol) in dry benzene (150 ml) was heated under reflux in inert conditions for 8h, the water produced being removed azeotropically. All volatiles were removed from the clear and transparent reaction mixture under vacuum and the dry mass extracted with hot petroleum ether (60-80°C, 50 ml). Pale yellow liquid of the desired product were obtained by cooling the solution at room temperature after the removal of the solvent under vacuum at room temperature.

(B) To a solution of sodium salt of 2-mercapto isothiocyanate (1g, 5.29 mmol) in methanol was added to a methanolic solution of n-Bu₃SnCl (1.72g, 1.43 ml, 5.29 mmol). The mixture was continued to stir for 3h. The reaction mixture was then heated under reflux for 6h under inert conditions. The volatile were removed and the dry mass extracted with hot petroleum ether (60-80°C, 50 ml). Pale yellow liquid of the desired product was obtained by cooling the solution at room temperature and removing the solvent distilling under vacuum at room temperature.

3.4.5.5 Synthesis of triphenyltin(IV) 2-mercapto isothiocyanate, Ph₃SnL (3)

(A) A mixture of Ph₃SnOH (0.6g, 1.56 mmol) and 2-mercapto isothiocyanate (0.26g, 1.56 mmol) in dry benzene (150 ml) was heated under reflux in inert conditions for 8h, the water produced being removed azeotropically. All volatiles were removed from the clear and transparent reaction mixture and the dry mass extracted with hot petroleum ether (60-80°C, 50 ml). White crystals of the desired product were obtained by cooling the solution at room temperature.

(B) To a solution of sodium salt of 2-mercapto isothiocyanate (0.6g, 3.17 mmol) in methanol was added to a methanolic solution of Ph₃SnCl (1.22g, 3.17 mmol). The mixture was continued to stir for 3h. The solution was clear initially but after 1.30h started to a precipitate white in colour appeared. The reaction mixture was then heated under reflux for 6h under inert conditions. After 2h of refluxation the solution was clear. The volatile were removed and the dry mass extracted with hot petroleum ether (60-80°C, 50 ml). White crystals of the desired product were obtained by cooling the solution at room temperature.

3.4.5.6 Synthesis of tribenzyltin(IV) 2-mercapto isothiocyanate, Bz₃SnL (4)

(A) A mixture of Bz₃SnOH (2.45g, 5.99 mmol) and 2-mercapto isothiocyanate (1g, 5.99 mmol) in dry benzene (150 ml) was heated under reflux at inert conditions for 9h, the water thus produced being removed azeotropically. All volatiles were removed from the clear and transparent reaction mixture under vacuum and the dry mass extracted with hot petroleum ether (60-80°C, 50 ml). White crystals of the desired product were obtained by cooling the solution at room temperature.

(B) To a solution of sodium salt of 2-mercapto isothiocyanate (1g, 5.29 mmol) in methanol was added to a methanolic solution of n-Bz₃SnCl (2.26g, 5.29 mmol). The mixture was continued to stir for 3h. The reaction mixture was then heated under reflux for 6h under inert conditions. The volatile were removed under vacuum and the dry mass extracted with hot petroleum ether (60-80°C, 50 ml). White crystals of the desired product were obtained by cooling the solution at room temperature.

3.4.5.7 Synthesis of tricyclohexyltin(IV) 2-mercapto isothiocyanate, c-Hex₃SnL (5)

To a solution of sodium salt of 2-mercapto isothiocyanate (0.95g, 5.02 mmol) in methanol was added to a methanolic solution of c-Hex₃SnCl (2.03g, 5.02 mmol). The mixture was continued to stir for 3h. The reaction mixture was then heated under reflux for 6h under inert conditions. The volatile were removed under vacuum and the dry mass extracted with hot petroleum ether (60-80°C, 50 ml). White crystals of the desired product were obtained by cooling the solution at room temperature.

3.4.5.8 Synthesis of dimethyltin(IV) 2-mercapto isothiocyanate, Me₂Sn(L)₂ (6)

A mixture of Me₂SnO (0.6g, 3.64 mmol) and 2-mercapto isothiocyanate (1.22g, 7.28 mmol) in dry benzene (150 ml) was heated under reflux and inert conditions for 10h, the water produced being removed azeotropically. All volatiles were removed from the clear and transparent reaction mixture by vacuum distillation and the dry mass first washed out with hot petroleum ether (60-80°C) and then extracted with benzene (50 ml). Light yellow crystals of the desired product were obtained by cooling the solution at room temperature.

3.4.5.9 Synthesis of n-dibutyltin(IV) 2-mercapto isothiocyanate, n-Bu₂Sn(L)₂ (7)

A mixture of n-Bu₂SnO (1g, 4.02 mmol) and 2-mercapto isothiocyanate (1.34g, 8.04 mmol) in dry benzene (150 ml) was heated under reflux and inert conditions for 10h, the water produced being removed azeotropically. All volatiles were removed from the clear and transparent reaction mixture under vacuum and the

dry mass extracted with hot petroleum ether (60-80°C, 50 ml). White crystals of the desired product were obtained by cooling the solution at room temperature.

3.4.5.10 Synthesis of diphenyltin(IV) 2-marcapto isothiocyanate, Ph₂Sn(L)₂ (8)

A mixture of Ph₂SnO (1g, 3.46 mmol) and 2-marcapto isothiocyanate (0.58g, 3.46 mmol) in dry benzene (150 ml) was heated under reflux and inert conditions for 10h, the water produced being removed azeotropically. All volatiles were removed from the clear and transparent reaction mixture under vacuum and the dry mass washed with hot petroleum ether (60-80°C, 50 ml) then the mass was extracted with dry benzene (50 ml). White crystals of the desired product were obtained by cooling the solution at room temperature.

3.4.5.11 Synthesis of dibenzyltin(IV) 2-marcapto isothiocyanate, Bz₂Sn(L)₂ (9)

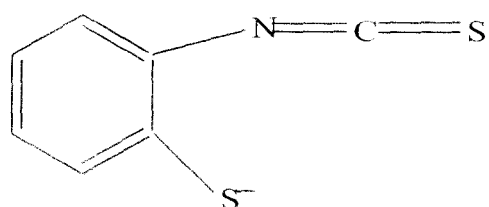
A mixture of Bz₂SnO (1.4g, 4.42 mmol) and 2-marcapto isothiocyanate (1.48 g, 8.84 mmol) in dry benzene (150 ml) was heated under reflux in inert conditions for 10h, the water produced being removed azeotropically. All volatiles were removed from the clear and transparent reaction mixture under vacuum and the dry mass extracted with hot petroleum ether (60-80°C, 50 ml). White crystals of the desired product were obtained by cooling the solution at room temperature.

3.5 Result and Discussion

All the compositions, formulae and the proposed structures of the newly synthesised compounds are drawn on the basis of the analytical data- supported well by the spectroscopic and other data available in our laboratory conditions. In some cases, data *e.g.*, ¹¹⁹Sn NMR could not be obtained due to lack of facilities.

3.5.1 Preparation of 2-marcapto isothiocyanate

The ligand used here was derived from 2-aminothiophenol with carbon disulphide and hydrazine hydrate. The 2-marcapto isothiocyanate was obtained in good yield. The products were recrystallized from ethanol. Sodium salt of the ligand was prepared by neutralization with equimolar methanolic solution of sodium hydroxide. The ligand 2-marcapto isothiocyanate was soluble in methanol, ethanol, chloroform, benzene but insoluble in petroleum ether (60-80°C) and had a sharp melting point. The synthetic detail and characterization data for LH and LNa are described in section 3.4.4.1 and 3.4.4.2. The formula of the ligand and the abbreviations of the complexes are presented in scheme 3.1.



1. Me_3SnL ; 2. $n\text{-Bu}_3\text{SnL}$; 3. Ph_3SnL ; 4. Bz_3SnL ; 5. $c\text{-Hex}_3\text{SnL}$
6. $\text{Me}_2\text{Sn}(\text{L})_2$; 7. $n\text{-Bu}_2\text{Sn}(\text{L})_2$; 8. $\text{Ph}_2\text{Sn}(\text{L})_2$; 9. $\text{Bz}_2\text{Sn}(\text{L})_2$

Scheme 3.1

3.5.2 Synthesis of tri- and diorganotin(IV) complexes 2-marcapto isothiocyanate

In this section the synthesis, characterization of tri- and di-organotin derivatives of 2-marcapto isothiocyanate are presented. Two different methods for the synthesis were adopted for the tri- and di-organotin complexes of the 2-marcapto isothiocyanate reported here. The objective was to compare the yields obtained by following two different synthetic routes. The procedures have been described in details in section 3.4.4.3-3.4.4.11.

3.5.2.1 Synthesis of triorganotin(IV) complexes of 2-marcapto isothiocyanate (LH)

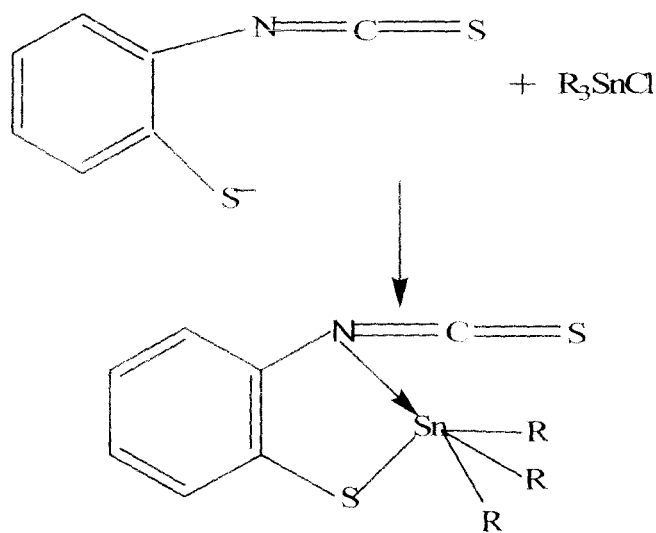
Method A:

The triorganotin(IV) derivatives of 2-marcapto isothiocyanate (R= Me, n-Bu, Ph, Bz, c-Hex) were obtained with moderate yields by the equimolar reaction of triorganotin(IV) chlorides with the sodium salt of the ligand in methanol as solvent.

The sodium salt of the ligand was generated by the addition of methanolic solution of NaOH to the methanolic solution of 2-mercapto isothiocyanate and stirred for 5h (Eq. 4 and Eq. 5).



The reactions were completed in 6-9h time. The solvents from the reaction mixture was distilled off to dryness and then the mass obtained subsequently extracted with hot petroleum ether (60-80°C) in quantities of 3-4 ml for 10 times. The synthetic methodology is described in scheme 3.2.



1. R = Me; 2. R = n-Bu; 3. R = Ph; 4. R = Bz; 5. R = c-Hex

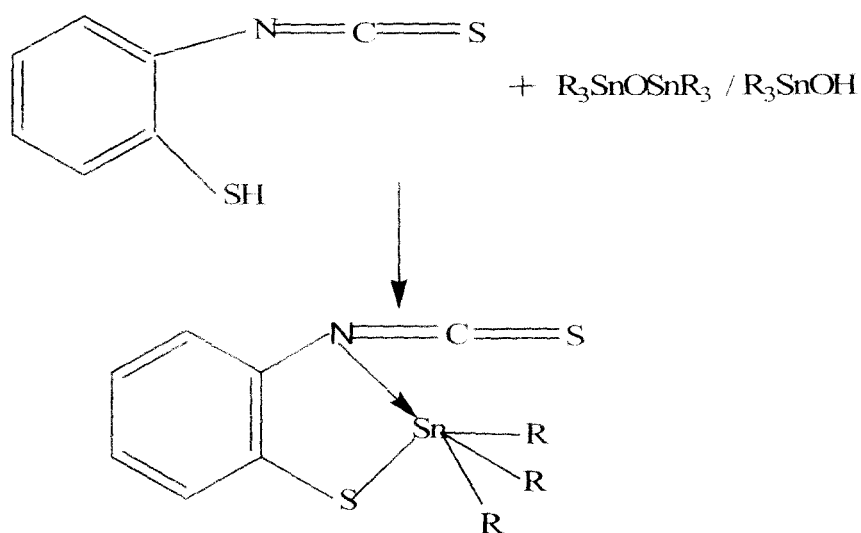
Scheme 3.2

3.5.2.2 Synthesis of triorganotin(IV) complexes of 2-mercapto isothiocyanate (LH)

Method B:

The triorganotin(IV) complexes of 2-mercapto isothiocyanate were synthesized by the reaction of the triorganotin oxides or hydroxides with the ligand in 1:2 or 1:1 molar ratio respectively (Eq. 6 and Eq. 7). Benzene was used as the solvent. The water produced during the reaction was removed using a Dean-Stark Trap to facilitate faster completion of the reactions. The compounds were obtained in

moderate to good yields. The solvents after the reaction was over in all cases were removed to obtain a dry mass which was then extracted with hot petroleum ether (60-80°C). The compounds are relatively stable in air and moisture and were recrystallized from suitable organic solvent. All the complexes were soluble in chloroform, methanol, benzene and petroleum ether (60-80°C). The synthetic methodology is described in scheme 3.3. The physical and analytical data are summarized in table 3.5



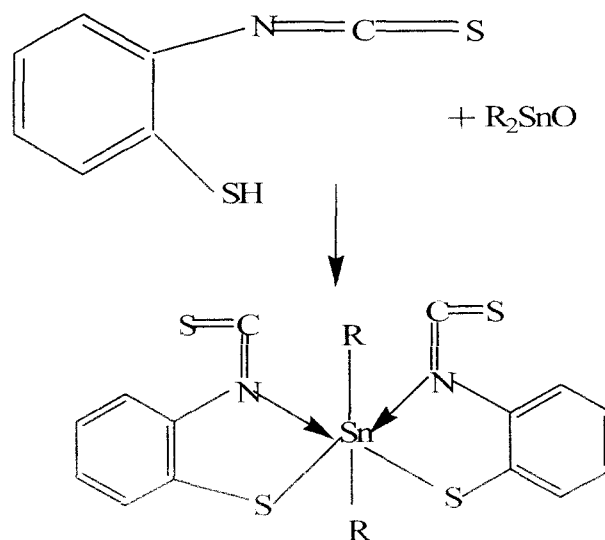
2. R= n-Bu; 3. R= Ph; 4. R=Bz

Scheme 3.3

3.5.2.3 Synthesis of diorganotin(IV) complexes of 2-mercapto isothiocyanate (LH)

The diorganotin(IV) complexes of 2-mercapto isothiocyanate were synthesized by the reaction of the diorganotin oxides with the ligand in 1:2 molar ratio in benzene as a solvent for refluxion (Eq. 8). The water produced during the reaction was removed using a Dean-Stark Trap to facilitate faster completion of the reactions. The compounds were obtained in moderate to good yields. The solvents after the reaction was over in all cases were removed by distillation to dryness and then extracted with hot petroleum ether (60-80°C). The compounds were relatively stable in air and moisture and recrystallized from suitable organic solvent. All the complexes

were found to be soluble in chloroform, methanol, benzene and petroleum ether (60-80°C). The synthetic methodology is described in scheme 3.4. The physical and analytical data are summarized in Table 3.5



6. R= Me; 7. R= n-Bu; 8. R= Ph, 9. R= Bz

Scheme 3.4

3.5.3 Spectroscopic characterization of tri-and diorganotin(IV) complexes

The complexes were characterized by IR, NMR (¹H and ¹³C) and elemental analysis.

3.5.3.1 Differential Scanning Calorimetric analysis

All the compounds have single sharp peak indicates the compounds are pure and this is the corresponding melting point of those compounds. The enthalpy of compound **3** was ($\Delta H_{\text{melting}} = 43.01 \text{ J/g}$). The enthalpy of compound **4** was ($\Delta H_{\text{melting}} = 52.88 \text{ J/g}$). Like as compound **5** ($\Delta H_{\text{melting}} = 2.53 \text{ J/g}$), compound **7** ($\Delta H_{\text{melting}} = 40747 \text{ J/g}$), compound **9** ($\Delta H_{\text{melting}} = 43.33 \text{ J/g}$), compound **8** ($\Delta H_{\text{melting}} = 64.14 \text{ J/g}$) were the enthalpy of the melting point.

3.5.3.2 IR Spectra

Selected IR band and their assignments for the tri- and di organotin complexes have been presented in Table 3.6. The infrared spectral data together with the stoichiometric composition of these organotin(IV) complexes suggested that the 2-mercapto isothiocyanate acts as mononegative S,N bidentate ligand, with the central tin (IV) coordinated to the deprotonated thiol S^- and isothiocyanate N atom. This mode of chelation was confirmed by NMR data also. The $\nu(\text{N}=\text{C})$, $\nu(\text{Sn}-\text{C})$ and $\nu(\text{C}-\text{S})$ bands were identified based on literature value [56,61,62]. The $\nu(\text{N}=\text{C})$ (of $\text{N}=\text{C}=\text{S}$ group) stretching vibrations of the ligands appear in the range $2082\text{--}2095\text{ cm}^{-1}$. These bands did not shift but slightly vary (not significant) upon complex formation. But in the new complexes a new band appears in the range between 795 cm^{-1} and 875 cm^{-1} indicating coordination of isothiocyanate ions to the metal [61] via the N atom. Hence it indicates the ligand to be a bidentate ligand through S and N coordinations. The $\nu(\text{SH})$ stretching in free 2-mercapto isothiocyanate occurs around 2680 cm^{-1} but after complex formation the band disappears indicating S atom's involvement in complex formation and confirms the deprotonation of the thiol group [63, 64]. The $\nu(\text{C}-\text{S})$ (of $\text{N}=\text{C}=\text{S}$ group) vibration in free ligand does not change significantly in the complex. It ($\nu(\text{C}-\text{S})$) appears around 748 cm^{-1} suggesting no coordination via S atom of $\text{N}=\text{C}=\text{S}$ group. The $\nu(\text{Sn}-\text{C})_{\text{asym}}$ and $\nu(\text{Sn}-\text{C})_{\text{sym}}$ bands have been identified tentatively at $540\text{--}600\text{ cm}^{-1}$ and $420\text{--}510\text{ cm}^{-1}$ respectively.

Table 3.5 Physical and analytical data for compounds 1-9

Composition	Yield	M.P/B.P(°C)	Elemental composition found (calcd)			
			C	H	N	Sn
1. C ₁₀ H ₁₃ NS ₂ Sn	75	69°C 10 ⁻² Torr	36.42 (36.39)	3.86 (3.97)	4.20 (4.24)	35.80 (35.9)
2. C ₁₉ H ₃₁ NS ₂ Sn	68	82°C 10 ⁻² Torr	50.32 (50.01)	6.87 (6.84)	3.02 (3.07)	25.92 (26.01)
3. C ₂₅ H ₁₉ NS ₂ Sn	65	91	58.08 (58.16)	3.76 (3.71)	2.74 (2.71)	22.77 (22.99)
4. C ₂₈ H ₂₅ NS ₂ Sn	60	81	60.18 (60.23)	4.31 (4.51)	2.54 (2.51)	21.02 (21.26)
5. C ₂₅ H ₃₇ NS ₂ Sn	63	67	56.42 (56.19)	7.08 (6.98)	2.60 (2.62)	22.05 (22.21)
6. C ₁₆ H ₁₄ N ₂ S ₄ Sn	59	162-166	39.75 (39.93)	2.90 (2.93)	5.80 (5.82)	24.46 (24.66)
7. C ₂₂ H ₂₆ N ₂ S ₄ Sn	70	84	46.59 (46.74)	4.60 (4.63)	4.90 (4.95)	20.84 (20.99)
8. C ₂₆ H ₁₈ N ₂ S ₄ Sn	62	160	51.34 (51.58)	2.93 (3.00)	4.65 (4.63)	19.52 (19.61)
9. C ₂₈ H ₂₂ N ₂ S ₄ Sn	67	101	53.33 (53.09)	3.48 (3.50)	4.36 (4.42)	18.58 (18.74)

Table 3.6 IR spectral data (cm⁻¹) for compounds 1-9

Compound	$\nu(\text{C}=\text{N})$	$\nu(\text{C}-\text{S})$	$\nu(\text{Sn}-\text{C})$
1.	2122(m)	725(w)	536(m), 513(w)
2.	2097(s)	725(m)	597(m), 505(w)
3.	2067(m)	729(s)	601(w), 447(s)
4.	2112(m)	756(s)	551(w), 447(m)
5.	2082(m)	725(m)	565(w), 417(w)
6.	2070(s)	752(m)	560(w), 420(w)
7.	2045(m)	752(m)	572(w), 420(w)
8.	2090(m)	747(m)	570(s), 454(m)
9.	2105(m)	756(m)	551(m), 424(w)

w, weak; m, medium; s, strong

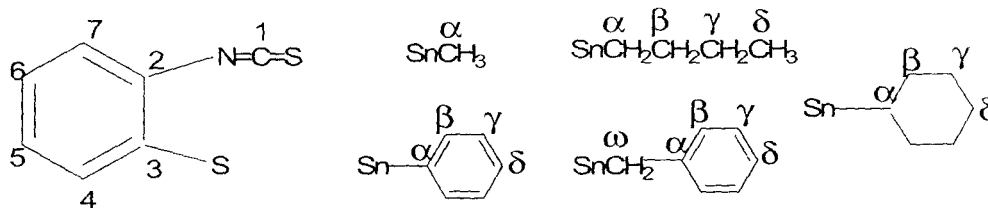
3.5.3.3 NMR Spectra

The ¹H NMR data for the tri- and di-organotin(IV) complexes of 2-mercapto isothiocyanates are presented in Table 3.7. The observed resonances were assigned on the basis of their integration and multiplicity patterns. The ligand and tin-bound organic group protons gave signals in the expected ranges [62, 65].

The spectrum of tribenzyl-, triphenyl-, dibenzyl-, diphenyl- compounds show complex patterns for the aromatic protons (both ligand and Sn-Ph appear in the same range of the spectra). In compounds **3**, **4**, **8** and **9** the C-H and aromatic protons appear as complex multiplets in the range 7.71 to 7.11, 7.68 to 6.86, 7.66 to 7.18, 7.68 to 6.98 respectively. The Sn-Me protons(**1**) appear as a sharp singlet at δ 0.65. The percentage s-character of the tin-methyl orbital has been related to the $^2J(^1\text{H}-^{119/117}\text{Sn})$ coupling constants [66]. The value of the coupling constant for $^2J(^1\text{H}-^{119/117}\text{Sn})$ is 57.69 Hz falls in the range of tetrahedral geometry in solution [67]. The Sn-nBu, Sn-cyhex and Sn-benzyl protons has been assigned satisfactorily and tabulated in Table 3.7.

The ^{13}C NMR data for the tri- and di-organotin(IV) complexes of 2-mercapto isothiocyanates are presented in Table 3.8 and 3.9. The number of ^{13}C signals found correspond with the number of magnetically non-equivalent carbon atoms in the complexes. The R groups attached to the tin atom have their signals in different specific regions in correspondence with the literature [68, 69]. The author was inclined to propose C-1 signal to be the most deshielded carbon atom followed by the C-7 carbon of the phenyl ring of the ligand. As can be seen from Table 3.9 the $J(^{119}\text{Sn}-^{13}\text{C})$ coupling constants range from 327.69-366.76 Hz for the alkyl compounds. These values are consistent with the values for similar compounds with a tetrahedral geometry in solution [70]. Therefore, ^1H and ^{13}C NMR spectral data reveal that the weak interaction between central tin and N(4) (as existing in the solid state supported by IR) weakens further in the solution, leading to the distorted tetrahedral pseudo-tetrahedral.

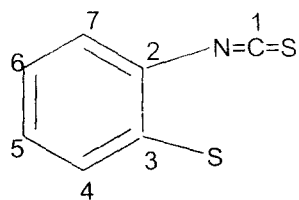
Table 3.7 ^1H NMR chemical shifts and coupling data (ppm and Hz) for compound 1-9^a



Compound	H-4	H-5	H-6	H-7	H- α	H- β	H- γ	H- δ	-CH ₂ (ω)
1.	7.64 (d, 1H) [8.1] ^e	7.34 (t, 1H) [7.8] ^e	7.22 (t, 1H) [8.7] ^e	7.72 (d, 1H) [8.1] ^e	0.65 (s, 9H) [57.62] ^b	-	-	-	-
2.	7.67 (d, 1H) [8.1] ^e	7.34 (t, 1H) [8.4] ^e	7.22 (t, 1H) [7.8] ^e	7.70 (d, 1H) [8.1] ^e	1.70- 1.60 (m, 6H)	1.64- 1.60 (m, 6H)	1.46- 1.25 (m, 6H)	0.85- 0.69 (t, 9H) [15.3] ^d	-
3.	7.60 (d, 1H) [8.1] ^e	7.32 (t, 1H) [8.1] ^e	7.20 (t, 1H) [8.1] ^e	7.68 (d, 1H) [8.1] ^e	-	multiplet at centre 7.39 and 7.04 (m, 15H)			-
4.	7.68 (d, 1H) [8.1] ^e	7.40 (t, 1H) [8.1] ^e	7.27 (t, 1H) [8.1] ^e	7.72 (d, 1H) [8.1] ^e	-	7.24- 7.09 (m, 6H)	7.14- 7.02 (m, 6H)	6.86 (m, 3H)	2.81- 2.51 (s, 6H) [63.6] [65.7] ^c
5.	7.64 (d, 1H) [7.5] ^e	7.36 (t, 1H) [8.4] ^e	7.23 (t, 1H) [8.4] ^e	7.69 (d, 1H) [9.0] ^e	1.30 (m, 3H)	2.03- 1.47 (m, 12H)	1.75- 1.47 (m, 12H)	1.33- 1.24 (m, 6H)	-
6.	7.61 (d, 2H) [8.1] ^e	7.38 (d, 2H) [8.1] ^e	7.25 (d, 2H) [8.1] ^e	7.65 (d, 2H) [8.1] ^e	0.85 (s, 6H) [70.8] ^b	-	-	-	-
7.	7.65 (d, 2H) [8.1] ^e	7.40 (t, 2H) [8.1] ^e	7.28 (t, 2H) [8.1] ^e	7.69 (d, 2H) [8.1] ^e	1.92- 1.86 (m, 4H)	1.84- 1.76 (m, 4H)	1.40 (m, 4H)	0.82 (t, 6H) [7.2] ^d	-
8.	7.59 (d, 2H) [8.1] ^e	7.31 (t, 2H) [8.4] ^e	7.18 (t, 2H) [8.1] ^e	7.66 (d, 2H) [8.1] ^e	-	7.72- 7.74 (m, 4H)	7.35 (m, 4H)	7.44 (m, 2H)	-
9.	7.65 (d, 2H) [8.1] ^e	7.34 (t, 2H)	7.29 (t, 2H)	7.68 (d, 2H) [8.1] ^e	-	7.29- 7.24 (m, 4H)	7.0 (m, 4H)	6.98 (m, 2H)	3.34 (s, 4H) [84.6] ^c

^a Spectra recorded in CDCl₃ downfield to TMS; Multiplicity is given as s, singlet; d, doublet; t, triplet; m, multiplet; ^b $^2J(^1\text{H}-^{119/117}\text{Sn})$ Hz, ^c $^2J(^1\text{H}-^{119/117}\text{Sn})$ Hz, ^d $^4J(^1\text{H}-^{119/117}\text{Sn})$ Hz, ^e $^2J(^1\text{H}-^1\text{H})$ Hz.

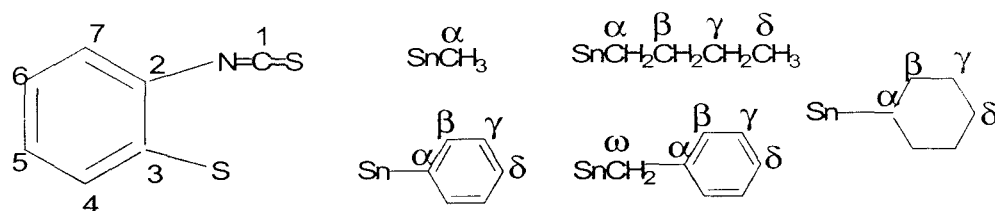
Table 3.8 ^{13}C NMR chemical shifts and coupling data (ppm and Hz) for compound **1-9**^a ligand portion.



Compound	C-1	C-2	C-3	C-4	C-5	C-6	C-7
1.	172.66	131.13	130.12	142.47	129.15	125.66	158.37
2.	168.10	125.59	123.64	137.75	120.77	120.52	153.46
3.	167.50	137.07	129.81	138.98	123.89	120.95	152.72
4.	168.04	125.84	123.93	137.79	120.96	120.45	152.95
5.	168.19	125.57	123.54	138.09	120.76	120.43	153.54
6.	170.43	127.23	124.71	140.34	121.42	112.95	152.21
7.	172.89	126.07	123.85	137.13	121.24	119.16	151.39
8.	168.23	138.17	130.48	139.01	120.95	120.22	152.72
9.	168.35	125.12	123.95	137.13	121.08	120.80	152.55

^a Spectra recorded in CDCl_3 solution, downfield to TMS;

Table 3.9. ^{13}C NMR chemical shifts and coupling data (ppm and Hz) for **1-9**^a
 R_3Sn portion [R= $-\text{CH}_3$ or $-(\text{CH}_2)_3\text{CH}_3$, or $-\text{CH}_2\text{C}_6\text{H}_5$ or $-\text{C}_6\text{H}_{12}$] and R_2Sn
portion [R= $-(\text{CH}_2)_3\text{CH}_3$, or $-\text{C}_6\text{H}_5$ or $-\text{CH}_2\text{C}_6\text{H}_5$].



Compound	C- α	C- β	C- γ	C- δ	$-\text{CH}_2(\omega)$
1.	2.55 [366.76,350.16] ^b	-	-	-	-
2.	16.42 [334.33,327.69] ^b	27.06 [65.84] ^c	28.69 [22.46] ^d	13.72	-
3.	138.50	136.80 [47] ^c	128.80 [62.2] ^d	124.01 [13.5] ^e	-
4.	139.77 [42.26] ^b	127.83 [30.20] ^c	128.65 [16.60] ^d	124.42 [10.56] ^e	24.68 [288.31,275.48] ^f
5.	33.48 [277.74] ^b	31.90 [16.60] ^c	29.50 [64.90] ^d	26.90	-
6.	5.45 [549.84] ^b	-	-	-	-
7.	28.99 [370.22] ^b	28.02 [36.22] ^c	25.61 [101.13] ^d	13.69	-
8.	125.86 [297.37] ^b	136.78 [46.03] ^c	128.81 [60.38] ^d	123.89 [10.51] ^e	-
9.	138.97 [40.23] ^b	128.09 [29.27] ^c	128.51 [16.62] ^d	124.66 [10.41] ^e	30.99 [289.33,276.43] ^f

^a Spectra recorded in CDCl_3 solution, downfield to TMS; ^b $^1\text{J}(^{119}\text{Sn}-^{13}\text{C})$ in Hz, ^c $^2\text{J}(^{119}\text{C}-^{13}\text{C})$ in Hz, ^d $^3\text{J}(^{119}\text{Sn}-^{13}\text{C})$ in Hz, ^e $^4\text{J}(^{119}\text{Sn}-^{13}\text{C})$ in Hz, ^f $^2\text{J}(^{119}\text{Sn}-^{13}\text{C})$ in Hz.

In spite of the best effort the compounds did not yield crystals suitable for X-ray crystal structure determination. Therefore, in the absence of such data some inference on the composition and the probable structures of the synthesized compounds were done on the basis of analytical data, IR and ^1H and ^{13}C spectra only. The literature data is also very limited for this type of complexes.

The compounds **1-5** are formulated as R_3SnL and **6-9** are the $\text{R}_2\text{Sn}(\text{L})_2$ type respectively. On the basis of the spectral data the structure for R_3SnL type a trigonal bipyramidal displaying a pentacoordinate Sn atom may be suggested where a chelated bidentate isothiocyanate moiety is indicated (Fig. 3.16).

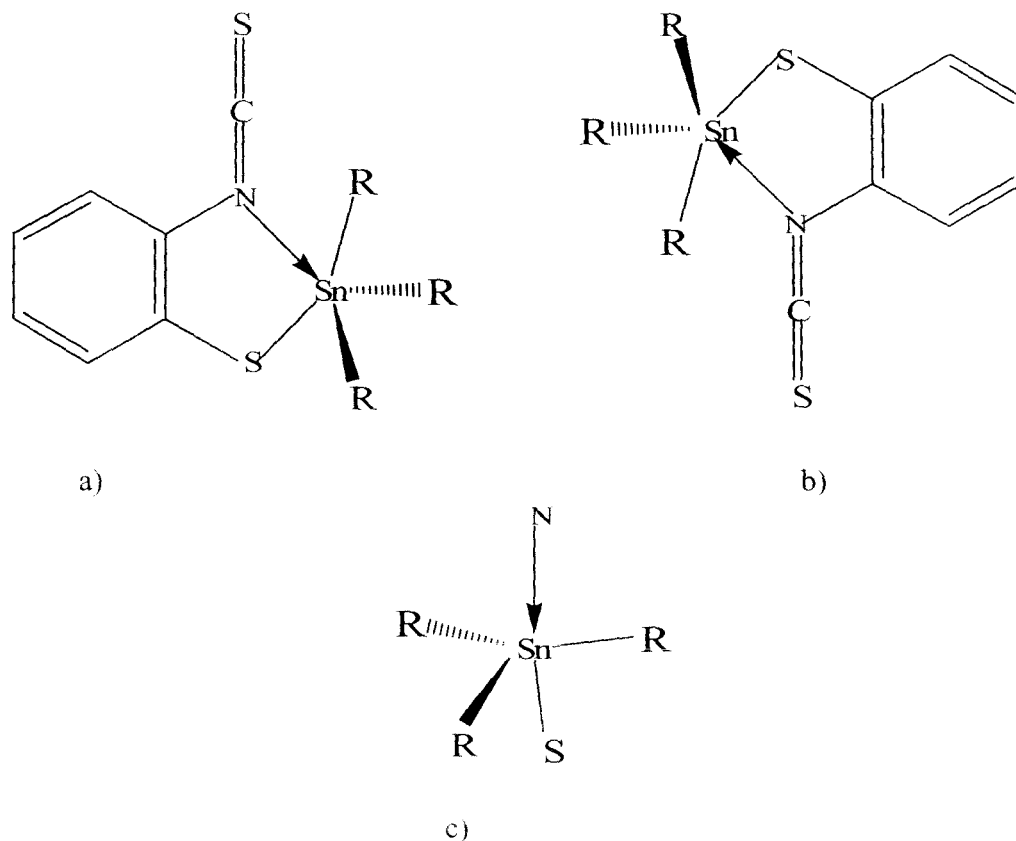


Fig. 3.16 a), b), and c) Proposed structure of compounds **1-5** formulated as R_3SnL .

For the $R_2Sn(L)_2$ type, on the other hand, an octahedral disposition around the hexacoordinate Sn atom is a likely proposition. Hence the structures may be drawn as follows: (Fig. 3.17).

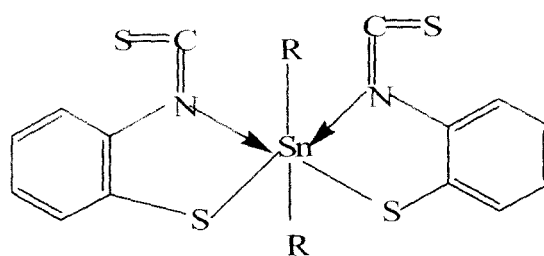


Fig. 3.17 Proposed structure of compounds **6-9** formulated as $R_2Sn(L)_2$.

3.5.3.4 A brief note on Crystal structure of compound **B**

Compound (**B**) is formed by discrete molecule in which the tin atom is bound to the sulphur atom. This together with benzyl (**B**) groups constitutes a distorted

tetrahedron around the metal atom. The maximum acuteness of C-Sn-S bond angles are observed to be $96.9(2)^\circ$ [C(14)-Sn(1)-S(1) in **B**]. The proximity of the carbonyl group (C=O) to the sulphur atom is most probably responsible for the acuteness of the angles. It appears that there is neither Sn(1)-O(1) nor Sn(1)-N(1) intra- or inter atomic interactions present in the molecules. The O(1)-C(5) bond length 1.221(9) Å and N(1)-C(5) 1.309(10) Å bond length in **B** respectively correspond well for uncoordinated C=O and C-N [71] confirming further the mono-dentate mode of coordination of the ligand. On the other hand, the largest deviations observed for C-Sn-C angles being $112.7(3)^\circ$ [C(17)-Sn(1)-C(14) in **B**]. The Sn(1)-S(1) bond lengths 2.430(2) Å is only slightly larger than that of the sum of the covalent radii 2.42 Å of Sn and S [72].

3.6 References

1. *Tin Chemistry: Fundamentals, Frontiers, and Applications* Edited by Gielen M, Davies AG, Pannel K, Tiekink ERT. John Wiley & Sons, Ltd. 2008.
2. Musgrave MJP. *Proc.Roy.Soc.*1963; **227A**: 503.
3. <http://www.plastics.com/articles/10/3/RIGID-PVC-EXTRUSION-HANDBOOK-RAW-MATERIALS-SELECTION> 2007.
4. Davies AG, Smith PJ. *Comprehensive Organometallic Chemistry*, Pergamon Press, New York, 1982.
5. Willem R, Biesemans M, Boualam M, Delmotto A, El-Khloufi A, Gielen M. *Appl. Organomet. Chem.* 1993; **7**: 311.
6. Davies AG, *Organotin Chemistry*, Wiley-VCH, Verlag, GmbH & Co., KGaA, Weinheim, 2004.
7. Hänssgen D, Reuter P, Döllein G. *J.Organomet.Chem.* 1986; **317**: 159.
8. D'yachenko OA, Zolotoi AB, Atovmyan LO, Mirskov RG. *Dokt. Phys. Chem.* 1988; **27**: 4636.
9. Kersch S, Wrackmeyer B. *Z. Naturforsch.*1987; **42B**: 387.
10. Batchelor RJ, Einstein FWB, Jones CHW, Sharma RD. *Inorg. Chem.* 1988; **27**: 4636.
11. Menzebach B, Bleckmann P. *J. Organomet. Chem.*1975; **91**: 291.
12. Farina Y, Baba I, Othman AH, Razak IA, Fun HK, Ng SW. *Acta Crystallogr.Sect. E.* 2001; **E57**: m37.
13. Puff H, Gattermayer R, Hundt R, Zimmer R. *Angew. Chem. Int. Ed. Engl.*1977; **16**: 547.
14. Lange H, Herzog H, Böhme U, Rheinald G, *J. Organomet Chem.* 2002; **660**: 43.
15. Davies AG, Harrison PG. *J. Chem. Soc. (C).* 1970; 2035.
16. Beckmann J, Dakternieks D, Duthie A, Jones C, Jurkschat K, Teckink ERT. *Main Group Metal Chem.* 2002; **25**: 77.
17. Capozzi G, Menichetti S, Ricci A, Taddei M. *J. Organomet. Chem.* 1988; **344**: 285.
18. Stalke D. *Proc. Indian Acad. Sci. (Chem. Sci.).* 2000; **112**: 155.
19. Singh HL, Varshney AK, *Bioinorg. Chem. Appl.* 2006; 2006: 23245.
20. Peach ME. *Can. J. Chem.* 1968; **46**: 211.

21. Bratspies GK, Smith JF, Hill JO, Derrick PJ. *J. Thermal Analysis*. 1979; **16**: 369.
22. Xanthopoulou MN, Hadjikakou SK, Hadjiliadis N, Schürmann M, Jurkschat K, Michaelides A, Skoulika S, Bakas T, Binolis J, Karkabounas S, Charalabopoulos K. *J. Inorg. Biochem.*. 2003; **96**: 425.
23. Rehman Z, Shahzadi S, Ali S, Jin GX. *Turk. J. Chem.* 2007; **31**: 435.
24. Munguia T, Cervantes-Lee F, Párkányi L, Pannell KH.
Organotin-Sulfur Intramolecular Interactions. In: An Overview of Current and Past Compounds and the Biological Implications of Sn---S Interactions
Modern Aspects of Main Group Chemistry Chapter 30, *ACS Symposium Series*, Publication Date (Print): December 01, 2005; **917**: 422.
25. Engel G, Mattern G. *Z. Kristallogr.* 2008; **223**: 465.
26. Ma C, Jiang Q, Zhang R.. *Can. J. Chem.* 2003; **81**(7): 825.
27. Haiduc I, Silvestru C, Roesky HW, Schmidt HG, Noltemeyer M. *Polyhedron*.1993; **12**: 69.
28. Silvestru C, Haiduc I, Klima S, Thewalt U, Gielen M, Zuckerman JJ
J. Organomet. Chem. 1987; **327**: 181.
29. Ramirez RG, Toscano RA, Silvestru C, Haiduc I. *Polyhedron*. 1996; **15**: 3857.
30. Silvestru A, Drake JE, Yang J. *Polyhedron*. 1997; **16**: 4113.
31. Dumitrescu LS, Haiduc I, Weiss J. *J. Organomet. Chem.* 1984; **263**: 159.
32. Cea-Olivares R, Lomelí V, Hernández-Ortega S, Haiduc I. *Polyhedron*. 1995; **14**: 747.
33. Dunstan PO. *Thermochimica Acta*. 2000; **345**: 117.
34. Dunstan PO. *Thermochimica Acta*. 2001; **369**: 9.
35. Smith FE, Ee Kl. *Cellular and Molecular Life Sciences*. 1980; **36**: 391.
36. Lozano-Lewis LI, John-Rajkumar SV, Islas SA, Pike RD, Rabinovich D. *Main Group Chem.* 2007; **6**: 133.
37. Teoh SG, Teo SB, Lee LK, Arifin Z, Ng SW. *J. Coord. Chem.* 1995; **34**: 253.
38. Singh R, Kaushik NK. *Spectrochimica Acta Part A*. 2008; **65**: 950.
39. Singh R, Kaushik NK. *Spectrochim Acta Part A. Molecular and Biomolecular Spectroscopy*. 2008; **71**: 669.
40. Singh RV, Joshi SC, Gajraj A, Nagpal P. *Appl. Organomet Chem.* 2002; **16**: 713.
41. Nath M, Sulaxna, Song X, Eng G. *J. Organomet Chem.* 2006; **691**: 1649.

42. Nath M, Sulaxna, Song X, Eng G. *Spectrochimica Acta Part A*. 2006; **64**: 148.
43. Nath M, Sulaxna, Song X, Eng G, Kumar A. *Spectrochim Acta Part A. Molecular and Biomolecular Spectroscopy*. 2008; **71**: 766.
44. Shahzadi S, Saqib Ali S, Fettouhi M. *J Chem Crystallogr*. 2008; **38**: 273.
45. Chauhan HP, Shaik NM. *J. Inorg. Biochem*. 2005; **99**: 538.
46. Holmes RR. *Acc. Chem. Res*. 1989; **22**: 190.
47. Schmid CG, Day RO, Holmes RR. 5th International Symposium on Inorganic Ring Systems, Amherst, MA, Aug 1988; No. 11, 8; *Phosphorus, Sulfur, Silicon* 1989; **41**: 69.
48. The following drawings were reprinted with permission from the source indicated. [(n-BuSn(S)OP-(OH)(O-t-Bu)₂)₃S] [O₂P(O-t-Bu)₂].2H₂S.H₂O: ref 46. Copyright 1989 Gordon and Breach Science Publishers. Cube center and core structure of [{n-BuSnS(O₂PPh₂)₃O]₂Sn: ref 48. Copyright 1988 American Chemical Society. [(n-BuSn)₃(S)(O)(O₂CPh)₅]: ref 46. Copyright 1989 Gordon and Breach Science Publishers.
49. Kumara Swamy KC, Day RO, Holmes RR, *J. Am. Chem. Soc.* 1988; **110**: 7543.
50. Day RO, Kumara Swamy KC, Schmid CG, Holmes RR. 5th International Symposium on Inorganic Ring Systems, Amherst, MA, Aug 1988; No. P-12. 31.
51. Wang LS, Sheng TL, Zhang JJ, Hu SM, Fu RB, Wu XT, Li YM, Huang XH. *J. Coord. Chem*. 2006; **59**: 1991.
52. Evans CJ, Karpel S. Organotin compounds in modern technology, Adv. In: *Organometal Chem*. 1985,16.
53. Lockhart TP. *Organometallics*. 1988; **7**: 1438.
54. Sarkar B, Choudhury B, Sen Sharma M, Kamruddin SK, Choudhury AK, Roy A. *Archv. Phytopath. Plant Prot*. 2009 **(In Press)** DOI: 10.1080/03235401003633667.
55. Sarkar B, Choudhury AK, Roy A, Biesemans M, Willem R, Ng SW, Tiekink ERT. *Appl. Organomet. Chem*. 27 JUL 2010. DOI: 10.1002/aoc.1698.
56. Holloway JH, McQuillan GP, Ross DS. *J. Chem Soc. (A)*. 1969; 2505.
57. Kamruddin Sk. Ph.D Thesis, University of North Bengal, West Bengal, India 1996.
58. Sisido K, Takeda Y, Kinugawa Z. *J. Am. Chem. Soc*. 1961; **83**: 538.

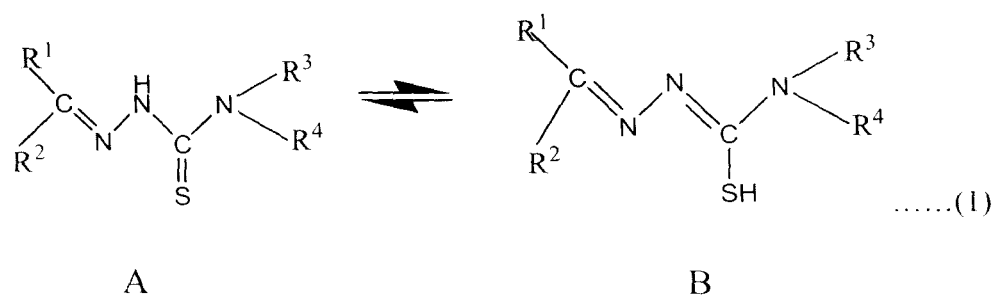
59. Sheldrick GM, SHELXS-86 Program for crystal structure determination, University of Gottingen, Gottingen, Germany (1986) *Acta Crystallogr.* 1990; **A35**: 467.
60. Johnson CK. ORTEP. Report ORNL-5138; Oak Ridge National Laboratory, TN, 1976.
61. Socrates G. Infrared and Raman Characteristic Group Frequencies Tables and Chart. 3rd Ed., John Wiley and Sons Ltd., 2001.
62. Sen Sharma M, Mazumder S, Ghosh D, Roy A, Duthie A, Tiekink ERT. *Appl. Organomet. Chem.* 2007; **21**: 890.
63. Bellamy LJ. The Infrared Spectra of Complex molecules, 3rd Ed., Chapman and Hall, London, 1975.
64. Demertzi DK, Tauridou P, Russo U, Gielen M. *Inorg. Chim. Acta.* 1995; **239**: 177.
65. Sahu RK, Magan A, Gupta B, Sondhi SM, Srimal RC, Patnaik GK. *Phosphorus, Sulfur and Silicon and the related Elements.* 1994; **88**: 45.
66. Eng G, Song X, Duong Q, Strickman D. *Appl. Organomet. Chem.* 2003; **17**: 218.
67. Song X, Zapata A, Hoerner J, de Dios AC, Casablanca L, Eng G. *Appl. Organomet. Chem.* 2007; **21**: 545.
68. Ali S, Khokhar MN, Bhatti MH, Mazhar M, Masood MT, Shahid K, Badshah A. *Synth. React. Inorg. Met.-Org. Chem.* 2002; **32**: 1373.
69. Ahmad F, Ali S, Parvez A, Munir A, Mazhar M, Khan KM, Shah TA. *Heteroatom. Chem.* 2002; **13**: 638.
70. Holecek J, Lycka A. *Ing. Chim. Acta.* 1986; **118**: L15.
71. *Handbook of Chemistry and Physics*, Ed. Weast RC, Chemical Rubber Co., Ohio, 57th Edition (1976-1977) F216.
72. Bravo J, Cordero MB, Casas JS, S'anchez A, Sordo J, Castellano EE, Zuckerman-Schpector J. *J. Organomet. Chem.* 1994; **482**: 147.

CHAPTER 4

**SYNTHESIS, SPECTROSCOPIC CHARACTERIZATION
AND X-RAY CRYSTAL STRUCTURES
OF SOME DIORGANOTIN(IV) COMPLEXES OF
SALICYLALDEHYDE THIOSEMICARBAZONE
AND RELATED LIGANDS**

4.1 Introduction

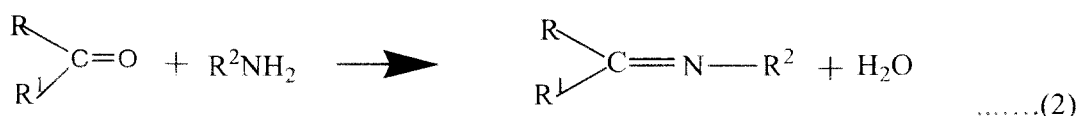
The organotin complexes have been the subject of interest for years because of their versatile bonding modes [1, 2] as well as their commercial [3] and agricultural applications [4-6]. An important class of organotin(IV) complexes are those derived from Schiff bases. Schiff bases continue to occupy an important position as ligands in metal coordination chemistry even after almost a century since their discovery [7]. Schiff bases with organotin (IV) moieties have received considerable attention with respect to their potential applications in antimicrobial activity, medicinal chemistry and biotechnology [8-16]. These classes of compounds for their biological activities including antitumor activities have been attracting our attention [15, 17-21]. Schiff base complex exhibits catalytic activity towards electro-reduction of oxygen [22]. Some metal complexes of a polymer bound Schiff base show catalytic activity on decomposition of hydrogen peroxide and oxidation of ascorbic acid [23]. Schiff base in neutral and deprotonated forms react with organotin(IV) moieties and the complexes that are formed exhibit variable stoichiometry and different modes of coordination [24, 25]. Schiff bases continue to attract attention as they are known to be capable of stabilizing uncommon oxidation states, [26-29] to give rise to unusual coordination numbers and redox reactions [30-32] in their transition metal complexes. Thiosemicarbazones are thiourea derivatives and the studies on their chemical and structural properties have received much attention due to the widespread application in different fields. Thiosemicarbazones, with the general formula $R^1R^2C=N-NH-C(S)-NR^3R^4$, generally exist in the thione form in the solid state but exist in equilibrium mixture of thione and thioneol tautomarism forms in solution (A and B, in Eq. 1) which is essential for their versatile chelating behavior. [33]



As mentioned earlier the chemistry of thiosemicarbazone complexes has gained considerable attention due to their significant biological activities. The biological activity of certain thiosemicarbazones is believed to be due to the ability to form terdentate chelates with organotin(IV) compounds, bonding through oxygen, nitrogen and sulphur atoms. [15] A brief survey on the relevant literatures is presented below.

4.2 Literature

Schiff base ligands, which are the condensation products of primary amines and aldehydes or ketones ($\text{RCH}=\text{NR}'$, where R & R' represents alkyl and / or aryl substituents) (Eq. 2) [34], since their synthesis was first reported by Schiff [35].



In 1970, Dayagi and Degani had reviewed the other methods of synthesis of the Schiff bases [36]. Organotin(IV) complexes of Schiff base moieties had been reported and reviewed [7-8, 37-39]. In 2006, Sen Sharma *et al.* [40] have reported mononuclear organotin complexes of the Schiff base where the Schiff base acts either as a dianionic tridentate or as a monobasic bidentate moiety and coordinating through an alkoxy group. Di- μ_2 -methoxo-bis[benzyl{5-chloro-2-oxido-benzaldehyde thiosemicarbazonato}tin(IV)] was obtained from the reaction of Bz_2SnCl_2 and the sodium salt of 5-chlorosalicylaldehyde thiosemicarbazone where debenylation had taken place because sometimes, solvent may be the strongest nucleophilic agents. In presence of polar nucleophilic solvent such as methanol or acetic acid the nucleophilic assistance is rendered by coordination of the solvent to the tin atom there by increasing the polarity of Sn-C bonds and hence debenylation occur [41]. They have also reported another nine compounds of Schiff bases derived from salicylaldehyde/substituted salicylaldehyde and thiosemicarbazide. The compounds, with general formulae $[\text{R}_2\text{Sn}(\text{OArCH}=\text{N}-\text{N}=\text{CSNH}_2)]$, where R= Me, n-Bu, Ph and Ar= $-\text{C}_6\text{H}_4$, $-\text{C}_6\text{H}_3(-5\text{Cl})$, $-\text{C}_6\text{H}_3(-5\text{Br})$, were characterized by UV, IR and NMR (^1H , ^{13}C , ^{119}Sn) spectroscopy and elemental analysis. The X-ray crystallographic studies of five of these complexes indicate penta-coordination of tin within a distorted C_2NOS

trigonal bipyramidal geometry in each case. The biological activity of these compounds against fungal pathogens, and some bacteria were investigated. Their cytotoxicity was also investigated against several human cancer cell lines [15].

In 1980, Saxena *et al.* [42] have synthesized the inorganic tin(IV) derivatives of ligands derived from dithiocarbazic acids and to study their stereochemistry along with their biological activity. In 1982, tin(IV) complexes of tridentate dithiocarbazate Schiff bases have been synthesized by Saxena *et al.* [43] and characterized by their elemental analyses and UV, IR, ^1H NMR, and Mössbauer spectroscopies and X-ray powder diffraction. Complexes having the general formulae, $\text{Sn}(\text{OCOCH}_3)_2\text{L}$, where $\text{L} =$ dianion of S-benzyl- β -N-(2-hydroxyphenyl) methylene and methyl dithiocarbazate (Fig. 4.1), are five-coordinated in distorted trigonal bipyramidal geometry, whereas complexes of the type SnL_2 show hexa-coordination around the tin atom which is arranged in a distorted octahedral geometry with an orthorhombic lattice.

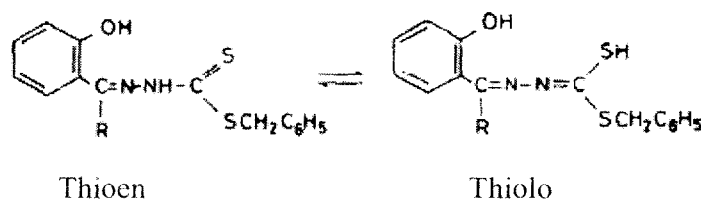


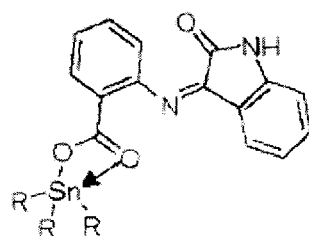
Fig. 4.1 Thioen and Thiolo tautomerism of ligand L [43].

In 1984, Saxena and Tendon have synthesized five- and six- coordinated di- and tri-n-butyl tin(IV) semi- and thio-semi carbazates. The characterization of these complexes, by IR, NMR (^1H , ^{13}C , ^{119}Sn), ^{119}Sn Mössbauer and mass spectroscopies along with X-ray diffraction, reveals that complexes of bionic ligands of the type $\text{Bu}_2\text{SnL}''$ [$\text{L}'' = (\text{o-HO})\text{C}_6\text{H}_4\text{CHNN}=\text{C}(\text{SH})\text{NH}_2$] are five-coordinated having trigonal bipyramidal geometry. However, complexes of monoionic ligands of the type $\text{Bu}_2\text{SnL}'_2$ [$\text{L}' = \text{C}_6\text{H}_5\text{CHNN}=\text{C}(\text{SH})\text{NH}_2$] are six-coordinated in a distorted cis-octahedral geometry and $\text{Bu}_3\text{SnL}'$ are five-coordinated with a trigonal bipyramidal structure. X-ray structural studies on the compound $\text{Bu}_2\text{Sn}(\text{O.C}_6\text{H}_4.\text{CH:N.N.CS.NH}_2)$, show that it crystallizes in a monoclinic lattice [44].

They also have synthesized five- and six-coordinated di- and tri-n-butyl tin(IV) complexes of the type Bu_2SnL , Bu_2SnL_2 and Bu_3SnL (where L is the anion of a monofunctional bidentate or bifunctional tridentate Schiff base) and characterized

them on the basis of microanalyses, molecular weight determinations, IR, NMR (^1H , ^{13}C , ^{119}Sn) and ^{119}Sn Mössbauer spectroscopy. These complexes are highly active towards bacteria [7].

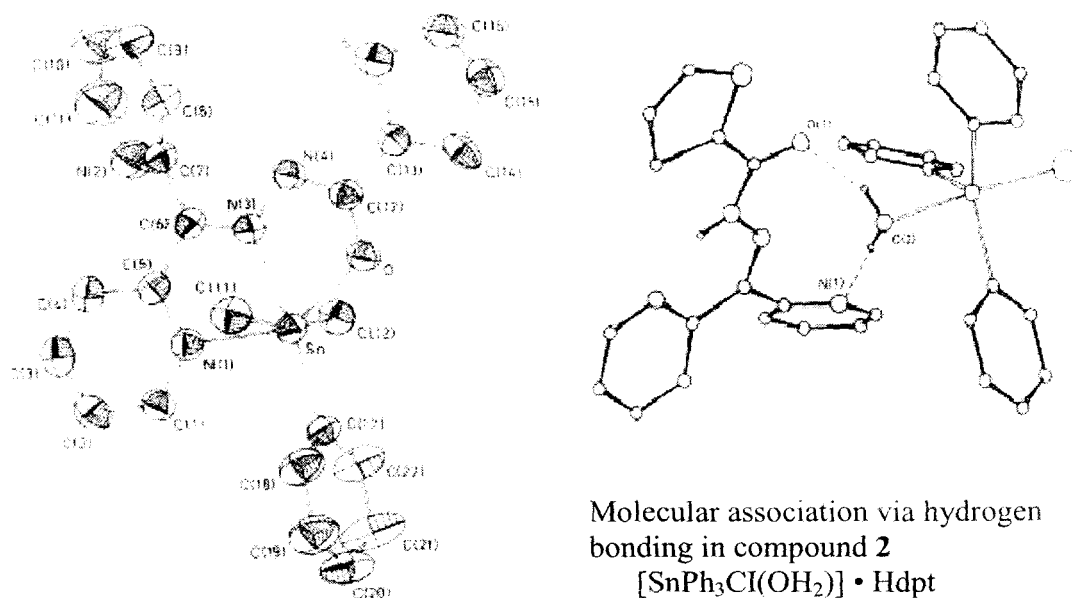
In 2009, J. Khan and his coworkers [45] have prepared organotin (IV) complexes with the general formulae R_3SnL (R: Me, Ph and Bz; and L: [2-{2-oxoindolin-3-ylideneamino}benzoic acid] which is derived from indoline-2,3-dione and 2-aminobenzoic acid) (Fig. 4.2) and their antibacterial activity was investigated by using the agar well diffusion methods. The synthesized compounds were capable of showing biocidal activity against *Staphylococcus aureus*. The order of increasing activities was: ligand $< \text{Me}_3\text{SnL} < \text{Bz}_3\text{SnL} < \text{Ph}_3\text{SnL}$. On the basis of (^1H , ^{13}C) NMR, IR and elemental analysis the trigonal bipyramidal geometry is proposed for the synthesized compounds.



R= Me, Ph and Bz

Fig. 4.2 Structure of Schiff base L and its complexes [45].

Carcelli *et al.* [46] synthesized two organotin compounds i.e $[\text{SnPh}(\text{dpt})\text{Cl}_2]$ (**1**) and $[\text{SnPh}_3\text{Cl}(\text{OH}_2)] \cdot \text{Hdpt}$ (**2**) (Hdpt = di-2-pyridylketone 2-thenoylhydrazone) (Fig. 4.3) which were characterized by IR spectroscopy and X-ray diffraction. Hdpt behaves differently in the two compounds: it is deprotonated and ONN tridentate in **1** and uncoordinated in **2**, where pairs of hydrogen-bonded $[\text{SnPh}_3\text{Cl}(\text{OH}_2)]$ and Hdpt molecules are present. The tin environment is octahedral in **1** and trigonal bipyramidal in **2**. Compound **2** has shown good antimicrobial activity against gram-positive bacteria and moulds *in vitro*. Neither compound showed genotoxic properties.



Structure of Compound **1** $[\text{SnPh}(\text{dpt})\text{Cl}_2]$

Fig. 4.3 Structure of the compounds **1** and **2** [46].

In 1997, they also reported that the reactivity of the polydentate ligands bis(2-acetylpyridine) corbanohydrazone (H_2apc) and 2-acetylpyridine semicarbazone (Haps) as well as of their sulphur containing analogous bis(2-acetylpyridine) thiocarbonohydrazone (H_2apt) and 2-acetylpyridine thiosemicarbazone (Hapts) was investigated towards organotin compounds. An X-ray crystal structure determination carried out on $\text{Ph}_2\text{Sn}(\text{Hapt})\text{Cl} \cdot \text{H}_2\text{O}$ (**1**) (Fig. 4.4) and $(n\text{-Bu})_2\text{Sn}(\text{apts})(\text{OAc})$ (**5**) revealed that in both compounds the hydrazonic ligand was terdentate via a sulphur atom and two nitrogen atoms. The tin atom was six-coordinated in **1** and seven-coordinated in **5**. The similarities observed in the IR and ^1H NMR spectra are indicative of a similar behavior of the ligand in the complexes, thus suggesting a six-coordinated tin in the chloro derivatives and a seven-coordinated tin in the acetato-ones [47].

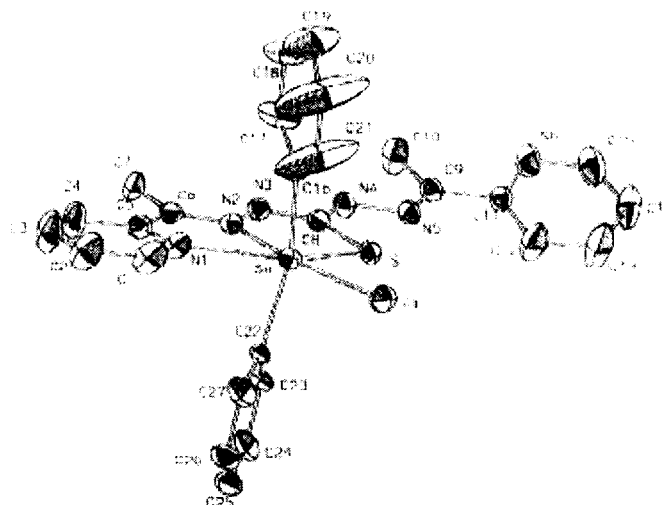


Fig. 4.4 Structure of Compound 1 $\text{Ph}_2\text{Sn}(\text{Hapt})\text{Cl}\cdot\text{H}_2\text{O}$ [47].

In 2003, Carcelli *et al.* [48] have also synthesized and spectroscopically characterized the new potentially hexadentate ligand (2,9-diformylphenanthroline) bis(benzoyl) hydrazone (H_2L). It reacted with dibutyltin diacetate giving the complex $[(\text{C}_4\text{H}_9)_2\text{SnL}]$ (Fig. 4.5). The X-ray crystal structure of the complex belonged to the monoclinic system and the systematic absences identified the correct space group as $\text{P}2_1/\text{c}$. Its spectroscopic characterization does not show any remarkable aspects: it is possible to note that, in solution, the molecule shows C_{2v} symmetry and, accordingly, only one set of signals is present in the ^1H NMR spectrum. The IR spectrum suggests a complete deprotonation of the ligand and the coordination of the hydrazonic $\text{C}=\text{O}$ groups, in fact the $\nu(\text{N}-\text{H})$ and $\nu(\text{C}=\text{O})$ bands disappear. These data are confirmed by the ^1H NMR spectrum, where the $\text{N}-\text{H}$ proton signals disappear and the aldehyde protons undergo an upfield shift. The resonances of the alkyl groups linked to the tin are present at high fields.

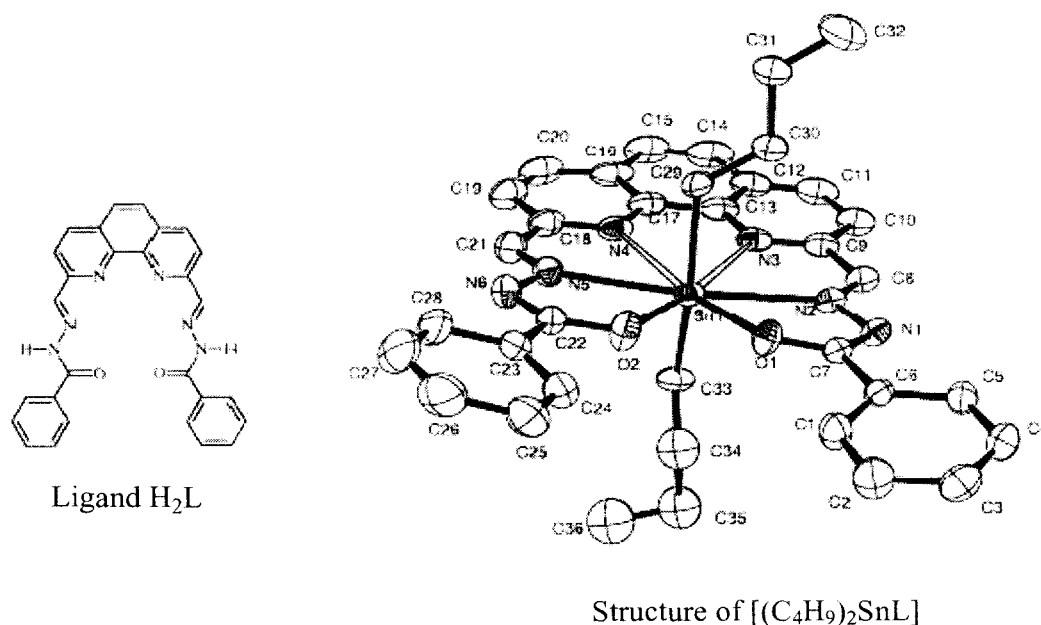
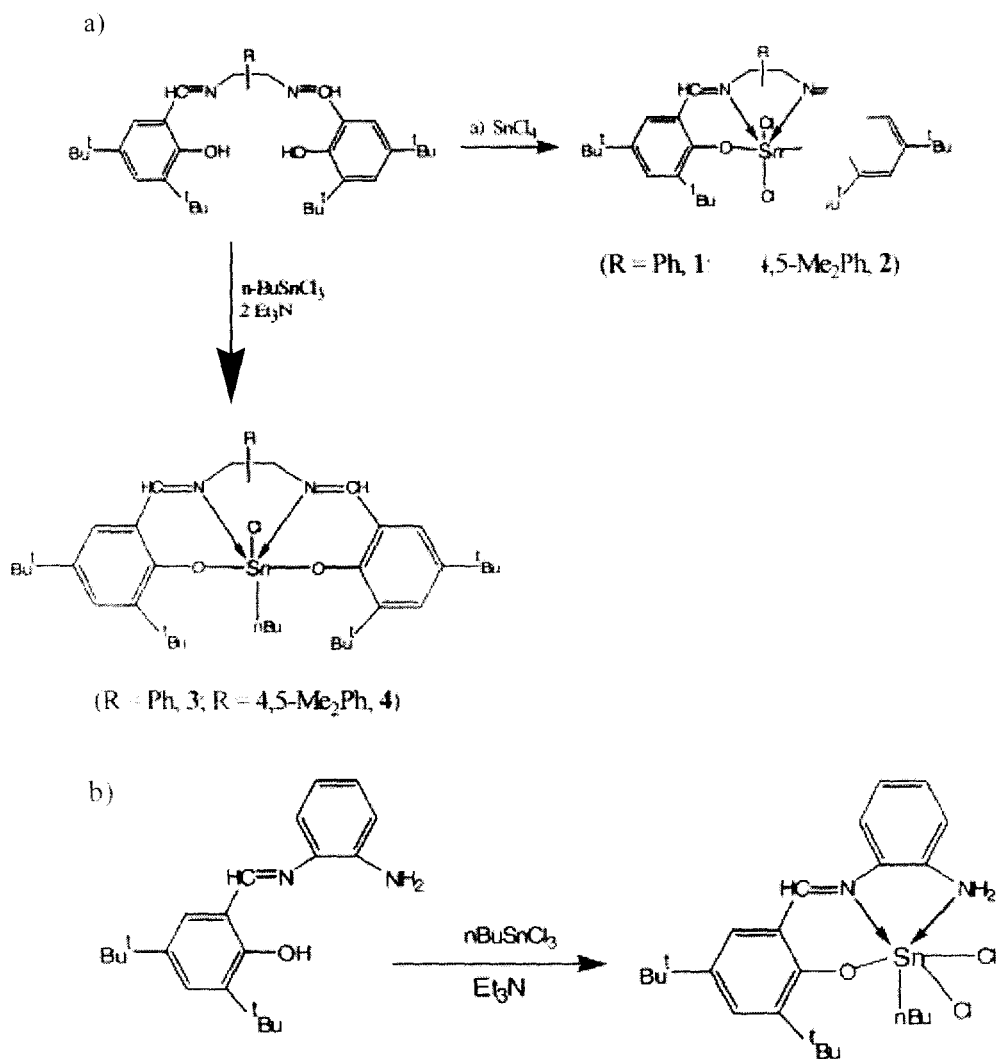


Fig. 4.5 Schiff base ligand (2,9-diformylphenanthroline) bis(benzoyl) hydrazone (H₂L) and Crystal structure of [(C₄H₉)₂SnL] [48].

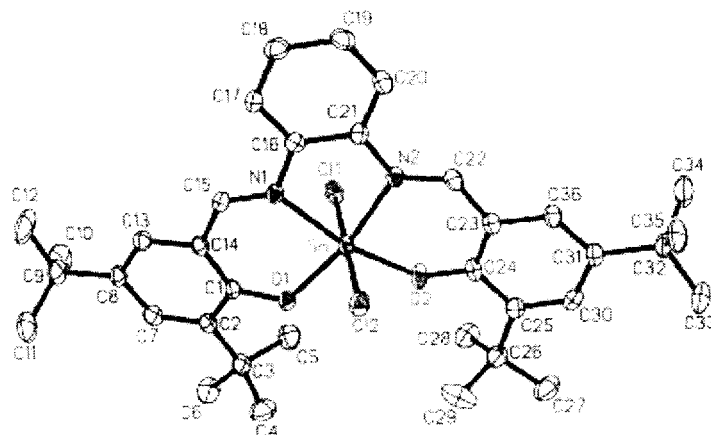
B. Yearwood and his coworkers [49] have described the synthesis and characterization of five organotin compounds containing Salophen(^tBu) [Salophen(^tBu)= N,N'-phenylene-bis(3,5-di-tert-butylsalicylideneimine)], Salomphen(^tBu) [Salomphen(^tBu)= N,N'-(4,5-dimethyl)phenylene-bis(3,5-di-tert-butylsalicylideneimine)] and Phensal(^tBu) [Phensal(^tBu)= 3,5-di-tert-butylsalicylidene(1-aminophenylene-2-amine)] ligands. These compounds include the monomeric complexes LSnCl₂ (where L= Salophen(^tBu) **1**, L= Salomphen(^tBu) **2**) (Fig. 4.6) . L(ⁿBu)SnCl (where L= Salophen(^tBu) **3**, Salomphen(^tBu) **4**), L(ⁿBu)SnCl₂ (where L= Phensal(^tBu) **5**). Compounds **1** and **2** were prepared by combining SnCl₄ with LH₂ in the presence of triethylamine. Synthesis of compounds **1** and **2**, along with **3** and **4**, can also be achieved by combining (ⁿBu)SnCl₃ with LH₂ in the presence of triethylamine (Scheme 4.1). This reaction leads to a mixture of L(ⁿBu)SnCl and LSnCl₂. The formation of LSnCl₂ may be due to a disproportionate reaction (Eq. 3) or a redistribution (Eq. 4) occurring in solution. Spectroscopic techniques including ¹¹⁹Sn NMR and X-ray crystallography were used in the characterization of the compounds.



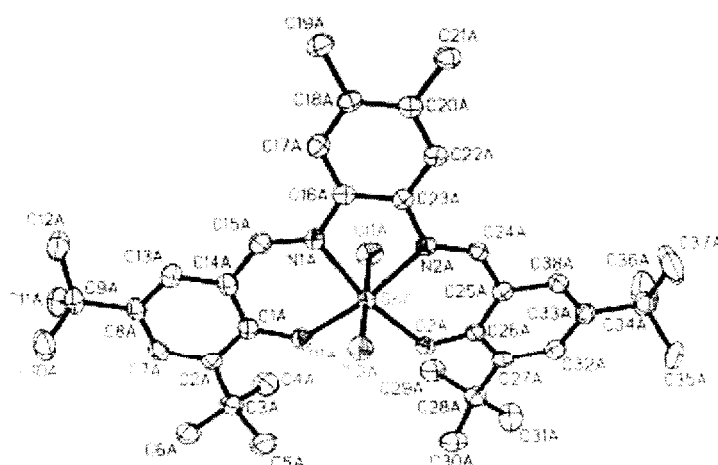


Scheme 4.1. a) General syntheses of compounds 1-4.

b) General syntheses of compound 5.



a) Crystal structure of Complex 1



b) Crystal structure of Complex 2

Fig.4.6 a) Crystal Structure of N,N' -phenylene-bis (3,5-di-tert-butylsalicylideneimine) $SnCl_2$
 b) Crystal Structure of N,N' -(4,5-dimethyl)phenylene-bis(3,5-di-tert-butylsalicylideneimine) $SnCl_2$ [49].

Diorganotin(IV) complexes of the general formula R_2SnL ($R=Ph$, n -Bu and Me) have been prepared by Dey *et al.* [24] from diorganotin(IV) dichlorides (R_2SnCl_2) and tetradentate Schiff bases (H_2L) containing N_2O_2 donor atoms in the presence of triethylamine in benzene. The Schiff bases, H_2L , were derived from salicylaldehyde, 3-methoxysalicylaldehyde (*o*-vanillin), 1-phenyl-3-methyl-4-benzoyl-5-pyrazolone and diamines such as *o*-phenylenediamine and 1,3-propylenediamine. The complexes were characterized by IR, NMR (1H , ^{13}C , ^{119}Sn)

and elemental analysis. The structure of the complex, *n*-Bu₂Sn(Vanophen) (Fig. 4.7), was determined using single crystal X-ray diffraction. The tin atom has a distorted octahedral coordination, with the Vanophen ligand occupying the four equatorial positions and the *n*-butyl groups in the *trans* axial positions. Six-coordinated distorted octahedral structures have been proposed for all diorganotin(IV) complexes studied here, as they possess similar spectroscopic data.

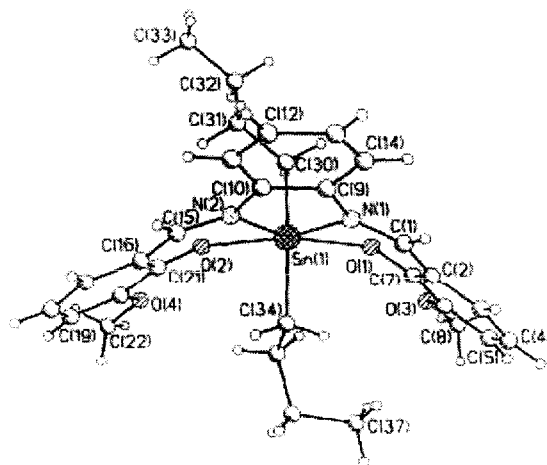


Fig. 4.7 Structure of *n*-Bu₂Sn(Vanophen) [24].

de Sousa *et al.* [50] have reported the multidentate ligand, 2,6-diacetylpyridine bis(3-hexamethyleneiminylthiosemicarbazone) monohydrate, H₂2,6Achexim·H₂O, crystallizes with one thiosemicarbazone moiety in an intramolecular hydrogen bonded, bifurcated *E'* form. The other thiosemicarbazone moiety is *E* and is not involved in intramolecular hydrogen bonding, but is involved in hydrogen bonding with the hydrate water molecule. The molecular structure of H₂2,6Achexim·H₂O is planar, except for the hexamethyleneimine rings, which are tilted in opposite directions from the plane of the molecule and make dihedral angles with the pyridine ring. In complex formation (Fig. 4.8) with tin(IV), the dianion (loss of N3a and N3b hydrogens) of H₂2,6Achexim (Fig. 4.8) acts as a pentadentate ligand, 2,6Achexim, in a planar conformation to a central tin(IV) ion. The tin(IV) is heptacoordinate in a distorted pentagonal dipyramidal configuration, with the five SNNNS donor atoms of 2,6Achexim in the pentagonal plane and the two *n*-butyl groups in the axial positions. They have also reported the crystal structures of heptacoordinate tin(IV) complexes, namely [MeSnCl(H₂,6Ac4DH)]Cl·MeOH [51] and [Ph₂Sn(H₂,6-Ac4DH)]Cl [52].

where $H_22,6Ac4DH=2,6$ -diacetylpyridine bis(thiosemicarbazone). Casas *et al.* [53] reported on $H_22,6Ac4DH$ complexes include the following: a third tin(IV) heptacoordinate complex of formule $[Ph_2Sn(2,6Ac4DH)] \cdot 2DMF$. Another two cases of heptacoordination in organotin(IV) complexes are described by de Sousa *et al.* [54]. Both possess pentagonal bipyramidal geometry and show the organic groups on the axial positions, with the ligands forming five bonds to tin(IV) on the equatorial plane. The first complex, $[^nBu_2Sn(H_2daptsc)]Cl_2 \cdot MeNO_2$ (**1**) (Fig 4.9) is entirely new, whereas the second, $[Me_2Sn(H_2dapsc)][Me_2SnCl_4]$ (**2**), although previously reported, only now had its structure determined. In both **1** and **2** the heptacoordinate species are cationic, but whereas in **1** the counterion is simply Cl^- , in **2** it is a complex anion, namely $[Me_2SnCl_4]^{2-}$. In 2001, de Sousa *et al.* [55] also have done, the reactions of 2-acetylpyridine-N(4) phenylthiosemicarbazone, HAP4P (Fig. 4.10), and 2-hydroxyacetophenone-N(4)-phenylthiosemicarbazone, H_2DAP4P (Fig. 4.10), with R_mSnX_m ($m = 2, 3$; $R = Me, ^nBu, Ph$ and $X = Cl, Br$) led to the formation of hexa- and penta-coordinated organotin(IV) complexes, which were studied by microanalysis, IR, 1H -NMR and Mössbauer spectroscopies. The molecular structures of $[SnMe_2(DAP4P)]$ and $[Sn^nBu_2(DAP4P)]$ (Fig. 4.10) were determined by single crystal X-ray diffraction studies. In the compounds $[SnClMe_2(AP4P)]$ and $[SnBrMe_2(AP4P)]$, the deprotonated ligand $AP4P^-$ is N,N,S-bonded to the Sn(IV) atoms, which exhibit strongly distorted octahedral coordination. The structures of $[SnMe_2(DAP4P)]$ and $[Sn^nBu_2(DAP4P)]$ revealed that the $DAP4P^{2-}$ anion acts as a O,N,S-tridentate ligand. In these cases, the Sn(IV) atoms adopt a strongly distorted trigonal bipyramidal configuration where the azomethine N and the two C atoms are on the equatorial plane while the O and the S atoms occupy the axial positions. In 2004, the preparation and characterization of $[Sn(C_{14}H_{13}N_4S)(CH_3)Cl_2]$ (Fig. 4.11), an organotin(IV) complex containing the ligand 2-acetylpyridine(4)-phenylthiosemicarbazone, HAP4P, was described by Francisco *et al.* [56]. The molecular structure was studied by single crystal X-ray diffraction and IR and Mössbauer spectroscopies. The compound crystallizes in the centric triclinic as discrete neutral complexes, with the Sn(IV) ion in a distorted octahedral coordination geometry, with the thiosemicarbazone derivative in a meridional configuration and the chlorides in *trans* positions. The complex, $[Sn(C_{14}H_{13}N_4S)(CH_3)Cl_2]$, was synthesized to the investigation of the coordination modes of thiosemicarbazones with organotin(IV) compounds. The chelating behavior of N,N,S-donor

thiosemicarbazones revealed three coordination modes. They can act as a neutral N(azomethine),S-bidentate ligand, [57] as an anionic (-1) ligand bonded through N,N,S and as an anionic (-1) ligand bonded through N(azomethine),S. [58,59]

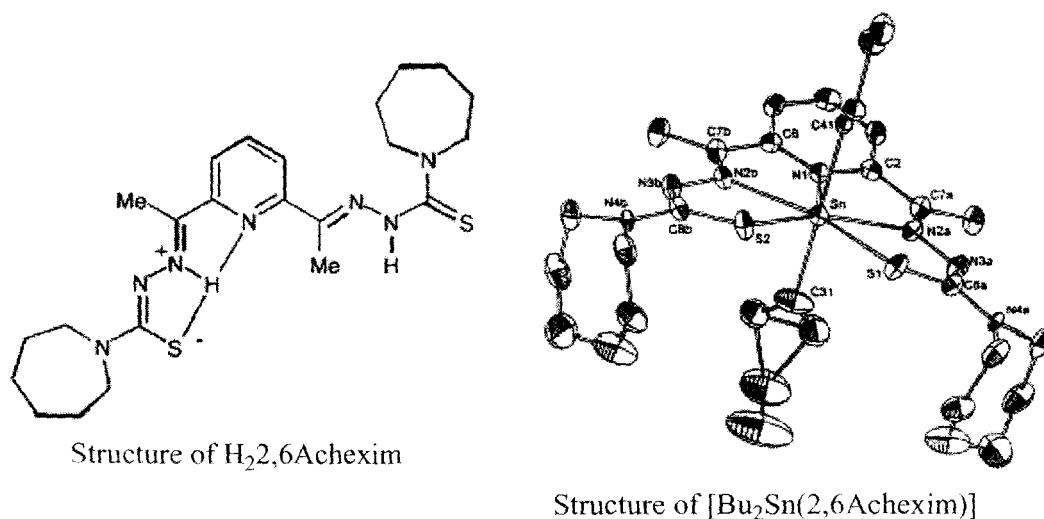


Fig 4.8 The Structure of ligand H₂,6Achexim and its complex [Bu₂Sn(2,6Achexim)] [50].

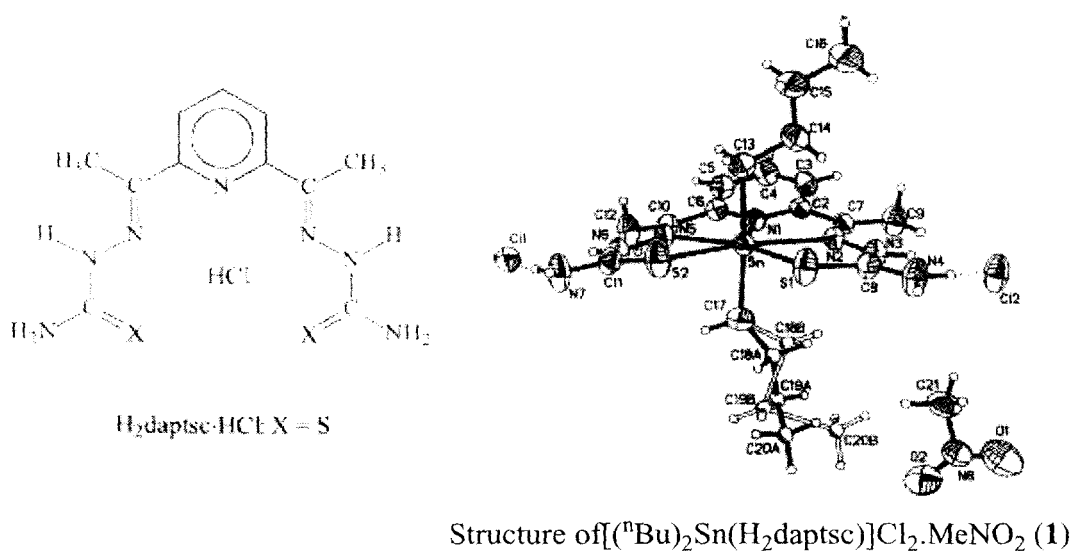


Fig 4.9 The Structure of the ligand H₂daptsc·HCl·X=S and its complex [54].

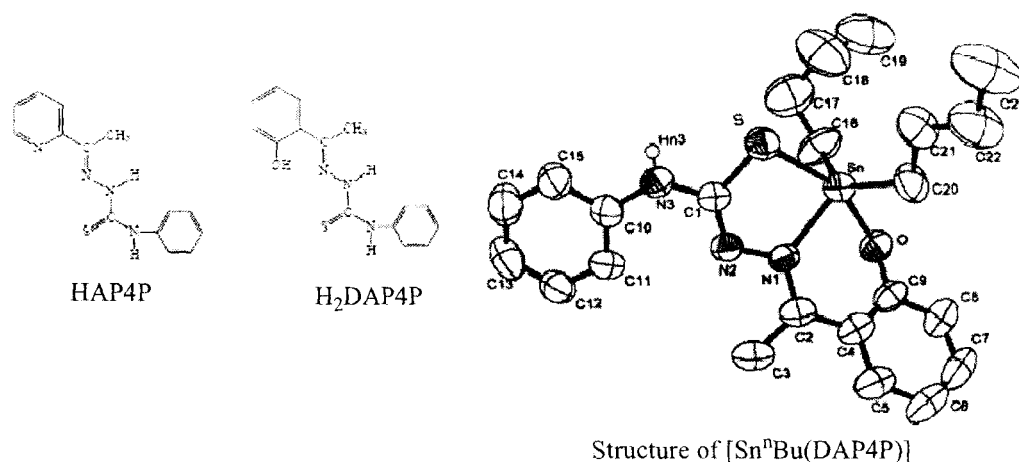


Fig. 4.10 The Structure of ligand 2-acetylpyridine-N(4) phenylthiosemicarbazone, HAP4P; The Structure of ligand 2-hydroxyacetophenone-N(4) phenylthiosemicarbazone, H₂DAP4P; And the structure of its complex [SnⁿBu₂(DAP4P)] [55].

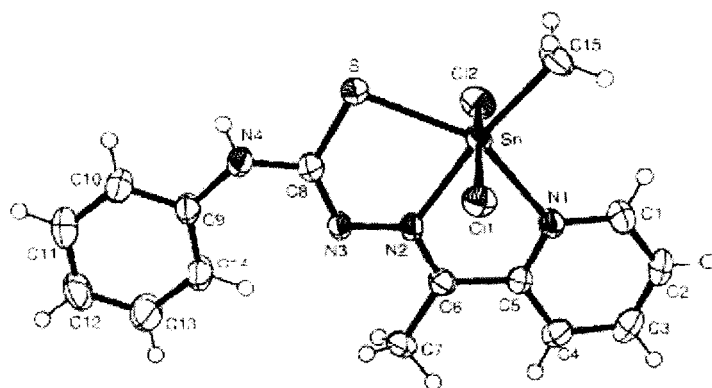


Fig 4.11 Structure of [Sn(C₁₄H₁₃N₄S)(CH₃)Cl₂] [56]

Pettinari *et al.* [60] reported that the interaction of 2-[(2-hydroxyphenyl)imino] methyl} phenol (salopH₂) (Fig. 4.12) with tin and organotin(IV) acceptors, the derivatives [SnR₃(salopH)] (R=Me or Buⁿ), [SnR₂(salop)] (R=Me, Buⁿ, Bu^t, Vin or Ph) (Fig. 4.12a), [SnRX(salop) (solvent)] (R=Me, Buⁿ, Ph or X; X=Cl, Br or I; solvent=CH₃OH or H₂O), [Sn(salop)₂], [R₂SnCl₂(salopH₂)] (R=Me or Buⁿ) have been obtained and characterized. The chelates, containing the Schiff base in mono or dianionic form, are generally stable both in the solid state and in solution, whereas the [SnR₂Cl₂(salopH₂)] adducts slowly decompose in acetone or DMSO yielding [SnR₂(salop)] and releasing HCl. All the [SnR₂(salop)] and [SnRX(salop) (solvent)] complexes are fluxional in solution. The ¹¹⁹Sn NMR chemical shift is a function of

the number of R groups. The X-ray single crystal diffraction study of $[\text{SnVin}_2(\text{salop})]$ shows the metal to be five-coordinate in a distorted square pyramidal environment. The whole structure consists of molecular units connected by weak intermolecular Sn–O interactions. In the complexes $[\text{SnX}_2(\text{salop})(\text{CH}_3\text{OH})]\cdot\text{CH}_3\text{OH}$ complexes ($\text{X}=\text{Cl}$ or Br) (Fig. 4.12b and Fig 4.13b), the tin atom is found in a strongly distorted octahedral environment. The salopH_2 is a typical potentially ONO tridentate Schiff base ligand forming stable complexes with many transition and post-transition metal ions [61-63]. Metal– salopH_2 complexes of the Group IV elements is rather sparse [64, 65], only three tin(IV) complexes structurally characterized being reported, i.e. $[\text{SnMe}_2(\text{Salop})]$ [66], $[\text{SnPh}_2(\text{salop})]$ [67] (Fig. 4.13a) and $[\text{Sn}(\text{salop})]_2$ [68].

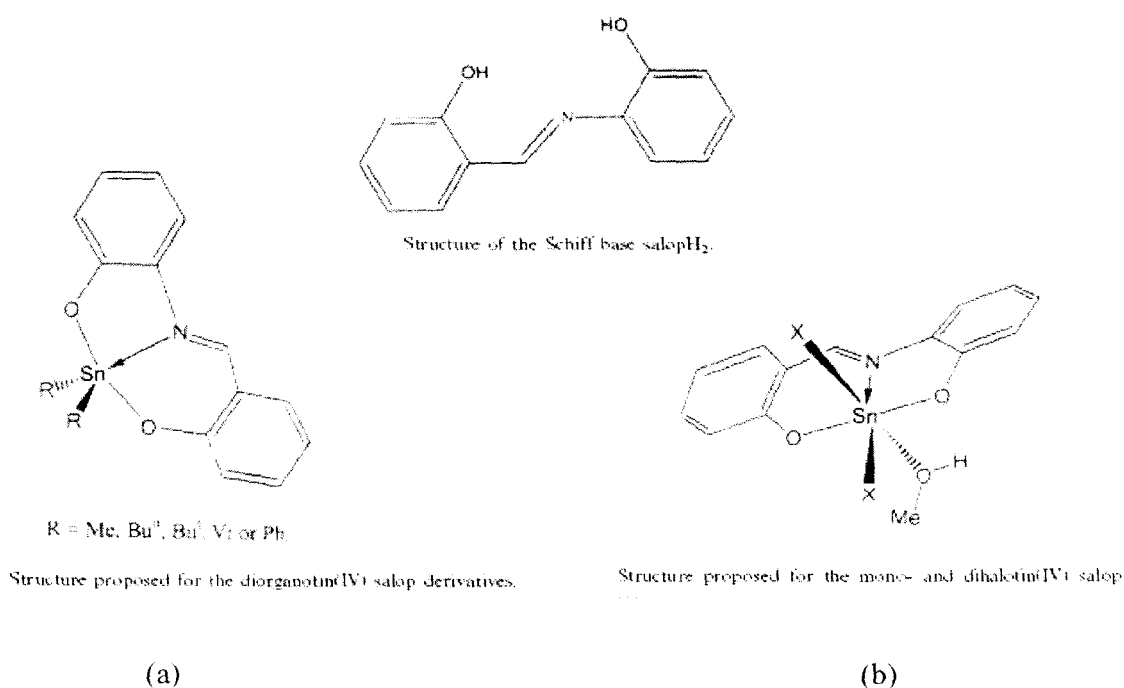


Fig. 4.12 The structure of the Schiff base ligand salopH_2 ; Structure proposed for
 (a) the diorganotin(IV) salop derivatives;
 (b) mono- and dihalotin(IV) salop derivatives [60].

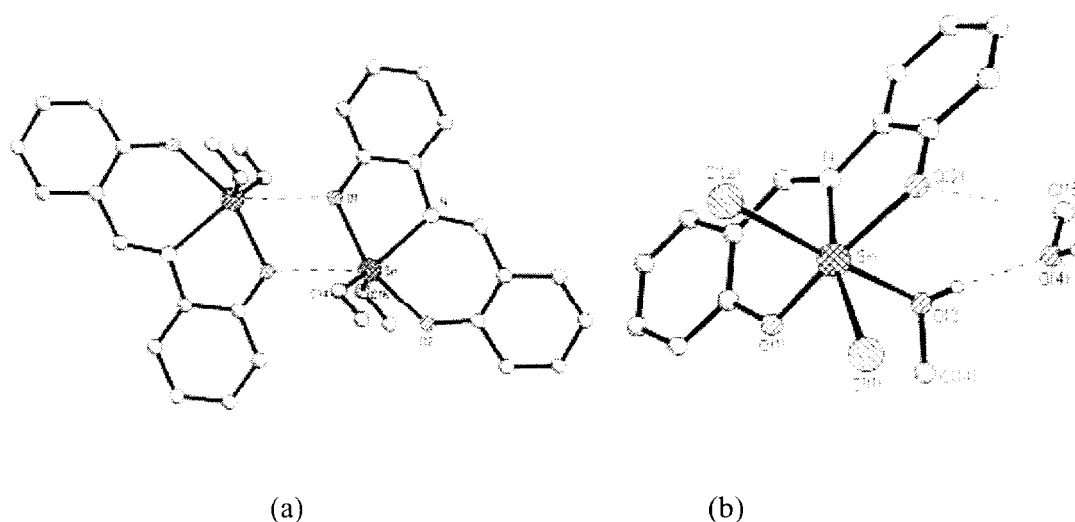
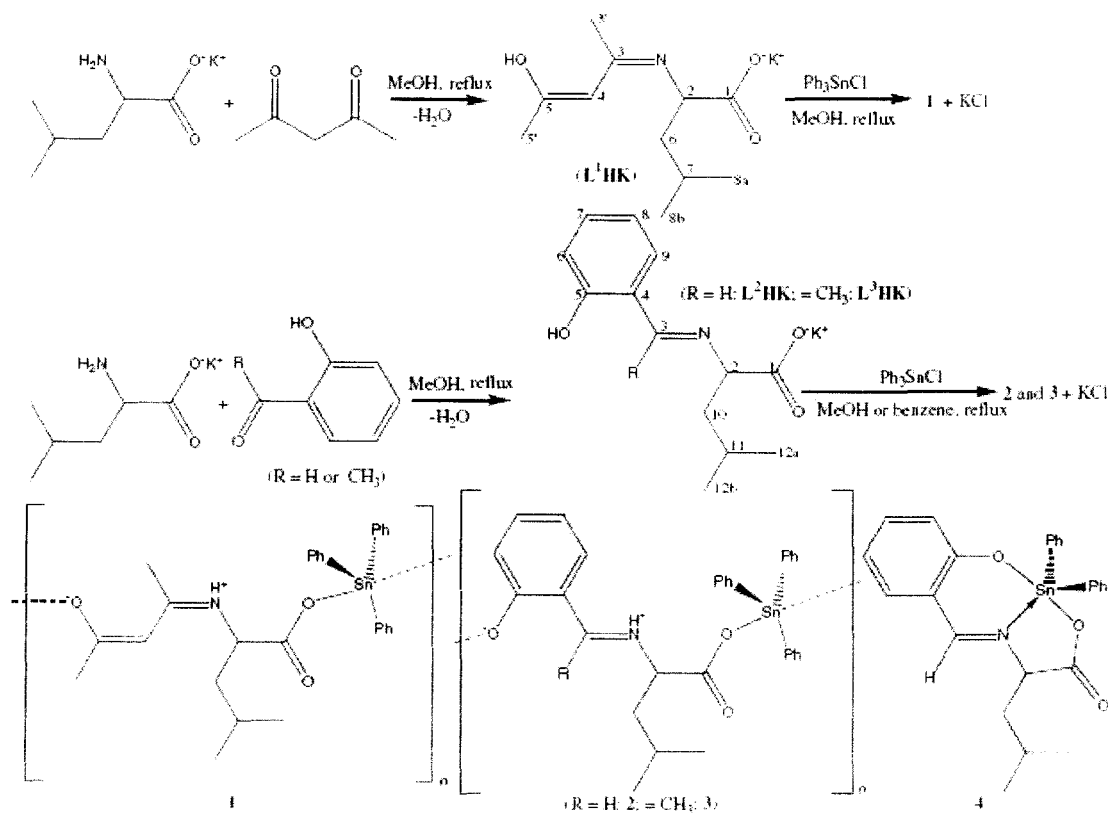


Fig. 4.13 a) Structure of $[\text{SnPh}_2(\text{salop})]$ [67].

b) Structure of $[\text{SnCl}_2(\text{salop})(\text{CH}_3\text{OH})] \cdot \text{CH}_3\text{OH}$ [60].

T.S. Basu Baul and his coworkers [69] described that potassium 2- $\{[(2Z)$ -3-hydroxy-1-methyl-2-butenylidene]amino $\}$ -4-methyl-pentanoate (L^1HK) and potassium 2- $\{[(E)$ -1-(2-hydroxyphenyl)alkylidene]amino $\}$ -4-methyl-pentanoates (L^2HK - L^3HK) underwent reactions with $\text{Ph}_n\text{SnCl}_{4-n}$ ($n=2$ and 3) to give the amino acetate functionalized Schiff base organotin(IV) complexes $[\text{Ph}_3\text{SnLH}]_n$ (1-3) and $[\text{Ph}_2\text{SnL}]$ (4), respectively [scheme 4.2]. These complexes have been characterized by ^1H , ^{13}C , ^{119}Sn NMR, IR spectroscopic techniques in combination with elemental analyses. The crystal structures of 1 and 3 were determined. The crystal structures reveal that the complexes exist as polymeric chains in which the L-bridged Sn-atoms adopt a $\text{trans-R}_3\text{SnO}_2$ trigonal bipyramidal configuration with the Ph groups in the equatorial positions and the axial locations occupied by a carboxylate oxygen atom from one carboxylate ligand and the alcoholic or phenolic oxygen atom of the next carboxylate ligand in the chain. The carboxylate ligands coordinate in the zwitterionic form with the alcoholic/phenolic proton moved to the nearby nitrogen atom. The solution structures were predicted by ^{119}Sn NMR spectroscopy. These organotin(IV) complexes were tested against human tumor cell lines. Interestingly, the most cytotoxic triphenyltin(IV) compound was (3) with an average ID_{50} value of around 35 ng/ml for all the cell lines.



Scheme 4.2 Syntheses of potassium salts (L^1HK - L^3HK) and their triphenyltin(IV) complexes (1–3). The structure of diphenyltin(IV) complex (4) is included [69].

Previous studies [70] have shown that the metal salicylaldimine complexes with $\text{X}=\text{H}$ are effective ligands for both inorganic and organotin species. Replacement of X by a methoxy group, the nature of the metal salicylaldimine complexes as ligands is, not surprisingly, radically altered, transforming them from bidentate to extremely effective tetradentate ligands. Much more surprising, however, is the finding that the behaviour of the complexes as ligands is markedly and dramatically influenced by the nature of the bridging group B (Fig. 4.14). Clarke *et al.* [71] studied that dinuclear complexes $[\text{M}(\text{3MeO-sal-}m\text{-phen})(\text{H}_2\text{O})_2]$ [$\text{M}=\text{Cu}$, Ni and Zn ; $\text{3MeO-H}_2\text{sal-}m\text{-phen}=\text{N,N'$ -bis(3-methoxysalicylidene) benzene-1,3-diamine] (Fig. 4.14b) and $[\text{M}(\text{3MeO-sal-}p\text{-phen})(\text{H}_2\text{O})_2]$ [$\text{M}=\text{Cu}$, Ni and Zn ; $\text{3MeO-H}_2\text{sal-}p\text{-phen}=\text{N,N'$ -bis(3-methoxysalicylidene)benzene-1,4-diamine] which were synthesized and reacted with diorganotin(IV) dihalides, dinitrates and dithiocyanates. Only in the case of those reactions involving $[\text{M}(\text{3MeO-sal-}m\text{-phen})(\text{H}_2\text{O})_2]$ with $\text{M}=\text{Ni}$ or Zn were adducts

obtained as the sole products of reaction; the adducts were all tetranuclear complexes. $\text{SnMe}_2(\text{NCS})_2$ reacts with $\text{Ni}(\text{3MeO-sal1,2pn})[\text{H}_2\text{3MeO-sal1,2pn}=\text{N,N}'\text{-bis(3-methoxysalicylidene) propane-1,2-diamine}]$ to give a brick red diamagnetic 1/1 adduct whereas a similar reaction with $\text{Ni}(\text{3MeO-sal1,3pn})[\text{H}_2\text{3MeO-sal1,3pn}=\text{N,N}'\text{-bis(3-methoxysalicylidene)propane-1,3-diamine}]$ results in the formation of a deep purple paramagnetic 1/1 adduct. Because the number of carbon atoms linking the imine nitrogen atoms increases beyond three, the effectiveness of the metal salicylaldimines as ligands is greatly reduced. For example, practically no organotin(IV) Lewis acids react with the complex $\text{Ni}(\text{3MeO-sal1,5pent})[\text{H}_2\text{3MeO-sal1,5pent}=\text{N,N}'\text{-bis(3-methoxysalicylidene)pentane-1,5-diamine}]$.

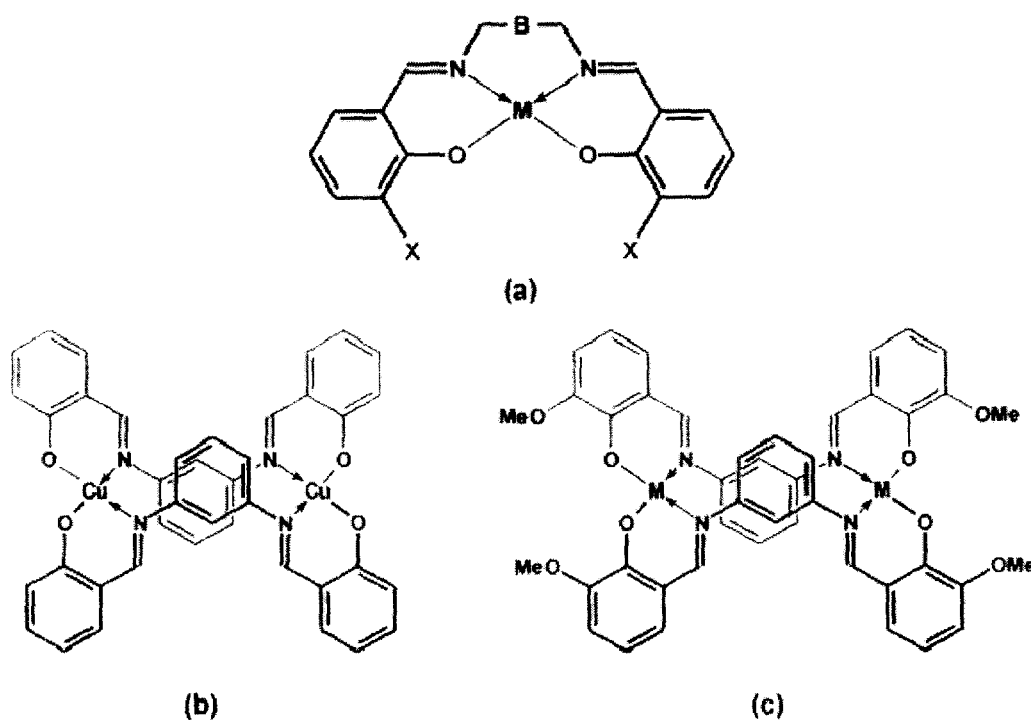


Fig. 4.14 Structure of $\text{M}(\text{sal-}m\text{-phen})$ complexes [70,71].

Jamil *et al.* [72] were screened novel organotin complexes with the general formulae R_3SnL (R: alkyl and L: Schiff base) (Fig. 4.15) for their *in vitro* antimicrobial properties. These complexes were synthesized by the reaction of organotin (IV) halide with ligand in the presence of a base; their antibacterial activity

was investigated by using the agar well diffusion methods while their antifungal activity was determined by drop method. The chemical bondings of the complexes have been discussed with the help of their IR, $^1\text{H-NMR}$ and $^{13}\text{C-NMR}$ spectral studies. All the compounds possessed excellent antimicrobial activities. The order of increasing activities was ligand $\text{Me}_3\text{SnL} < \text{Bz}_3\text{SnL} < \text{Ph}_3\text{SnL}$. The results provided evidence that the studied complexes might indeed be potential sources of antimicrobial agents and these would further enable us to evaluate their utility in biomedical field.

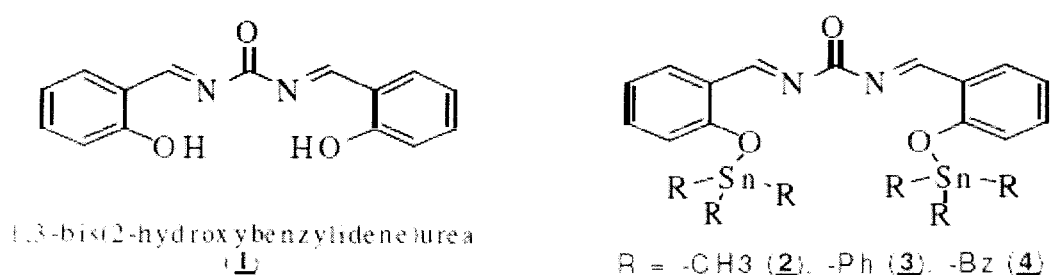
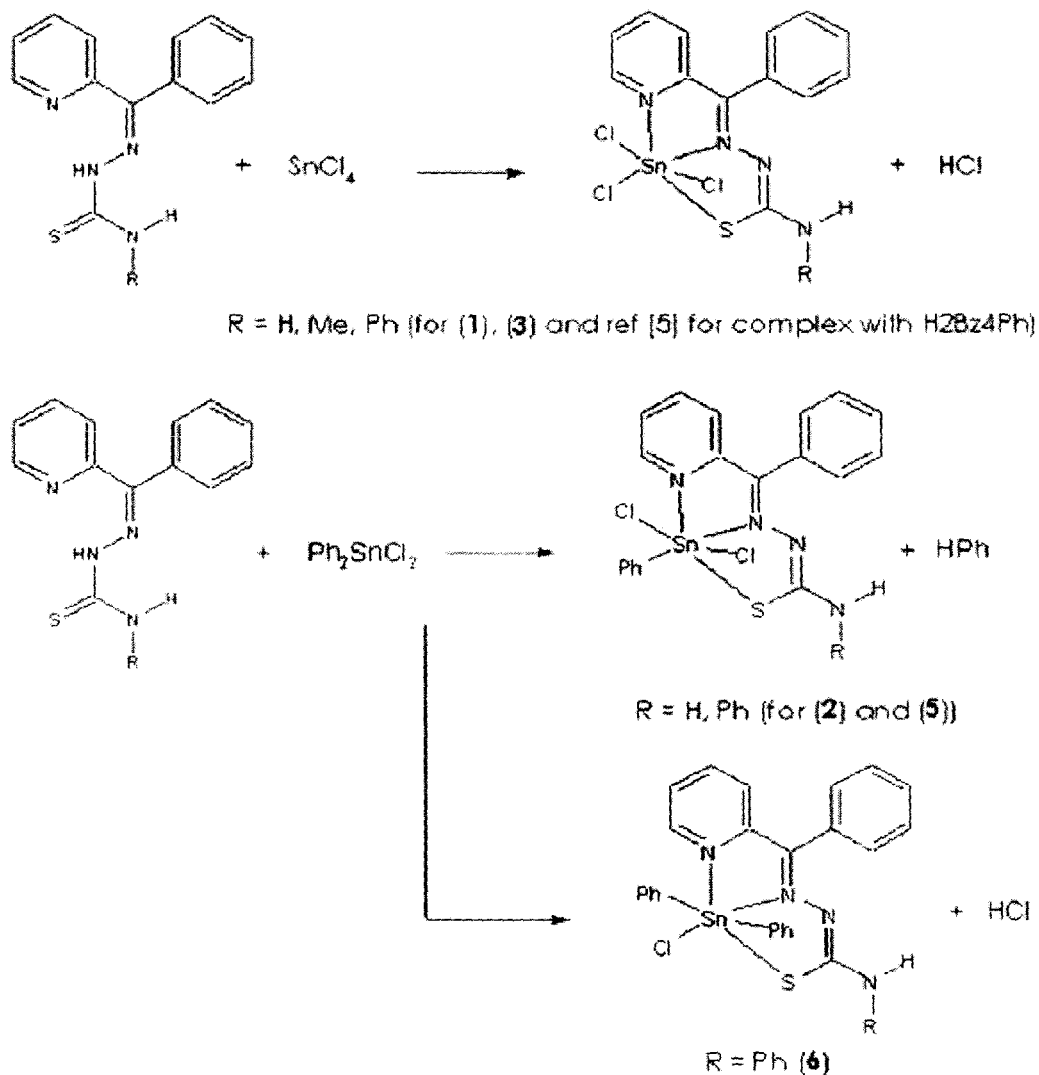


Fig. 4.15 General structures of Schiff base and Complexes [72].

Previously, Rebolledo *et al.* [73] have prepared tin(IV) complexes of N(4)-phenyl-2-benzoylpyridine thiosemicarbazone (H2Bz-4Ph) and studied their antifungal properties. They also demonstrated the cytotoxic activity of n-butyltin complexes of H2Bz4Ph against three human tumor cell lines. The di-n-butyl compound proved to be particularly effective [74]. In 2006, they studied the reaction of 2-benzoylpyridine thiosemicarbazone (H2Bz4DH, HL1) and its N(4)-methyl (H2Bz4Me, HL2) and N(4)-phenyl (H2Bz4Ph, HL3) derivatives with SnCl_4 and diphenyltin dichloride (Ph_2SnCl_2) gave $[\text{Sn}(\text{L1})\text{Cl}_3]$ (1), $[\text{Sn}(\text{L1})\text{PhCl}_2]$ (2), $[\text{Sn}(\text{L2})\text{Cl}_3]$ (3), $[\text{H}_2\text{L2}]^+_2$ $[\text{Ph}_2\text{SnCl}_4]^{-2}$ (4) $[\text{Sn}(\text{L3})\text{PhCl}_2]$ (5) and $[\text{Sn}(\text{L3})\text{Ph}_2\text{Cl}]$ (6) [Scheme 4.3]. Infrared and ^1H , ^{13}C and ^{119}Sn NMR spectra of 1–3, 5 and 6 are compatible with the presence of an anionic ligand attached to the metal through the $\text{N}_{\text{py}}\text{-N-S}$ chelating system and formation of hexacoordinated tin complexes. The crystal structures of 1–3, 5 and 6 show that the geometry around the metal is a distorted octahedron formed by the thiosemicarbazone and either chlorides or chlorides and phenyl groups. The crystal structure of 4 reveals the presence of $[\text{H}_2\text{L2}]^+_2$ and trans $[\text{Ph}_2\text{SnCl}_4]^{-2}$ [75]. The formation of the $[\text{Ph}_2\text{SnCl}_4]^{-2}$ dianion as in (4) is not an uncommon process in tin

chemistry. In fact, there are a number of papers describing complexes where such ion is present [76].



Scheme 4.3 The formation of complexes 1–3, 5 and 6 are summarized [73].

Affan *et al.* [77] have synthesized five new organotin(IV) complexes with pyruvic acid isonicotinoyl hydrazone [H_4PAI (**1**)] (Fig. 4.16) of the general formula [$\text{Me}_2\text{Sn}(\text{H}_2\text{PAI})$] (**2**), [$\text{R}_2\text{Sn}(\text{H}_2\text{PAI})\cdot\text{H}_2\text{O}$] [$\text{R}=\textit{n}$ -Bu, (**3**) or Ph, (**4**)], [$\text{RSnCl}(\text{H}_2\text{PAI})\cdot\text{H}_2\text{O}$] [$\text{R}=\text{Me}$ (**5**) or Ph (**6**)] in the presence of base in absolute methanol in 1:2:1 mole ratio (metal:base:ligand). All organotin(IV) complexes are

characterized by elemental analyses, molar conductance values, UV-Visible, IR and ^1H NMR spectral studies. The crystal structure of organotin(IV) complex (**3**) has also been determined by X-ray crystallography diffraction analyses. Complex [*n*-Bu₂Sn(H₂PAI).H₂O] (**3**) is orthorhombic with space group *P2(1)/c*. The complex [*n*-Bu₂Sn(H₂PAI).H₂O] (**3**) (Fig. 4.16) shows a distorted octahedral geometry with coordination for the central tin(IV) atom and exhibits two monomeric structures in one unit cell. In the complex (**3**), the pyruvic acid isonicotinoyl hydrazone ligand is coordinated to the tin(IV) as dinegative tridentate chelating agent via the carboxylic-O, enolic-O and imine-N atoms. Hydrazone ligand (**1**) and its organotin(IV) complexes have also been screened for their antimicrobial activities and found to be relatively active. Previously, several novel molecular structures of organotin(IV) complexes with hydrazone ligands have been reported by Affan *et al.* [78, 79]. In 2009, they have synthesized another series of six organotin(IV) complexes of pyruvic acid thiosemicarbazone ligand [H₂PAT, (**1**)] with general formula [R_nSnCl_{n-1} PAT] [R = Me₂, n = 1 (**2**); R = Bu₂, n = 1 (**3**); R = Ph₂, n = 1 (**4**); R = Me, n = 2 (**5**); R = Bu, n = 2 (**6**); R = Ph, n = 2 (**7**)] were synthesized by direct reaction of thiosemicarbazone ligand (**1**), base and organotin(IV) chloride(s) in absolute methanol under N₂ atmosphere. These organotin(IV) complexes were characterized by elemental analyses, molar conductivity, UV-visible, FTIR, ^1H and ^{13}C NMR spectral studies. Among them, dimethyltin(IV) complex (**2**) was also characterized by X-ray crystallography diffraction analyses. The cytotoxicity of the ligand (**1**) as well as its organotin(IV) complexes (**2-7**) were determined by *Artemia salina*, shrimp test lethality bioassay [80].

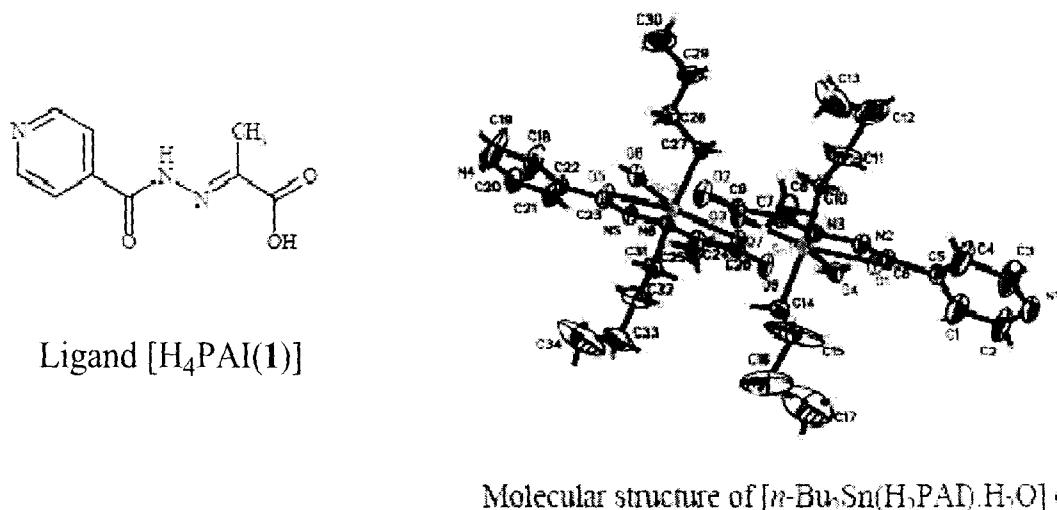
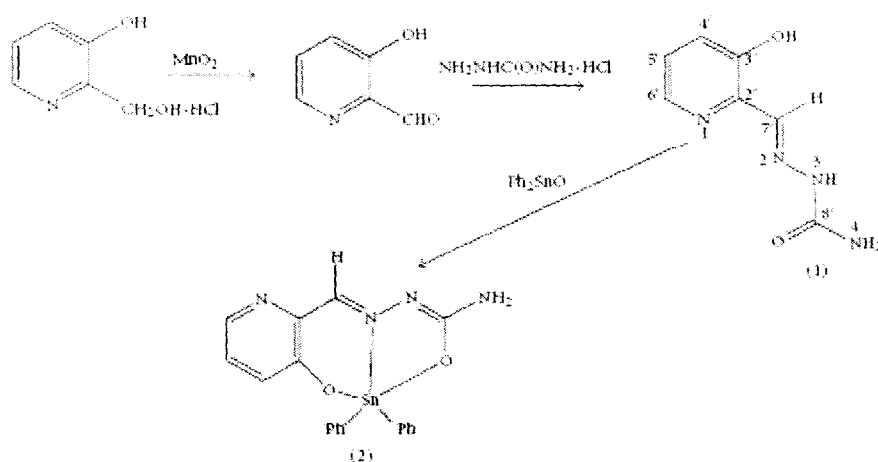


Fig. 4.16 Structure of the ligand pyruvic acid isonicotinoyl hydrazone [H₄PAI (1)] and its complex [77].

Wiecek *et al.* [81] were reported that the novel diphenyltin(IV) compound [Ph₂(HyFoSc)Sn] (2), where H₂HyFoSc (1) (Scheme 4.4) is 3-hydroxy-2-formylpyridine semicarbazone, was prepared and characterized by vibrational and NMR (¹H, ¹³C) spectroscopy. The structure of [Ph₂(HyFoSc)Sn] was confirmed by single-crystal X-ray crystallography. The doubly deprotonated ligand is coordinated to the tin atom through the enolic-oxygen, the azomethine-nitrogen, and phenolic-oxygen, and so acts as an anionic tridentate ligand with the ONO donors. Two carbon atoms complete the fivefold coordination at the tin(IV) center. Intermolecular hydrogen bonding, C–H → π, and π → π interactions combine to stabilize the crystal structure. Compounds 1 and 2 have been evaluated for antiproliferative activity *in vitro* against the cells of three human tumor cell lines and a mouse cancer cell line.



Scheme 4.4 For the preparation of 1 and 2 [81].

The ligand behavior of di-2-pyridylketone 2-aminobenzoylhydrazone (Hdpa) (Fig 4.17), and phenyl(2-pyridyl)ketone 2-aminobenzoylhydrazone (Hdba) (Fig. 4.17) towards organotin derivatives was investigated by Ianelli *et al.* [82]. The synthesis and the IR and ^{119}Sn NMR spectroscopic characterization of the compounds is reported, together with the X-ray crystal structures of Hdpa and $\text{Sn}(\text{C}_6\text{H}_5)_3\text{Cl}(\text{OH}_2)$. Hdpa (Fig. 4.17), which are discussed and compared. The *in vitro* evaluation of antimicrobial properties revealed the strong activity of $\text{Sn}(\text{C}_6\text{H}_5)_2(\text{Hdpa})\text{Cl}_2$ and $\text{Sn}(\text{C}_6\text{H}_5)_3\text{Cl}(\text{OH}_2)\cdot\text{Hdpa}$ complexes. None of the compounds showed genotoxicity in the *Bacillus subtilis* rec-assay and in the *Salmonella-microsome* test. Previously they have reported the synthesis and structural characterization of two organotin compounds of formula $\text{Sn}(\text{C}_6\text{H}_5)(\text{dpa})\text{Cl}_2$ and $\text{Sn}(\text{C}_6\text{H}_5)_2(\text{Hdpa})\text{Cl}_2$, derived from the interaction of dichlorodiphenyltin with di-2-pyridylketone 2-aminobenzoylhydrazone (Hdpa), a molecule showing an interesting ligand behavior [83]. Along these lines and in continuation of their investigations on the chemical, structural, and biological properties of organotin-hydrazone compounds, they have further investigated the ligand behavior of Hdpa as well as that of Hdba, a new hydrazone obtained from the reaction of 2-aminobenzoylhydrazine with phenyl(2-pyridyl)ketone [84, 85].

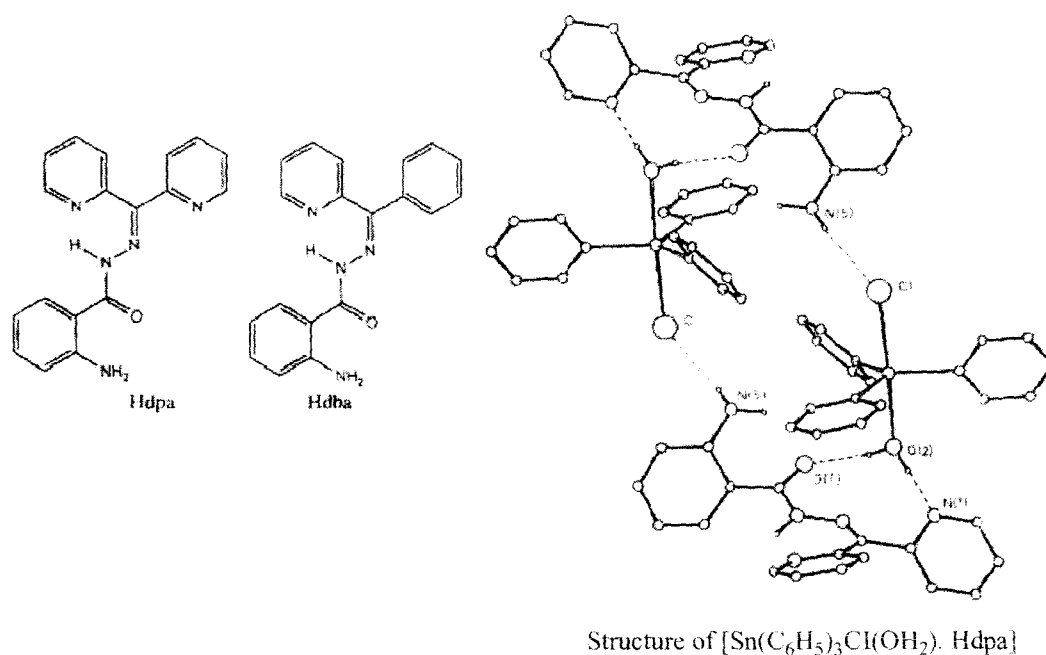


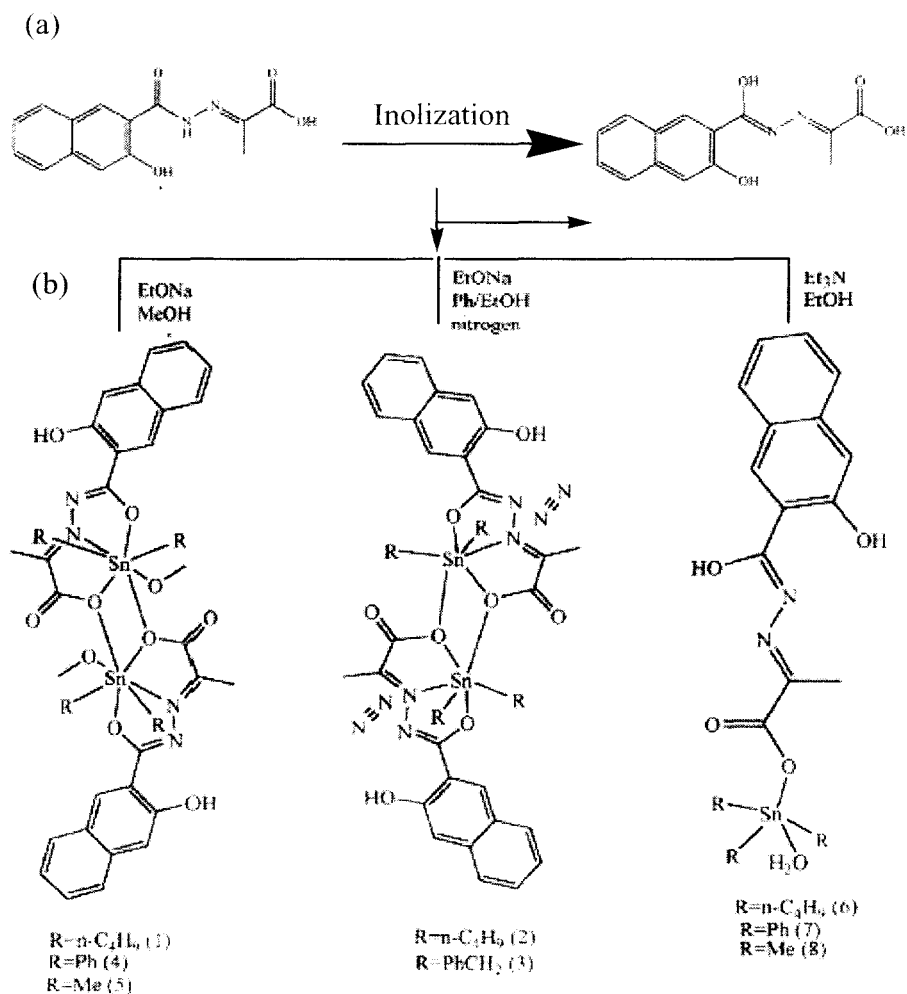
Fig. 4.17 The structure of the ligand phenyl(2-pyridyl)ketone 2-aminobenzoylhydrazone (Hdba); di-2-pyridylketone 2-aminobenzoylhydrazone (Hdpa) and its complex [82].

Bergamaschi *et al.* [86] have investigated a series of organotin complexes with pyrrole-2-carboxaldehyde 2-hydroxybenzoylhydrazone (H₃mfps) and pyrrole-2-carboxaldehyde 2-picolinoylhydrazone (H₂mfpp). The IR, ¹H, and ¹¹⁹Sn nuclear magnetic resonance spectroscopic characterization of all the compounds is reported and discussed in connection with the ligand behaviour of the hydrazone and the structure of the organotin complex. Complexes exhibit antibacterial properties bigger than those of the corresponding ligands but they turn out to be less potent than the parent organotin compounds. Sn(H₃mfps)(C₆H₅)₂Cl₂·2H₂O and Sn(Hmfpp)(n-C₄H₉)₂Cl are the most active antibacterial compounds showing MIC values between 3-6 µg/ml against *Bacillus subtilis* and *Staphylococcus aureus* and between 6-25 µg/ml against *Escherichia coli* the first compound also strongly inhibits the growth of *Aspergillus niger*. All the ligands and complexes are devoid of DNA-damaging activity in the *Bacillus subtilis* rec-assay. H₂mfpp and its complexes Sn(Hmfpp)(C₂H₅)₂Cl and Sn₃(Hmfpp)₃(mfpp)(C₆H₅)₃Cl₆ are shown by the Salmonella-microsome assay to be mutagenic substances in the presence of a

metabolic activation system. The obtained results are discussed on the basis of structure-activity relationships.

Several examples are heterocycles prepared from dicarboxylic acids and Schiff bases [87-89]. Obafemi *et al.* [9] are reported that some representative six-membered heterocyclic organotin(IV)-nitrogen and -oxygen compounds were prepared by the condensation of dialkyltin oxides with hydroxycarboxylic acids, substituted aminocarboxylic acids and diols. These compounds were characterized by infrared and mass spectra. The compounds were screened against nine species of bacteria and five species of fungi.

Yin and Chen [90] have prepared a series of organotin(IV) complexes with Schiff base ligand pyruvic acid 3-hydroxy-2-naphthoyl hydrazone $[R_2SnLY]_2$, L = 3-HO-C₁₀H₆-2-CONHN=C(CH₃)COOH, R = n-C₄H₉, Y = CH₃OH (**1**), R = n-C₄H₉, Y = N (**2**), R = PhCH₂ (**3**), R = Ph, Y = CH₃OH (**4**), R = Me, (**5**) and $[R_3SnLY]$, L = 3-HO-C₁₀H₆-2-CONHNC(CH₃)COOH, R = n-C₄H₉, Y = H₂O, (**6**), R = Ph (**7**), R = Me (**8**). The complexes **1-8** (Scheme 4.5) were produced by the reaction of the Schiff base and trialkyltin in 1:1 stoichiometry. They have used strong base in the reaction of complexes **1-5** and mild base in the complexes **6-8**, the enolization was observed in all the complexes. These complexes have been characterized by elemental analysis, IR, ¹H and ¹¹⁹Sn NMR spectra. The crystal and molecular structure of complexes **1**, **2** and **6** have been determined by X-ray single crystal diffraction. Results show that complex **1** has a dimeric structure and the central tin atom is rendered seven-coordinate in a distorted pentagonal-bipyramid configuration. The complex **2** has a monoclinic structure and the central tin atom is rendered six-coordinate in octahedrally configuration with a planar of SnO₃N unit and two apical aryl C atoms. And the whole structure consists of molecular units connected by weak intermolecular Sn----N and O-H---N interactions. In the complex **6**, the central tin atom is five-coordinate in distorted trigonal-bipyramidal geometry. Several reactions of the Schiff base ligand and the alkyltin in different solutions have received different products; they have previously reported some di-organotin complexes of pyruvic acid isonicotinyl hydrazone and pyruvic acid salicylhydrazone [91-94].



Scheme 4.5 (a) Inolization of ligand (b) synthesis and description of compounds 1-8 [90].

Mendes *et al.* [95] were investigated that the reaction of n-butylin trichloride [(n-Bu)SnCl₃] with 2-pyridineformamide thiosemicarbazone (H₂Am₄DH) and its N(4)-methyl (H₂Am₄Me) and N(4)-ethyl (H₂Am₄Et) derivatives gave [(n-Bu)Sn(2Am₄DH)Cl₂] (1), [(n-Bu)Sn(2Am₄Me)Cl₂] (2), and [(n-Bu)Sn(2Am₄Et)Cl₂] (3). Thiosemicarbazones as well as their tin complexes are active as antimicrobials against the growth of *Candida albicans* and *Salmonella typhimurium* and were highly active against malignant glioblastoma. The cytotoxic activity of complexes 1-3 is similar. Among the studied compounds [(n-Bu)Sn(2Am₄DH)Cl₂] (1) was the most active as antiproliferative (cytostatic) agent. Thiosemicarbazones and their tin(IV)

complexes proved to be more potent as cytotoxic agents than cisplatin. All the compounds were able to induce apoptosis.

Nath *et al.* [96] have synthesized some new triphenyltin(IV) complexes with semicarbazones and thiosemicarbazones of the general formula $\text{Ph}_3\text{SnCl.L}$ (L= semicarbazone or thiosemicarbazone of salicylaldehyde, o-hydroxynaphthaldehyde, 2-methoxybenzaldehyde, 4-methoxybenzaldehyde, furfuraldehyde, o-hydroxyacetophenone, benzyl methyl ketone and benzil) and characterized on the basis of elemental analysis, conductance measurements, IR, ^1H NMR and electronic spectral studies. An octahedral structure has been proposed for all these complexes.

Three bidentate Schiff bases having nitrogen and sulphur donor sequences were prepared by condensing S-benzylthiocarbamate ($\text{NH}_2\text{NHCS}_2\text{CH}_2\text{C}_6\text{H}_5$) with heterocyclic aldehydes. The reaction of diphenyltin dichloride with Schiff bases leads to the formation of a new series of organotin(IV) complexes (Fig. 4.18). An attempt has been made to prove their structures on the basis of elemental analyses, conductance measurements, molecular weights determinations, UV, infrared, and multinuclear magnetic resonance (^1H , ^{13}C , and ^{119}Sn) spectral studies. Organotin(IV) complexes were five- and six-coordinate. Schiff bases and their corresponding organotin complexes have also been screened for their antibacterial and antifungal activities and found to be quite active in this respect [97]. These authors have published several works about organotin(IV) complexes of biologically active Schiff bases derived from sulpha drugs [98] and coordination compounds of organotin(IV) with nitrogen and sulfur donor ligands [99]. This group has also reported some tin(II) complexes with semicarbazones and thiosemicarbazones of heterocyclic ketones [100].

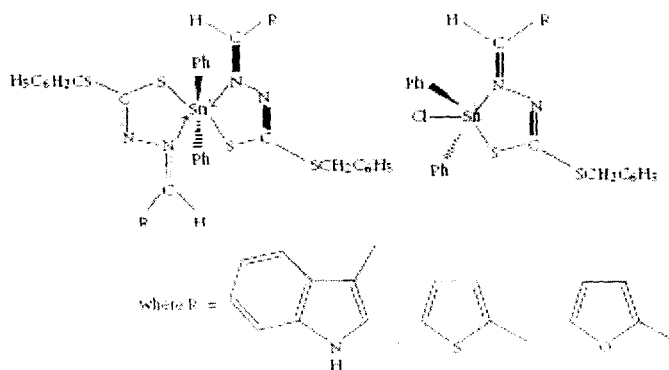


Fig. 4.18 Geometry of the organotin(IV) complexes [97].

W. Rehman and his coworkers [101] have synthesized five novel organotin(IV) derivatives by refluxing trimethyl, triethyl, tributyl, and triphenyl and tribenzyltin chloride with Schiff base derived from salicylaldehyde and adenine (Fig. 4.19). These compounds were characterized by spectroscopic (IR, ^1H , ^{13}C , ^{119}Sn -NMR, $^{119\text{m}}\text{Sn}$ Mössbauer) techniques and elemental analysis. Based on these results, trigonal bipyramidal geometry is suggested. The synthesized compounds were also treated with various microorganisms and found to be active. In order to expand the scope of investigations on the coordination behavior of various donor ligands towards organotins, previously they carried out the investigations on organotin(IV) compounds containing various ligands and established their bioactivities [102-105].

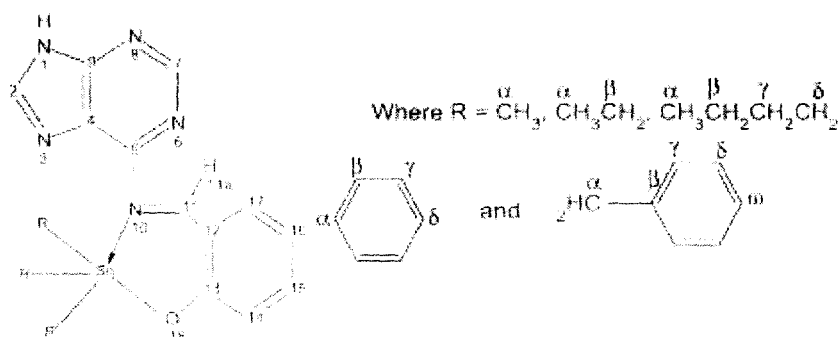


Fig. 4.19 Proposed structure of trialkyltin (IV) complexes of the ligand. [101].

In 2002, Singh *et al.* [106] reported the description of synthetic procedure and structural characterization on the basis of analytical and spectroscopic techniques of a new class of coordination compounds of organotin(IV) with a sulfur-containing ligand moiety L derived by the condensation of 1-acetylferrocene and thiosemicarbazide (Fig. 4.20). Finally, attempts have been made to establish a correlation between a variety of biointeraction activities, including antimicrobial activity and antifertility activity, on male rats and the structures of the resulting products on the basis of different constituents and chemical phenomena. Previously, Belwal and Singh [107] have synthesized diorganotin(IV) derivatives of the types $\text{R}_2\text{SnCl}(\text{TSCZ})$ and $\text{R}_2\text{Sn}(\text{TSCZ})_2$ (where TSCZ is the anion of a thiosemicarbazone ligand, $\text{R}=\text{Ph}$ or Me). The ligands were prepared by the condensation of heterocyclic ketones, i.e. 1,3-dihydro-3-(2-

phenyl-2-oxoethylidene)-2H-indol-2-one, and 2-phenyl-3-(3-phenyl-3-oxoprop-1-enyl)indole with hydrazine carbothioamide in 1 : 1 molar ratio in absolute ethanol to give L_1 and L_2 (Fig. 4.21). Synthesized diorganotin(IV) derivatives were characterized by elemental analyses, molecular weight determinations and conductivity measurements. The mode of bonding has been established on the basis of IR and ^1H , ^{13}C , ^{29}Si and ^{119}Sn NMR spectroscopic studies. Some of the representative complexes have also been evaluated for their antimicrobial effects on different species of pathogenic fungi and bacteria *in vivo* as well as *in vitro*. The results of these investigations were reported.

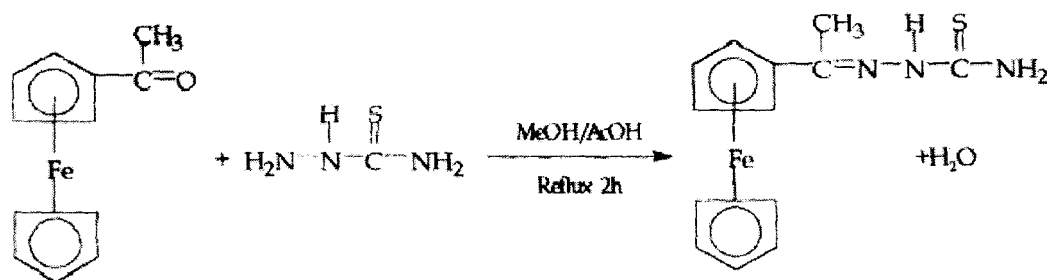


Fig. 4.20 Preparation of the ligand L [106].

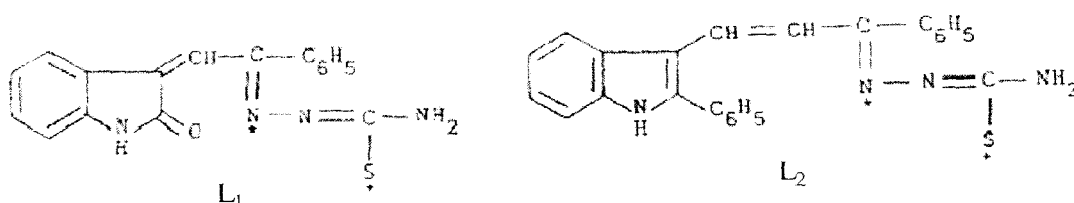


Fig. 4.21 Structure of ligands L_1 and L_2 [107].

Some new organotin(IV) complexes having general formulae $\text{R}_2\text{SnCl}[\text{L}]$ and $\text{R}_2\text{Sn}[\text{L}]_2$. Singh *et al.* [108] were synthesized by the reactions of Me_2SnCl_2 with Schiff bases, derived from condensation of pyrrol-2-carboxaldehyde with different triazoles [5-Mercapto-4-(pyrrolcarboxalideneamino)-*s*-triazole, 5-Mercapto-3-methyl-4-(2pyrrolcarboxalideneamino)*s*-triazole, 3-Ethyl-5-mercapto-4-(2-pyrrolcarboxalideneamino)-*s*-triazole] in 1:1 and 1:2 molar ratios (Fig. 4.22). All of the compounds were characterized by elemental analysis, molar conductance, IR, UV, ^1H , ^{13}C and ^{119}Sn NMR spectral studies. The IR and ^1H NMR spectral data suggest

the involvement of azomethine nitrogen in coordination with the central metal atom. With the help of the above-mentioned spectral studies, penta- and hexacoordinated environments around the central metal atoms in the 1:1 and 1:2 complexes, respectively, have been proposed. Finally, the free ligands and their metal complexes were tested *in vitro* against some pathogenic bacteria and fungi to assess their antimicrobial properties.

T. S. Basu Baul and his coworkers [109] reported the studies on several organotin(IV) compounds such as diorganotin(IV) compounds of the types Ph_2SnLH (monomer), ${}^n\text{Bu}_2\text{SnLH}\cdot\text{OH}_2$ (monomer), $[\text{Me}_2\text{SnLH}\cdot\text{OH}_2]_2$ (centrosymmetric dimer), $[\text{nBu}_2\text{SnLH}]_3$ (cyclic trinuclear), $[\text{Ph}_2\text{SnLH}]_n$ (polymer), $\{[{}^n\text{Bu}_2\text{Sn}(\text{LH})]_2\text{O}\}_2$ (centrosymmetric tetranuclear), dinuclear di-/tri-mixed organotin(IV) compounds $\text{Ph}_2\text{SnLH}\cdot\text{Ph}_3\text{SnCl}$ (monomer) and triorganotin(IV) compounds of the types $[\text{Bz}_3\text{SnLH}]_2$ (centrosymmetric dimer) and $[\text{Me}_3\text{SnLH}]_n$ (Polymer) (LH=Schiff base carboxylate) in the solid state at liquid nitrogen temperature using ${}^{119}\text{Sn}$ Mössbauer spectroscopy. The tin coordination geometry of the compounds determined from crystallography was correlated with the ${}^{119}\text{Sn}$ Mössbauer results.

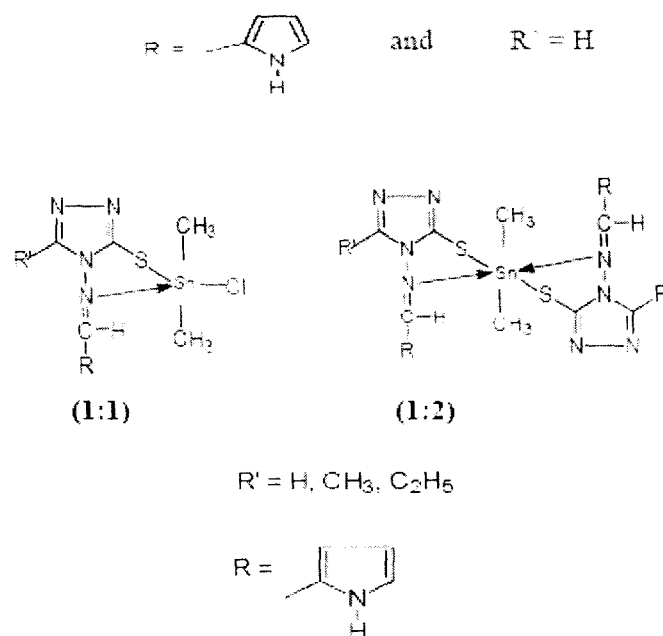


Fig. 4.22 Proposed structures of the 1:1 and 1:2 complexes [108].

A tin complex with coordination number four has been reported by Ng *et al.* [110] that of $[\text{SnPh}_3(\text{HMeSTSC})]$, (Fig. 4.23) which was obtained by slow evaporation of a solution of triphenyltin hydroxide and the thiosemicarbazone in 1:1 mole ratio in ethanol. In this compound the S-coordinated TSC retains the E-configuration it has in the hemihydrate of the free ligand. The thiosemicarbazonato fragment is twisted rather than planar. Three C atoms of the phenyl group and the TSC S atom defines a distorted tetrahedral coordination polyhedron for the tin atom. Ng *et al.* [111] have also prepared the dibutyltin salicylaldehyde semicarbazone $[\text{SnBu}_2(\text{SSC})]$ (Fig.4.24) and the dibutyltin salicylaldehyde thiosemicarbazone $[\text{SnBu}_2(\text{STSC})]$ (Fig. 2.24) by melting together equimolar amounts of dibutyltin oxide and the appropriate ligand. The structure of these two compounds are almost identical with an (O,N,O)- or (S,N,O)-tridentate ligand in Z-configuration and cis-trigonal bipyramidal coordination polyhedron with the phenolic hydroxyl O in one axial position and the semicarbazone O or thiosemicarbazone S in the order.

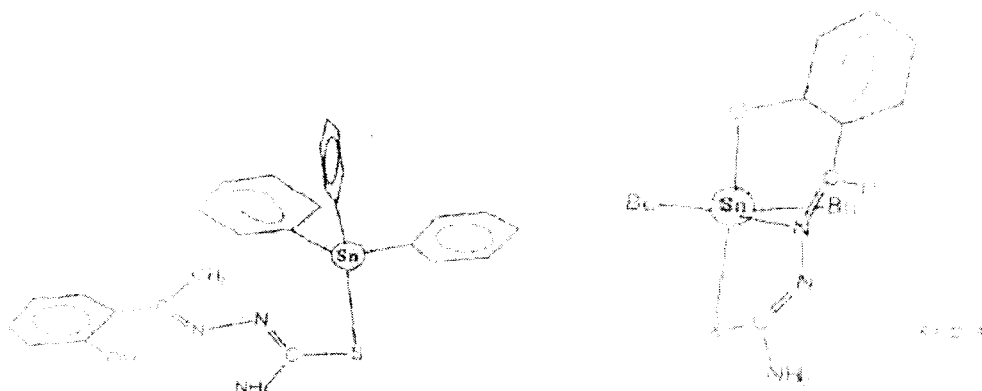


Fig. 4.23 Structures of $[\text{SnPh}_3(\text{HMeSTSC})]$ [110]. **Fig. 4.24** Structure of $[\text{SnBu}_2(\text{SSC})]$ and $[\text{SnBu}_2(\text{STSC})]$ [111].

The structures have been reported for $[\text{SnMe}_2(\text{STSC})]$ and $[\text{SnPh}_2(\text{STSC})]$, the slight differences in them being due to the different organotin units [112]. Both these compounds are obtained by azeotropic distillation of $\text{SnR}_2(\text{O})$ and salicylaldehyde thiosemicarbazone in benzene. The ligand pyridine-2-carbaldehyde thiosemicarbazone is only [S,N(3)]-bidentate in $[\text{SnMe}_2(\text{PyTSC})\text{Cl}]\cdot 0.5 \text{ H}_2\text{O}$ (Fig. 4.25) [59]. The authors argue that the coordination of the pyridine N atom is prevented by a severe distortion together with steric hindrance by the two methyl

groups. The ligand is deprotonated and the tin atom is five-coordinated in a severely distorted trigonal bipyramidal arrangement.

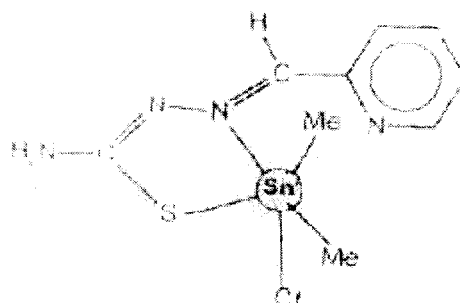


Fig. 4.25 Structure of $[\text{SnMe}_2(\text{PyTSC})\text{Cl}] \cdot 0.5 \text{H}_2\text{O}$. [59].

Equimolar reactions of Bu_2SnO with ion of a new series of Schiff bases derived from amino acids led to the formation of a new series of $\text{Bu}_2\text{Sn}(\text{IV})^{2+}$ complexes of general formula Bu_2SnL (L=dianion of tridentate Schiff bases derived from the condensation of 2-hydroxy-1-naphthaldehyde or acetyl acetone with Gly, L- β -Ala, DL-Val, DL-4-aminobutyric acid, L-Met, L-Leu and PhGly). The central tin $\text{Sn}(\text{IV})$ ions in all these complexes are pentacoordinated with a monodentate carboxylic group. The complexes have been tested against various bacteria and exhibited moderate activity [113].

In $[\text{SnCl}_3(\text{PyTSC})]$ (Fig. 4.26) the distorted octahedral coordination polyhedron of the tin atom is completed by three Cl atoms. The difference in coordination mode with respect to $[\text{SnMe}_2(\text{PyTSC})\text{Cl}] \cdot 0.5 \text{H}_2\text{O}$ in which the same ligand, with very similar geometry, is attributable to the replacement of two Me groups by Cl atoms on the tin atom, which eliminates steric hindrance and increases the acceptor strength of the tin atom [58].

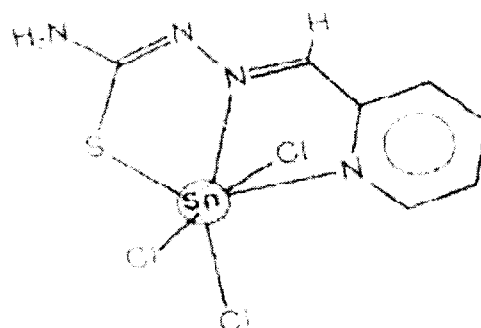


Fig. 4.26 Structure of $[\text{SnCl}_3(\text{PyTSC})]$ [58].

Teoh *et al.* [114] obtained $[\text{SnPh}_2\text{Cl}_2(\text{HATSC})_2]$ (Fig. 4.27) by reacting a solution of SnPh_2Cl_2 in ethanol with a solution of thiosemicarbazide in a mixture of ethanol and acetone. This compound has interesting biological activity. The ligand is monodentate, coordinating to the tin via its S atom. The C–S bond is longer than in the free ligand. The coordination polyhedron is a distorted all-trans octahedron.

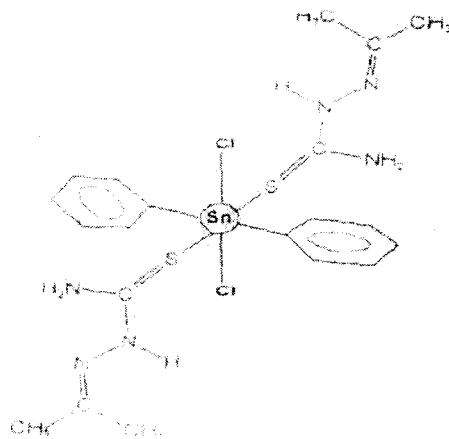


Fig. 4.27 Structure of $[\text{SnPh}_2\text{Cl}_2(\text{HATSC})_2]$ [114].

Refluxation of a mixture of HPyTSC and $\text{SnMe}_2(\text{OAc})_2$ in dry methylene chloride yielded $[\text{SnMe}_2(\text{PyTSC})(\text{OAc})]\cdot\text{HOAc}$ [115] (Fig. 4.28). In this compound the PyTSC ligand is planar and (N,N,S)-tridentate. Although the acetate anion is monodentate, the non-coordinated O atom probably plays an important role in determining the geometry of the coordination polyhedron around the tin atom, which may be described as a distorted pentagonal bipyramid with the methyl group occupy axial and one of the equatorial positions.

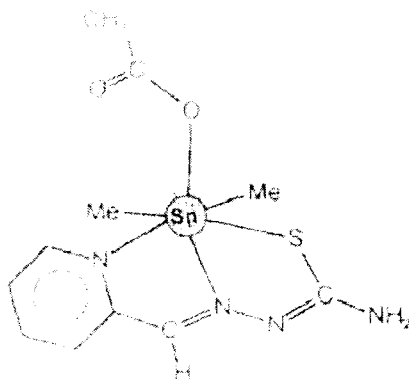


Fig 4.28 Structure of $[\text{SnMe}_2(\text{PyTSC})(\text{OAc})]\cdot\text{HOAc}$ [115].

Tin has attained coordination number seven with the derivatives of diacetylpyridine: 2,6-diacetylpyridine bis(semicarbazone) (H₂DAPSC) and its thio analogue, 2,6-diacetylpyridine bis(thiosemicarbazone) (H₂DAPTSC). Two tin complexes of H₂DAPSC and three tin complexes of H₂DAPTSC have been characterized. By reacting (CH₄N)₃[Pt(SnCl₃)₅] with H₂DAPSC, Sommerer and Palenik [116] unexpectedly obtained [SnCl₂(H₂DAPSC)]Cl₂·2H₂O. In the [SnCl₂(H₂DAPSC)]²⁺ cation, the planar H₂DAPSC moiety is (N,N,O,O)-pentadentate, defining around the tin in the equatorial plane of a slightly distorted pentagonal bipyramid in which the two Cl atoms are axial. A similar structure is possessed by the cation [SnMeCl(H₂DAPSC)]²⁺, which is found in [SnMeCl(H₂DAPSC)]Cl₂·2H₂O [51]. Replacement of a Cl by a Me group does not significantly change the Sn–N bond lengths. By reacting H₂DAPTSC with diphenyltin(IV) oxide in DMF, Casas *et al.* [117] obtained [SnPh₂(DAPTSC)]·2DMF, in which the bis(thiosemicarbazone) ligand is deprotonated and pentadentate.

4.3 Scope and Objective

The Schiff bases obtained by the condensation of salicylaldehyde and substituted salicylaldehyde with thiosemicarbazide and 4-alkyl-thiosemicarbazide to give a class of versatile O,N,S donor ligands. Schiff bases continue to attract attention as they are known to be capable of stabilizing uncommon oxidation states, [26-29] to give rise to unusual coordination numbers and redox reactions in their transition metal complexes [30-32, 118-120]. In the context of the present investigation, it is the potential biological applications of Schiff base compounds which is paramount. Motivated by this imperative, the chemistry of organotin compounds with Schiff bases is well established in the literature [11, 44, 90, 121]. Unusual coordination mode of salicylaldehyde thiosemicarbazone was observed in a group of [M(PPh₃)₂(saltsc)₂] complexes, where R= Ru, Os and saltsc= anion of salicylaldehyde thiosemicarbazone [122, 123]. This work was also motivated by the desire to investigate the ligating behaviour of the versatile thiosemicarbazones towards the organotin(IV) moieties. Our particular interest in these compounds relates to delineating their biological properties specially act as a fungicide in agriculture.

4.4 Experimental

4.4.1 General comments

The solvents used in reactions were of AR grade and were obtained from commercial sources (Merck, India). The solvents were dried using standard literature procedures. Petroleum ether (60-80°C) and benzene were distilled from sodium where as methanol was distilled after reacting it with solid iodine and magnesium. While working with benzene as a solvent, proper health precaution was undertaken.

4.4.2 Materials

The 3-Bromo-5-chloro-salicylaldehyde (Aldrich, USA), 3,5-dibromo-salicylaldehyde (Aldrich, USA), salicylaldehyde (Fluka AG, Switzerland), thiosemicarbazide (Loba Chemie, India), tin powder (Merck, India), benzyl chloride (s.d. fine-chem, India), ortho-amino thio phenol (s.d.fine-chem, India), cyclohexyl amine (s.d.fine-chem, India), (NH₄OH (Merck, India), carbon di sulphide (s.d.fine-chem, India), Ethanol (Bengal Chemical, India), chloro acetic acid (BDH Lab Chem Glaxo, India), Hydrazine hydrate (s.d.fine-chem, India), n-dibutyltin oxide (Alfa, USA), Me₂SnCl₂ (Fluka, Germany), Ph₂SnCl₂ (Aldrich, USA), and n-Bu₂SnCl₂ (Merck, Germany), were purchased from commercial sources. Sodium chloroacetate was prepared by neutralization the solution of chloroacetic acid with NaOH. The Bz₂SnCl₂, was prepared using the method of Sisido *et al.* [124]. Me₂SnO and Ph₂SnO were prepared by the alkaline hydrolysis of respective di- organotin chlorides in water/ether mixtures.

4.4.3 Measurements

The ¹H, ¹³C and ¹¹⁹Sn NMR spectra were recorded in CDCl₃ solution using TMS as an internal standard (for ¹H and ¹³C) on a Bruker DPX 300 and Bruker Avance II 500 (operating at 500.08, 125.76, and 186.46 MHz, respectively) spectrometers. The ¹¹⁹Sn spectra were recorded under broadband ¹H decoupling during acquisition and were referenced to $\Xi = 37.290665$ MHz [125]. The IR spectra in the range 4000-400 cm⁻¹ were recorded on FTIR-8300 Shimadzu spectrophotometer with samples investigated as KBr palate on a CsI window. The

electronic absorption spectra were recorded on a Shimadzu UV 2450 spectrophotometer and emission data were recorded on a Spex Fluorolog 2 spectrophotometer in methanol. Microanalyses were performed at the ICAS, Kolkata, India. Differential calorimetric analyses were carried out on a Perkin-Elmer Thermal analyzer from 100-230°C at a heating rate of 10°C/min. Tin was estimated as SnO₂ gravimetrically using standard procedure in our laboratory.

4.4.4 Synthetic procedure

The methods employed for the preparation of Schiff bases of salicylaldehyde/ substituted salicylaldehyde from thiosemicarbazide/ 4-alkyl-thiosemicarbazide/ 2-amino thio phenol are described in section 4.4.4.1-4.4.4.5. It may be mentioned here that due to poor solubility of the ligands in CDCl₃ or C₆D₆, the NMR spectra for them could not be recorded. However, the x-ray crystal structures of the organotin compounds synthesized confirm the identity of the ligands as well. The synthesis of organotin(IV) complexes of the thiosemicarbazones are described in 4.4.4.6-4.4.4.16. Their characterization, analytical and spectroscopic data are given in section 4.5.

The author gratefully acknowledges the work of Ms. Babita Chowdhury who synthesised the compounds 1-4 [152] included hereunder. The procedure described here produced higher product yields utilizing different solvent media and less reaction time..

4.4.4.1 Preparation of 4-cyclohexyl thiosemicarbazide

Cyclohexyl amine (100 mmol, 11.44 ml, 9.92g) was dissolved in ammonia solution (20 ml, d 0.88) and CS₂ (8 ml) was added to it gradually with stirring and cooling below 30°C. Ethanol (25 ml) was then added and the stirring continued till CS₂ had completely dissolved. The reaction mixture was allowed to stand for 2h and a solution of sodium chloroacetate (100 mmol, 11.69 g) was added, followed by hydrazine hydrate (10 ml, 50%). After warming it was filtered. The filtrate was concentrated to half its volume and allowed to stand overnight. The crystals separating were filtered and recrystallized from ethanol to give 4-cyclohexyl thiosemicarbazide (4-c-hexTSC) [126].

4-c-hexTSC: yield: 5.4 g, 54.43%, M.P.: 142°C

Elemental analysis (Calcd. For C₇H₁₅N₃S)

Calcd.: C, 48.52; H, 8.73; N, 24.25%

Found: C, 48.40; H, 8.86; N, 24.28%

IR (cm⁻¹): ν(N-H), 3155(w,b); ν(NH₂)_{asym}, 3442(w,b); ν(NH₂)_{smy}, 3350(w); ν(C=S), 752 (s).

4.4.4.2 Preparation of salicylaldehyde 4-cyclohexyl thiosemicarbazone (L¹H)

The 4-cyclohexyl thiosemicarbazone (2.5g, 14.42 mmol) was dissolved in ethanol (50 ml) and salicylaldehyde (1.76g, 1.04 ml, 14.42 mmol) was added to the solution. The mixture was heated to reflux for 1h and was allowed to stand for over night. The pale yellow crystals separated were filtrated and then recrystallized from ethanol. The product was dried *in vacuo*.

L¹H: yield: 3.6g, 84.50%, M.P.: 194-196°C

Elemental analysis (Calcd. For C₁₄H₁₉N₃OS)

Calcd.: C, 60.62; H, 6.90; N, 15.15%

Found: C, 60.45; H, 6.86; N, 15.10%

IR (cm⁻¹): ν(N-H), 3150(w,b); ν(C=N), 1622 (m); ν(C=S), 750 (s).

4.4.4.3 Preparation of salicylaldehyde ortho-amino thio phenol (L²H)

Ortho-amino thio phenol (1g, 0.85 ml, 7.99 mmol) was dissolved in ethanol (10 ml) and to it dropwise salicylaldehyde (0.98g, 0.57 ml, 7.99 mmol) was added with continuous stirring. The stirring was continued for 1h at room temperature. Thus yielded pale yellow crystals which were collected by filtration. The product was recrystallized from ethanol and dried *in vacuo*.

L²H: yield: 1.75g, 88.38%, M.P.: 124°C

Elemental analysis (Calcd. For C₁₃H₁₁NOS)

Calcd.: C, 68.09; H, 4.84; N, 6.11%

Found: C, 68.25; H, 4.80; N, 6.10%

IR (cm⁻¹): ν(O-H), 3254 (s); ν(C=N), 1653 (w); ν(S-H), 2605 (w).

4.4.4.4 Preparation of 3-bromo-5-Chloro-salicylaldehydethiosemicarbazone (L³H)

A hot ethanolic solution (50 ml) of 3-bromo-5-Chloro-salicylaldehyde (4g, 16.98 mmol) was added to a hot 1:1 ethanol-water (75 ml) of thiosemicarbazide (1.55g, 16.98 mmol) with continuous stirring. The stirring was continued for 2h at hot conditions which resulted solid (white crystalline) formation which was then filtrated. The product was recrystallized from ethanol and dried *in vacuo*.

L³H: yield: 4.60g, 83.63%, M.P.: 265°C

Elemental analysis (Calcd. For C₈H₇N₃OSClBr)

Calcd.: C, 31.14; H, 2.29; N, 13.62%

Found: C, 31.09; H, 2.40; N, 13.60%

IR (cm⁻¹): $\nu(\text{NH}_2)_{\text{asmy}}$, 3448(w,b); $\nu(\text{NH}_2)_{\text{smy}}$, 3355(w); $\nu(\text{C}=\text{N}-\text{N}=\text{C})$, 1612(w); $\nu(\text{C}=\text{S})$, 728(m).

4.4.4.5 Preparation of 3,5-dibromo-salicylaldehydethiosemicarbazone (L⁴H)

A hot ethanolic solution (50 ml) of 3,5-dibromo-salicylaldehyde (4g, 14.29 mmol) was added to a hot 1:1 ethanol-water (75 ml) of thiosemicarbazide (1.30g, 14.29 mmol) with continuous stirring. The stirring was continued for 2h at hot conditions, resulted solid (white crystalline) formation which was then filtrated and collected. The product thus obtained was recrystallized from ethanol and dried *in vacuo*.

L⁴H: yield: 3.75g, 87.20%, M.P.: 253°C

Elemental analysis (Calcd. For C₈H₇N₃OSBr₂)

Calcd.: C, 27.22; H, 2.00; N, 11.90%

Found: C, 27.11; H, 2.04; N, 11.86%

IR (cm⁻¹): $\nu(\text{NH}_2)_{\text{asmy}}$, 3449(w,b); $\nu(\text{NH}_2)_{\text{smy}}$, 3354(w); $\nu(\text{C}=\text{N}-\text{N}=\text{C})$, 1614(w); $\nu(\text{C}=\text{S})$, 724(m).

4.4.4.6 Synthesis of dimethyltin(IV) salicylaldehyde 4-cyclohexyl thiosemicarbazone, Me_2SnL^1 (1)

A mixture of Me_2SnO (1g, 6.07 mmol) and salicylaldehyde 4-cyclohexyl thiosemicarbazone (1.68g, 6.07mmol) in dry toluene (150 ml) was heated under reflux in nitrogen atmosphere for 12h; the water thus produced being removed azeotropically. The solvent were removed from the yellow reaction mixture and the dry mass extracted with hot petroleum ether (60°-80°C, 50 ml). Yellow crystals of the desired product were obtained by cooling the solution to 10°C.

4.4.4.7 Synthesis of n-dibutyltin(IV) salicylaldehyde 4-cyclohexyl thiosemicarbazone, $\text{n-Bu}_2\text{SnL}^1$ (2)

A mixture of $\text{n-Bu}_2\text{SnO}$ (0.9g, 3.60 mmol) and salicylaldehyde 4-cyclohexyl thiosemicarbazone (1.0g, 3.60 mmol) in dry toluene (150 ml) was heated under reflux in nitrogen atmosphere for 14h; the water thus produced being azeotropically. The solvent were removed from the yellow reaction mixture and the dry mass extracted with hot petroleum ether (60°-80°C, 50 ml). A viscous deep yellow liquid was obtained as the product. The product was then dried further in *vacuo* and then distilled for purification and then stored in a dessicator.

4.4.4.8 Synthesis of diphenyltin(IV) salicylaldehyde 4-cyclohexyl thiosemicarbazone, Ph_2SnL^1 (3)

A mixture of Ph_2SnO (1.05g, 3.60 mmol) and salicylaldehyde 4-cyclohexyl thiosemicarbazone (1.0g, 3.60 mmol) in dry toluene (150 ml) was heated under reflux in nitrogen atmosphere for 12h; the water thus produced being azeotropically removed. The solvent were removed from the yellow reaction mixture under vacuum and the dry mass extracted with hot petroleum ether (60°-80°C, 50 ml). Yellow crystals of the desired product were obtained by cooling the solution to 10°C.

4.4.4.9 Synthesis of n-dibutyltin(IV) salicylaldehyde ortho-amino thio phenol, $\text{n-Bu}_2\text{SnL}^2$ (4)

A mixture of $\text{n-Bu}_2\text{SnO}$ (1.08g, 4.36 mmol) and salicylaldehyde ortho-amino thio phenol (1.0g, 4.36 mmol) in dry toluene (150 ml) was heated under reflux in nitrogen atmosphere for 12h; the water thus produced being removed azeotropically. The solvent were removed from the yellow reaction mixture under vacuum and the

dry mass extracted with hot petroleum ether (60°-80°C, 50 ml). A viscous deep yellow colour liquid was obtained as the product. The product was then dried further in *vacuo* at room temperature and then distilled for purification and then stored in a dessicator.

4.4.4.9 Synthesis of dimethyltin(IV) 3-bromo-5-chlorosalicylaldehyde thiosemicarbazone, Me_2SnL^3 (5)

A mixture of Me_2SnO (0.53g, 3.23 mmol) and 3-bromo-5-chlorosalicylaldehyde thiosemicarbazone (1.00g, 3.23 mmol) in dry benzene (140 ml) was heated under reflux in a nitrogen atmosphere for 10h; the water thus produced was removed azeotropically. The solvent was removed from the yellow reaction mixture under vacuum and the dry mass first washed with hot petroleum ether (60°-80°C) and then extracted with benzene (50 ml). Yellow crystals of the desired product were obtained by cooling the solution to 10°C.

4.4.4.10 Synthesis of di n-butyltin(IV) 3-bromo- 5-chlorosalicylaldehyde thiosemicarbazone, $\text{n-Bu}_2\text{SnL}^3$ (6)

A mixture of $\text{n-Bu}_2\text{SnO}$ (0.80g, 3.23 mmol) and 3-bromo-5-chlorosalicylaldehyde thiosemicarbazone (1.00g, 3.23 mmol) in dry benzene (140 ml) was heated under reflux and inert conditions for 10 h; the water produced was removed azeotropically. All volatiles were removed from the yellow reaction mixture and the dry mass extracted with hot petroleum ether (60°-80°C, 50 ml). Yellow crystals of the desired product were obtained by cooling the solution to room temperature.

4.4.4.11 Synthesis of diphenyltin(IV) 3-bromo-5-chloro salicylaldehyde thiosemicarbazone, Ph_2SnL^3 (7)

A mixture of Ph_2SnO (0.94g, 3.23 mmol) and 3-bromo-5-chlorosalicylaldehyde thiosemicarbazone (1.00g, 3.23 mmol) in dry benzene (140 ml) was heated under reflux and inert conditions for 10 h; the water produced was removed azeotropically. The volatiles were removed from the yellow reaction mixture and the dry mass washed with hot petroleum ether (60°C-80°C) and then extracted with dry benzene (50 ml). Crystals of the product (yellow) were obtained by cooling the solution to room temperature.

4.4.4.12 Synthesis of dibenzyltin(IV) 3-bromo-5-chloro-salicylaldehyde thiosemicarbazone, Bz_2SnL^3 (8)

A 0.10M methanolic NaOH (63.48 ml, 0.25g, 6.47 mmol) solution was added dropwise to a solution of 3-bromo-5-chloro-salicylaldehyde thiosemicarbazone (1.00g, 3.23 mmol) in methanol, while stirring. The mixture was stirred for another 2 h and then a methanolic solution of Bz_2SnCl_2 (1.20 g, 3.23 mmol) was added. The yellow reaction mixture was subsequently heated under reflux for 8 h under inert conditions. The volatiles were removed and the dry mass extracted with several aliquots of benzene (50 ml). Slow cooling to room temperature gave rise to a yellow precipitate of the product.

4.4.4.13 Synthesis of dimethyltin(IV) 3, 5-dibromo-salicylaldehyde thiosemicarbazone, Me_2SnL^4 (9)

A mixture of Me_2SnO (0.69g, 4.24 mmol) and 3,5-dibromo-salicylaldehyde thiosemicarbazone (1.50g, 4.24 mmol) in dry benzene (140 ml) was heated under reflux under inert conditions for 10h; the water produced was removed azeotropically. The solvent was removed from the yellow reaction mixture by distilling under low pressure and the dry mass thus obtained was washed with hot petroleum ether (60°-80°C) and extracted with dry benzene (50 ml). Yellow crystals of the desired product were obtained by allowing the solution to cool to room temperature.

4.4.4.14 Synthesis of di-n-butyltin(IV) 3, 5-dibromo-salicylaldehyde thiosemicarbazone, $\text{n-Bu}_2\text{SnL}^4$ (10)

A mixture of $\text{n-Bu}_2\text{SnO}$ (0.70g, 2.83 mmol) and 3,5-dibromo-salicylaldehyde thiosemicarbazone (1.00g, 2.83 mmol) in dry benzene (140 ml) was heated under reflux under inert conditions for 10 h; the water produced was removed azeotropically. The volatiles were removed from the yellow reaction mixture and the solid mass was extracted with hot petroleum ether (60°-80°C, 50 ml). Yellow crystals of the desired product appeared upon cooling of the solution to room temperature.

4.4.4.15 Synthesis of diphenyltin(IV) 3, 5-dibromo-salicylaldehyde thiosemicarbazone, Ph_2SnL^4 (11)

A mixture of Ph_2SnO (1.07g, 3.68 mmol) and 3,5-dibromo-salicylaldehyde thiosemicarbazone (1.30g, 3.68 mmol) in dry benzene (140 ml) was heated under

reflux and inert conditions for 10h; the water produced was removed azeotropically. The volatiles were removed from the yellow reaction mixture, the solid thus obtained was washed with hot petroleum ether (60°-80°C), and then extracted with dry benzene (50 ml). Yellow crystals of the desired product were obtained by cooling the solution to room temperature.

4.4.4.16 Synthesis of dibenzyltin(IV)3,5-dibromo-salicylaldehyde thiosemicarbazonate, Bz_2SnL^4 (12)

A 0.10M methanolic NaOH (50.44 ml, 0.23g, 5.66 mmol) solution was added dropwise to a solution of 3,5-dibromo-salicylaldehyde thiosemicarbazone (1.00g, 2.83 mmol) in methanol, while stirring. The mixture was stirred for another 2h and then a methanolic solution of Bz_2SnCl_2 (1.05g, 2.83 mmol) was added. The yellow reaction mixture was subsequently heated under reflux for 8 h under inert conditions. The volatiles were removed and the dry mass extracted with several aliquots of benzene (50 ml). Slow cooling to room temperature gave rise to a yellow precipitate of the titled product.

4.4.5 Crystal structure determination

The crystals of (5), (6), (7), (9) and (10) suitable for the X-ray diffraction study were prepared by slow crystallization of benzene solutions of the respective compounds; the crystallographic analysis of (7) showed the sample had crystallised as a hemi-benzene solvate. Intensity data were collected at room temperature on a Bruker SMART APEX CCD fitted with Mo $K\alpha$ radiation. The data set was corrected for absorption based on multiple scans [127] and reduced using standard methods [128]. The structures were solved by direct-methods with SHELXL-97 [129] and refined by a full-matrix least-squares procedure on F^2 using SHELXL-97 [129] with anisotropic displacement parameters for non-hydrogen atoms, hydrogen atoms in their calculated positions and a weighting scheme of the form $w = 1/[\sigma^2(F_o^2) + (aP)^2 + bP]$ where $P = (F_o^2 + 2F_c^2)/3$. In the analysis of (7), two positions for each of the tin-bound phenyl rings were resolved. In the refinement, the anisotropic displacement parameters for matched pairs of atoms were constrained to be equivalent and to be approximately isotropic by utilising the EADP and ISOR commands in SHELXL-97 [129]. Refinement showed that each component of the disorder had a site occupancy

factor = 0.5. In the refinements of the di-*n*-butyl compounds, **(6)** and **(10)**, high thermal motion was noted for the *n*-butyl groups. As multiple positions were not resolved, the 1-,2- and 1-,3-C–C distances were restrained to $1.54 \pm 0.01 \text{ \AA}$ and $2.51 \pm 0.01 \text{ \AA}$, respectively. Crystal data and refinement details are given in Table 1. The molecular structures showing crystallographic numbering schemes were drawn with 35% displacement ellipsoids using ORTEP-3 [130] and the remaining figures were drawn with DIAMOND [131]. Additional data analysis was accomplished using PLATON [132].

4.4.6 Crystallographic data and refinement details for 5, 6, 7, 9 and 10.

Table 4.1 Crystallographic data and refinement details for [Me₂SnL³]

Empirical formula	C ₁₀ H ₁₁ BrClN ₃ OSSn
Formula weight	455.33
Crystal habit, colour	cube, yellow
Crystal system	Monoclinic
Space Group	<i>C2/c</i>
<i>A</i> (Å)	14.7612(9)
<i>B</i> (Å)	13.3430(8)
<i>C</i> (Å)	15.2054(9)
α (°)	90
β (°)	91.6906(9)
γ (°)	90
Volume (Å ³)	2993.5(3)
<i>Z</i>	8
Density (calculated, g cm ⁻³)	2.021
Absorption coefficient (mm ⁻¹)	4.686
<i>F</i> (000)	1744
Crystal size (mm)	0.20 x 0.20 x 0.20
θ range for data collection (°)	2.1 – 27.5
Reflections collected	14038
Independent reflections	3432
<i>R</i> _{int}	0.025
Reflections with <i>I</i> ≥ 2σ (<i>I</i>)	2802
Number of parameters	171
<i>A</i> , <i>b</i> for weighting scheme	0.022, 5.987
Final <i>R</i> indices [<i>I</i> ≥ 2σ (<i>I</i>)]	<i>R</i> = 0.025
	<i>wR</i> ₂ = 0.055
<i>R</i> indices [all data]	<i>R</i> = 0.036
	<i>wR</i> ₂ = 0.060
Largest difference peak and hole (Å ⁻³)	0.91, -0.68

Table 4.2 Crystallographic data and refinement details for [n-Bu₂SnL³]

Empirical formula	C ₁₆ H ₂₃ BrClN ₃ OSSn
Formula weight	539.48
Crystal habit, colour	block, yellow
Crystal system	Monoclinic
Space Group	<i>P2₁/c</i>
<i>a</i> (Å)	17.2188(12)
<i>b</i> (Å)	8.7465(6)
<i>c</i> (Å)	14.9051(10)
α (°)	90
β (°)	108.4257(9)
γ (°)	90
Volume (Å ³)	2129.7(3)
<i>Z</i>	4
Density (calculated, g cm ⁻³)	1.683
Absorption coefficient (mm ⁻¹)	3.307
<i>F</i> (000)	1664
Crystal size (mm)	0.10 x 0.25 x 0.35
θ range for data collection (°)	2.5–27.5
Reflections collected	12543
Independent reflections	4871
<i>R</i> _{int}	0.035
Reflections with <i>I</i> ≥ 2σ (<i>I</i>)	3568
Number of parameters	225
<i>a</i> , <i>b</i> for weighting scheme	0.030, 2.458
Final <i>R</i> indices [<i>I</i> ≥ 2σ (<i>I</i>)]	<i>R</i> = 0.037 <i>wR</i> 2 = 0.080
<i>R</i> indices [all data]	<i>R</i> = 0.062 <i>wR</i> 2 = 0.091
Largest difference peak and hole (Å ⁻³)	0.76, -0.89

Table 4.3 Crystallographic data and refinement details for [Ph₂SnL³]

Empirical formula	C ₂₃ H ₁₈ BrClN ₃ OSSn
Formula weight	618.51
Crystal habit, colour	block, yellow
Crystal system	Triclinic
Space Group	<i>P</i> 1
<i>a</i> (Å)	9.1612(7)
<i>b</i> (Å)	9.8617(8)
<i>c</i> (Å)	13.5553(11)
α (°)	94.159(1)
β (°)	92.155(1)
γ (°)	99.109(1)
Volume (Å ³)	1204.53(17)
<i>Z</i>	2
Density (calculated, g cm ⁻³)	1.705
Absorption coefficient (mm ⁻¹)	2.937
<i>F</i> (000)	606
Crystal size (mm)	0.10 x 0.20 x 0.30
θ range for data collection (°)	1.5 – 27.5
Reflections collected	11506
Independent reflections	5488
<i>R</i> _{int}	0.030
Reflections with $I \geq 2\sigma(I)$	3860
Number of parameters	274
<i>a</i> , <i>b</i> for weighting scheme	0.046, 1.141
Final <i>R</i> indices [$I \geq 2\sigma(I)$]	<i>R</i> = 0.043 <i>wR</i> 2 = 0.010
<i>R</i> indices [all data]	<i>R</i> = 0.071 <i>wR</i> 2 = 0.114
Largest difference peak and hole (Å ⁻³)	0.90, -0.80

Table 4.4 Crystallographic data and refinement details for [Me₂SnL⁴]

Empirical formula	C ₁₀ H ₁₁ Br ₂ N ₃ OSSn
Formula weight	499.79
Crystal habit, colour	block, yellow
Crystal system	Monoclinic
Space Group	<i>C2/c</i>
<i>a</i> (Å)	14.9682(12)
<i>b</i> (Å)	13.4107(10)
<i>c</i> (Å)	15.2213(12)
α (°)	90
β (°)	92.040(1)
γ (°)	90
Volume (Å ³)	2993.5(3)
<i>Z</i>	8
Density (calculated, g cm ⁻³)	2.174
Absorption coefficient (mm ⁻¹)	7.036
<i>F</i> (000)	1888
Crystal size (mm)	0.30 x 0.35 x 0.40
θ range for data collection (°)	2.0 – 27.5
Reflections collected	13737
Independent reflections	3491
<i>R</i> _{int}	0.043
Reflections with $I \geq 2\sigma(I)$	2581
Number of parameters	171
<i>a</i> , <i>b</i> for weighting scheme	0.030, 10.080
Final <i>R</i> indices [$I \geq 2\sigma(I)$]	<i>R</i> = 0.034
	<i>wR</i> ₂ = 0.078
<i>R</i> indices [all data]	<i>R</i> = 0.058
	<i>wR</i> ₂ = 0.088
Largest difference peak and hole (Å ⁻³)	0.99, -0.76

Table 4.5 Crystallographic data and refinement details for [n-Bu₂SnL⁴]

Empirical formula	C ₁₆ H ₂₃ Br ₂ N ₃ OSSn
Formula weight	583.94
Crystal habit, colour	block, yellow
Crystal system	Monoclinic
Space Group	<i>P</i> 2 ₁ / <i>c</i>
<i>a</i> (Å)	17.2465(13)
<i>b</i> (Å)	8.7688(6)
<i>c</i> (Å)	14.7170(11)
α (°)	90
β (°)	108.893(1)
γ (°)	90
Volume (Å ³)	2105.8(3)
<i>Z</i>	4
Density (calculated, g cm ⁻³)	1.842
Absorption coefficient (mm ⁻¹)	5.116
<i>F</i> (000)	1136
Crystal size (mm)	0.10 x 0.15 x 0.35
θ range for data collection (°)	1.3 – 27.5
Reflections collected	19497
Independent reflections	4838
<i>R</i> _{int}	0.048
Reflections with <i>I</i> ≥ 2σ (<i>I</i>)	3592
Number of parameters	225
<i>a</i> , <i>b</i> for weighting scheme	0.045, 0.325
Final <i>R</i> indices [<i>I</i> ≥ 2σ (<i>I</i>)]	<i>R</i> = 0.033 <i>wR</i> 2 = 0.079
<i>R</i> indices [all data]	<i>R</i> = 0.054 <i>wR</i> 2 = 0.089
Largest difference peak and hole (Å ⁻³)	0.57, -0.62

4.4.7 Biological studies

4.4.7.1 Antifungal activity

The virulent fungal strains of *Bipolaris sorokiniana*, *Helminthosporium oryzae*, *Altreneria brassicae*, *Alternaria kikuchiana*, *Stemphylium pori*, and *Colletotrichum capsici* were collected from the Type culture collection, Department of Plant Pathology, Uttar Banga Krishi Viswavidyalaya, Cooch Behar, West Bengal, India. The *B. sorokiniana* was maintained in an oat meal agar medium while the remaining fungi were grown on potato-dextrose agar medium at 27°C. The fungicidal activities were determined following spore germination bioassay as described by Rouxel *et al.* [133]. Purified eluants (15 µl) were placed on two spots 3 cm apart on a clean grooved slide. One drop of spore suspension (15 µl), which was prepared from 15 day old cultures of the fungi, was added to the treated spots. The slides were incubated in trays at 27°C for 24h under humid conditions. After incubation, one drop of Lactophenol mixture was added to each spot to fix the germinated spores. The number of spore germination events was compared with the spore germination of the control.

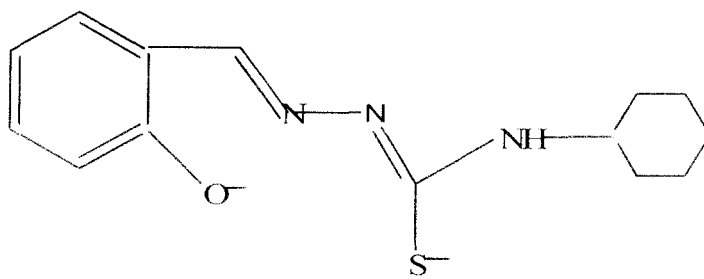
4.4.7.2 Phytotoxic effect

Seeds of Indian wheat (*Triticum aestivum* L.), cultivar *Sonalika* were obtained from the Directorate of Wheat Research, Karnal, India. Seeds of *Oryza sativa*, *Brassica nigra*, *Capicum annum*, and *Brassica oleracea* were collected from the Directorate of Farm, Uttar Banga Krishi Viswavidyalaya, Cooch Behar, West Bengal, India. Seeds were first surface sterilized with 0.1% mercuric chloride for 3 min, washed with distilled water and then the phytotoxic effects of the new organotin compounds (dissolved in 2 ml methanol then diluted with 10 ml water) were determined [134]. Seeds were incubated with different concentration of organotin compounds for different time periods. After incubation, the seeds were washed with distilled water and incubated in a B.O.D. incubator for 48h at 27°C. The percentage of seed germination was calculated and compared with the control.

4.5 Result and discussion

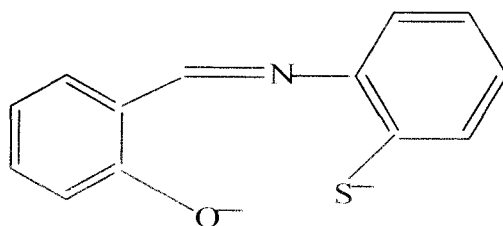
4.5.1 Syntheses of the Schiff base ligands

The ligands used here Schiff bases which are derived from salicylaldehyde/substituted salicylaldehyde (3-bromo-5-chloro-salicylaldehyde, 3,5-dibromo-salicylaldehyde) with thiosemicarbazide/4-cyclohexyl-thiosemicarbazide/ortho-amino thio phenol. These are reacting by equimolar amounts in ethanol or ethanol/water mixture. [123] The products were recrystallized from ethanol. The thiosemicarbazones and were obtained in good yield. The ligands are high melting ($>200^{\circ}\text{C}$) solids, soluble in hot ethanol and methanol but insoluble in benzene, petroleum ether ($60\text{-}80^{\circ}\text{C}$), chloroform and carbon tetrachloride. The formulae of the ligands and complexes are described in Scheme 4.6.



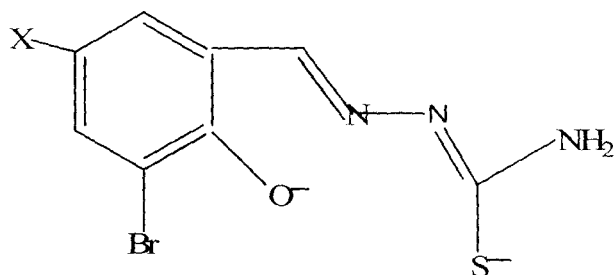
L^1

1. Me_2SnL^1 , 2. $n\text{-Bu}_2\text{SnL}^1$, 3. Ph_2SnL^1



L^2

4. $n\text{-Bu}_2\text{SnL}^2$



- | | |
|---|---|
| <p>L³: X=Cl,</p> <p>5. Me₂SnL³</p> <p>6. n-Bu₂SnL³</p> <p>7. Ph₂SnL³</p> <p>8. Bz₂SnL³</p> | <p>L⁴: X=Br</p> <p>9. Me₂SnL⁴</p> <p>10. n-Bu₂SnL⁴</p> <p>11. Ph₂SnL⁴</p> <p>12. Bz₂SnL⁴</p> |
|---|---|

Scheme : 4.6

4.5.2 Syntheses of the diorganotin(IV) complexes of Schiff base ligands

Two different methods for the synthesis of the diorganotin(IV) complexes of Schiff base ligands were described here. The products were obtained by following both of the synthetic procedures in good yields:

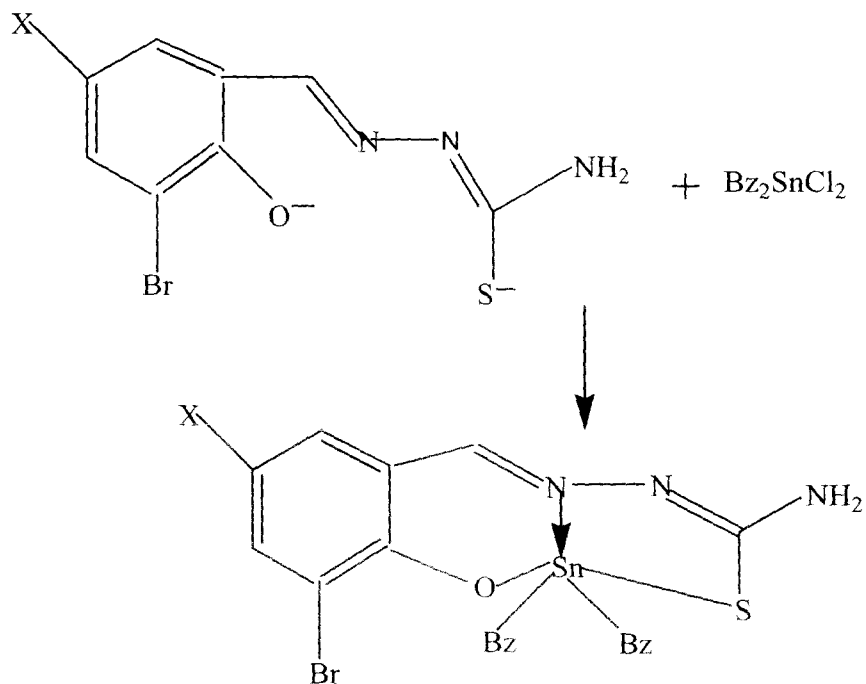
Procedure I

The diorganotin(IV) complexes of Schiff bases were obtained in moderate yields by the equimolar reaction of diorganotin(IV) chlorides with the sodium salt of the ligand in methanol. The sodium salt of the ligand was prepared by the addition of methanolic solution of NaOH to the hot methanolic solution of the ligands and stirred for 2h (Eq. 5 and Eq. 6)



R= benzyl (Bz),

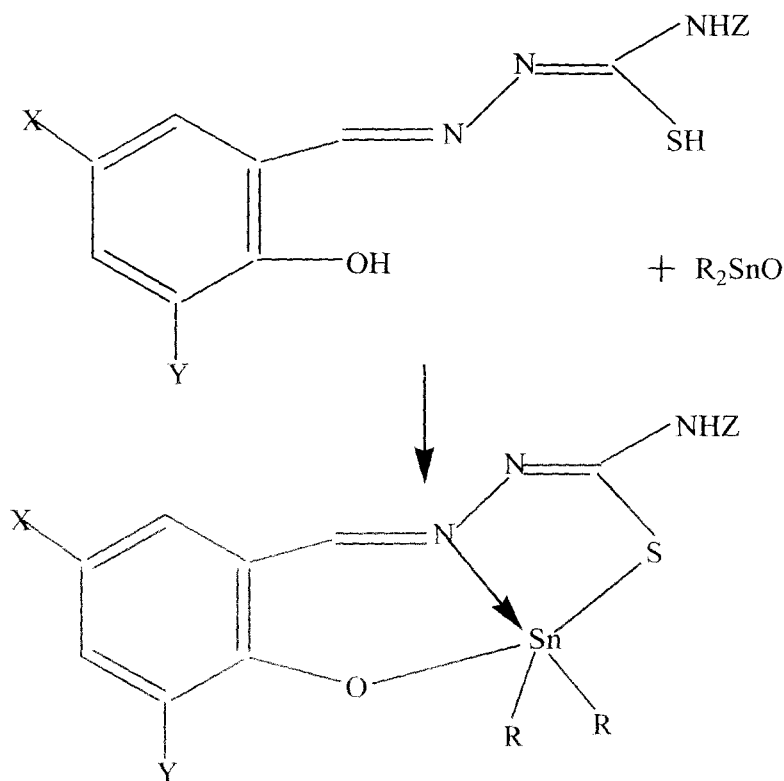
The reactions were completed in 8h. The reaction mixture was evaporated to dryness and extracted with several aliquots of benzene. The synthetic procedure was described in Scheme 4.7.



Procedure II

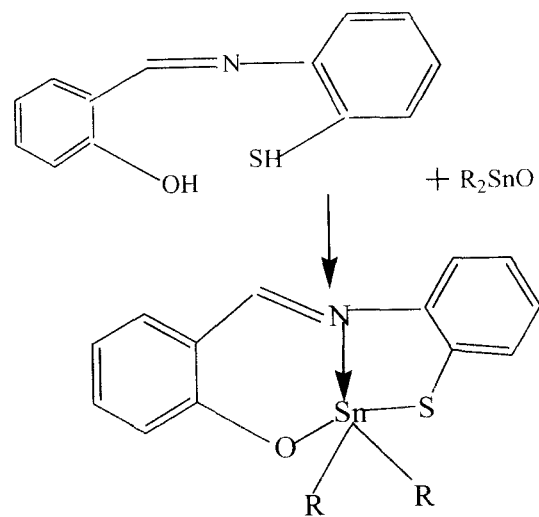
In this procedure the diorganotin(IV) complexes of Schiff bases were obtained in moderate yields by the equimolar reaction of diorganotin(IV) oxide with the respective ligands in dry benzene/toluene (Eq. 7). Schiff bases (i.e, the ligands used) are insoluble in benzene/toluene, the reaction mixture turned to be heterogenous. During the reaction the water produced was removed azeotropically by Dean-Stark Trap for faster completion of the reactions. The volatiles were removed from the yellow reaction mixture, the solid thus obtained was extracted with dry benzene/ hot petroleum ether (60-80°C), (50 ml). Interestingly, the compound **7** was isolated with hemibenzene (0.5) solvate. The compounds are stable in air and recrystallized from suitable solvents. All the compounds are soluble in chloroform,

methanol, benzene, n-hexene and petroleum ether (60-80°C). The synthetic procedure was described in Scheme 4.8 and 4.9.



- | | |
|---|------------------------------------|
| 1: R =Me, X=H, Y=H, Z= Cyclohexyl | 5: R=Me, X=Cl, Y=Br, Z=H |
| 2: R=n-Bu, X=H, Y=H, Z= Cyclohexyl | 6: R=n-Bu, X=Cl, Y=Br, Z=H |
| 3: R=Ph, X=H, Y=H, Z= Cyclohexyl | 7: R=Ph, X=Cl, Y=Br, Z=H |
| | 9: R=Me, X=Br, Y=Br, Z=H |
| | 10: R=n-Bu, X=Br, Y=Br, Z=H |
| | 11: R=Ph, X=Br, Y=Br, Z=H |

Scheme 4.8



4: R=n-Bu

Scheme 4.9

Table 4.6 Physical and analytical data for compound 1-12

Compound number Composition	Yield (%)	m. pt. (°C)	Elemental composition found (calcd) (%)			
			C	H	N	Sn
1. C ₁₆ H ₂₃ N ₃ SOSn	75	98	45.56 (45.31)	5.43 (5.46)	9.78 (9.90)	27.67 (27.98)
2. C ₂₂ H ₃₇ N ₃ SOSn	58	Sticky liquid	51.57 (51.78)	7.25 (7.30)	8.45 (8.23)	23.43 (23.25)
3. C ₂₆ H ₃₁ N ₃ SOSn	60	144	56.68 (56.45)	5.75 (5.66)	7.80 (7.60)	21.59 (21.49)
4. C ₂₁ H ₂₇ NSOSn	53	Sticky liquid	54.79 (54.81)	5.98 (5.91)	3.24 (3.04)	25.86 (25.79)
5. C ₁₀ H ₁₁ N ₃ OSClBrSn	82	157	26.30 (26.38)	2.32 (2.35)	9.21 (9.23)	25.91 (26.07)
6. C ₁₆ H ₂₅ N ₃ OSClBrSn	74	82	35.36 (35.49)	4.61 (4.65)	7.75 (7.76)	21.89 (21.92)
7. C ₂₀ H ₁₅ N ₃ OSClBrSn.0.5C ₆ H ₆	80	212	44.38 (44.66)	2.60 (2.93)	7.20 (6.79)	20.38 (19.19)
8. C ₂₂ H ₁₉ N ₃ OSClBrSn	63	>240	43.44 (43.50)	3.12 (3.15)	6.80 (6.92)	19.42 (19.54)
9. C ₁₀ H ₁₁ N ₃ OSBr ₂ Sn	85	156	23.91 (24.03)	2.25 (2.28)	8.39 (8.41)	23.59 (23.75)
10. C ₁₆ H ₂₅ N ₃ OSBr ₂ Sn	75	108	32.68 (32.80)	4.27 (4.30)	7.14 (7.17)	20.18 (20.26)
11. C ₂₀ H ₁₅ N ₃ OSBr ₂ Sn	83	188	38.41 (38.50)	2.41 (2.42)	6.65 (6.73)	18.88 (19.02)
12. C ₂₂ H ₁₉ N ₃ OSBr ₂ Sn	65	200	40.40 (40.53)	2.75 (2.94)	6.40 (6.44)	18.33 (18.20)

4.5.3 Spectral characterization and X-ray structure determination of diorganotin(IV) complexes

The complexes were characterized by Fluorescence, UV, IR, NMR (¹H, ¹³C, ¹¹⁹Sn) and elemental analysis. X-ray crystal structures were also analyzed for some of these compounds. The discussion on the data obtained is presented below in brief.

4.5.3.1 IR spectra

Selected IR bands and their assignments for the diorganotin(IV) complexes are presented Table 4.7 and 4.8. The IR spectral data of these diorganotin(IV) complexes suggested that the ligands act as tridentate S,N,O ligands, central tin atom coordinating via the thiolate-S, phenoxide-O and imino-N atoms. This is confirmed by the X-ray crystallographic structures.

Table 4.7 IR spectral data (cm^{-1}) for compounds **1-4**^a

Compound	$\nu(\text{NH}_2)$	$\nu(\text{C}=\text{N}-\text{N}=\text{C})$	$\nu(\text{C}-\text{S})$	$\nu(\text{Sn}-\text{C})$
1.	3395 (m,b)	1580 (s),1543 (s)	752 (s)	549(w),486 (w)
2.	3388 (m,b)	1576 (s),1540 (s)	730 (s)	540(w),475 (w)
3.	3384 (m,b)	1575 (s),1541 (s)	727 (s)	535(w),480(w)
4.	-	1580(s)	735 (s)	542(w),478 (w)

^a s, strong; m, medium; w, weak; b, broad.

Table 4.8 IR spectral data (cm^{-1}) for compounds **5-12**^a

Compound	$\nu(\text{NH}_2)_{\text{asym}}$	$\nu(\text{NH}_2)_{\text{sym}}$	$\nu(\text{C}=\text{N}-\text{N}=\text{C})$	$\nu(\text{C}-\text{S})$	$\nu(\text{Sn}-\text{C})$
5.	3438 (m)	3168 (w)	1608 (s)	734 (s)	520, 464 (w)
6.	3462 (m)	3344 (w)	1601 (m)	750-729 (m)	570, 457 (w)
7.	3463 (w)	3286 (w)	1627 (m)	736 (m)	570, 462 (w)
8.	3452 (b,w)	3008 (w)	1621 (m)	728-671 (w)	528, 460 (w)
9.	3427 (b)	3200 (w)	1606 (m)	724 (w)	535, 475 (w)
10.	3431 (b)	3175 (w)	1627 (m)	722 (w)	538, 472 (w)
11.	3409 (b)	3135 (w)	1626 (m)	724 (w)	540, 468 (w)
12.	3462 (b)	3350 (w)	1600(s)	721 (w)	552,458(w)

^a s, strong; m, medium; w, weak; b, broad.

The $\nu(\text{NH}_2)$, $\nu(\text{C}=\text{N}-\text{N}=\text{C})$ and $\nu(\text{Sn}-\text{C})$ bands are assigned on the basis of literature data. [135, 59] The $\nu(\text{NH}_2)$ stretching vibrations due to the ligands in **1-4** appear in the range 3395-3384 cm^{-1} as medium broad bands, both $\nu_{(\text{C}=\text{N})}$ azomethine, and other $\nu_{(\text{N}=\text{C}-)}$ frequencies are present at 1580-1540 cm^{-1} as strong sharp bands,

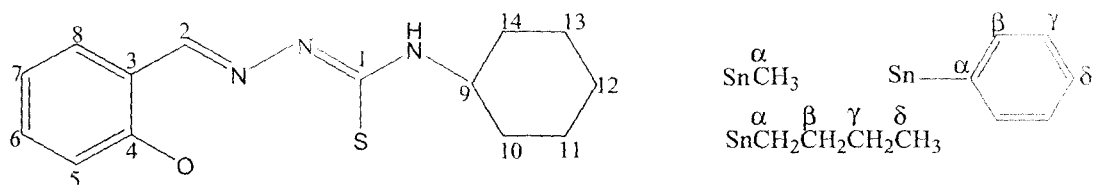
$\nu_{(C-S)}$ stretching frequencies are present in all the compounds at 752-727 cm^{-1} as sharp and strong bands, whereas, $\nu_{(Sn-C)}$ show two frequencies (*asym* and *sym*) respectively at 549-535 cm^{-1} and 486-475 cm^{-1} indicating departure from C-Sn-C bond linearity. The $\nu(\text{NH}_2)_{\text{asym}}$ and $\nu(\text{NH}_2)_{\text{sym}}$ stretching vibrations due to the ligands in **5–12** appear in the range 3248 to 3454 cm^{-1} . These bands in the free ligands do not shift significantly upon coordination indicating that the amino-nitrogen atom is hardly or not involved in an interaction with tin. The spectra also show medium to strong absorptions in the range of 1600-1627 cm^{-1} due to $\nu(\text{C}=\text{N}-\text{N}=\text{C})$ [59]. The spectra show weak absorptions within the range 721-750 cm^{-1} , as expected for $\nu(\text{C}-\text{S})$. The $\nu(\text{Sn}-\text{C})_{\text{asym}}$ and $\nu(\text{Sn}-\text{C})_{\text{sym}}$ bands are tentatively assigned to absorptions in the regions 520-570 cm^{-1} and 430-468 cm^{-1} , respectively.

4.5.3.2 NMR spectra

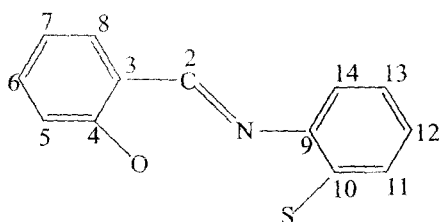
The ^1H NMR data for the diorganotin(IV) complexes are presented in Table 4.9 and 4.10. The observed resonances were assigned on the basis of their integration and multiplicity patterns, as well as for a selected number of compounds, by 2D ^1H - ^{13}C HMQC and HMBC experiments and were compared with literature data [15, 112, 136, 137]. The ligand and tin-bound organic group protons give signals in expected regions of the spectra. The azomethine proton resonance (around 8.4 ppm) has been identified and is flanked by its $^3J(\text{HC}=\text{N}\dots^{119}\text{Sn})$ coupling satellites ranging from 34 to 41 Hz between 7.88 and 8.39 ppm, whereas the NH_2 protons gave signals in the range 4.70 to 5.19 ppm. The presence of the coupling satellites for these azomethine proton resonances is an indication for the existence in solution of an intramolecular coordination between the tin and nitrogen atom [138]. For the dimethyltin derivatives, the $^2J(^1\text{H}-^{119}\text{Sn})$ coupling satellites are clearly visible, which allowed estimation of the C-Sn-C angle from the Lockart equation, [139] $\Theta = 0.016|^2J(^1\text{H}-^{119}\text{Sn})|^2 - 1.32|^2J(^1\text{H}-^{119}\text{Sn})| + 133.4$. For both **5** and **9** a value of 122° was found, comparing well with the 128 and 127° angles found, respectively, in the solid state according to X-ray crystallography (Table 4.16 and 4.17). The ^{13}C resonances were well separated and readily assigned with the aid of 2D ^1H - ^{13}C HMQC and HMBC spectra and $^nJ(^{117/119}\text{Sn}-^{13}\text{C})$ coupling constants. The values for the $^1J(^{119}\text{Sn}-^{13}\text{C})$ coupling constants were consistent with pentacoordinated tin for which the fifth coordination

site originates from the interaction with the imine nitrogen atom of the Schiff base [140]. The $^1J(^{119}\text{Sn}-^{13}\text{C})$ coupling constants also allowed estimation of the C–Sn–C angle, from a relationship established by Lockart *et al.* for dimethyltin compounds, $^1J(^{119}\text{Sn}-^{13}\text{C}) = 10.7 (\pm 0.5) \ominus -778 (\pm 64)$, [141–143] and by Holeček *et al.* [144–147] for dibutyl and diphenyl derivatives, $^1J(^{119}\text{Sn}-^{13}\text{C}) = 9.99 (\pm 0.73) \ominus -746 (\pm 100)$ and $^1J(^{119}\text{Sn}-^{13}\text{C}) = 15.56 (\pm 0.84) \ominus -1160 (\pm 101)$, respectively. The calculated values were 128 ± 12 and $127 \pm 12^\circ$ for, respectively, **5** and **9**, 130 ± 20 and $128 \pm 20^\circ$ for, respectively, **6** and **10**, and 132 ± 14 and $130 \pm 14^\circ$ for, respectively, **7** and **11**; all compared well with the angles found in the solid state, ranging from 119 to 128° (Table 4.16–4.20). The intramolecular coordination was further confirmed by the rather high (17–21 Hz) $^nJ(^{117/119}\text{Sn}-^{13}\text{C})$ coupling constant found for carbon 7, which without this interaction would implicate four bonds over a heteroatom for which no measurable coupling constant was expected. In the 2D $^1\text{H}-^{13}\text{C}$ HMBC correlation experiment, satellites originating from the coupling with the passive ^{119}Sn spin were clearly observed for correlation peaks associated with proton 7. From the tilt of the satellites the relative sign of the $^1\text{H}-^{119}\text{Sn}$ and $^{13}\text{C}-^{119}\text{Sn}$ coupling constants can be obtained [148]. In this respect, a positive tilt for carbon 1 and a negative one for carbon 2 were noted, meaning that, if the $^1\text{H}-^{119}\text{Sn}$ coupling for proton 7 can be considered as a 3J coupling pathway, giving usually negative coupling constants, the coupling constant between the tin atom and carbon 1 is also negative, while the one with carbon 2 is positive. This observation is in accord with the fact that $^2J(^{13}\text{C}-^{119}\text{Sn})$ coupling constants are generally positive, while $^3J(^{13}\text{C}-^{119}\text{Sn})$ coupling constants are usually negative. However, it should be emphasized that, for carbon 1, two coupling pathways, both involving three bonds, need to be considered, one through the oxygen atom and another one through the coordinating nitrogen atom and a double bond [149]. The ^{119}Sn chemical shifts, around -200 ppm for the aliphatic tin compounds and around -320 ppm for the diphenyltin compounds, were also in agreement with penta-coordination at tin.

Table 4.9. ^1H NMR chemical shifts and coupling data (ppm and Hz)* for 1-4.



Compounds 1-3



Compound 4

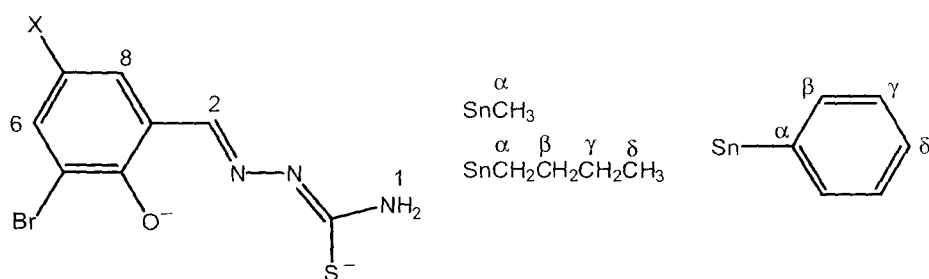
Compound	H-1	H-2	H-5	H-6	H-7	H-8	H-9	H-10	H-11	H-12	H-13	H-14	H- α	H- β	H- γ	H- δ
1	4.85 - 4.83 (d,1H)	8.51 (s,1H)	7.1 (d,1H)	7.23 (t,1H)	6.71 (t,1H)	6.78 - 6.75 (d,1H)	3.90 (qt,1H)	e	e	e	h	k	0.85 (s,6H)			
		[40.23] ^a											[71.49] ^b			
2	5.46 (d,1H)	8.44 (s,1H)	6.87 - 6.86 (d,1H)	6.83 (t,1H)	6.60 (t,1H)	6.79 - 6.75 (d,1H)	3.95 (qt,1H)	e	e	e	h	k	e	e	e	e
		[38.23] ^a														
3	4.97 - 4.94 (d,1H)	8.53 (s,1H)	f	6.68 (t,1H)	i	i	3.90 (qt,1H)	g	g	g	h	k	-	7.92 - 7.90 (d,4H)	f	7.07 (t,2H)
		[43.42] ^a												[83.25] ^b		
4	-	8.28 (s,1H)	i	i	i	i	-	-	i	i	i	i	1.60 - 1.45 (m,4H)	1.27 - 1.11 (m,2H)	1.38 - 1.32 (m,4H)	0.71 (t,6H)
		[25.35] ^a														

* Spectra recorded in CDCl₃, downfield TMS.

h = C-13 = C-11, k = C-14 = C-10, s: singlet, d: doublet, t: triplet, qt: quintet, m: multiplet

i = 7.46–6.54 (m, 8H), a = $^3J(\text{Sn-H})\text{Hz}$, b = $^2J(^{117/119}\text{Sn-CH}_3)\text{Hz}$, c = 2.06–1.07 (m, 10H), e = 2.00–0.75 (m, 28H), f = centered at 7.35 (5H), g = 2.05–1.49 (m, 10H).

Table 4.10. ^1H NMR chemical shifts and coupling constants (ppm and Hz) for 5–12^a



Compound	H-1	H-2	H-6	H-8	H- α	H- β	H- γ	H- δ
5.	5.18 (s, 2H)	8.39 (s, 1H) [38] ^b	7.58 (d, 1H) [2.5] ^c	7.06 (d, 1H) [2.5] ^c	0.93 (s, 6H) [72] ^b	-	-	-
6.	5.05 (s, 2H)	8.40 (s, 1H) [34] ^b	7.58 (d, 1H) [2.5] ^c	7.06 (d, 1H) [2.5] ^c	1.64-1.52 (m, 4H)	1.74-1.64 (m, 4H) [106] ^b	1.44- 1.28 (m, 4H)	0.91 (t, 6H)
7.	5.21 (s, 2H)	8.41 (s, 1H) [41] ^b	7.65 (d, 1H) [2.5] ^c	7.03 (d, 1H) [2.5] ^c	not obs.	8.03 (d, 4H) [82] ^b	7.50- 7.40 (m, 4H)	7.50-7.40 (m, 2H)
8. ^f	4.71 (s, 2H)	7.88 (s, 1H) [36] ^b	7.70 (d, 1H) [2.5] ^c	7.19 (d, 1H) [2.5] ^c	not obs.	7.26-7.88 (m, 4H)	7.26- 7.88 (m, 4H)	7.26-7.88 (m, 2H)
9.	5.14 (s, 2H)	8.39 (s, 1H) [38] ^b	7.70 (d, 1H) [2.2] ^c	7.20 (d, 1H) [2.2] ^c	0.93 (s, 6H) [72] ^b	-	-	-
10.	5.05 (s, 2H)	8.39 (s, 1H) [35] ^b	7.70 (d, 1H) [2.3] ^c	7.18 (d, 1H) [2.3] ^c	1.64-1.52 (m, 4H)	1.74-1.64 (m, 4H) [106] ^b	1.44- 1.28 (m, 4H)	0.91 (t, 6H)
11.	5.19 (s, 2H)	8.41 (s, 1H) [41] ^b	7.76 (d, 1H) [2.5] ^c	7.17 (d, 1H) [2.5] ^c	not obs.	8.02 (d, 4H) [82] ^b	7.50- 7.40 (m, 4H)	7.50-7.40 (m, 2H)
12. ^g	4.63 (s, 2H)	8.37 (s, 1H) [36] ^b	7.57 (d, 1H) [2.5] ^c	7.19 (d, 1H) [2.5] ^c	not obs.	7.01-7.61 (m, 4H)	7.01- 7.61 (m, 4H)	7.01-7.61 (m, 2H)

^aSpectra recorded in saturated CDCl_3 solution, and data are reported downfield to TMS;

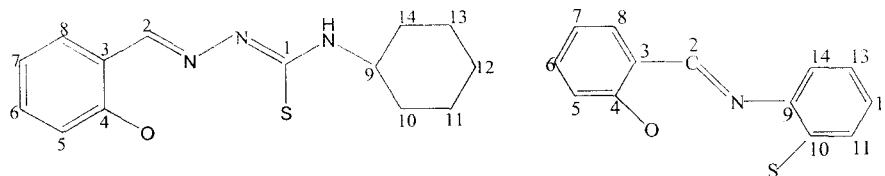
s: singlet, d: doublet, t: triplet, m: multiplet,

^b $^{2,3}J(^1\text{H}-^{117/119}\text{Sn})$ coupling constants between [].

^c $^4J(^1\text{H}-^1\text{H})$ coupling constants in parentheses

^f $\text{Sn}-\text{CH}_2 - \delta$ 1.58(d,4H); ^g $\text{Sn}-\text{CH}_2 - \delta$ 1.54(d,4H);

Table 4.11. ^{13}C NMR chemical shifts and coupling data (ppm and Hz)* for **1-4** and Ligand portion.



Compound 1-3

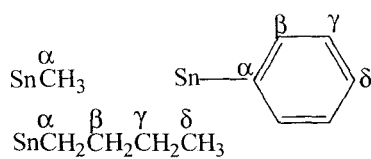
Compound 4

Compound	C-1	C-2	C-3	C-4	C-5	C-6	C-7	C-8	C-9	C-10	C-11	C-12	C-13	C-14
1.	165.64	165.82	121.31	159.38 [20.84] [†]	117.04	133.23	117.19	134.02	51.39	33.22	24.81	25.59	a	b
2.	158.32?	165.25	120.26	157.51 [16.88] [†]	116.32	132.24	117.45	133.08	51.37	32.24	24.67	25.27	a	b
3.	164.20	166.36	121.52	159.67 [20.91] [†]	117.25	133.39	121.52	134.25	51.37	33.17	24.77	25.55	a	b
4.	-	174.43	118.88	166.56 [18.23] [†]	117.54	131.66	118.64	135.62	143.96	137.07	135.62	127.72	128.44	124.55

a = C-13 = C-11 b = C-14 = C-10; * = spectra recorded in CDCl_3 , downfield TMS.

[†] = $^2J(^{119}\text{Sn}-^{13}\text{C})$ in Hz.

Table 4.12. ^{13}C NMR chemical shifts and coupling data (ppm and Hz) for **1-4**
 R_2Sn portion [R= $-\text{CH}_3$ or $-(\text{CH}_2)_3\text{CH}_3$, or $-\text{C}_6\text{H}_5$].



Compound	C- α	C- β	C- γ	C- δ
1.	5.67 [688.41] [*]	-	-	-
2.	25.60 [563.78] [*]	26.67 [30.97] †	26.29 [92.22] [‡]	12.65
3.	142.80 [872.43] [*]	136.03 [59.41] [†]	128.53 [87.37] [‡]	129.80 [17.26] [§]
4.	25.02 [656.04] [*]	26.79 [24.64] †	27.66 [77.10] [‡]	13.68

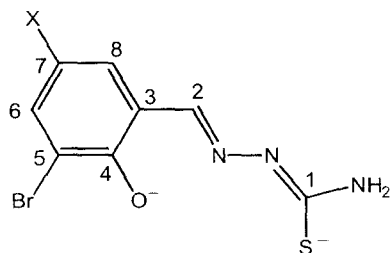
^{*} = $^1\text{J}(^{13}\text{C}-^{119}\text{Sn})\text{Hz}$

† = $^2\text{J}(^{13}\text{C}-^{119}\text{Sn})\text{Hz}$

‡ = $^3\text{J}(^{13}\text{C}-^{119}\text{Sn})\text{Hz}$

§ = $^4\text{J}(^{13}\text{C}-^{119}\text{Sn})\text{Hz}$

Table 4.13. ^{13}C NMR chemical shifts coupling constants (ppm and Hz) for the Schiff base dianion in **5** – **7** and **9** – **11**^{a,c}



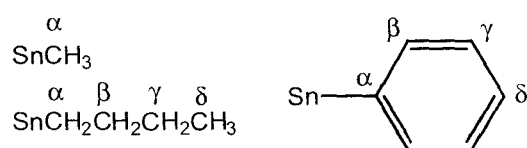
Compound	C-1	C-2	C-3	C-4	C-5	C-6	C-7	C-8
5.	168.8	158.4 [20] ^b	117.7 [24] ^b	160.1 [32] ^b	116.0 [8] ^b	136.3	121.2	131.1
6.	169.1	158.5 [16] ^b	117.7 [19] ^b	160.6 [32] ^b	116.6 [8] ^b	136.3	120.8	131.1
7.	167.2	158.7 [21] ^b	117.8 [22] ^b	160.4 [33] ^b	117.0 [10] ^b	136.6	121.6	131.4
9.	168.8	158.4 [21] ^b	118.5 [23] ^b	160.5 [31] ^b	117.0 [8] ^b	138.8	107.1	134.1
10.	169.1	158.4 [17] ^b	118.6 [19] ^b	160.0 [33] ^b	117.0 [n.o.]	138.8	107.1	134.2
11.	167.2	158.6 [21] ^b	118.0 [21] ^b	160.8 [34] ^b	117.3 [10] ^b	139.0	107.9	134.5

^aSpectra recorded in saturated CDCl_3 solution, and data are reported downfield to TMS;

^cdata was not obtained for **8** and **12** owing to poor solubility in CDCl_3 ; $c^2J(^{119}\text{Sn}-\text{O}-^{13}\text{C})$ in Hz

^bunresolved $^nJ(^{13}\text{C}-^{117/119}\text{Sn})$ and resolved $^1J(^{13}\text{C}-^{117/119}\text{Sn})$ are indicated between brackets.

Table 4.14 ^{13}C and ^{119}Sn NMR chemical shifts and coupling constants (ppm and Hz) for the diorganotin residues in **5–7** and **9–11**^{a,b}



Compound	^{119}Sn	C- α	C- β	C- γ	C- δ
5.	-194.0	6.18 [567/593] ^c	-	-	-
6.	-212.8	26.4 [532/557] ^c	27.3 [31] ^d	26.5 [87] ^e	13.6
7.	-320.1	141.4 [854/895] ^c	135.9 [59] ^d	128.9 [84] ^e	130.4 [17] ^f
9.	-193.6	6.19 [567/594] ^b	-	-	-
10.	-212.5	26.4 [531/557] ^c	27.3 [31] ^d	26.8 [88] ^e	13.6
11.	-319.9	141.4 [860/894] ^c	135.9 [59] ^d	128.9 [85] ^e	130.4 [17] ^f

^a Spectra recorded in saturated CDCl_3 solution, and data are reported downfield to TMS;

^b data was not obtained for **8** and **12** owing to poor solubility in CDCl_3 ;

^c $^1\text{J}(^{13}\text{C}-^{119}\text{Sn})$ in Hz; ^d $^2\text{J}(^{13}\text{C}-^{119}\text{Sn})$ in Hz; ^e $^3\text{J}(^{13}\text{C}-^{119}\text{Sn})$ in Hz; ^f $^4\text{J}(^{13}\text{C}-^{119}\text{Sn})$ in Hz

4.5.3.3 Electronic spectra

The spectral data for **5–12** are summarized in Table 4.15. Towards the visible region, the electronic spectra show multiple absorptions, giving rise to the yellow appearance of the compounds and is due likely to a $n \rightarrow \pi^*$ transition within the thiosemicarbazide chromophore owing to extensive conjugation, [15] which is most likely reason for the observed fluorescence in methanol solution Table 4.15. The

emission spectral data in solution indicate the fluorescence property of these compounds qualitatively which is not unexpected for the extended conjugation present in the structures as mentioned.

Table 4.15. Electronic absorption spectra of compounds **5–12** recorded in methanol solution

Compound	λ_{\max} (nm)	Absorption (λ_{\max} , nm)	Emission (λ_{\max} , nm)
5.	410	410, 340, 236	495 ($\lambda_{\text{exc}} = 400\text{nm}$)
6.	415	415, 340, 238	495 ($\lambda_{\text{exc}} = 415\text{nm}$)
7.	407	407, 339, 260	490 ($\lambda_{\text{exc}} = 410\text{nm}$)
8.	395	-	-
9.	409	409, 340, 238	493 ($\lambda_{\text{exc}} = 410\text{nm}$)
10.	414	414, 343, 240	496 ($\lambda_{\text{exc}} = 410\text{nm}$)
11.	408	408, 340, 268	491 ($\lambda_{\text{exc}} = 410\text{nm}$)
12.	398	-	-

4.5.3.4 X-ray Crystal Structures

This section deals with the X-ray crystallographic studies of diorganotin(IV) complexes of the type R_2SnL ($R=Me$, $n\text{-Bu}$ and Ph ; $L= L^3$ and L^4). In the present study efforts were undertaken to obtain single crystals for the X-ray analysis of the diorganotin(IV) derivatives of the ligands described before. Compounds **5**, **6**, **7**, **9** and **10** provided single crystals suitable for the X-ray crystal structure determination. The crystal structures of all these complexes are described below.

4.5.3.4.1 Crystal structure of Me_2SnL^3 (**5**) and Me_2SnL^4 (**9**)

The X-ray quality single crystal of **5** and **9** from the benzene solution of the compounds were successfully isolated. The molecular structure of **5** and **9** along with the crystallographic number are given in (Fig. 4.29a) and (Fig. 4.29b) respectively. The crystal data and refinement parameters are presented in Table 4.1 for **5** and Table

4.4 for **9**. Selected geometric parameters are given in Table 4.16, for **5** and **9**. Both the compounds **5** and **9** crystallizes into a monoclinic lattice with $C2/c$ space group. The molecular structures reveal a tridentate mode of coordination to the tin atom through the thiolate-S1, phenoxide-O1 and imino-N1 atoms of the dianion derived from the respective Schiff base, with the penta-coordinate geometry being completed by two methyl carbon atoms. The similarity in the structures is emphasized by the isomorphous relationship between the two di-methyl compounds, **5** and **9**. An evaluation key bond distances of **5** with Br/Cl substituents and **9** with Br/Br ones, indicates that the substituents do not influence the electronic structure of the ligand as the comparable distances are equal within experimental error. The coordination geometry about the tin atom in each structure as the coordination geometries vary depending on the nature of the tin-bound group. Thus, the di-methyltin compounds adopt almost intermediate geometries between square pyramidal and trigonal bipyramidal. This is quantified by the value of τ , i.e. $\tau = 0.47$ for **5** and 0.49 for **9**, which compares with $\tau = 0.00$ for an ideal square pyramid and $\tau = 1.00$ for an ideal trigonal bipyramid [150]. In the crystal structures of isomorphous **5** and **9**, molecules are connected into supramolecular chains aligned along $[1\ 0\ 1]$, through a variety of hydrogen bonding interactions. The most prominent supramolecular synthon in the crystal packing is an eight-membered $\{\dots\text{HN}(\text{C})\text{N}\}_2$ motif disposed about a two-fold axis; geometric parameters for the intermolecular interactions are given below. The second hydrogen of the amine forms a hydrogen bond to the Br1 atom with the resulting chain stabilised by an internal C-H...Cl interaction. The supramolecular chains thus formed, (Fig. 4.30a), pack into layers with an undulating topology that stack along the b axis, (Fig. 4.30c). In the absence of the chloride in **9**, a C-H...S interaction occurs instead, and these provide connections between the chains to form two-dimensional arrays in the ac plane, (Fig. 4.30b). The layers have an undulating topology and stack as illustrated for **5**, (Fig. 4.30c). By contrast to the situation in **5** and **9**, simpler supramolecular aggregation patterns are observed in the crystal structures of isomorphous **6** and **10**, and in **7**. This is correlated with the increased size of the tin-bound substituents and the participation of only one of the amine-H atoms in significant intermolecular interactions.

Table 4.16 Selected geometric parameters (Å, °) for Me₂SnL³ (**5**)

Parameter	5
Sn-S1	2.5493(10)
Sn-O1	2.086(2)
Sn-N1	2.231(2)
C1-S1	1.723(3)
N1-N2	1.391(3)
C1-N2	1.299(4)
C2-N1	1.298(4)
S1-Sn-O1	156.24(7)
C-Sn-C	128.25(18)

Table 4.17 Selected geometric parameters (Å, °) for Me₂SnL⁴ (**9**)

Parameter	9
Sn-S1	2.5451(15)
Sn-O1	2.085(3)
Sn-N1	2.232(4)
C1-S1	1.721(5)
N1-N2	1.396(5)
C1-N2	1.300(6)
C2-N1	1.290(6)
S1-Sn-O1	156.17(11)
C-Sn-C	127.0(3)

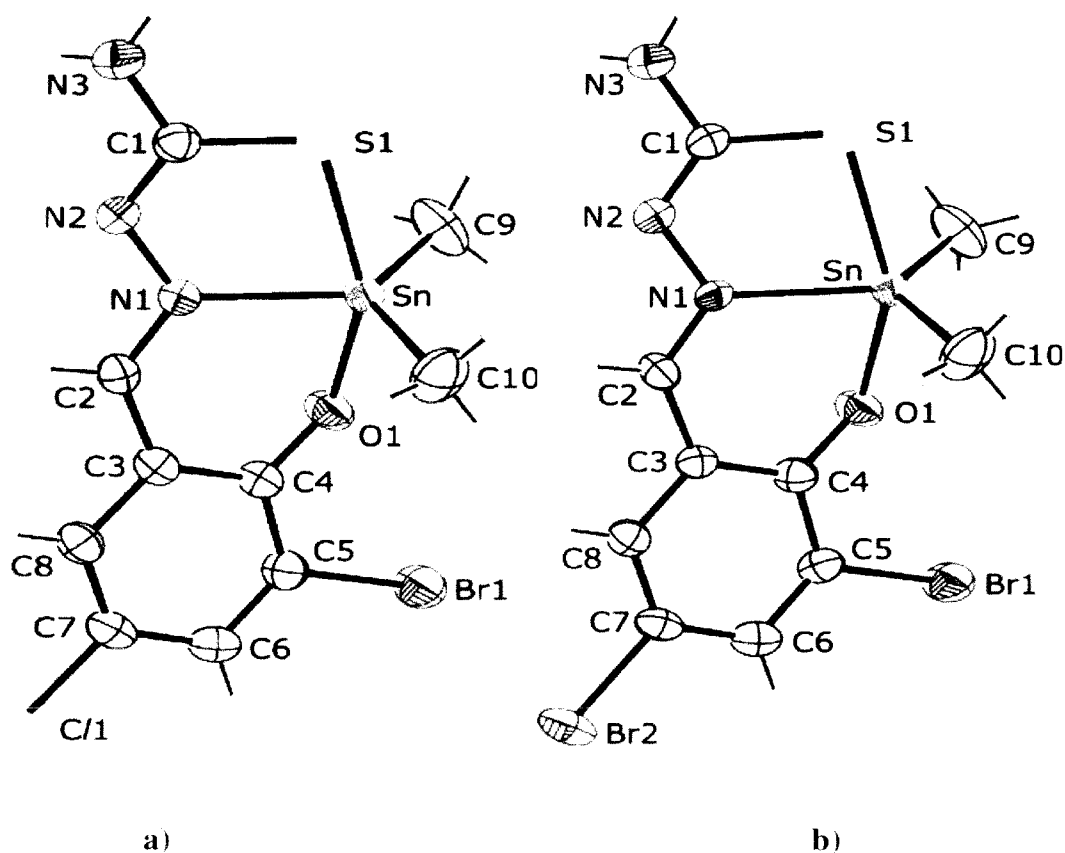
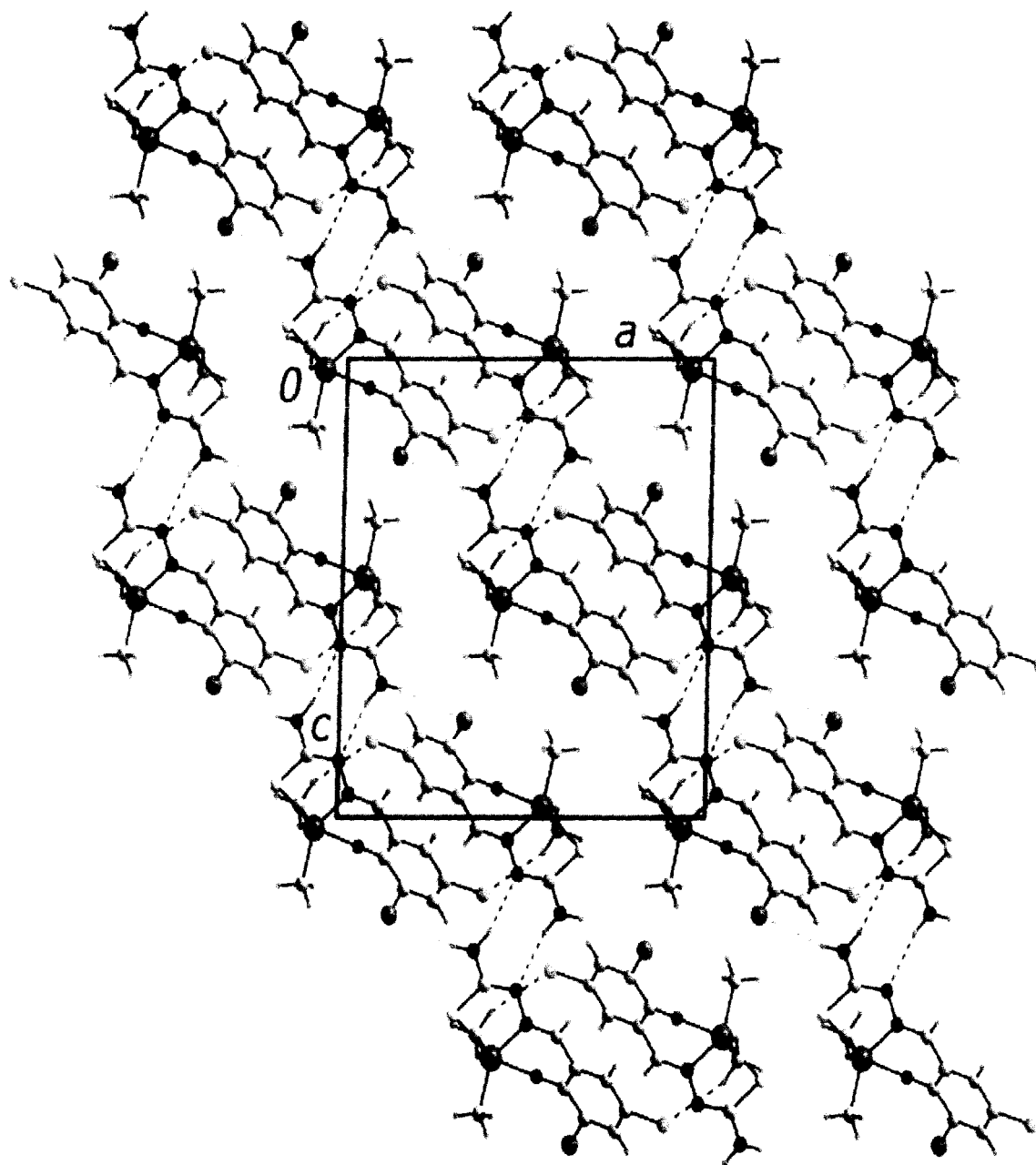


Fig. 4.29 a) Molecular structure and crystallographic numbering scheme for Me_2SnL^3 (**5**)
 b) Molecular structure and crystallographic numbering scheme for Me_2SnL^4 (**9**)

Details of the geometric parameters describing the supramolecular aggregation in the structures of 5 and 9.

(5): $\text{N3-H1n} \dots \text{N2}^i = 2.37(4) \text{ \AA}$, $\text{N3} \dots \text{N2}^i = 3.176(4) \text{ \AA}$, angle at H1n = $152(3)^\circ$ for symmetry operation i: $1-x, y, 1/2-z$. $\text{N3-H2n} \dots \text{Br1}^{ii} = 2.84(4) \text{ \AA}$, $\text{N3} \dots \text{Br1}^{ii} = 3.626(3) \text{ \AA}$, angle at H2n = $162(3)^\circ$ for symmetry operation ii: $1/2+x, 1/2-y, 1/2+z$. $\text{C9-H9c} \dots \text{C1}^{iii} = 2.80 \text{ \AA}$, $\text{C9} \dots \text{C1}^{iii} = 3.669(5) \text{ \AA}$, angle at H9c = 150° for symmetry operation iii: $1/2-x, 1/2-y, 1-z$.

(9): $\text{N3-H1n} \dots \text{N2}^i = 2.33(6) \text{ \AA}$, $\text{N3} \dots \text{N2}^i = 3.175(6) \text{ \AA}$, angle at H1n = $163(6)^\circ$ for symmetry operation i: $1-x, y, 1/2-z$. $\text{N3-H2n} \dots \text{Br1}^{ii} = 2.88(6) \text{ \AA}$, $\text{N3} \dots \text{Br1}^{ii} = 3.679(5) \text{ \AA}$, angle at H2n = $163(6)^\circ$ for symmetry operation ii: $1/2+x, 1/2-y, 1/2+z$. $\text{C9-H9b} \dots \text{S1}^{iii} = 2.81 \text{ \AA}$, $\text{C9} \dots \text{S1}^{iii} = 3.710(6) \text{ \AA}$, angle at H9b = 157° for symmetry operation iii: $1/2-x, 1/2-y, 1-z$.



a)

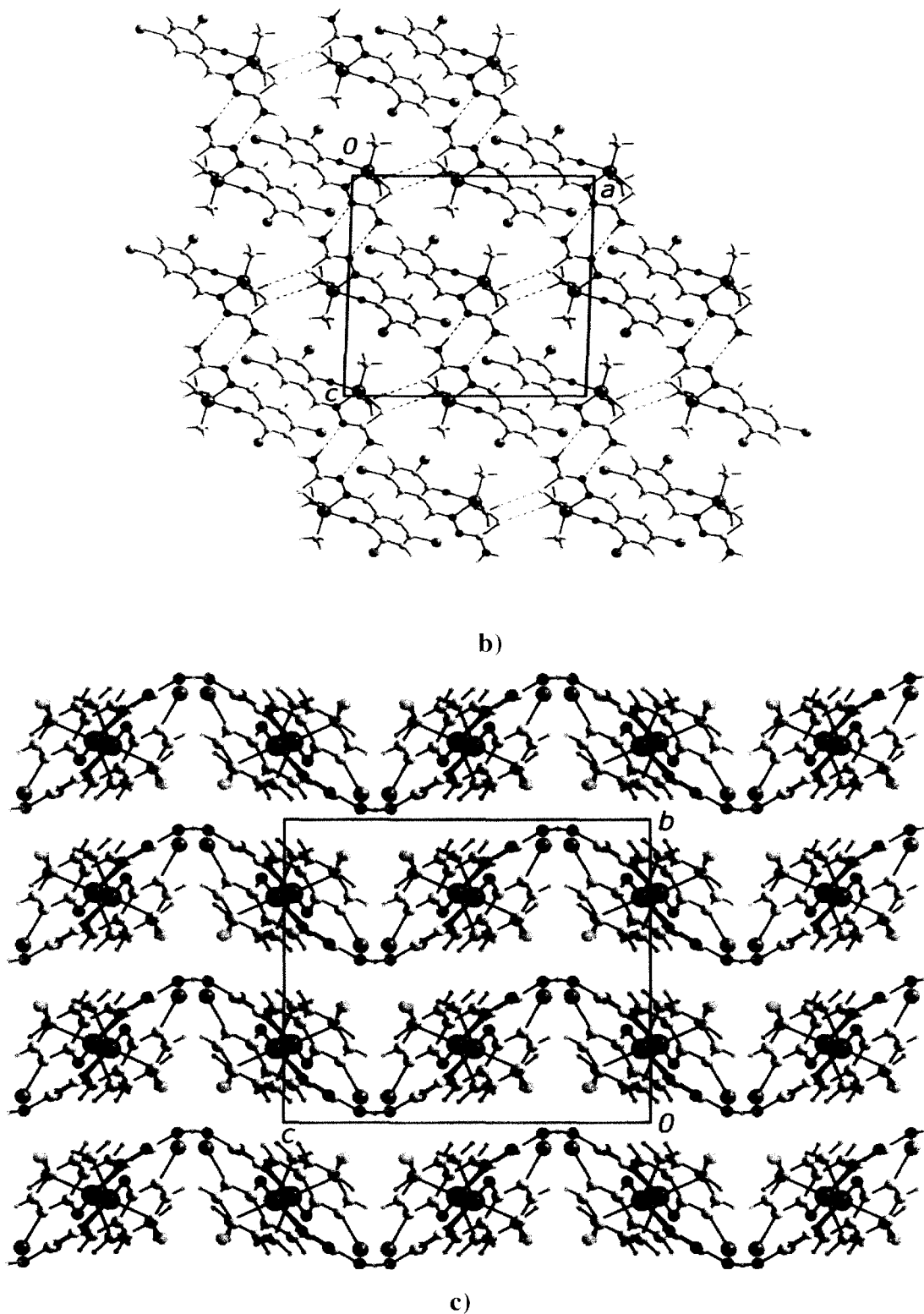


Fig. 4.30 Crystal packing in the isomorphous structures of **5** and **9**:

- a) view of the supramolecular chain in **5** mediated by $\text{N-H} \cdots \text{N}$ and $\text{N-H} \cdots \text{Br}$ interactions and sustained by internal $\text{C-H} \cdots \text{Cl}$ contacts.
- b) view of the supramolecular chain in **9** mediated by $\text{N-H} \cdots \text{N}$ and $\text{N-H} \cdots \text{Br}$ interactions for **5**, and connected into a two-dimensional array by $\text{C-H} \cdots \text{S}$ contacts.
- c) stacking of layers in **5** representative of both **5** and **9**.

4.5.3.4.2 Crystal structure of $n\text{-Bu}_2\text{SnL}^3$ (**6**) and $n\text{-Bu}_2\text{SnL}^4$ (**10**)

X-ray quality single crystal of **6** and **10** from the petroleum ether (60-80°C) solution of the compounds were successfully isolated. The molecular structure of **6** and **10** along with the crystallographic number are given in Fig. 4.31 and Fig. 4.32 respectively. The crystal data and refinement parameters are presented in Table 4.2 for **6** and Table 4.5 for **10**. Selected geometric parameters are given in Table 4.18 for **6** and Table 4.19 for **10**. Both the compounds **6** and **10** crystallizes into a monoclinic lattice with $P2_1/c$ space group. The molecular structures reveal a tridentate mode of coordination to the tin atom through the thiolate-S1, phenoxide-O1

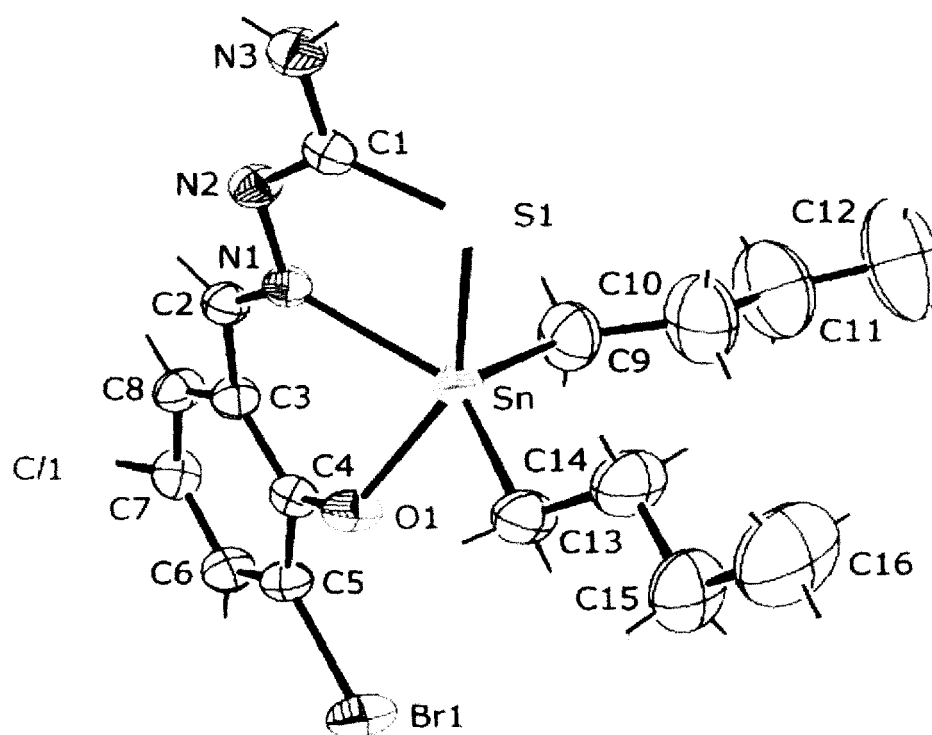


Fig. 4.31 Molecular structure and crystallographic numbering scheme for $n\text{-Bu}_2\text{SnL}^3$ (**6**)

and imino-N1 atoms of the dianion derived from the respective Schiff base, with the penta-coordinate geometry being completed by two *n*-butyl carbon atoms. The similarity in the structures is emphasised by the isomorphous relationship between the two di-*n*-butyl derivatives, **6** and **10**. Small, but chemically insignificant, [151] differences are noted between the Sn-S1 bond distances in the structures of **6** and **10**. Within the dianion, the C1-S1 and N1-N2 bond distances are consistent with single

bonds, whereas double bond character is evident in each of the C1–N2 and C2–N1 bonds. Arguably, the most significant differences in the geometric parameters about the tin atoms are found in the S1–Sn–O1 and C–Sn–C angles. These are pivotal in determining the coordination geometry about the tin atom in each structure as the coordination geometries vary depending on the nature of the tin-bound group. The distortion is even greater for the di-*n*-butyltin compounds where $\tau = 0.15$ and 0.16 for **6** and **10**, respectively. Therefore, there is a correlation between the magnitude of C–Sn–C and the distortion away from an ideal square pyramid. Simple supramolecular aggregation patterns are

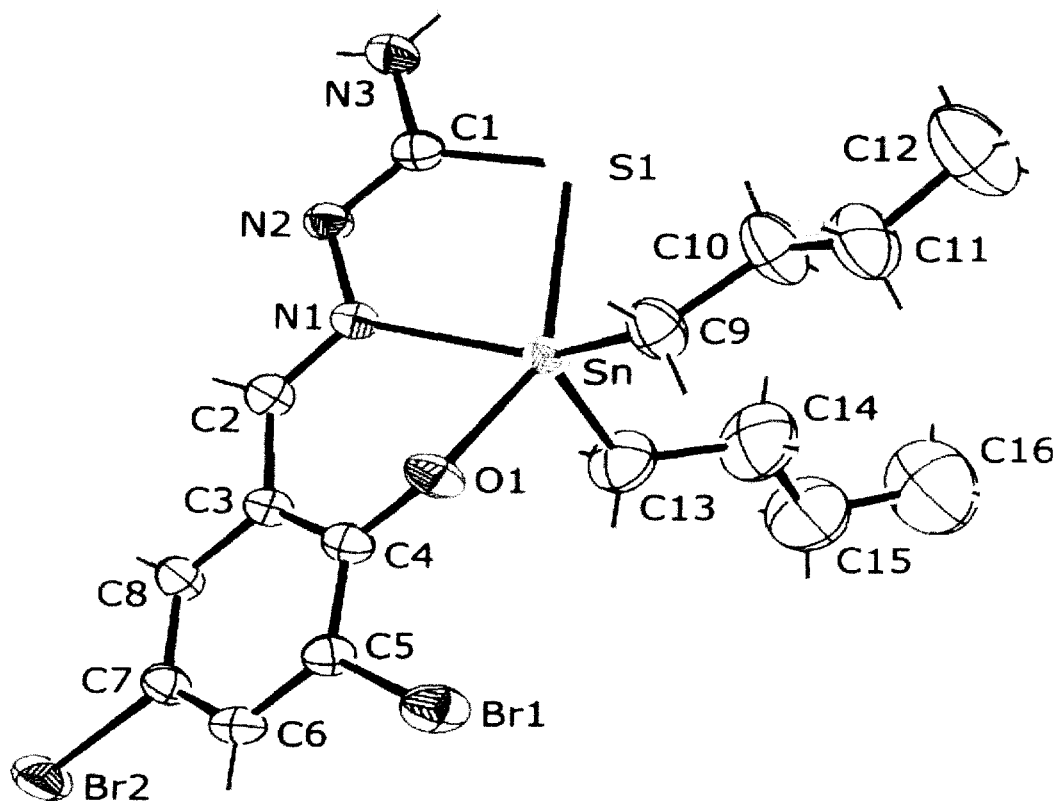


Fig. 4.32 Molecular structure and crystallographic numbering scheme for $n\text{-Bu}_2\text{SnL}^4$ (**10**)

observed in the crystal structures of isomorphous **6** and **10**. This is correlated with the increased size of the tin-bound substituents and the participation of only one of the amine-H atoms in significant intermolecular interactions. Supramolecular chains, mediated by N–H...O hydrogen bonding, along the *c* axis are found in each of **6**. (Fig.

Figure 10. In **10**, the chains are reinforced by hydrogen-bonding interactions so that the hydrogen-bonding chain is bifurcated.

*Table 1. Values of the geometric parameters describing the supramolecular aggregation in the structures of **6** and **10**.*

(6): N3-H1n...O1ⁱ = 2.36(5) Å, N3...O1ⁱ = 3.076(5)Å, angle at H1n = 145(5)° for symmetry operation i: x, 1½-y, ½+z.

(10): N3-H1n...O1ⁱ = 2.36(4) Å, N3...O1ⁱ = 3.055(5) Å, angle at H1n = 141(4)° for symmetry operation i: x, 1½-y, ½+z. N3-H1n...Br1ⁱ = 2.92(5) Å, N3...Br1ⁱ = 3.661(5) Å, angle at H1n = 148(4)°.

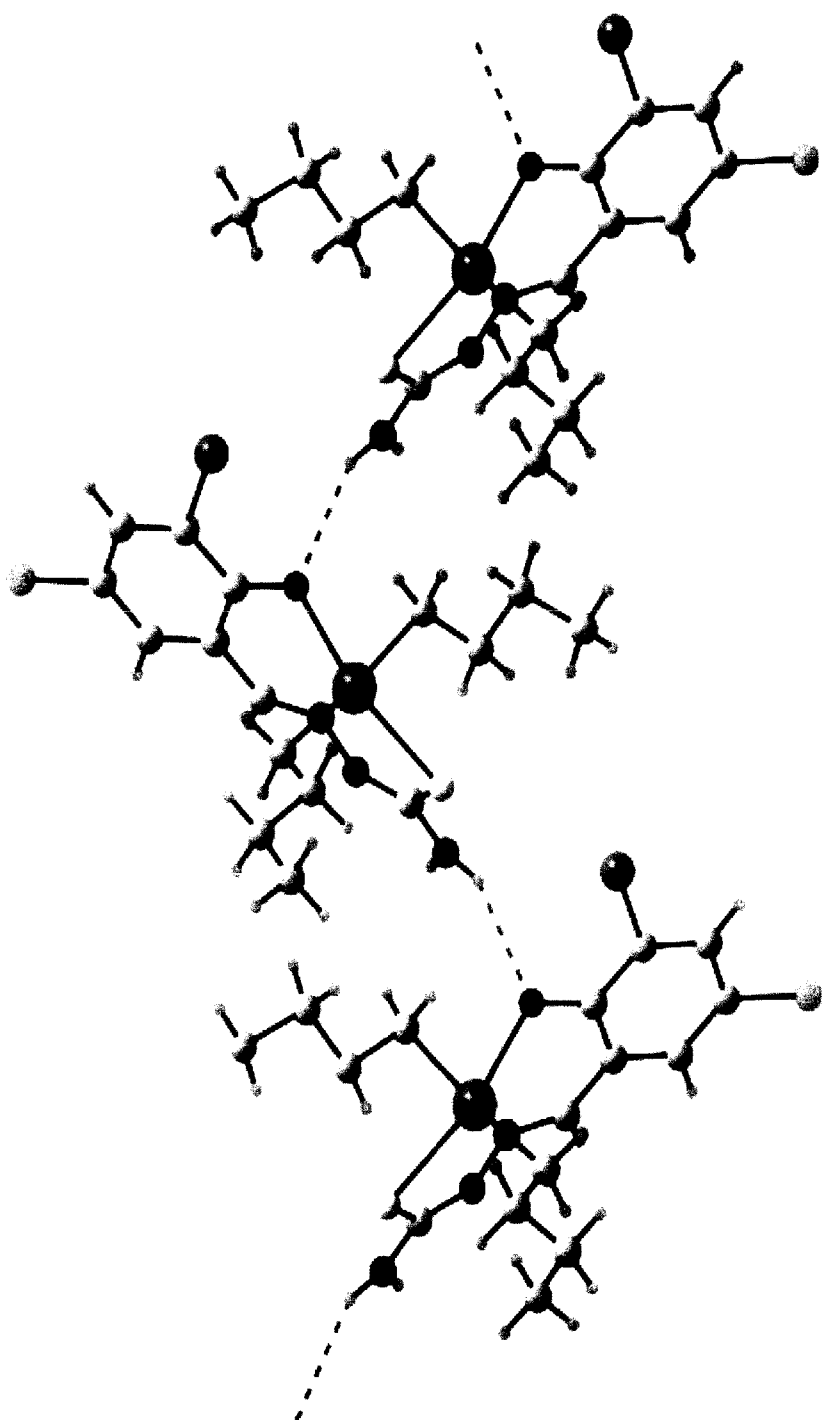


Fig. 4.33 Crystal packing in the isomorphous structures of **6** and **10**: view of the supramolecular chain in **6** mediated by N–H···N hydrogen bonding, representative of both **6** and **10**.

Table 4.18 Selected geometric parameters (Å, °) for n-Bu₂SnL³ (**6**)

Parameter	Value
Sn–S1	2.3151(13)
Sn–O1	2.118(3)
Sn–N1	2.242(3)
C1–S1	1.728(5)
N1–N2	1.385(4)
C1–N2	1.307(5)
C2–N1	1.300(5)
S1–Sn–O1	148.08(9)
C–Sn–C	119.0(2)

Table 4.19 Selected geometric parameters (Å, °) for n-Bu₂SnL⁴ (**10**)

Parameter	Value
Sn–S1	2.4975(12)
Sn–O1	2.104(2)
Sn–N1	2.232(3)
C1–S1	1.724(4)
N1–N2	1.376(4)
C1–N2	1.299(5)
C2–N1	1.294(5)
S1–Sn–O1	148.70(9)
C–Sn–C	118.5(2)

4.5.3.4.3 Crystal structure of Ph₂SnL³ (**7**)

The X-ray quality single crystal of **7** from the benzene solution of the compound was successfully isolated. The molecular structure of **7** along with the crystallographic number are given in (Fig. 4.34). The crystal data and refinement parameters are presented in Table 4.3. Selected geometric parameters are given in Table 4.20. The compound **7** crystallizes into a triclinic lattice with *P*1 space group. The molecular structure, reveal a tridentate mode of coordination to the tin atom

through the thiolate-S1, phenoxide-O1 and imino-N1 atoms of the dianion derived from the Schiff base, with the penta-coordinate geometry being completed by two phenyl carbon atoms. The crystallographic analysis of **7** showed the sample had crystallized as a hemi-benzene solvate. The coordination geometry about the tin atom

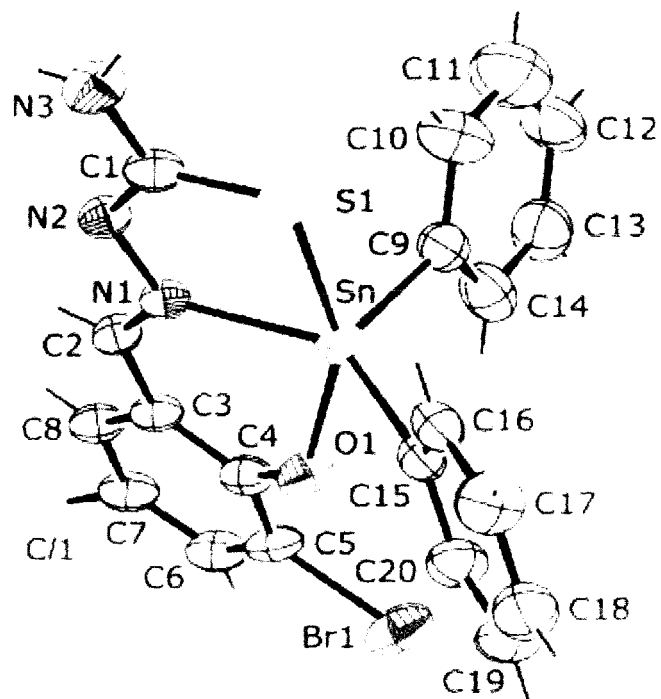


Fig. 4.34 Molecular structure and crystallographic numbering scheme for Ph_2SnL_2 (**7**). For **7**, only one component of the disordered *tin*-bound phenyl groups is shown for clarity.

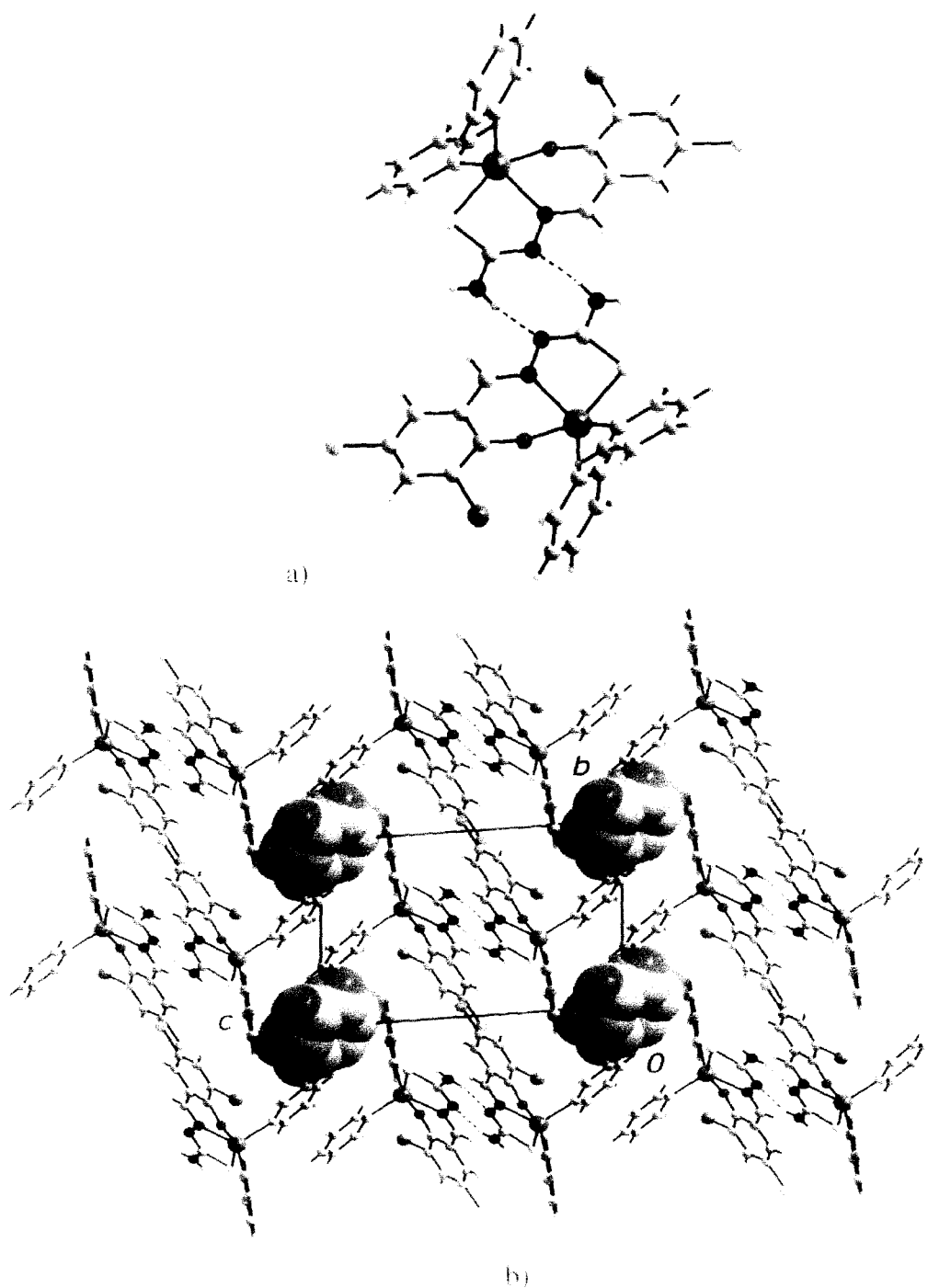


Fig. 4.35 Crystal packing in the structure of **7**:
 a) dimeric aggregates mediated by N–H...N hydrogen bonds; and
 b) stacking of the aggregates shown in (a) to form channels along the *a*
 axis in which reside the solvent benzene molecules, highlighted in
 space filling mode.

is varying depending on the nature of the tin-bound group. For the di-phenyltin
 compound, **7**, a distortion towards square pyramidal is evident, $\tau = 0.29$. Simple

supramolecular aggregation patterns are observed in the crystal structure of isomorphous **7**. The crystal structure of **7** comprises diorganotin molecules and benzene molecules in the ratio 2:1. The presence of the eight-membered $[...HNCN]_2$ synthon leads to centrosymmetric dimeric aggregates (Fig. 4.35a). These stack along the *a* axis to define channels in which reside the solvent benzene molecules (Fig. 4.35b).

Details of the geometric parameters describing the supramolecular aggregation in the structure of 7.

(7): N3-H1n...N2ⁱ = 2.25(6) Å, N3...N2ⁱ = 3.052(6) Å, angle at H1n = 163(5)° for symmetry operation i: 2-x, 1-y, 1-z.

Table 4.20 Selected geometric parameters (Å, °) for Ph₂SnL³ (**7**).

Parameter	7
Sn-S1	2.5074(15)
Sn-O1	2.082(3)
Sn-N1	2.236(3)
C1-S1	1.718(5)
N1-N2	1.387(5)
C1-N2	1.300(5)
C2-N1	1.292(5)
S1-Sn-O1	153.52(11)
C-Sn-C	119.2(8)
	124.6(8) ^a

^a The C-Sn-C angle for the second component of the disordered phenyl groups.

4.5.3.5 Differential Scanning Calorimetric analysis

All the compounds have single sharp peak indicates the compounds are pure and this is the corresponding melting point of those compounds. The enthalpy of compound **10** was ($\Delta H_{\text{melting}} = 57.65$ J/g). The enthalpy of compound **9** was ($\Delta H_{\text{melting}} = 35.07$ J/g). Like as compound **11** ($\Delta H_{\text{melting}} = 69.41$ J/g), compound **5** ($\Delta H_{\text{melting}} = 57.47$ J/g), compound **6** ($\Delta H_{\text{melting}} = 59.45$ J/g), compound **7** ($\Delta H_{\text{melting}} = 65.45$ J/g) were the enthalpy of the melting point.

4.5.4. Biological properties of diorganotin(IV) complexes of substituted salicyldehyde thiosemicarbazone.

4.5.4.1 Anti-fungal activities

The anti-fungal properties of the diorganotin compounds **5–7** and **9–11** are summarized in Tables 4.21, 4.22 and 4.23. The fungitoxic effect of the organotin compounds was screened at three concentrations, 25, 50, and 100 ppm, on spore germination of six different pathogens of rice (*Helminthosporium oryzae*), wheat (*Bipolaris sorokiniana*), mustard (*Alternaria brassicae*), cabbage (*Alternaria kikuchiana*), chilli (*Colletotrichum capsici*) and onion (*Stemphylium pori*). All test chemicals markedly inhibit the spore germination of each of the above fungi at concentrations above 50 ppm. At 100 ppm, almost complete inhibition of spore germination ensued, irrespective of the pathogen, which indicates high fungitoxicity against different groups of pathogen.

Table 4.21. Spore germination (%) of *Bipolaris sorokiniana* and *Helminthosporium oryzae* in the presence of compounds **5–7** and **9–11**.

Compound	Spore germination % of <i>B. sorokiniana</i>			Spore germination % of <i>H. oryzae</i>		
	Conc. (ppm)			Conc. (ppm)		
	25	50	100	25	50	100
5.	9.6	3.5	0	10.9	5.0	1.5
6.	5.9	2.5	0	6.7	4.0	0.5
7.	4.7	2.0	0	5.8	3.2	0
9.	10.1	5.0	1.0	10.5	4.8	1.2
10.	5.6	3.3	0	6.2	3.5	0
11.	4.9	2.0	0	5.3	3.2	0
Control(water)	83.1			85.4		

Table 4.22 Spore germination (%) of *Alternaria brassicae* and *Alternaria kikuchiana* in the presence of compounds 5–7 and 9–11.

Compound	Spore germination % of <i>A. brassicae</i>			Spore germination % of <i>A. kikuchiana</i>		
	Conc. (ppm)			Conc. (ppm)		
	25	50	100	25	50	100
5.	5.8	3.3	0	4.4	3.1	0
6.	4.4	2.4	0	3.9	2.5	0
7.	9.9	4.0	1.1	9.5	4.6	1.0
9.	9.5	4.0	1.0	9.4	4.0	0.9
10.	5.8	3.0	0	4.5	3.3	0
11.	4.5	2.1	0	4.1	2.9	0
Control(water)	80.9			79.5		

Table 4.23 Spore germination (%) of *Colletotrichum capsici* and *Stemphylium pori* in the presence of compounds 5–7 and 9–11.

Compound	Spore germination % of <i>C.</i> <i>capsici</i>			Spore germination % of <i>S. pori</i>		
	Conc. (ppm)			Conc.(ppm)		
	25	50	100	25	50	100
5.	8.1	4.9	0.8	7.9	5.0	0.9
6.	7.0	4.2	0.5	6.70	3.7	0
7.	12.2	5.6	2.1	11.9	6.1	2.2
9.	13.7	5.9	1.9	12.3	6.7	2.0
10.	7.9	4.3	0.9	7.3	4.9	0.8
11.	6.92	3.9	0	6.1	3.4	0
Control(water)	78.2			75.9		

4.5.4.2 Phytotoxic properties

The phytotoxic effects of compounds **5–7** and **9–11** as a function of the concentration are summarized in Tables 4.24 and 4.25. For this purpose, the seed germination of four economically important crops, *Oryzae sativa*, *Brassica nigra*, *Capcicum annum*, and *Brassica oleracea* was evaluated at a concentration of 100 ppm. The results indicate that none of the organotin compounds displays any inhibitory effect on seed germination and some even show stimulated germination. In other experiments (Table 4.24) with *Triticum aestivum* with cultivar Sonalika, it was found that concentrations as low as 25 ppm are equally effective.

It was observed that the general activity of the organotins towards fungi decreased when alkyl groups were replaced by aryl groups, irrespective of the fungi under study [15]. By contrast, in the present study fungitoxicity did not follow one common general trend but rather appeared to be dependent on the individual fungi under investigation. Hence, the order of activity decreased from alkyl to phenyl in one case and reversed for the other. The compounds containing phenyltin groups **11** were more fungitoxic than the alkyl-substituted tin compounds **9** and **10**.

Table 4.24. Phytotoxicity of compounds **5–7** and **9–11**, after seed treatment of Indian wheat (*Triticum aestivum* L.), cultivar Sonalika.

Compound	Percentage (%) of seed germination after 4h treatment			Percentage (%) of seed germination after 12h treatment		
	Conc. (ppm)			Conc. (ppm)		
	25	50	100	25	50	100
5.	93	96	95	94	93	95
6.	92	95	93	94	96	92
7.	95	99	99	94	97	95
9.	98	95	92	96	91	94
10.	91	94	93	93	95	94
11.	92	99	94	92	97	92
Control ^a	95			94		

^aThe control seeds were incubated in methanol/water (1:5) for the indicated period.

Table 4.25. Phytotoxic effect compounds **5–7** and **9–11**, after seed treatment of rice (*Oryzae sativa*), mustard (*Brassica nigra*), chilli (*Capcicum annum*), and cabbage (*Brassica oleracea*) at 100 ppm concentration.

Compound	Percentage (%) of seed germination after 12h treatment			
	Rice (<i>Oryzae sativa</i>)	Mustard (<i>Brassica nigra</i>)	Chilli (<i>Capcicum annum</i>)	Cabbage (<i>Brassicaoleracea</i>)
5.	82	85	79	89
6.	84	86	80	91
7.	86	87	83	94
9.	77	89	81	89
10.	81	85	82	92
11.	85	84	84	91
Control ^a	83	87	81	93

^aThe control seeds were incubated in methanol/water (1:5) for the indicated period.

4.3 References

1. Rasper ES. *Coord. Chem. Rev.* 1985; **61**: 115.
2. Kemmer M, Dalil H, Biesemans M, Martins JC, Mahieu B. *J. Organomet. Chem.* 2000; **608**: 63.
3. de Mora SJ. in de Mora SJ (Ed.), *Tributyltin: Case Study of an Environmental Contaminant*, Cambridge University Press, London, 1996, pp. 1-20.
4. Molly KC, Quill K, Nowell IW. *J. Chem. Soc., Dalton Trans.* 1986; **5**: 85.
5. Molly KC, Quill K, Nowell IW. *J. Chem. Soc., Dalton Trans.* 1987; 101.
6. Zubeita JA, Zuckerman JJ. *Inorg. Chem.* 1987; **24**: 251.
7. Saxena A, Tendon JP, Crowe AJ. *Polyhedron.* 1985; **4**: 1085.
8. Saxena A, Koacher JK, Tandon JP, Das SR. *J. Toxicol. Environ. Health.* 1982; **10**: 709.
9. Obafemi CA, Ejenavi AB, Kolawole DO, Oloke JK. *Inorg. Chim. Acta.* 1988; **151**: 21.
10. Nath M, Goyal S. *Main Group Met. Chem.* 1993; **16**: 167.
11. Nath M, Goyal S, Sharma CL. *Synth. React. Inorg. Met.-Org. Chem.* 1995; **25**: 821.
12. Nath M, Goyal S, Sharma CL. *Main Group Met. Chem.* 1995; **18**: 51.
13. Pellerito L, Nagy L. *Coord. Chem. Rev.* 2002; **224**: 111.
14. Mishra S, Goyal M, Singh A. *Main Group Met. Chem.* 2002; **25**: 437.
15. M. Sen Sharma, S. Mazumder, D. Ghosh, A. Roy, A. Duthie, E. R. T. Tiekink, *Appl. Organomet. Chem.* **2007**, *21*, 890.
16. Belsky I, Gerther D, Zilkla A. *J. Med. Chem.* 1968; **1**: 92.
17. Saxena A, Tandon JP. *Cancer Lett.* 1983; **19**: 73.
18. Ruisi G, Silvestri A, Lo Giudice MT, Barbieri R, Atassi G, Huber F, Gratz K, Lamartina L. *J. Inorg. Biochem.* 1985; **25**: 229.
19. Saxena AK, Huber F. *Coord. Chem. Rev.* 1989; **95**: 109.
20. Crowe AJ. *Drugs Future.* 1987; **2**: 40.
21. Gielen M. *Metal-Based Drugs.* 1994; **1**: 213.
22. Zhao YD, Pang DW, Zong Z, Cheng Jk, Luo ZF, Feng CJ, Shen HY, Zhung XC. *Huaxe Xuebao.* 1988; **56**: 178.
23. Sreekala R, Yusuff KK, Mohammed. *Catal (Pap Natl Symp)*, 1994, 507.
24. Dey DK, Saha MK, Das MK, Bhartiya N, Bansal RK, Rosair G, Mitra S. *Polyhedron.* 1999; **18**: 2678.
25. Kawakami BS, Miya-Uchi M, Tanaka T. *J. Inorg. Nucl. Chem.* 1980; **42**: 805.
26. Purohit S, Koley AP, Prasad LS, Manoharan PT, Ghosh S, *Inorg. Chem.* 1989; **28**: 3735.
27. Koley AP, Purohit S, Ghosh S, Prasad LS, Manoharan PT, *J. Chem. Soc., Dalton Trans.* 1988; 2607.
28. Koley AP, Purohit S, Prasad LS, Ghosh S, Manoharan PT. *Inorg. Chem.* 1992; **31**: 305.
29. Koley AP, Nirmala R, Prasad LS, Ghosh S, Manoharan PT, *Inorg. Chem.* 1992; **31**: 1764.
30. Christiansen J, Tittsworth RC, Hales BJ, Cramer SP, *J. Am. Chem. Soc.* 1995; **117**: 1017.
31. Greenwood RJ, Wilson GL, Pilbrow JR, Wedd AG, *J. Am. Chem. Soc.* 1993; **117**: 5385.
32. Laughlin LJ, Young CG, *Inorg. Chem.* 1996; **35**: 1050.
33. Sreekanth A, Fun H-K, Kurup MRP. *J. Mol. Str.* 2005; **737**: 61.

34. Kumar S, Dhar DN, Saxena PN. *J. Sci. Ind. Res.* 2009; **68**: 181.
35. Schiff H. *Inorg. Chim.* 1864; **131**: 118.
36. Dayagi S, Degani Y. in: Patai S (Ed.), *The Chemistry of the Carbon-Nitrogen Double Bond*. Wiley-Interscience, New York, 1970, pp. 71.
37. Casas JS, Garcia-Tasende MS, Sordo J. *Coord. Chem. Rev.* 2000; **209**: 197.
38. Tiwari R, Srivastava G, Mehrotra RC, Crowe AJ. *Inorg. Chim. Acta.* 1986; **111**: 167.
39. Saraswat BS, Srivastava G, Mehrotra RC. *J. Organomet. Chem.* 1977; **164**: 153.
40. Sen Sharma M, Ellis CA, Moitra N, Roy A, Tiekink ERT. *Acta Cryst.* 2006; **E62**: m2067.
41. Poller RC. *The Chemistry of Organotin Compounds*, Logos Press, London, 1970, pp.274.
42. Saxena A, Tandon JP, Molloy KC, Zuckerman JJ. *Inorg. Chim. Acta.* 1982; **63**: 71.
43. Saxena AK, Singh HB, Tandon JP. *Synth. React. Inorg. Met.-Org. Chem.* 1980; **10**: 177.
44. Saxena A, Tandon JP. *Polyhedron.* 1984; **3**: 681.
45. Khan J, Wajid R, Muhammad B, Danish M, Mahmood Q, Bukhari N, *World Appl. Sci. J.* 2009; **6**: 1563.
46. Carcelli M, Pelizzi C, Pelizzi G, Mazza P, Zani F. *J. Organomet. Chem.* 1995; **488**: 55.
47. Carcelli M, Delledonne D, Fochi A, Pelizzi G, Rodriguez-Argiuelles MC, Russo U. *J. Organomet. Chem.* 1997; **544**: 29.
48. Carcelli M, Corazzari G, Ianelli S, Pelizzi G, Solinas C. *Inorg. Chim. Acta.* 2003; **353**: 310.
49. Yearwood B, Parkin S, Atwood DA. *Inorg. Chim. Acta.* 2002; **333**: 124.
50. de Sousa GF, West DX, Brown CA, Swearingen JK, Valdés-Martínez J, Toscano RA, Hernández-Ortega S, Manfredo Hörner, Bortoluzzi AJ. *Polyhedron.* 2000; **19**: 841.
51. de Sousa GF, Filgueiras CAL, Abras A, Al-Juaid SS, Hitchcock PB, Nixon JF. *Inorg. Chim. Acta* 1994; **218**: 139.
52. Moreno PC, Francisco RHP, do MP, Gambardella P, de Sousa GF, Abras A. *Acta Crystallogr. Sect.* 1997; **C53**: 1411.
53. Casas JS, Castiñeiras A, Sánchez A, Sordo J, Vázquez-López A, Argüelles MC, Russo U, *Inorg. Chim. Acta* 1994; **221**: 61.
54. de Sousa GF, Valdés-Martínez J, Pérez GE, Toscano RA, Filgueiras CAL. *J. Braz. Chem. Soc.* 2002; **13**: 559.
55. de Sousa GF, Francisco RHP, Gambardella M Teresa do P, Santos RHdeA, Abras A. *J. Braz. Chem. Soc.* 2001; **12**: 722.
56. Francisco RHP, Gambardella M Teresa do P, de Sousa GF. *J. Chem. Crystallogr.* 2004; **34**: 39.
57. Bamgboye TT, Bamgboye OA. *Inorg. Chim. Acta.* 1988; **144**: 249.
58. Barbieri RS, Beraldo HO, Filgueiras CAL, Abras A, Nixon JF, Hitchcock PB. *Inorg. Chim. Acta.* 1993; **206**: 169.
59. Labib L, Khall TE, Iskander MF, Refaat LS. *Polyhedron.* 1996; **15**: 349.
60. Pettinari C, Marchetti F, Pettinari R, Martini D, Drozdov A, Troyanov S. *Inorg. Chim. Acta.* 2001; **325**: 103.
61. Dwivedi BK, Bhatnagar K, Srivastava AK, *Synth. React. Inorg. Met.-Org. Chem.* 1986; **16**: 715.

62. Gunduz T, Atakol O, *Synth. React. Inorg. Met.-Org. Chem.* 1989; **19**: 441.
63. Maurya MR, Jayaswal MN, Puranik VG, Chakrabarti P, Gopinathan S, Gopinathan G, *Polyhedron*. 1997; **16**: 3977.
64. Ruddick JNR, Sams JR, *J. Organomet. Chem.* 1973; **60**: 233.
65. Srivastava TN, Chauhan AKS, Agarwal M, *J. Inorg. Nucl. Chem.* 1979; **41**: 896.
66. Evans DL, Penfold BR, *J. Cryst. Mol. Struct.* 1975; **5**: 93.
67. Diamantis AA, Gulbis JM, Manikas M, Tiekink ERT, *Phosph. Sulf. Silicon* 1999; **151**: 251.
68. van der Bergen A, Cashion JD, Fallon GD, West BO, *Aust.J. Chem.* 1990; **43**: 1559.
69. Basu Baul TS, Basu S, de Vos D, Linden A. *Invest New Drugs*. 2009; **27**: 419.
70. Boyce M, Clarke B, Cunningham D, Gallagher JF, Higgins T, McArdle P, Ni Cholchúin M, O'Gara M, *J. Organomet. Chem.* 1995; **498**: 241.
71. Clarke B, Clarke N, Cunningham D, Higgins T, McArdle P, Ni Cholchúin M, O'Gara M. *J. Organomet. Chem.* 1998; **559**: 55.
72. Jamill K, Bakhtiar M, Khan AR, Rubina F, Rehana R, Wajid R, Qaisar M, Khan AF, Khan AK, Danish M, Awais M, Bhatti ZA, Rizwan M, Naveed A, Hussani M, Pervez A. *Afr. J. Pure Appl. Chem.* 2009; **3**: 66.
73. Rebolledo AP, de Lima GM, Gambi LN, Speziali NL, Maia DF, Pinheiro CB, Ardisson JD, Cortés ME, H. Beraldo, *Appl. Organomet. Chem.* 2003; **17**: 945.
74. Rebolledo AP, Ayala JD, de Lima GM, Marchini N, Bombieri G, Zani CL, Souza-Fagundes EM, Beraldo H, *Eur. J. Med. Chem.* 2005; **40**: 467.
75. Rebolledo AP, de Lima GM, Speziali NL, Piro OE, Castellano EE, Ardisson JD, Beraldo H. *J. Organomet. Chem.* 2006; **691**: 3919.
76. Casas JS, Castiñeiras A, Couce MD, Martinez G, Sordo J, Varela JM, *J. Organomet. Chem.* 1996; **517**: 165.
77. Affana MA, Fasihuddina BA, Liewa YZ, Foa SW, Ismailb J. *J. Sci. Res.* 2009; **1(2)**: 306.
78. Affan MA, Liew YZ, Fasihuddin BA, Mustaffa BS, Bohari MY. *ACGC Chem. Research. Comm.* 2005; **20**: 38.
79. Affan MA, Liew YZ, Fasihuddin BA, Bohari MY, Mustaffa BS. *Ind. J. Chem.* 2007; **46A**: 1063.
80. Affan MA, Wan FS, Ngaini Z, Shamsuddin M. *The Malaysian J. Anal. Sci.* 2009; **13**: 63.
81. Wiecek J, Kovala-Demertzi D, Ciunik Z, Wietrzyk J, Zervou M, Demertzis MA. *Bioinorg. Chem. Appl.* 2010; doi:10.1155/2010/718606.
82. Ianelli S, Mazza P, Orcesi M, Pelizzi C, Pelizzi G, Zani F. *J. Inorg. Biochem.* 1995; **60**: 89.
83. Ianelli S, Orcesi M, Pelizzi C, Pelizzi G, Predieri G, *J. Organomet. Chem.* 1993; **451**: 59.
84. Carcelli M, Ferrari C, Pelizzi C, Pelizzi G, Predieri G, Solinas C, *J. Chem.Soc. Dalton Trans.* 1992; 2127.
85. Mazza P, Orcesi M, Pelizzi C, Pelizzi G, Predieri G, Zani F. *J. Inorg. Biochem.* 1992; **48**: 251.
86. Bergamaschi G, Bonardi A, Leporati E, Mazza P, Pehzgatti P, Pelizzi C, Pelizzi G, Argüelles MCR, Zuni F. *J. Inorg. Biochem.* 1997; **68**: 295.
87. Ohara M, Okawara R, Nakamura Y. *Bull. Chem.Sot. Jpn.*, 1965; **38**: 1379.
88. Ruddick JNR, Sams JR. *J. Organomet. Chem.* 1973; **60**: 233.
89. Honnick WD, Zuckerman JJ, *Znorg. Chem.* 1979; **18**: 1437.

90. Yin HD, Chen SW. *Inorg. Chim. Acta.* 2006; **359**: 3330.
91. Yin HD, Hong M, Wang QB, Xue SC, Wang DQ. *J. Organomet. Chem.* 2005; **690**: 1669.
92. Yin HD, Hong M, Wang QB. *Indian J. Chem.* 2004; **43A**: 2301.
93. Yin HD, Wang QB. *Appl. Organomet. Chem.* 2004; **18**: 493.
94. Yin HD, Hong M. *Appl. Organomet. Chem.* 2005; **19**: 401.
95. Mendes IC, Moreira JP, Ardisson JD, Santos RG, da Silva PR, Garcia I, Castiñeiras A, Beraldo H. *Eur. J. Med. Chem.* 2008; **43(7)**:1454.
96. Nath M, Sharma N, Sharma CL. *Syn. React. Inorg. Met-Org. Nano-Met. Chem.* 1989; **19**: 339.
97. Singh HL, Varshney AK. *Bioinorg. Chem. Appl.* 2006; DOI 10.1155/BCA/2006/23245.
98. Gupta MK, Singh HL, Varshney S, Varshney AK. *Bioinorg. Chem. Appl.* 2003; **1**: 309.
99. Singh HL, Varshney AK. *Appl. Organomet. Chem.* 2001; **15**: 762.
100. Singh HL, Sharma M, Varshney AK. *Syn. React. Inorg. Met-Org. Chem.* 1999; **29**: 817.
101. Rehman W, Baloch MK, Badshah A. *Eur. J. Med. Chem.* 2008; doi:10.1016/j.ejmech.2008.01.019.
102. Rehman W, Baloch MK, Badshah A, Ali S. *J. Chin. Chem. Soc.* 2005; **52**: 231.
103. Rehman W, Badshah A, Baloch MK, Ali S, Hameed G, Khan KM. *J. Chin. Chem. Soc.* 2004; **51**: 929.
104. Rehman W, Baloch MK, Muhammad B, Badshah A, Khan KM. *Chin. Sci. Bull.* 2004; **49**: 119.
105. Rehman W, Baloch MK, Badshah A, Ali S, 65. *Spectrochim. Acta A.* 2006; **65**: 689.
106. Singh RV, Joshi SC, Gajraj A, Nagpal P. *Appl. Organomet. Chem.* 2002; **16**: 713.
107. Belwal S, Singh RV. *Appl. Organomet. Chem.* 1998; **12**: 39.
108. Singh K, Dharampal, Dhiman SS. *J. Iran. Chem. Soc.* 2010; **7**: 243.
109. Basu S, Mizar A, Basu Baul TS, Rivarola E. *Hyperfine Interact.* 2008; **185**: 95.
110. Ng SW, Kumar Das VG, Skelton BW, White AH. *J. Organomet. Chem.* 1989; **377**: 211.
111. Ng SW, Kumar Das VG, Luo BS, Mak TCW. *Z. Kristallogr.* 1994; **209**: 961.
112. Casas JS, Sánchez A, Sordo J, Vázquez-López A, Castellano EE, Zukerman-Schpector J, Rodriguez-Argüelles MC, Russo U. *Inorg. Chim. Acta.* 1994; **216**: 169.
113. Nath M, Yadav R, Gielen M, Dalil H, de Vos D, Eng G. *Appl. Organomet. Chem.* 1997; **11**: 727.
114. Teoh S-G, Ang S-H, Teo S-B, Fun H-K, Khew K-L, Ong C-W. *J. Chem. Soc. Dalton Trans.* 1997; 465.
115. Casas JS, Gracia-Tasende MS, Maichle-Mössner C, Rodriguez-Argüelles MC, Sánchez A, Sordo J, Vázquez-López A, Pinelli S, Lunghi P, Albertini R. *J. Inorg. Biochem.* 1996; **62**: 41.
116. Sommerer SO, Palenik GJ. *Inorg. Chim. Acta.* 1991; **183**: 217.
117. Casas JS, Castiñeiras A, Sánchez A, Sordo J, Vázquez-López A, Rodriguez-Argüelles MC, Russo U. *Inorg. Chim. Acta.* 1994; **221**: 61.
118. Kruger HJ, Peng G, Holm RH. *Inorg. Chem.* 1991; **30**: 734.

119. Holm RH, *Coord. Chem. Rev.* 1990; **100**: 183.
120. George G N, Prince RC, Kipke CA, Sunde RA, Enemark JH, *J. Biochem.* 1988; **256**: 307.
121. El-Tabl AS, El-Saied FA, Plass W, Al-Hakime AN, *Spectrochim Acta*, 2008; **71A**: 90.
122. Basuli F, Peng SM, Bhattacharya S. *Inorg. Chem.* 1997; **36**: 5645.
123. Basuli F, Ruf M, Pierpont CG, Bhattacharya S. *Inorg. Chem.* 1998; **37**: 6113.
124. Sisido K, Takeda Y, Kinugawa Z. *J. Am. Chem. Soc.* 1961; **83**: 538.
125. Mason J. *Multinuclear NMR*, Plenum Press, New York, 1987, p. 627.
126. Sen AB, Gupta SK. *J. Indian Chem. Soc.* 1962; **39**: 628.
127. Sheldrick GM. SADABS. University of Göttingen, Germany, 1996.
128. Bruker. APEX2 and SAINT. Bruker AXS Inc., Madison, Wisconsin, USA. 2008.
129. Sheldrick GM. *Acta Crystallogr.* 2008; **A64**: 211.
130. Farrugia LJ. *J. Appl. Cryst.* 1997; **30**: 565.
131. Brandenburg K, DIAMOND. Crystal Impact GbR, Bonn, Germany, 2006.
132. Spek AL. *J. Appl. Crystallogr.* 2003 ; **36** : 7.
133. Rouxel T, Sarniguet A, Kollmann A, Bousquet JF. *Physiol. Mol. Plant Pathol.* 1989; **34**: 507.
134. Kamruddin Sk, *Ph.D. Thesis*. North Bengal University, West Bengal, India, 1996.
135. Silverstein RM, Bassler GC, Morrill TC, *Spectrometric Identification Of Organic Compounds*, 5th Edn, Wiley: Toronto, 1991.
136. Basu Baul TS, Dutta S, Rivarola E, Scopelliti M, Choudhuri S. *Appl. Organomet. Chem.* 2001; **15**: 947.
137. Martinez EG, Sanchez A, Gonzalez A, Casas JS, Sordo J. *J. Organomet. Chem.* 1993; **453**: 47.
138. Iskander MF, Labib L, Nour El-Din MMZ, Tawfik M. *Polyhedron*, 1989; **8**: 2755.
139. Lockhart TP, Manders WF. *Inorg. Chem.* 1986; **25**: 892.
140. Ahmad F, Ali S, Parvez M, Munir A, Mazhar M, Khan KM, Shah TA. *Heteroatom Chem.* 2002; **13**: 638.
141. Lockhart TP, Manders WF, Schlemper EO, Zuckerman JJ. *J. Am. Chem. Soc.* 1986; **108**: 4074.
142. Lockhart TP, Manders WF, Holt EM. *J. Am. Chem. Soc.* 1986; **108**: 6611.
143. T. P. Lockhart, W. F. Manders. *J. Am. Chem. Soc.* **1987**, *109*, 7015.
144. Nadvornik M, Holecek J, Handlir K, Lycka A. *J. Organomet. Chem.* 1984; **275**: 43.
145. Holecek J, Lycka A. *Inorg. Chim. Acta*, 1986; **118**: L15.
146. Holecek J, Nadvornik M, Handlir K, Lycka A. *J. Organomet. Chem.* 1986; **315**: 299.
147. Holecek J, Handlir K, Nadvornik M, Lycka A. *Zeitschrift Chemie*, 1990; **30**: 265.
148. Wrackmeyer B. in *Physical Organometallic Chemistry-Advanced Applications of NMR to Organometallic Chemistry*, Vol. 1 (Eds:Gielen M, Willem R, Wrackmeyer B.), pp. 87–122, Wiley:London, 1996.
149. Wrackmeyer B. *Annu. Rep. NMR Spectrosc.* 1999; **38**: 203.

150. Addison AW, Rao TN, Reedijk J, van Rijn JJ, Verschoor GC,. *J. Chem. Soc. Dalton Trans.* 1984; 1349.
151. Buntine MA, Hall VJ, Kosovel FJ, Tiekink ERT. *J. Phys. Chem. A* 1998; **102**: 2472.
152. Sarkar B, Choudhury B, Sen Sharma M, Kamrudin SK, Choudhury AK, Roy A. *Archv. Phytopath. Plant Prot. (In Press)*, 2009.
DOI: 10.1080/03235401003633667.

CHAPTER 5

**BIOCIDAL ACTIVITY OF ORGANOTIN(IV)
COMPLEXES ON FOLIAR BLIGHT DISEASES OF
WHEAT (*Triticum aestivum* L.)**

5.1 Introduction

India is one of the main wheat producing and consuming countries of the world. After the advent of Green Revolution, the production of wheat has shown a gigantic increase from 10.4 to 80.58 million tones during 2008-09 [1]. The crop is known to suffer from a large number (at least 50 fungal, 7 bacterial and 36 viral) of diseases [2] which may reduces the yield up to 24.3%. Among the different pathogens, foliar blights have been recognized as one of the major production constraint of worldwide wheat cultivation, particularly in warmer growing areas of eastern plains of South Asia including India characterized by an average temperature in the coolest month above 17°C [3-9].

There are numerous foliar blights either of seed borne and/or soil borne diseases reported on wheat [10, 11]. The three blight diseases (spot blotch, tan spot and *Alternaria* blight) have been recorded in most of the wheat growing areas of India [12-14], Bangladesh [15], Nepal [16] and Pakistan [17]. In Eastern India, the leaf blight diseases represent a complex and are collectively referred to as *Helminthosporium* Leaf Blight (HLB). Two of the most common diseases, spot blotch and tan spot, are caused by the fungi *B. sorokiniana* (Sacc. in Sorok.) Shoem (Fig. 5.1a); and *Pyrenophora tritici-repentis* (Died) Drechs, respectively. Another leaf blight fungus is *Alternaria triticina* (Fig. 5.1b) reported by Prasad and Prabhu [18]. In the conducive weather conditions i.e. continuous rain for 5-6 day followed by warmer temperatures (day average of 20–30°C), spot blotch epidemic can develop very rapidly [19]. In recent surveys, the relative frequency of *A. triticina* seems to be declining, possibly due to availability of more resistant varieties of wheat [20]. Besides, another leaf spot disease, zonate eye-spot (*Drechslera gigantea*) has also been reported by Chowdhury *et al.* [21] from *terai* zone of West Bengal. Symptoms of these three leaf blights are difficult to distinguish in the field, even microscopic observation does not clearly resolves the problem of correct diagnosis. However, the spot blotch pathogen, *B. sorokiniana* is the major one and responsible for yield loss in northern districts of West Bengal [22]. Though organotin has been widely used as fungicide [23-25], however, till today no attempts have been made to evaluate the organotin or its derivatives as fungicide against wheat foliar diseases caused by *B. sorokiniana*, the role of which are elaborated below.

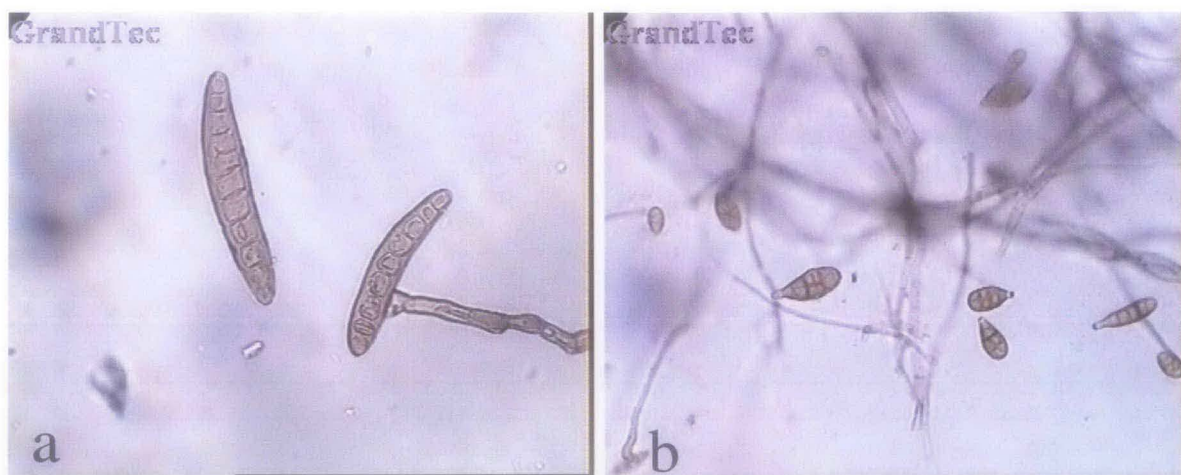


Fig. 5.1 a) Spore of the fungi *B. sorokiniana* and; b) Spore of the fungi *A. triticina*.

5.2 Literature

5.2.1 Use of organotin as biocide

Investigation of fungicidal and bacteriocidal properties of organotin compound and its derivatives was carried out by many scientists world over. Among them a few are cited below. In case of the agricultural applications since the present investigation is carried out in Indian soil, similar important works are referred below preferentially. Fentin acetate was found to be effective against many diseases such as leaf spot diseases of bitter melon [26], leaf spot and fruit rot diseases of brinjal [27], *Phytophthora* diseases of cacao [28], gray blight diseases of coconut [29], sugar cane downy mildew diseases of maize [30], Alternaria disease of sesame [31], kernel bunt [32] and spot blotch diseases of wheat [33]. Similarly, fentin hydroxide was also found to be effective against some diseases of cereal [34-36]. Several other compounds such as fentin chloride [37], non-commercialized triphenyl tin derivatives [38, 39] and some anionic complexes [40] were found to be effective as fungicide or as bactericide. Kamruddin *et al.* [41] have reported that among the three $R_3SnO_2(O_2CCH_2N(H)C(O)NH_2)$ [$R=Ph, C-Hex(Cyclohexyl)$ or $n-Bu$], $n-Bu$ was more toxic against the fungi *A. alternata*, *H. sativum*, *H. maydis* and *P. oryzae*. Chakraborty *et al.* [42] have reported the synthesis and biocidal activity of $[R_3Sn(O_2CCH_2SC_5H_4N-4)]$ where $R=Ph$, benzyl(Bz), Cyclohexyl(C-hex), $n-Bu$ and $[R_3Sn\{O_2CCH_2SC_4H_3N-2,6\}]$ where $R=Me$, Ph and $n-Bu$ against the fungi *H. maydis* (ITCC 2675) and *H.*

oryzae (ITCC 2537) both of which damage the crops such as maize and rice. Also they have observed that these compounds show no adverse phytotoxicity up to the concentration 10^{-3} M. Sen Sarma *et al.* [43] have described the biological activity of these compounds, with general formulae $[R_2Sn(OArCH=N-N=CSNH_2)]$, where $R=Me, n-Bu, Ph$ and $Ar= -C_6H_4, -C_6H_3(5-Cl), -C_6H_3(5-Br)$, against four fungal pathogens (*Curvularia eragrostidi*, *Alternaria porri*, *Dreschlerea oryzae* and *Macrophomina phaseolina*) of four different crops (*Camellia sinensis*, *Guizotia abyssinica*, *Oryzae sativa* and *Solanum melongena*).

A wide range of organotin substitute show biocidal activity such as organotin compound with oxygen and nitrogen donor legends [44-47]. Even, the organotin complexes of sulphur containing legends have been found biological applications [48-49]. Rehman *et al.* [50] presented the synthesis and *in vitro* antifungal activity of some Schiff bases and their organotin(IV) complexes against plant pathogenic fungi and it was found that they pose excellent fungicidal activity. The application of multi criteria decision-making methods to the results of *in vitro* antifungal properties of organotin compounds of the type Ph_xSnX_z ($x=2$ or 3 ; $X=O_2CC_6H_4OH, O_2CC_6H_4OCOCH_3, Cl$ or O_2CCH_3 ; $z=1$ or 2) and of free 2 hydroxybenzoic and 2-acetoxybenzoic acids against many fungi such as *Aspergillus niger* and *Aspergillus flavus* etc. was described by Gorwin *et al.* [51]. The $[nBu_3Sn(N-phthaloylglycinate)OH_2]$ and 3 other triorganotin derivatives of N-phthaloyl-protected amino acids were tested by Ng *et al.* [52] and the complexes were having a varying degree of inhibitory effect against several economically important plant pathogenic fungi like *Alternaria padwickii*, *Batryodiplodia theobromae*, *Colletotricum musae*, *Pestalotiopsis guepin* and *Phytophthora palmivora*. Triorganotin(IV) compounds appear to inhibit the mitochondrial function in Dutch elm diseases of American elm tree [53,54]. Eng *et al.* [55] observed that complexes of several $Ph_3Sn(IV)^+$ carboxylates and of some 1:1 addition compounds of Ph_3SnCl and 2,3-disubstituted thiazolium 4-ones were effective against *Ceratocystis ulni*, a pathogen of Dutch elm diseases.

Additionally, $Ph_3Sn(IV)^+$ compounds of p-ethoxybenzoic acid and acetyl salicylic acid contain molecular units with distorted tetrahedral Sn center. These complexes have significant inhibitory activity against a range of fungi [56]. Kalsoom *et al.* [57] reported that a series of di- and tri-organotin complexes of 2-thionaphthene had

moderate biological activities against various bacteria and fungi. The fungicidal activities of ArSn(IV) compound $(p\text{-Z C}_6\text{H}_4)_3\text{SnX}$ where $\text{X} = \text{OAC group, } ^-\text{OH or } \frac{1}{2}\text{O}$, $\text{Z} = \text{F, Cl, CH}_3, \text{CH}_3\text{O, C}_2\text{H}_5$ or $[(\text{CH}_3)_3\text{C}]$ was reported by Whaef *et al.* [58]. They found that *p*-substitution reduces biocidal activity but *p*- CH_3O was completely ineffective. Based on these experiments, they proposed a model for the fungicidal action [58]. In view of the promising results, some organotin(IV) dithiocarbamates of the formula $\text{R}_n\text{Sn(SCSNR}_1\text{R}_2)_{4-n}$ ($\text{R} = \text{Ph or Bz}$; $\text{R}_1 = \text{R}_2 = \text{alkyl or aryl}$; $n = 1$ or 2) were synthesized as well and evaluated *in vitro* against five fungi [59]. Triphenyltin(IV) phenylthiocarbamate had the best overall antimicrobial activity. A series of organotin(IV) complexes of pipyridyl dithiocarbamates of the types R_2SnL_2 , R_3SnL [60] and R_2SnLCl [61,62] also exhibited high activity compared to free ligand against bacteria and fungi. A large number of organotin(IV) complexes of compositions $\text{Ph}_3\text{SnL}\cdot\text{bipy}$ and $\text{Me}_2\text{SnLCl}\cdot\text{bipy}$ ($\text{L} = \text{anion of amino acid, e.g. tyrosine or phenylalanine}$) have been screened against a number of fungi and bacteria to assess their growth inhibition potential [63]. The organotin(IV) derivatives of the amino acids have been of interest as possible biocides [64–66]. Tricyclohexyltin(IV) alaninate has been found to be active as a fungicide and bactericide for seeds and plants [67]. Organotin(IV) complexes of amino acids [68–70] of the type R_3SnL and R_2SnL_2 ($\text{R} = \text{Me, Ph or n-Bu}$, $\text{L} = \text{anion of various amino acids}$) were found to be active against a wide spectrum of bacteria and fungi. Organotin(IV) complexes of extended systems derived from the condensation of 2-amino-5-(*o*-anisyl)-1,3,4-thiadiazole with salicylaldehyde, 2-hydroxynaphthaldehyde and 2-hydroxyacetophenone, were also screened *in vitro* against the same panel of bacteria and fungi [71,72]. The effect of fentin acetate against various fungi and bacteria was investigated. They are *Phytophthora palmivora* of black pepper [73], *Pyrenopeziza brassicae* of brassicas [74], *Perenoporm destructor* of onion [75], basal stem rot diseases of cowpea [76]. The fentin hydroxide was also effective against various fungi e.g. *Cercospora beticola* of sugarbeet [77] and *Stemphylium solani* of wheat [78] etc.

5.2.2 Economic importance of *B. sorokiniana*

The theoretical aspects including methodology of yield losses in general crops as well as for economically important commercially cultivated crops have been

reviewed [79-84]. The importance of yield losses in relation to host age is the most important particularly in designing strategy of management and decision making. In a conservative estimation, it has been reported that the yield losses due to foliar blights in wheat ranges from 20 to 100% [4-5] depending on genotypes and environmental factors (Fig. 5.2).



Fig. 5.2 Foliar blight diseases appeared in wheat plant on the field trial condition.

(Inset: a close up view in the top right corner)

At Poza Rica, in Mexico which is the hot spot for screening the resistance to spot blotch diseases, 49-90% yield losses have been recorded by Duveiller *et al.* [85]. In the Mixteca region of Mexico, on-farm trials under severe natural infection by tan spot diseases indicated plots under zero tillage suffer loss in yield around 37% even with one spray of propiconazole [86]. In Argentina, tan spot is recognized as major leaf blight in wheat and severity level beyond 50% is a common feature with potential yield losses up to 20% [87]. In Paraguay, during 1972, losses due to the disease complex in the wet year reached as high as 70% [88,89]. In Pakistan, previously the spot blotch was considered to be of the minor importance [90]. However in 2000 during a survey of wheat fields in various districts of Punjab, foliar spots were observed in different frequencies [91]. Later *B. sorokiniana* was found the

predominant pathogen of foliar spot in all wheat growing areas of Pakistan [92]. Due to this destructive pathogen, the yield loss was estimated at 18-22% in India [20] and 23.8% in Nepal [93].

In farmers' fields of Bangladesh, the average yield losses due to foliar blights were estimated to be 15% [94] whereas yield losses due to spot blotch were about 20% in Sonalika cultivar, whereas 14 and 8% losses have been reported in Akbar and Kanchan cultivar respectively [95]. Sowing time also dramatically increases yield loss. For an example, in Bangladesh, the late sowing of the two leaf rust susceptible cultivars Sonalika and Kanchan resulted in a yield loss of 71% and 41%, respectively [96]. A study conducted at Bangladesh into the effect of *B. sorokiniana* on wheat production revealed that upon the artificial inoculation of plants at the flag leaf stage reduced the number of grains per ear head and 1000-grain weight by 7-100 % and 12-100 %, respectively compared with the control [97]. In Nepal, the yield losses have been registered around 27 % [98].

The losses caused by *A. triticina* and *Helminthosporium* spp. have been estimated separately in India. Flag leaf in almost all cereals has major impact on yield potential of the concerned crop. Chenulu and Singh [99] estimated losses due to *A. triticina* to the extent of 99% in a highly susceptible variety, Sonalika under artificial conditions of inoculations at the boot stage in pot experiment. Nema and Joshi [100] correlated reduction in grain weight to the number of lesions incited by *Helminthosporium sativum* and disease intensity per unit area of flag leaf in pot experiments. Prabhu and Singh [101] estimated the relative effects of *A. triticina* and *Helminthosporium sativum*, independently and in combination on yield and magnitude of losses. They observed that losses increased at the rates of 0.92, 0.52 and 0.36 per unit increase of the disease incited by *Helminthosporium sativum*, *A. triticina* and combined infection of both the pathogens respectively. Studies conducted at Rajendra Agricultural University, Pusa, India revealed that 20-25% loss in grain yield is inflicted due to blights in different wheat cultivars under normal years, which may be more in epiphytotic years [102].

The yield losses due to foliar blight at Faizabad, India during 1994-95 crop season, was estimated to be 20 and 22% in the wheat varieties UP 262 and HD 1633, respectively [103]. Yield loss assessment conducted at Cooch Behar, West Bengal

showed 42% yield loss in highly susceptible varieties in experimental plots and on farm studies up to 21% [104].

5.2.3 Symptoms of *B. sorokiniana* infection

The *B. sorokiniana* is an aggressive pathogen that causes spot blotch, root and crown rots, node cankers, ear head and seedling blight in wheat [105]. Lesions in leaves are small, chlorotic and oval shaped with dark centers. Lesions have reddish brown centers with yellow margins and tapered ends. They may reach several centimeters before coalescing and inducing the death of the leaf. If spikelets are affected, it can result in shriveled grain and black point, a dark staining of the embryo at the end of the seed [106].

5.2.4 Management of foliar blight

The management of foliar blight by different pathogens was the centre of interest for controlling the severity of the diseases. It becomes critical particularly under favourable environmental regime for fungal pathogens, as they are highly sporulating with shorter life cycle as well as easy dissemination. Generally multipronged strategy becomes essential and application of a single tactics results in obvious failure. Conventionally foliar spray has been a first choice to researchers, extension officers and to a practicing farmer. Integrated pest management (IPM) with various stages of development in different countries has been attempted, however, not yet accepted in larger scale among the growers' community. Researches relevant to foliar blight management can be considered and categorized as component for developing IPM.

5.2.4.1 Seed treatment

Seed treatment with different fungicide and various other substances including non-conventional chemical may provide variable protection against foliar blight incidence of wheat. Hait and Sinha, [107] reported that phytoalexin inducers like cupric chloride, ferric chloride at 10^{-3} M protected the wheat seedlings from foliar

blight infection. The other effective fungicides include captan, mancozeb, thiram, pentachloronitrobenzene, praline and triademefon [108,109]. The foliar pathogen can be controlled with seed treating fungicides like guazatine and guazatine along with imazalil [110]. Pavlova *et al.* [111] indicated that seed treatment with some dual fungicides combination such as flutriafol and thiabendazole carboxin and thiram, difenoconazole and cyproconazole, tebuconazole and diniconazole provided protection against root rot caused by *Fusarium*, *Helminthosporium*, *Bipolaris* and *Rhizoctonia* spp. In 2002, Domanov [112] conducted field trials to test carbendazim along with carboxin which gave good control of root rots and increased yield of wheat. The efficacy of Raxil (tebuconazole) was studied on spring wheat cultivar as seed treatment with tebuconazole and found to control root rots caused by *B. sorokiniana* (*Cochliobolus sativus*) and *Alternaria* spp. [113]. Seed treatment with Vitavax 200 B and Bavistin increased seed germination by 43% and reduced seedling infection by *B. sorokiniana* in Nepal [114]. Seed and soil borne inoculum are the most important sources in the establishment of spot blotch on wheat. Seed treatment with Vitavax-200TM was consistent in a 10% yield increase or higher, across Bangladesh [115]. In 2009, Malaker and Mian [116] reported the efficacy of seed treatment and foliar spray with fungicides in controlling black point caused mainly by *B. sorokiniana* and *A. alternata* incidence of wheat seeds was evaluated in the field. Two seed treating fungicides, namely Vitavax-200 and Homai-80WP were used @ 0.25% of dry seed weight and foliar spray with Tilt-250EC (0.05%) was applied in six different schedules.

The seed treatment of a newly developed fungicidal formulation, Vitavax 200 WS (carboxin + thiram in a ratio of 1:1) @ 2.0, 2.5 and 3.0 g/kg gave good results in reducing seedling mortality, incidence of foliar diseases at multilocations of India including Uttar Banga Krishi Viswavidyalaya, West Bengal [117].

5.2.4.2 Chemical management

The use of fungicides for the control of foliar blight has been attempted in many countries including India with mixed success despite the harmful effect of fungicides; it had proved useful and economical in the control of tan spot and spot blotch [118].

In Brazil, Mehta [19] observed that foliar fungicides are an effective in controlling spot blotch. Non systemic and systemic foliar fungicides belonging to the dithiocarbamates (*namely*, mancozeb) and triazoles (*namely*, propiconazole, tebuconazole, flutriazol, prochloraz, and triadimenol) and dicarboximides (*namely*, iprodione) are known to be effective. The first spray should be applied soon after the onset of disease symptoms appear. In a non-endemic zone generally spraying may be done 45-55 day after sowing for the spring wheat cultivars [119]. Foliar applications especially with systemic fungicides such as tebuconazole, epoxiconazole, flutriafol, cyproconazole, flusilazole, epoxiconazole, and metaconazole, applied between heading and grain filling stages, have been proved to be cost effective. Under severe disease infestation, a second spray can result in a grain yield increase by 38-61% [120].

The fungicide, manzate reduced disease severity by 25%. There were no significant differences between two treatments reduced the average disease severity on both flag leaf (F) and (F-1) leaves by more than 75%. Only two sprays of tebuconazole (Folicur) caused a significantly larger reduction in disease severity (86%) [86].

In Argentina, Annone [121] observed positive response with foliar fungicides for reducing disease development under conditions of moderate to low inoculum pressure, but inconsistent results under high inoculum pressure. Among fungicides tested under field conditions, tebuconazole and propiconazole achieved the highest level of control, though results varied widely (30-80%).

In 2003, Tewari and Wako [122] reported that the mixture of tebuconazole and metacid applied as foliar spray at the boot stage of wheat crop effectively suppressed all the foliar diseases (brown and yellow rusts, powdery mildew and leaf blight) showing curative property with no phytotoxic effect on the plant. They also observed that Sencor and Propiconazole (Tilt) was incompatible and highly phytotoxic. They further noticed that the mixture of zinc sulphate and urea completely inhibited mycelial growth of *B. sorokiniana* and also inhibit 78% growth of *A. triticina*. Rashid *et al.* [123] reported propiconazole to be very effective against foliar blight of wheat (*B. sorokiniana*). The different fungicides like flusilazole, prochloraz, propiconazole and tebuconazole were effective against tan spot disease of wheat [124]. In 2008, Singh *et al.* [125] observed that the foliar sprays of Propiconazole @

0.1% beginning from the appearance of the disease and later at 15 days intervals thrice reduced the leaf blight incidence and increased grain yield at Karnal, Pantnagar, Faizabad, Dharwad and Cooch Behar in India. At Uttar Banga Krishi Viswavidyalya, the management of foliar blight has been attempted in an integrated approach and it was observed that seed treatment with carboxin and single spray with propiconazole (Tilt) at panicle initiation stage was effective in reducing the disease symptoms [22]. An experiment was undertaken to find out an effective integrated approach in controlling Bipolaris Leaf Blight (BpLB) as well as foot and root rot diseases of wheat under field condition. Sixteen treatments consisting of chemical fertilizer alone in combination with soil treatment (poultry refuse) and fungicide (Tilt 250EC) were considered for the management of Bipolaris leaf blight as well as foot and root rot diseases of wheat caused by *B. sorokiniana* and *Sclerotium rolfsii* or *Rhizoctonia solani* respectively. Considerable differences were observed among the treatments regarding the disease severity, incidence, disease control and grain yield. Disease severity increased both at lower and higher doses of N that is at '0' and '150' kg N/ha, respectively. Disease severity was reduced significantly through the use of recommended chemical fertilizers (N₁₀₀ P₂₆ K₅₀ S₂₀ B₁). Addition of poultry refuse (1.5 tons/ha) and Tilt 250EC (0.5 ml/L) with chemical fertilizers further reduced disease severity resulting the highest grain yield (4956 kg/ha). This yield was higher over the farmers practice, N₁₀₀ P₂₆ K₅₀ S₂₀ + poultry refuse + Tilt 250EC and N₅₀ P₁₃ K₂₅ S₁₀ B₁ + poultry refuse + Tilt 250EC, by 20%, 17% and 15% respectively [126]. The best chemical way to protect yield loss from spot blotch is to foliar spray a fungicide combined with seed treatment. From a number of years of experiments the average yield loss due to spot blotch was estimated at 15%. After conducting a series of experiments with varying rates of fungicides and from an economic and environmental viewpoint, a single spray of fungicide Tilt 250EC (125 a.i./ha) combined with seed treatment (Vitavax-200TM @ 3g/kg of seed) at the dose ml/L of water/20m², at 35-50 day after sowing (booting to heading) was found profitable for successful wheat production (Banu *et al.* Personal communication)

5.2.4.3 Induced resistance

Yield losses in wheat and barley leaf blight (*B. sorokiniana*) indicate the need to search for alternative strategies of disease control. Globally, one of the emerging

strategies is induced resistance. In the broadest sense, induced resistance means the control of causal agents by a prior activation of the plants own defense system. Defense was activated by necrotizing pathogen as well as by chemicals mimicking factors of the natural defense systems, such as salicylic acid [127,128]. Chemical induction of resistance to *B. sorokiniana* in barley by pre-treatment with inducers 2,6-dichloroisonicotinic acid (DCINA), benzo (1,2,3) thiadiazole-7-carbothioic acid-methylester (BTH) or jasmonates leads to reduction of the diseases in the range of 10-20% (Kumar and Ibeagha, personal communication). In 1986, Hait and Sinha [107] reported that seed treatment with heavy metal ions provides the protection to the wheat seedlings from *Helminthosporium* infection.

The biocontrol efficiency of *Epicoccum purpurascens*, *Gliocladium roseum*, three strains of *Bacillus subtilis*, and *Pseudomonas fluorescens*, isolated from the rhizosphere of wheat plants, was assessed in relation to seedling blight caused by *B. sorokiniana*. An *in vitro* study of the potential antagonist was performed using the dual culture technique and by 'sowing' wheat seeds pelleted with the saprophytes in plates with water agar along with the pathogen. *In vivo* assays were carried out in the greenhouse and in the field with pelleted seeds sown in artificially infested soil. Both the number of living plants and the number of plants with necrosis on the leaves and the base of the stems and roots were assessed 15 days after sowing. Under greenhouse conditions, *B. subtilis* and *G. roseum* reduced the level of infection of Buck Pucar and Trigomax 100 cultivars, respectively. In the field, biocontrol of the disease was not achieved [129].

5.2.5 Biochemical changes due to infection

The morphological, physiological and biochemical characterizations of *B. sorokiniana* have been the major aim of many studies [130-134]. However, knowledge about the genetic structure of this fungus is less available [135-137]. In general, plants respond in two different ways to pathogens. There is either no obvious interaction, or an interaction occurs and is, in the extreme cases, either incompatible (where the plant is resistant) or compatible (where the plant is susceptible). The biochemical events occurring in interactions between host or non-host plants with potential pathogens are basically similar but their timing of appearance and both the

intensities and patterns depend on their genomic as well as environmental conditions [138]. It has been established that different plant species, even varieties within a species may have fine differences in their biochemical make-up particularly in respect of phenolics, proteins and various other primary and secondary metabolites variation in respect of constitutive components as also in their enzyme components. They also differ in their responses to infection in most of these respects. Such biochemical differences in the host responses to inoculation with their potential pathogens have been studied for many host-pathogen combinations and the sum of all available data suggest that most, or all of them, are part of a typical resistant response of plants, one often determining over the others as the major defense mechanisms. Variations may occur more at the level of timing of induction, location and relative amounts, than in terms of all-or-none response.

Sixty-seven isolates of *B. sorokiniana* of barley, belonging to three groups (black, white and mixed) were studied to find an association of melanin with the spore production of the fungus. Conidiogenesis in black, white and mixed subpopulation of *B. sorokiniana* was positively correlated with melanin content/g of mycelium. Primary hyphae of black and mixed subpopulation differentiated into secondary hyphal structures which subsequently produced conidiophores and conidia. Primary hyphae could not differentiate into secondary hyphae and subsequently conidiophores and conidia in white subpopulation. A melanin containing mutant developed from white subpopulation regained its ability to differentiate into secondary hyphae, conidiophores and conidia. Results showed that melanization of mycelia *B. sorokiniana* mycelia is an important factor for conidia production [139].

5.2.5.1 Phenol

Since Newton and Anderson [140] suggested in their 'Phenol hypothesis' that resistance of wheat to rust fungus was due to the accumulation of phenol caused by the fungal entry and its subsequent inhibition of the parasite, there by imparting a large amount of information accumulated on the possible role of phenol in disease resistance. Later several reports suggested that rapid synthesis of phenolics following infection to be an important first line defense in plants [141].

The interaction of plants with the pathogens for post-infectious increase in phenol level has also been reported [141- 143]. Reddy *et al.* [144] reported post-infectious increase in phenol level in groundnut plants when infected with *Rhizoctonia solani*. The resistant groundnut varieties contain more phenols than susceptible ones and also responded to infection with *Cercospora* sp. with greater increase in phenol [145].

5.2.5.2 Ortho-dihydroxyphenol

Ortho-dihydroxyphenols like chlorogenic acid have often been implicated in disease resistance reactions. They are easily oxidized by polyphenoloxidases and the resulting quinones are highly reactive and toxic to pathogens by inhibitory to their enzymes, particularly chain splitting pectic enzymes [146].

5.2.5.3 Protein

Plants are known to undergo both quantitative and qualitative changes in their protein content upto infection. The synthesis of 'pathogenesis- related protein'(PR protein) is induced not only by infection with pathogens or treatment with pathogen derived elicitors but also by exposure of plant tissues or cultured plant cells to various inorganic or organic chemicals [147].

Synthesis of new proteins in resistant host varieties following infection with the pathogen has been reported for several plant species such as cucumber- *Colletotricum lagenarium* [148], tobacco- *Thielaviopsis basicola* [149] interactions. In tomato plants, resistant to *Cladosporium fulvum* some novel proteins appear soon after infection [150]. Working with brown spot of rice, Hait and Sinha [143] observed that the disappearance from the susceptible rice plants protected from *H. oryzae* by seed treatment with cysteine and sodium selenite, of three common proteins that they share with the pathogen and also the appearance at the same time of two new proteins in them having similar Rf values as two proteins present in resistant plants.

5.2.5.4 Polyphenoloxidase

Changes in host physiology following infection or induced resistance is often associated with an activation of oxidase activity and post-infectious rise in the level of such enzyme is a common phenomenon in diseased tissue, more so in an incompatible interaction. The activity of polyphenoloxidase would seem to be important as it can oxidize phenolics to quinones which may be more fungitoxic. The infected resistant tissue shows in many cases a higher oxidase activity than the infected susceptible tissue as also in healthy one. Such observations have led to the speculation that stimulated polyphenoloxidase activity possibly contributes to the resistance of plants against the pathogen, an idea though not fully accepted. Various observations on the role of polyphenoloxidase in host resistance are well documented in literature [151-153].

5.2.5.5 Peroxidase

Increased peroxidase activity in response to infection is a common phenomenon in different host-parasite interactions and the greater activity is generally linked with incompatible than with compatible interaction, i.e., linked with disease resistance in the host though contrary evidence is also available. Importance of peroxidase in phenylpropanoid metabolism as the terminal enzyme in lignin biosynthesis is important for containing the spread of the pathogen in host defense. The role of peroxidase in plant defense has been attributed to its ability to catalyze various types of oxidative reactions important in metabolism of the pathogen or of the host plant such as phenolics, toxins, hormones, etc. [151,152]. Heitefuss *et al.* [154] observed that peroxidase activity differed in resistant and susceptible cabbage varieties to *E. oxysporum* f. sp. *conglutinans* and resistant plants showed greater activity following infection. Greater post-infectious increases in peroxidase activity in the resistant variety has been reported in groundnut- *Puccinia arachidis* [155], groundnut-*Cercosporidium personatum* [145], rice-*Helminthosporium oryzae* [143], rice-*Pyricularis oryzae* [156,157]and wheat-*Erysiphe graminis* [158] interactions.

5.2.5.6 Phenylalanine ammonia-lyase

Phenylalanine ammonia-lyase (PAL) activity was strongly reduced in barley and wheat leaves after inoculation with highly or weakly aggressive isolates of *B. sorokiniana*. Aggressive isolates, however, generated much stronger early induction of PAL than less aggressive isolates. Prior inoculation of barley leaves with non-pathogenic strain provided partial protection against a subsequent challenge with *B. sorokiniana* after seven days. Induced plants showed unchanged PAL activity levels compared to those of non-induced plants after challenge inoculation. The results suggest that PAL plays a role in the active defenses of barley and wheat in response to pathogen attack, but apparently not in response to non-pathogens, wounding, or in plants expressing induced resistance [159]. Kervinen *et al.* [160] used gene-specific probes to assess the expression patterns of four different phenylalanine ammonia-lyase (PAL) genes in infected or elicitor-treated leaves and suspension cultured cells of barley. Genes corresponding to *hpa12*, *hpa13*, *hpa14* and *hpa16* were all induced by mercuric chloride and fungal infection by *B. sorokiniana* in barley leaves, but with considerable variation in their expression level and timing. Mycelial preparation of *B. sorokiniana* causes delayed induction of phenylalanine ammonia-lyase activity as compared to crude extract and purified glucan [161]. Paltonen and Karjalainen [162] suggested that second phase of PAL induction in wheat and barley is linked with resistance to *B. sorokiniana* infection.

5.2.5.7 Pathogenesis related (PR) proteins

Attempts have also been made to understand the molecular mechanism of this pathogen infection. Cross species hybridization was made using barley cDNA as probe against some rice transcript. The transcripts for the pathogenesis related proteins such as PR-1, PR-2, PR-3, PR-4, PR-5 and peroxidase were found to be up-regulated in response to *B. sorokiniana* in rice [163]. PR-protein transcripts accumulation was seen 12h after infection with *B. sorokiniana* as well as after exposure with UV light. These transcripts reached to maximum accumulation levels at 24 h and all declined thereafter with the exception of the PR-4 transcript in response to *B. sorokiniana*. Maximum accumulation of the peroxidase transcript occurred at 12 h in response to *B. sorokiniana* and UV light.

5.3 Scope and objective

Organotin chemistry is a subject of interest for years due to not only of its rich structural chemistry but also for its versatile applications. Author is interested to explore the biocidal activity, specially related to plant pathogenic organisms of newly synthesized as well as previously synthesized compounds in this laboratory. Diorganotin complexes of salicylaldehyde thiosemicarbazone or di- and triorganotin complexes of 2-mercapto isothiocyanate have contained O, N, S and N, S atom as donor. Organotin compounds of O, N, S donor ligands are well known for their biological activity [43-50]. Crops are vulnerable to the attack of various fungi and bacteria apart from insects and pests resulting in to the mass destruction of considerable amount of important crops annually. Therefore, it is needless to say that we need biologically active molecule to protect our crops. The synthesized compounds achieve effective control of foliar blight disease of wheat, which is the important limiting factor of wheat cultivation in North-East Indian plane zone. The mechanism of action of this compounds on host physiology in respect of phenolics pathogenesis-related protein, enzyme such as polyphenol oxydase, peroxidase and phenyl alanine ammonia lyase and other biochemical parameters commonly associated with diseases resistance is investigated. So the newly synthesized compounds may serve as alternative agrochemicals.

5.4 Materials and methods

5.4.1 General comments

The solvents used in biochemical reactions were of AR grade and were obtained from commercial sources (Merck, India). The solvents were dried using standard literature procedures. Double distilled water was used. Used reagents were received from commercial sources (HiMedia, India).

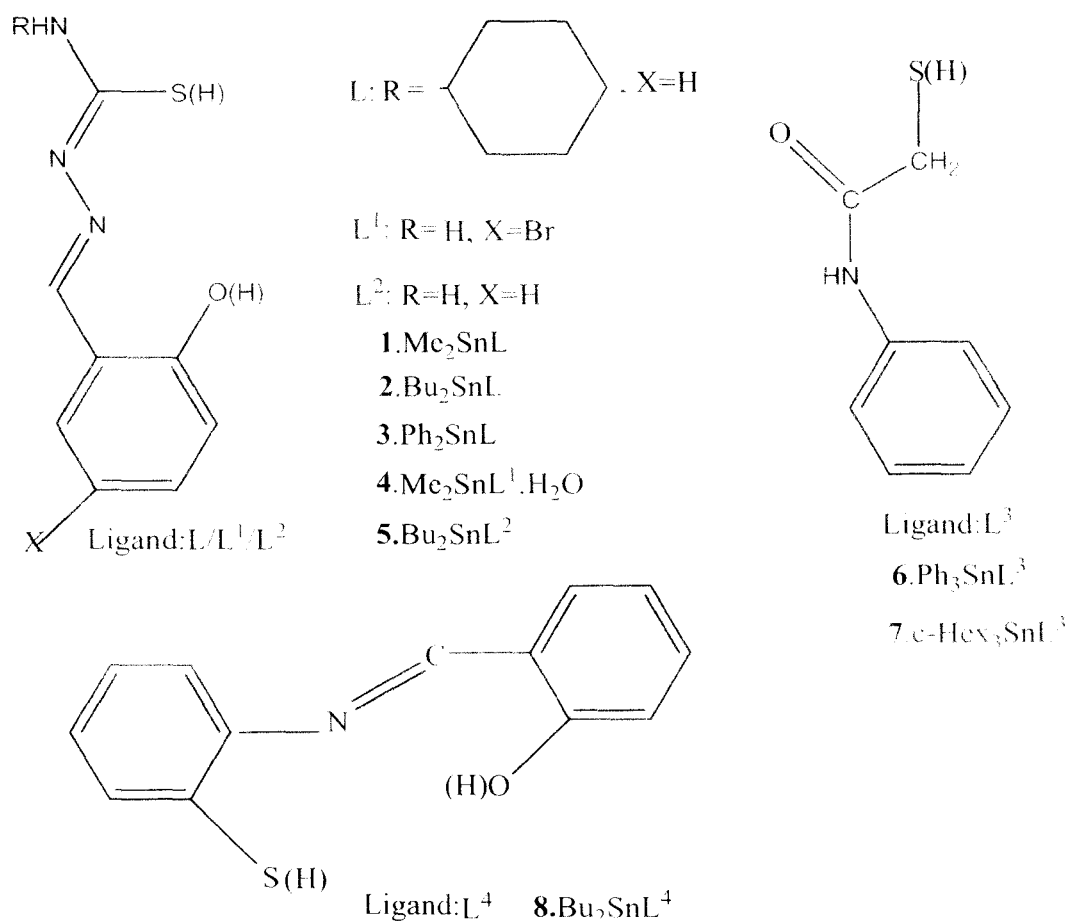
5.4.2 Measurements

The PAL enzyme activity was assayed by Parkin Elmer UV-Vis spectrophotometer in the optical density at 290 nm. The absorbance of the total phenol, ortho-dihydroxyphenol, protein, peroxidase activity, polyphenoloxidase

activity was measured by 722 Vis spectrophotometer, Jinghua instruments. Spore germination was counted by Lieca light microscope.

5.4.3 Synthesis and characterization of di and triorganotin(IV) complexes of Schiff bases

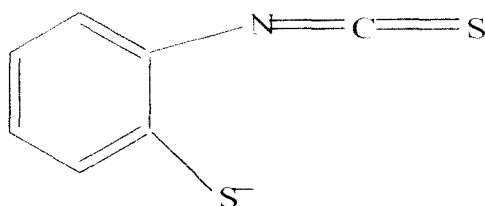
The synthesis and characterization of di and triorganotin(IV) of Schiff bases complexes (Set I) are described in Chapter 4 and in Sarkar *et al* [164]. In chapter 4, compound **8** is described as compound **4**. The formulae of the ligands and abbreviation of the complexes used for the present study are presented in Scheme 5.1.



Scheme 5.1.

5.4.3 Synthesis and characterization of di and triorganotin(IV) complexes of 2-mercapto isothiocyanate

The synthesis and characterization of di and triorganotin(IV) of 2-mercapto isothiocyanate complexes (Set II) are described in Chapter 3. The formulae of the ligands and abbreviation of the complexes used for the present study are presented in Scheme 5.2.



1. Me₃SnL; 2. n-Bu₃SnL; 3. Ph₃SnL; 4. Bz₃SnL; 5. c-Hex₃SnL
6. Me₂Sn(L)₂; 7. n-Bu₂Sn(L)₂; 8. Ph₂Sn(L)₂; 9. Bz₂Sn(L)₂

Scheme 5.2

5.4.4 Location

The experiments were carried out at Research Farm, Uttar Banga Krishi Viswavidyalaya, Pundibari Cooch Behar, West Bengal, situated between 25°57'N and 27°N latitude and 88°25'E longitude. The laboratory experiments were conducted at Department of Plant Pathology, Faculty of Agriculture, Uttar Banga Krishi Viswavidyalaya, Cooch Behar, West Bengal.

5.4.5 Weather

The experimental domain comes under terai agroclimatic zone of West Bengal. It is the northern aspect of West Bengal and is spread along the Bhutan Hills of Kalimpong and Karseong in northern side, Assam on its eastern border and Bihar on the west. This subtropical zone has a humid climate endowed with long rainy season starting from 1st week of May, continuing up to the end of September having low to heavy rainfall, ranges between 2100-3300 mm per year. Around 80% rainfall comes from the southwest monsoon during June-September when temperature varies between 24-33.2°C at the maximum and to 7-8°C at minimum with relative humidity 58% in March to 87% in July. Barring a period between December-February when

the winter sets in, this area as a whole remains warm and humid. This diverse climatic condition renders complicity to the agro ecological condition subjecting the region more prone to multiplication of pathogenic organisms.

5.4.6 Soil Characteristics

Soil of this zone is generally sandy loam to loam in texture, acidic in reaction, high in raw humus content, low in water retention capacity, low to medium in total nitrogen content with a low rate of nitrogen mineralization, low to medium in phosphorous status with high phosphorous fixation, low to medium in potash content and low in calcium and magnesium status. Micronutrients which are deficient in this zone are boron, molybdenum and zinc.

5.4.7 Media

All the glasswares were sterilized in hot air oven at 160°C for 30 min. The culture mediums were sterilized in an autoclave at 1.02 kg pressure/cm² for 15 min. The following medium was used for isolation, maintenance, sporulation characterization and mass multiplication of the fungi.

Wheat Dextrose Agar

Wheat leaves	100g
Dextrose	10g
Agar	7.5g
Distilled water	500 ml

Wheat leaves of 30-35 day old were first cut into pieces (2-3 cm) and boiled in 500ml of water till the colour of water becomes green and leaves become soften. Then it was filtered through cheesecloth. Required volume of water was added. Agar was dissolved in water to the required volume in warm condition and autoclaved at 15 lb pressure for 15 min.

Potato Dextrose Agar

Peeled Potato	250g
Glucose	20g
Agar	15g
Water	1000 ml
pH	6.0-6.5

Peeled potato was made into thin chips, boiled in 500 ml of distilled water till they were soft enough and extracted. The extract was filtered through cheese cloth. To the extract the weighed quantity of dextrose was added. Agar was melted in the other half of water and mixed in potato dextrose solution and the volume was made up to a litre. Finally it was autoclaved at 15 lb pressure for 15 min.

Oat Meal Agar

Oat Meal	15g
Agar	15g
Water	500 ml

Oat meal powder 15g was added in 500 ml of water. It was boiled for 15 min. volume was made upto 500 ml with water again. Finally the total solution was autoclaved at 15lb pressure for 15 min.

5.4.8 Planting material

Seeds of wheat were collected from Directorate of Wheat Research, ICAR Karnal, India and CYMMT (South Asia office, Kathmandu, Nepal). Seeds were air dried and stored in drier at 37°C. Wheat seeds were sown in sandy loam (field soil mixed with farmyard manure in 3:1 proportion) contained in pots (12-15 plant/ 25cm diameter pot). Prior of sowing, seeds were treated with 0.1% HgCl₂ for one min. to remove superficial contaminants, followed by several washing with sterile distilled water. During the summer season (April-June) and rainy season (July – September) the pot experiments were carried out in the environment controlled polyhouse.

5.4.9 Isolation of pathogens

Large number of blight infected wheat leaf sample were collected from different farm trials of Uttar Banga Krishi Viswavidyalaya Research farm. The infected leaf samples were washed with mercuric chloride (0.1%) solution and again rewashed with sterile distilled water. The leaf samples having typical blight symptoms were cut into small pieces (4 mm²). The leaf bits were placed in slant containing wheat bran extract dextrose medium and incubated at 22°C for 7 days. After 7 days these isolates were transferred in different medium to observe their sporulation.

5.4.10 Fungal culture

5.4.10.1 Source

The *B. sorokiniana* were isolated from Research Farm, Uttar Banga Krishi Viswavidyalaya, Pundibari, Cooch Behar. Cultures were first grown in wheat dextrose agar medium. Then the cultures were sporulated in Oat Meal Agar medium and then transferred to the Potato Dextrose Agar medium.

5.4.10.2 Completion of Koch's postulate

Wheat seeds were surface sterilized with 0.1% HgCl₂ solution for one minute washed with sterile distilled water and sown in earthenware pots containing sandy loam soil. Seedlings (21days old) were inoculated with *B. sorokiniana*. Infected leaves were collected, washed, cut into small pieces, treated with HgCl₂ (0.1%) for one min., rewashed with sterile distilled water and transferred to OMA (Oat Meal Agar) slants. After 10 days, the isolated organism were examined, compared with the original stock culture of *B. sorokiniana* and its identity was confirmed.

5.4.10.3 Maintenance of stock

The fungi were grown on OMA slants and stored under different conditions (5°C and 20°C). Apart from weekly transfer for experimental work at a regular interval culture of *B. sorokiniana* was examined in order to test its pathogenicity

5.4.11 Definition of field experiments parameters

Following unit were used for field experiment

Days to Heading (DH): An entry was considered to have headed when 50% of the shoots have the entire spike out of the flag leaf. Days to heading was calculated from the day of planting.

Days to Maturity (DM): When at least 50% of the peduncles are physiologically mature.

Plant Height (PHT): Distance in centimeter from soil level to the tips of the spikes excluding the awns of randomly selected plants.

1000-grain weight: One thousand kernels taken randomly from harvested in each plot were weighted to obtain-grain weight.

Grain yield: In grams per plot, adjusted to 12% moisture level.

5.4.12 Disease Assessment

The disease was visually scored using the double digit scale (00-99) developed as a modification of Saari and Prescott's severity scale to assess wheat foliar disease [165,166] caused by *B. sorokiniana* was recorded in the whole plot. [Double digit (DD) system: For example, if the reading was 93, i.e. 9 represent height of the plants on which disease was developed and 3 represent % infected by the disease or 30% necrotic or chlorotic lesions appeared on the leaves]. The AUDPC (Area Under Disease Progress Curve) was calculated using the following formula given by Das *et al.* [167].

$$\text{AUDPC} = \sum_{i=1}^{n-1} [(x_i + x_{i+1})/2] (t_{i+1} - t_i)$$

Where, x_i is the foliar blight severity on i th date, the t_i is the i th day and n is the number of scoring dates. The AUDPC measures the amount of disease as well as the rate of progress, and has no units.

5.4.13 Parameters of laboratory experiment

5.4.13.1 Detached leaf assay

Pads of absorbent cotton wool soaked with respective chemicals were laid inside 20 cm × 30 cm rectangular trays. Five excised pieces of leaves were parallelly placed in each of the trays and cut ends were covered with soaked cotton pads in the form of wicks. 10 ml of *B. sorokiniana* spore suspension (10^6 spores / ml) was inoculated in each tray.

Under field conditions, the respective chemicals were sprayed thrice at 10 days intervals starting from 45 days after sowing.

5.4.13.2 Phenol

Extraction

Fresh healthy leaves from plants were collected, washed with distilled water and used to extract phenol. Around 2g of fresh tissue was crushed in a mortar with a pestle in 5 ml of 80% ethanol. The homogenate was centrifuged at 10,000 rpm for 20 min. The supernatant was saved. The residue was re-extracted with another 5 ml of 80% ethanol, centrifuged for 10 min and the supernatants were pooled. The ethanol fraction was then evaporated to dryness in vacuum at 40°C. The residue was then dissolved in 2 ml of distilled water.

Estimation

The total phenol content was estimated using Folin-Ciocalteu reagent [168]. Around 0.1 ml of extract was pipetted into a graduated test tube and the volume was making up to 3 ml with distilled water. To each test tube 0.5 ml of Folin-Ciocalteu Reagent (1N) was added. After 3 min, 2 ml of 20% Na_2CO_3 solution was pipetted into each tube. The tubes were shaken well and heated on a boiling water bath for 1 min and then cooled under running tap water. The absorbance of the resulting blue solution was measured at 650nm in spectrophotometer. For comparison a reagent blank was run without any phenol extract was added in it. Total phenol was determined in catechol equivalent after comparing with the standard curve prepared from pure catechol. Total phenol was expressed as mg/g fresh wt of tissue.

5.4.13.3 Ortho dihydroxy phenol (OD Phenol)

Extraction

Fresh healthy leaves from plants were collected, washed with distilled water and used to extract OD phenol. 2g of fresh tissue was crushed in a mortar with a pestle in 5 ml of 80% ethanol water mixture. The homogenate was centrifuged at 10,000 rpm for 20 min. The supernatant was saved. The residue was re-extracted with another 5 ml of 80% ethanol, centrifuged for 10 min. and the supernatants were pooled. The ethanol fraction was then evaporated to dryness *in vacuam* at 40°C. The residue was then dissolved in 2 ml of distilled water.

Estimation

The OD phenol content was estimated following the methods of Mahadevan and Sridhar [168]. About 1ml of extract was pipetted out into a graduated test tube and the volume was made up to 1 ml 0.5(N) HCl. 1 ml of Arnou's reagent (NaNO₂:10g, Na₂MoO₄: 10g, distilled water: 100 ml), 2 ml of 1N NaOH were added and mixed thoroughly in room temperature following which the total volume of the reaction mixture was made up to 10 ml by adding water. Optical density was recorded in a Spectrophotometer at 515 nm. A blank was prepared for comparison by adding 1 ml of alcohol instead of tissue extract with all other reagents. Standard curve was prepared with different concentrations of catechol. Results were expressed as mg/g fresh wt of tissue.

5.4.13.4 Protein

Extraction

Fresh healthy leaves from plants were collected, washed with distilled water and used to extract protein. Leaf tissue 0.5g was mixed with 0.05 M Sodium Phosphate buffer (pH 7.2) in mortar with pestle at 4°C with sea sand. The mixture was centrifuged at 4°C for 10 min at 15,000 rpm and the supernatant was used as crude protein and immediately stored at -20°C for further use.

Estimation

Soluble protein was estimated following the method of Lowry *et al.* [169]. Around 25 µl of protein sample was pipetted out and made up the volume with water

to 1.0 ml in the test tube. To the sample, 5.0 ml alkaline reagent (0.5 ml of 1% CuSO₄ and 0.5 ml of 2% sodium potassium tartarate dissolve in 50 ml of 2% Na₂CO₃ in 0.1 N NaOH) was added. This was incubated for 15 min. at room temperature and then 0.5 ml of Folin-Ciocalteu reagent (diluted 1: 1 with distilled water) was added and again incubated for 15 min for colour development following which optical density (O.D) was measured at 660 nm. Quality of protein was estimated from the standard curve made using bovine serum albumin (BSA) as standard.

5.4.13.5 Polyphenol oxidase (PPO)

Extraction

Fresh healthy leaves from plants were collected, washed with distilled water and used to extract PPO. Leaf tissue were cut into pieces of 1-2 cm and crushed in ice with 5 ml of pre-chilled phosphate buffer (pH 6.6) per g of tissue. The crushed material was centrifuged at 2,000 rpm of 4°C for 30 min. The supernatant was decanted and stored at 4°C

Estimation

For enzyme estimation, around 1.0 ml of enzyme extract, 1.5 ml of phosphate buffer (pH 6.0) and 0.5 ml. of substrate pyrogallol solution were mixed thoroughly by repeated inverting the cuvette and immediately the initial reading was taken at 495 nm. Further readings were taken in every 5 min interval. The blank reading was taken with 3 ml of phosphate buffer [168].

5.4.13.6 Peroxidase (PO)

Extraction

Fresh healthy leaves from plants were collected, washed with distilled water and used to extract peroxidase. Leaf tissue were cut into pieces of 1-2 cm and 0.2g taken in a pre-cooled mortar with phosphate buffer of pH 6 (5 ml/g leaf tissue), a pinch of neutral sand which was ground with pestle at 4°C. The homogenate was then centrifuged at 15,000 rpm for 15 min at 4°C and the supernatant was used as the source of enzyme.

Estimation

For measuring the activity, 3.0 ml of 0.05 M pyrogallol, 0.05 ml of enzyme extract was taken and mixed thoroughly. The tube was then inserted into colorimeter at 420 nm. After the colorimeter had been adjusted to show 10% optical density, 0.5 ml of 3% H₂O₂ was quickly added to the tube which was then inverted once immediately reinserted into the colorimeter. The change in optical density (O.D) between 30 and 150 sec at 420 nm was used to plot peroxidase activity [170]. A change in the absorption by 0.01 per min was accepted as a unit of activity. Results were expressed as unit of activity / g fresh tissue / min.

5.4.13. 7 Phenylalanine ammonia-lyase (PAL)

Extraction

To prepare the enzyme extract about 5 g of tissue (leaves) were homogenized in 1.5 ml of 0.05 M Tris-HCl buffer (pH 8.5) containing 1.4 mM 2-mercaptoethanol (100µl). The resulting slurry was filtered through two layers of cheese cloth. The filtrate was centrifuged at 15000 rpm for 15 min at 4°C. The resulting supernatant used as crude enzyme extract.

Estimation

The reaction mixture contained the following chemicals:

50 mM Tris-HCL (pH 8.8)	1 ml
20 mM l-phenyl alanine	0.5 ml
Enzyme extract	0.1 ml
H ₂ O	0.4 ml
Total	2 ml

The above mentioned reaction mixture was incubated for 60 min at 30°C. The reaction was stopped by the addition of 0.25 ml 2N HCL. The cinnamic acid formed by vigorous shaking was extracted in 2 ml toluene (This was done by vigorous shaking of the reaction mixture and toluene). The toluene layer was separated. One ml of the separated toluene layer was dried with a pinch of anhydrous sodium sulphate and taken in 1 ml cuvette. The specific activity of the enzyme was expressed as µ moles of cinnamic acid produced/min/mg of protein. The PAL enzyme activity was

assayed by measuring the appearance of *trans*-cinnamic acid in the optical density at 290 nm [171]. Standard curve was prepared with different concentrations of cinnamic acid for comparison.

5.4.13 .8 SDS-polyacrylamide gel electrophoresis of total soluble protein

Preparation of slab gel

Stock solutions

For the preparation of gel, the following stock solutions were initially prepared as described by Laemmli [172].

(A) Acrylamide and N, N'-methylenebisacrylamide

Acrylamide	29 g
N, N'-methylene bisacrylamide	1 g
Distilled water	100 ml

Solution was filtered and pH adjusted to 7.

(B) Sodium dodecyl sulphate

SDS	10 g
Distilled water	100 ml

(Stored at room temperature)

(C) Lower gel buffer (1.5 M Tris)

Tris	18.18 g
Distilled water	100 ml

pH was adjusted to 8.8

(D) Upper gel buffer (0.5 M Tris)

Tris	6.06 g
Distilled water	100 ml

pH was adjusted 6.8

(E) Ammonium per sulphate (APS)

Ammonium per sulphate	0.1 g
Distilled water (freshly prepared each time)	1.0 ml

(F) Tris-glycine electrophoresis buffer

(25 mM Tris Base : 250 mM glycine)

For 5 X Stock

Tris Base	15.1 g
Glycine	94 g

In 900 ml of distilled water, pH was adjusted to 8.3. Then 50 ml of 10% SDS was added and volume made upto 1000 ml.

(G) For 1 X SDS gel loading buffer :

50 mM Tris Cl (pH 6.8)

10 mM β -Mercaptoethanol

2% SDS

0.1% bromophenol blue

10% glycerol.

Slab gel preparation

For slab gel preparation, two glass plates (17 X 19cm) were washed with dehydrated alcohol and dried. Then 1 mm thick spacers were placed between the glass plates and the two edges along with two sides of glass plates were sealed with grease and gel sealing tape which were then kept in the gel casting unit. Resolving gel solution was prepared as follows:-

H ₂ O	11.9 ml
30% Acrylamide mix	10.0 ml
1.5 M Tris (pH-8.8)	7.5 ml
10% SDS	0.3 ml

10% APS	0.3 ml
TEMED	0.012 ml

The gel solution was cast very slowly and carefully up to a height of 12 cm by a syringe. The gel was over layered with water and kept for 2-3 h for polymerization. Then stacking gel solution was prepared as follows:

H ₂ O	6.8
30% Acrylamide mix	1.7 ml
1 M Tris (pH-6.8)	1.25
10% SDS	0.1 ml
10% APS	0.1 ml
TEMED	0.01 ml

After polymerization of resolving gel, overlay was decanted off and a 13 wall 1 mm thick comb was placed. Stacking gel solution was poured carefully up to a height of 4 cm over the resolving gel and overlaid with water. Finally the gel was kept for 30 min for polymerization.

Sample preparation

Sample was prepared by mixing the sample protein with 1 x SDS gel loading buffer (final volume 80µl). All the samples were floated in boiling water bath for 3 min. After cooling , upto 80µl of each sample was loaded in a predetermined order into the bottom of the wells with a micro liter syringe. Along with the samples, protein markers consisting of a mixture of six proteins ranging in molecular weight from 30 to 200 KD [Carbonic anhydrase – 29,000 , Albumin (egg) - 45,000 , Albumin (bovine) – 66,000 , Phosphorylase b - 97,400 , β - galactosidase – 166,000 .and Myosin – 205,000 ,] was treated as the other samples and loaded in a separate well.

Electrophoresis

Electrophoresis was performed at 25 mA for a period of 3 h until the dye front reached the bottom of the gel.

Fixing and Staining

For fixing the fixer solution was prepared as follows :

Glacial Acetic Acid	10 ml
Methanol	20 ml
Distilled water	70 ml

The entire gel was removed from the glass plates and then the stacking portion was cut off from the resolving gel. After that gel was soaked for 2 h in the fixer for fixing.

The staining solution was prepared as follows:

Coomassie Brilliant Blue R250	0.25 g
Methanol	45 ml
Distilled water	45 ml
Acetic Acid	10 ml

At first, gel were stained by staining solution for 2-3 h and finally soaked with destaining solution (Methanol:Distilled water: Acetic acid :: 4.5: 4.5:1) until the background become clear.

5.5 Result and Discussion

To evaluate the efficacy of different organotin compounds to be tested against foliar blight disease of wheat were initially screened at a range of three concentrations (25, 50 and 100 ppm) each for their possible fungitoxic effect on the spore germination and radial growth of *B. sorokiniana*. The compounds were categorized as Set I comprising of eight chemicals and Set II comprising of nine chemicals. The fungicide Propiconazole (Tilt) was kept as standard/check.

5.5.1 Set I:

Table 5.1: Effect of different organotin compounds on spore germination and growth of *B. sorokiniana*

Compound	Spore Germination %			Radial Growth of <i>B. sorokiniana</i> (cm)		
	Con. (ppm)			Con. (ppm)		
	25	50	100	25	50	100
1.	9.62	2.38	0	1.5	Nil	Nil
2.	4.44	4.14	0	Nil	Nil	Nil
3.	3.56	1.21	0	Nil	Nil	Nil
4.	10.73	3.55	1.17	1.2	Nil	Nil
5.	4.80	2.45	0	Nil	Nil	Nil
6.	8.14	4.74	3.51	1.1	Nil	Nil
7.	8.41	4.55	3.03	1.1	Nil	Nil
8.	5.12	4.44	0	Nil	Nil	Nil
Propiconazole (0.15 %)	12.36	-	-	-	1.6	-
Control (Water)	85.91	-	-	-	7.5	-
CD (P=0.05)	0.213	0.182	0.162	-	-	-

5.5.1.1 Effect of organotin compounds on spore germination and growth

It appears from Table 5.1 that all the compounds significantly inhibited the spore germination even at 25 ppm and the inhibition was more pronounced with the increase in concentration (Fig. 5.3 and Fig. 5.4). At 25 ppm compounds **2**, **3**, **5** and **8** exhibited spore germination in the range 3-5% whereas 85 % was recorded in case of water control. These compounds were more effective than propiconazole at the recommended dose of 0.15 %. The radial growth of *B. sorokiniana* was almost completely inhibited in all the compounds tested indicating that the newly synthesized organotin compounds are highly effective against *B. sorokiniana*.

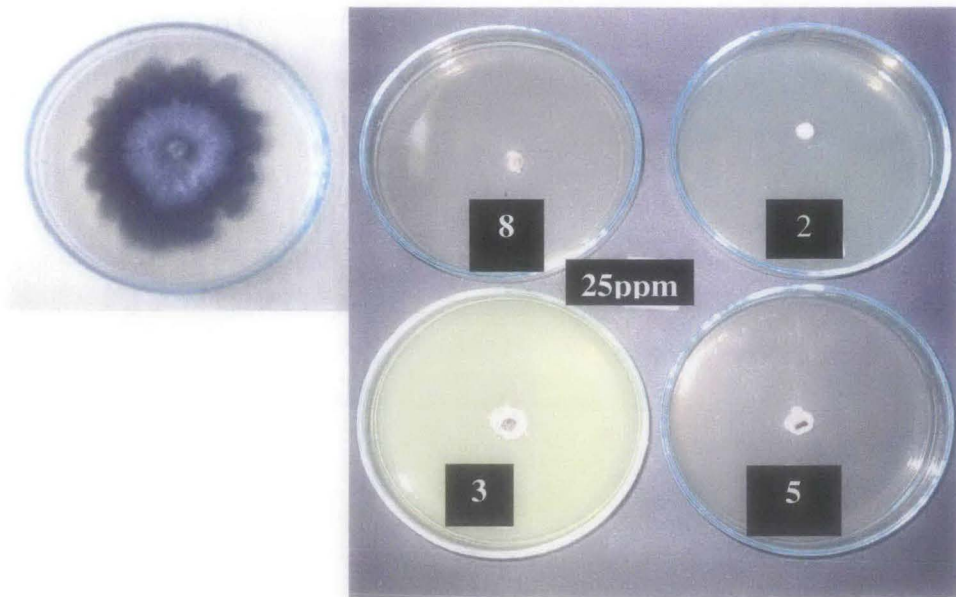


Fig. 5.3 Effects of test chemicals at 25 ppm on spore germination and growth of *B. sorokiniana* (control and treated).

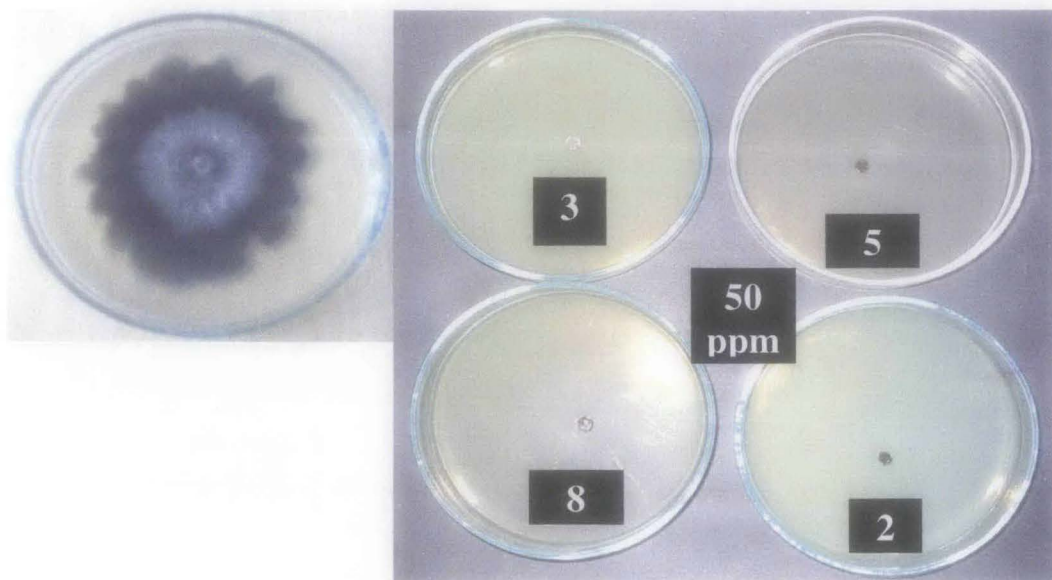


Fig. 5.4 Effects of test chemicals at 50 ppm on spore germination and growth of *B. sorokiniana* (control and treated).

5.5.1.2 Effect of organotin compounds on symptom expression and yield attributes in wheat plants

Eight organotin compounds have shown promise in the inhibition of spore germination of *B. sorokiniana* were further tested in field trials as well as detached wheat leaves by the methods described earlier for their effect on symptom expression and yield of wheat. The result is summarized in Table 5.2.

It appeared that susceptible plants in all the treatments showed very significant ($P=0.05$) differences in symptoms with the untreated plants both with excised wheat leaves and natural conditions as reflected by the reduced lesion area and AUDPC. As early as 72 h of inoculation, the lesion were fairly well developed in the untreated plants, those in different treatments showed only mild symptoms. Subsequently, symptom developments were distinctly higher in control, but in the treated plants 71% to 81% less symptoms than in the untreated plants were recorded. Among the different organotin compounds, **2**, **3**, **5** and **8** (Fig. 5.5) were more effective in reducing the disease symptoms. As recorded the average kernel weight (AKW), most of the treatments had little or no effect. The yield was also higher in the treated plants than in the untreated plants. The compounds, the most effective in reducing the disease symptom, also stimulated maximum yield of 46.7 Q/ha as that of the control which recorded 35.1 Q/ha (Fig. 5.6).



Fig. 5.5 A view of reduced disease symptoms compared to the control on excised wheat leaves by application of compounds **2,3,5** and **8**.



Healthy plants

Diseased plants

Fig. 5.6 A view of field trial for organotin treated healthy and control (untreated) diseased plant.

Table 5.2: Efficacy of different organotin compounds on excised wheat leaves (cv. Sonalika) as well as leaves under field condition challenged with against *B. sorokiniana*.

Compound	Con. (ppm)	Average lesion area in(cm)		Area under diseases progress curve	1000 kernel wt. (g)	Projected yield Q/ha
		After 72 h of inoculation	After 96 h of inoculation			
1.	50	0.80	0.92	191.35	37.9	37.407
2.	50	0.82	0.90	188.85	37.8	44.458
3.	50	0.70	0.75	145.54	38.5	46.777
4.	50	0.85	1.25	188.85	37.8	40.747
5	50	0.82	0.84	160.53	38.4	44.444
6	50	0.84	1.12	302.46	37.2	36.155
7.	50	0.85	1.21	332.71	37.4	37.252
8.	50	0.84	0.95	203.70	37.5	43.505
Propiconazole	0.15%	1.70	1.92	256.09	37.3	36.574
Control (water)	-	3.3	4.25	622.20	37.2	35.111
C.D.(P=0.05)	-	0.197	0.131	-	-	-

5.5.1.3 Studies on the biochemical changes associated with resistance in wheat plants

It has been observed that different organotin compounds cause substantial protection against *B. sorokiniana* infection that continued to active over a period. Such effect is presumed to be mediated through some sort of conditioning of host tissue leading to activated dynamic defense and this may be associated with significant alterations in host metabolism in response to treatment as well as to infection. This possibility was investigated in a series of biochemical studies aimed at determining the nature of changes that occurred in susceptible wheat plants cv. Sonalika. The areas of investigations include phenolics, proteins, polyphenol oxidase activity (PPO), peroxidase activity (PO), phenylalanine ammonia lyase activity (PAL), in healthy and infected tissues of cultivar Sonalika as influenced by organotin compounds.

Table 5.3: Effect of organotin compounds on phenol and OD-phenol contents in healthy and *B. sorokiniana* infected wheat leaves.

Compound	Phenol content (mg/g fresh tissue)						OD-phenol content (mg/g fresh tissue)					
	1 st Day		3 rd Day		7 th Day		1 st Day		3 rd Day		7 th Day	
	H	I	H	I	H	I	H	I	H	I	H	I
Water (Control)	4.43	4.48	5.14	4.51	4.81	3.31	0.223	0.228	0.224	0.221	0.224	0.187
Propiconazole	4.42	4.46	4.73	4.83	4.63	4.82	0.224	0.234	0.227	0.229	0.230	0.218
2.	4.90	5.05	4.20	5.15	4.41	5.10	0.223	0.236	0.227	0.240	0.229	0.235
3.	4.05	5.25	4.52	6.98	4.79	4.98	0.226	0.242	0.231	0.241	0.231	0.238
5.	4.45	5.13	4.18	5.96	4.45	5.67	0.224	0.233	0.230	0.236	0.230	0.235
8.	4.02	4.71	4.39	4.90	4.45	5.04	0.226	0.236	0.290	0.234	0.232	0.233
C.D. (P=0.05)	0.277		0.211		0.373		0.0094		0.0100		0.012	
H=Healthy, I= Inoculated												

5.5.1.3.1 Total phenols

Table 5.3 shows that inoculation resulted in a mild increase (5%) in phenol level in untreated leaves at 24h of inoculation but this effect rapidly decreased and infection resulted in small to perceptible fall (12-31%) in phenol level during the next 7 days. On the other hand, wheat leaves in different treatment recorded considerable increases in phenol level following inoculation at all three stages, 3-29% after 24 h, 11-52% after 72 h and 4-27% after 7 days. The final post-infection level of phenol in treated leaves was mostly significantly higher than that in the untreated plants. The wheat plants treated with propiconazole (Tilt) had moderate increases in phenol level at all stages of sampling but still fell slightly short of the levels in comparable organotin treated leaves.

5.5.5.3.2 Ortho-dihydroxy phenols

Treatment with organotin compounds either had no effect on the ortho-dihydroxyphenol level or caused only marginal to small increases in susceptible leaves (Table 5.3). In untreated susceptible leaves inoculation with *B. sorokiniana* resulted in a small increase (2%) in OD-phenol content, when sampled after 24 h, but at the later stages, between 3-7 day after inoculation, infected plants recorded moderate decreases (2-19%), the decline increasing with time. In different organotin compounds treatments, infection resulted in 4% to 7% increases in OD-phenol level within 24 h but the response gradually weakened with time. At all stages of sampling their post-infection levels were significantly higher than that in untreated plants. Among the different treatments, the different OD-phenol content is not statistically significant.

Table 5.4: Protein contents in wheat leave infected by *B. sorokiniana*

Compound	Protein Content (mg/g fresh tissue)					
	1 st Day		3 rd Day		7 th Day	
	H	I	H	I	H	I
Water (control)	21.95	19.65	22.40	15.85	21.35	12.45
Propiconazole	21.65	25.90	21.95	21.15	23.60	17.90
2.	22.55	25.45	24.25	22.40	23.60	18.65
3.	22.65	25.25	23.45	23.35	23.95	18.60
5.	23.35	24.40	23.10	21.00	23.20	18.95
8.	22.05	24.60	23.90	21.75	22.60	19.75
C.D. (P=0.05)	3.251		4.082		2.675	
H= Healthy , I= Inoculated						

5.5.1.3.3 Total protein

Results in Table 5.4 show that susceptible untreated plants responded to inoculation initially with a mild decrease (11%) in protein content but at the later stages this effect further declined and recorded 24% lower after 3 day and 41% lower than the normal level after 7 day of inoculation. Susceptible plants in different organotin compounds initially respond to inoculation with a very mild increase (4-12%) in protein content, but the stimulatory effect also weakened in them with time and practically disappeared within 3 day of inoculation and after 7 day, the protein content was reduced to 18-20% lower than the normal level. The treated plants always had higher post-infection levels of total protein as compared to the comparable untreated plants, the quantum of differences varying between 24 % and 31% after 24 h as well as 32% and 47% after 3 day and at the later stage of infection the differences became more pronounced recording 49-58% higher than untreated plants. The plants treated with propiconazole had similar protein content with organotin treated plants at all stages of sampling.

Preliminary studies on the extraction of protein through gel electrophoresis show the appearance of an additional band indicating the formation of lower molecular weight pathogen related protein.

Table 5.5: Activity of peroxidase and polyphenoloxidase enzymes on wheat leaves infected by *B. sorokiniana*

Compound	Peroxidase (unit of activity/g fresh tissue/min)						Polyphenoloxidase (unit of activity/g fresh tissue/min)					
	1 st Day		3 rd Day		7 th Day		1 st Day		3 rd Day		7 th Day	
	H	I	H	I	H	I	H	I	H	I	H	I
Water (control)	70.5	90.0	69.0	87.5	72.0	83.5	0.080	0.100	0.085	0.060	0.080	0.040
Propiconazole	70.0	89.5	71.0	94.5	70.5	86.0	0.085	0.110	0.095	0.850	0.075	0.065
2.	70.5	94.5	68.0	100.5	71.0	93.0	0.080	0.120	0.090	0.115	0.095	0.105
3.	70.0	93.5	72.0	100.0	69.5	91.0	0.085	0.120	0.085	0.120	0.090	0.105
5.	71.0	91.5	70.5	101.0	72.0	93.5	0.080	0.120	0.085	0.110	0.085	0.105
8.	72.0	93.5	71.0	99.5	71.0	91.0	0.085	0.115	0.080	0.120	0.085	0.115
C.D. (P= 0.05)	7.51		9.08		8.30		0.0292		0.0299		0.0293	
H = Healthy, I = Inoculated												

5.5.1.3.4 Peroxidase activity

It will be seen from Table 5.5 that the untreated susceptible plants responded to inoculation with considerable increases in (26-28%) enzyme activity between 1 and 3 days after inoculation, but during the next 4 days, the stimulated activity strongly declined to almost normal. The treated plants, responded to inoculation with pronounced increases, 30% to 33% after 24h and 43% to 47% after 3 days. Though this treatment induced effect declined with time, still after 7 days i.e. at the late stage of infection, 29% to 31% higher levels could be noticed. All the treatments recorded significantly higher post-infection levels of peroxidase activity. Though maximum effect of treatments mostly occurred within 3 days of inoculation, generally the peak period for pathogenic activity still significant effects persisted even at the late stage of infection.

5.5.1.3.5 Polyphenoloxidase activity

Treated susceptible plants recorded very mild increases in the level of polyphenoloxidase activity than the untreated plants at different stages of sampling (Table 5.5). Following inoculation, polyphenoloxidase activity appreciably (by 25%)

increased in untreated susceptible leaves after 24h, however, this effect sharply declined during the 7 days, to much lower values than normal level. At every stage of sampling, susceptible plants in different treatments responded to inoculation with greater increases in enzyme activity, as much as 22% to 50% after 24h, 29% to 41% after 3 days and 10% to 35% after 7 days. Their post-infection levels were also much higher than in the untreated plants.

5.5.2 Set II

The nine organotin chemicals (1-9), screened for their possible effect in controlling foliar blight disease in wheat, were also tested for their effect *in vitro* on spore germination and radial growth of the pathogen, *B. sorokiniana*. Three concentration of each chemicals were tested for such assay in germination of spore kept in grove slide.

It appears that all nine chemicals were highly toxic to the pathogen at all three concentrations tested i.e. 25, 50 and 100 ppm (Table 5.1). Among the nine chemicals, compound 2 and 3 significantly inhibited the spore germination and radial growth of *B. sorokiniana* at 50 ppm (Fig. 5.7).



Fig. 5.7 Effects of test chemicals at 50 ppm on spore germination and growth of *B. sorokiniana* (control and treated).

5.5.2.1 Effect of chemicals on *B. sorokiniana* in wheat

As a follow up of the results just described in Table 5.6, all the nine chemicals having significant inhibitory effects on spore germination and its growth were further tested for their possible effect on disease symptom inhibition on excised wheat leaves. Here only 50 ppm concentration of each chemical was selected. The results are shown in Table 5.7.

Susceptible plants in all the treatments showed very significant difference in symptoms with untreated plants as early as 72 h of inoculation (Table 5.2). Subsequently, symptom development was distinctly slower in the treated plants, so that after 96 h of inoculation these had very large difference in symptoms with control plants. Different treatments reduced disease symptoms by 54% to 83%. Best results were achieved with compounds 2 and 3, even much better their standard fungicide, propiconazole.

Table 5.6: Effect of the test chemicals on spore germination and growth of *B. sorokiniana*

Compound	Spore germination(%)			Radial growth of <i>B. sorokiniana</i> (cm)		
	Con. (ppm)			Con. (ppm)		
	25	50	100	25	50	100
1.	4.44	2.38	0	Nil	Nil	Nil
2.	3.78	1.49	0	Nil	Nil	Nil
3.	3.21	1.21	0	Nil	Nil	Nil
4.	4.8	2.91	0.96	Nil	Nil	Nil
5.	3.56	2.45	0	Nil	Nil	Nil
6.	9.62	4.44	0.91	1.5	Negligible	Nil
7.	4.12	2.72	0	Nil	Nil	Nil
8.	4.82	2.72	0	Nil	Nil	Nil
9.	8.14	5.32	1.20	Negligible	Negligible	Nil
Propiconazole (0.15%)	12.06	-	-	1.6	-	-
Control (Water)	87.81	-	-	7.5	-	-
C.D.(P=0.05)	0.285	0.364	0.226	-	-	-

Table 5.7 Efficacy of organotin compounds on excised wheat leaves (cv. Sonalika) infected by *B. sorokiniana*.

Compound	Con. (ppm)	Av. lesion area (cm)	
		After 72 h of inoculation	After 96 h of inoculation
1	50	0.74	0.79
2.	50	0.71	0.75
3.	50	0.67	0.70
4.	50	0.85	0.90
5.	50	0.79	0.82
6.	50	0.90	1.35
7.	50	0.75	0.81
8.	50	0.80	0.93
9.	50	0.85	1.21
Propiconazole	0.15 %	1.70	1.92
Control (Water)	-	3.3	4.25
C.D.(P=0.05)		0.1229	0.0823

5.5.2.2 Biochemical changes associated with resistance in the wheat plant (cv Sonalika) after infection

Results of *in vitro* and *in vivo* experiment on the effect of organotin chemicals on foliar blight infection of wheat plants appeared to be promising. So it became of some interest to investigate if there is any correlation between post-infection biochemical changes in the treated plants and the resistance induced in them. It was decided in this connection to investigate host responses in respect of total phenol, ortho-dihydroxyphenol and protein content and polyphenoloxidase and peroxidase activities, parameters that have often been found to be associated with expression of disease resistance in plants. For these purpose leaf materials were collected from diseased plants in the control plants and those with 9 compounds with standard check, propiconazole after 24h, 72h and 7 days of inoculation. Results were described in below

Table 5.8 Effect of test organotin compounds on phenol and OD-phenol contents in wheat leaves (cv. Sonalika) infected by *B. sorokiniana*

Compound	Phenol content (mg/ g fresh tissue)			OD-phenol content(mg/g fresh tissue)		
	1 st Day	3 rd Day	7 th Day	1 st Day	3 rd Day	7 th Day
1.	5.98	6.12	5.04	0.210	0.221	0.167
2.	5.25	5.70	4.79	0.239	0.246	0.155
3.	6.09	6.22	5.41	0.278	0.289	0.187
4.	5.09	5.54	3.67	0.232	0.243	0.142
5.	5.72	5.80	4.25	0.222	0.228	0.178
6.	4.97	4.29	3.39	0.192	0.198	0.111
7.	4.89	5.02	4.31	0.240	0.248	0.172
8.	4.55	4.89	4.33	0.203	0.212	0.142
9.	4.87	4.99	3.37	0.198	0.207	0.131
Propiconazole	4.42	4.52	3.34	0.183	0.196	0.112
Control (Water)	4.33	4.02	2.78	0.177	0.173	0.040
C.D.(P=0.05)	0.096	0.145	0.127	0.013	0.009	0.009

5.5.2.2.1 Total phenol

It seen in Table 5.8 that infected susceptible wheat plants in all the treatments recorded higher (5% to 40%) total phenol levels as compared to the untreated plants after 24 hr. of inoculation. After 3 days of inoculation, the phenol level further increased in the treated plants but at the later stage of infection, this effect somewhat declined. The final post-infection levels in different treatments were 6% to 59% higher after 3 days and 32% to 44% higher after 7 days of inoculation as compared to the control plants. Plants treated with compound **3** that provided maximum protection also recorded maximum increase in the phenol level followed closely by compound **1** and **2**.

5.5.2.2.2 Ortho-dihydroxyphenol

The trend for Ortho-dihydroxyphenol was nearly similar to that for total phenol. All the treatments lead to appreciable increase, 8% to 57% after 24 h, 14% to 67% after 3 days and 177% to 367% after 7 days of inoculation. The correlation between the increase in OD phenol content and resistance was good but no absolute.

Table 5.9 Effect of different organotin compounds on peroxidase and polyphenol oxidase activity in *B. sorokiniana* infected wheat leaves (cv. Sonalika)

Compound	Peroxidase activity (unit of activity/g fresh tissue /min)			Polyphenoloxidase activity (unit of activity/g fresh tissue /min)		
	1 st Day	3 rd Day	7 th Day	1 st Day	3 rd Day	7 th Day
1.	73.7	74.0	71.8	0.94	1.00	0.90
2.	73.4	74.0	72.2	1.02	1.05	0.96
3.	76.0	80.3	74.0	0.98	1.1	0.97
4.	72.5	73.0	71.6	0.95	0.99	0.90
5.	77.5	79.4	74.0	1.00	1.01	0.92
6.	71.1	72.0	69.0	0.89	0.88	0.82
7.	75.0	77.4	72.8	1.02	1.04	0.92
8.	75.0	77.2	72.9	0.96	1.03	0.90
9.	73.6	74.0	70.0	0.93	0.95	0.85
Propiconazole	64.2	68.2	62.2	0.90	0.94	0.82
Control (Water)	72.4	62.2	50.0	0.88	0.70	0.55
C.D.(P=0.05)	1.251	0.959	1.189	0.119	0.138	0.102

5.5.2.2.3 Peroxidase activity

Table 5.9 indicates that plants in all the treatments recorded moderately higher peroxidase than untreated plants after 24 h and after 3 and 7 days were quite high after 3 and 7 days of inoculation. Though all the treatments recorded significantly higher post infection level of peroxidase activity, the more effective compounds like 2, 3 and 5 recorded higher level of enzyme activity than less effective compounds, though the difference are not always significant (P =0.05).

5.5.2.2.4 Polyphenoloxidase activity

Following infection, the polyphenoloxidase activity was sharply declined with age in the untreated plants whereas the plants in all the treatments respond to inoculation with greater increase in enzyme activity. The final post-infection level varying between 2% to 15% after 24 h 25% to 57% after 3 days and 49% to 74% after 7 days. The maximum increase in the enzyme activity in all respect were recorded with the compound **3**, the most effective compound. Plants treated with propiconazole had intermediate effect in enzyme activity.

Table 5.10 Effect of organotin compounds on protein contents in *B. sorokiniana* infected wheat leaves cv. Sonalika.

Compound	Protein content (mg/ g fresh tissue)		
	1 st Day	3 rd Day	7 th Day
1.	20.32	17.96	12.57
2.	25.37	20.62	13.48
3.	25.54	20.66	13.57
4.	23.49	20.21	12.92
5.	21.31	18.71	12.91
6.	18.63	15.24	11.34
7.	20.66	17.95	12.04
8.	24.71	20.32	13.57
9.	22.01	18.63	12.73
Propiconazole	20.17	17.12	11.87
Control (Water)	16.94	12.57	5.39
C.D. (P=0.05)	0.148	0.124	0.146

5.5.2.2.5 Total protein

All nine treatments recorded higher post-infection protein level than the untreated plants (Table 5.10). All the initial stages of inoculation the protein content were higher in the treated plants but with the time the level gradually decreased in these plants. The final post-infectional levels were appreciably higher than that of

untreated plants and with time this difference became more pronounced after 7 days of inoculation.

5.5.3 Phenylalanine ammonia lyase activity

It has been clearly established that in the early experiments the degree of resistance was correlated with an increased biosynthesis of phenolics and stimulated oxidase activity at and around the site of host-pathogen interaction. It is well known that phenyl alanine ammonia lyase (PAL) activity is the first enzyme of the phenyl propanoid pathway and considered as the key enzyme in the regulation of the flux of the phenylpropanoid compounds such as lignin and their derivatives [173] and also appeared to be associated with hypersensitive reaction [174]. The PAL activity was measured in ten compounds that provided strong resistance against foliar blight pathogen excluding propiconazole after inoculation with *B.sorokiniana* and the results are presented in Table- 5.11

The PAL activity in the organotin compounds treated plants were always higher than untreated plants. A strong correlation were observed between resistance induced by the compounds and PAL activity mild variation.

Table 5.11 Effect of different organotin compounds on phenylalanine ammonia lyase activity in *B. sorokiniana* infected wheat leaves (cv. Sonalika)

Compound		PAL activity (μg cinnamic acid released/g/min)	
		24 h after inoculation	72 h after Inoculation
Set I:	2.	372.8	352.2
	3.	365.5	344.7
	5.	361.5	329.1
	8.	370.1	347.1
Set II:	1.	353.0	334.3
	2.	365.8	340.1
	3.	346.0	338.4
	5.	357.1	340.0
	7.	354.9	333.5
	9.	349.7	351.7
Propiconazole		329.9	315.2
Water (Control)		315.7	288.6

5.5.4 Effect of organotin compounds on seedling growth of wheat

The newly synthesized organotin compounds were further tested for their phytotoxic effect if any, on seed and its growth. For this purpose wheat seeds of Sonalika cultivar were tested with organotin compounds in set I and set II at 50 ppm concentration for 6 h and placed in the petridishes covered with moist blotter separately. The seed germination percentage was recovered after 72 h of treatments and root as well as shoot length were recorded after 7 days of treatment (Fig. 5.8). The results were presented in the Table 5.11



Fig. 5.8 Effect of organotin compounds on seedling growth.

Table 5.11: Effect of seed treatment with organotin compounds on seedling vigor of wheat (cv. Sonalika)

Set	Compound No.	Seed germination (%) ¹	Root length (cm)	Shoot length (cm)
I	1.	95.7	3.10	4.30
	2.	95.4	3.27	5.09
	3.	96.3	3.30	5.19
	4.	81.9	2.20	4.90
	5.	86.4	3.25	5.16
	6.	86.4	2.46	4.65
	7.	86.2	3.10	4.97
	8.	95.2	3.35	5.12
II	1.	92.4	3.16	5.02
	2.	94.5	3.21	5.15
	3.	93.2	3.23	5.21
	4.	87.5	3.02	4.95
	5.	83.4	2.94	4.72
	6.	88.6	2.74	4.62
	7.	89.5	2.85	4.75
	8.	89.5	3.01	4.99
	9.	83.4	2.92	5.01
	Control (Water)	95.5	3.32	5.27

¹Seed germination percentage was recorded after 72 h. Root and shoot length were recorded after 7 days.

It appears that the compounds shown effective against *B. sorokiniana* were also fungitoxic to *Alternaria triticina* and *Fusarium solani*. Among chemicals **2**, **3**, **5** and **8** in set I and **3**, **4**, **5** in set II almost completely inhibited spore germination of *Alternaria triticina* than other chemicals. These chemicals also inhibited spore germination of *Fusarium solani*. Though the extent of inhibition is slightly less, From the above result, it may be concluded that the newly synthesized organotin compounds have promise for the control of *Alternaria triticina* and *Fusarium solani* also.

It will be seen from the Table 5.11 that most of the compound either had no adverse or little effect on seed germination and its subsequent growth. Compounds like 4, 5, 6 and 7 in set I and 4, 5, 6, 7, 8 and 9 in set II caused mild inhibition of germination, recording 81-89% as compared to untreated check, recording 95% seed germination. Regarding root and shoot length, the result showed the same trend. No inhibition of seed germination was recorded with other chemicals like 1, 2, 3, 8 in set I and 1, 2, 3 in set II even some chemical stimulated seed germination and its growth.

5.5.5 Effect of organotin compounds on *Alternaria titricina* and *Fusarium solani*

The compounds were further tested for their fungicidal effect on spore germination of *Alternaria titricina* and *Fusarium solani*, the two major pathogen of wheat in this agroclimatic region. For this purpose, seventeen chemicals found effective against *B. sorokiniana* were tested at 50 ppm concentration for their effect *in vitro* on spore germination tests and results were shown in Table 5.12

Table 5.12 Effect of organotin compounds on spore germination of *Alternaria titricina* and *Fusarium solani*

Set	Compound (50ppm)	Spore germination (%)	
		<i>Alternaria titricina</i>	<i>Fusarium solani</i>
I	1.	4.2	2.8
	2.	0	1.7
	3.	0	3.1
	4.	2.5	4.7
	5.	1.6	1.3
	6.	9.2	11.2
	7.	7.5	9.2
	8.	1.2	8
II	1.	3.1	5.1
	2.	2.7	7.5
	3.	0	6.2
	4.	1.2	8.5
	5.	0	7.5
	6.	2.1	4.6
	7.	7.5	8.9
	8.	6.4	10.6
	9.	8.2	12.5
	Control (Water)	85.2	89.6
CD (P= 0.05)		3.25	2.98

Results from various studies involving wheat-*B. sorokiniana* combination, clearly established the fact that newly synthesized organotin compounds have the potential for inducing significant level of resistance in wheat plants against foliar blight pathogen. The results of *in vitro* fungitoxicity assay make it clear that the compounds directly suppressed the pathogen. These compounds acted through host mediated response. Supports for this view came from the studies in the biochemical changes in the host following treatment with the compounds. As a result of the treatment induced change in the host metabolites involving significant change in the phenolics, proteins and substantial increase in the PO and PPO activities.

The biochemical basis of resistance of plants to fungal pathogen have been associated with infection induced antimicrobial compounds [175]. At present a large amount of information has accumulated on the possible role of phenolics in disease resistance. Matern and Kneusel [141] proposed rapid synthesis of phenolics following infection to be an important first line defense in the plants. The present investigation showed that organotin compounds enhance the biosynthesis of phenolics.

Changes in the host physiology following infection is often associated with an activation of oxidase activity and a post-infectional increase in the level of such enzyme is a common phenomena in the diseased tissue more so is an incompatible interaction. Activation of polyphenol oxidase activity would seem to be more important as it can oxidize phenolics to quinines which may be more fungitoxic [176]. In the present investigation increased polyphenol oxidase activity was associated with the resistance induced by the test chemicals. Present reports agree with the earlier reports on the association of stimulated PPO activity against *B. sorokiniana* [22].

Response of both untreated and variously treated plants in respect of PO activity followed almost the same trend as reported for PPO. Increased PO activity in response to infection is a common phenomena in many host parasitic interactions and the greater activity is generally linked with resistance response. The role of PO plant defense has been attributed to its PO activity to catalyse various types of oxidative reactions important in metabolism of pathogens or of the host plant such as phenolics, toxins, hormones etc. [177]. Increase activity of PPO, the terminal enzyme in phenyle propanoid pathway, appears to be associated with an increased synthesis and deposition of lignin at the site of infection [178].

In the present investigation, it has been clearly established that resistant plants have less disease against *Bipolaris sorokiniana* infection as such resistance are mostly correlated with an increased biosynthesis of phenolics and stimulated oxydase activity at and around the site of host-pathogen interaction. It is well known that phenylalanine ammonia lyase is the first enzyme of the phenyl propanoid pathway and considered as the key enzyme in the regulation of the flux of the phenyl propanoid compounds such as lignin and their derivatives and also appeared to be associated with hypersensitive reaction. In the present study, the resistant plants always had a higher PAL and peroxidase activities in comparison to susceptible

genotypes. The increased peroxidase activity is presumed to be associated with enhanced lignifications and also for production of phytoalexins.

Plants are known to respond to infection with both quantitative and qualitative changes in their protein content. In the present investigation, it was noticed that protein content increased initially in the infected tissue in treated and untreated plants due to infection by *B. sorokiniana*, though in case of treated plants it is more than that of untreated Sonalika cultivar. Synthesis of new protein in resistant cultivar following fungal infection has been reported in rice, wheat, tobacco and some other plants [147,179].

In summing up, the series of observation on foliar blight of wheat, it may be concluded that the newly synthesized organotin compounds act both directly and indirectly by conditioning the susceptible plant towards induced resistance through series of changes in the host metabolism bringing about activation and strengthening of the host innate defense potential so that the pathogen or its pathogenic activity or both are suppressed. Initial studies also indicate that these chemicals are fungitoxic to other pathogens like *Alternaria triticina* incident of air borne leaf blight disease and *Fusarium solani* incident of soil borne foot rot disease in wheat, which is very significant.

5.6 References

1. Nepal. In: Wheat in Heat Stressed Environments: Irrigated, Dry Areas and Rice – Wheat Farming Systems Ed. Saunders DA, Hettel GP. Mexico, D F CIMMYT. 1991; Anonymous. Annual Report of All India Coordinated research project on wheat and barley, ICAR, 2009.
2. Prescott LM, Harley JP, Klein DA. Microbiology. 6th Ed. McGraw-Hill Co., New York. 2005.
3. Dubin HJ, Bimb HP. Effects of soil and foliar treatments on yield and diseases of wheat in lowland 484.
4. Dubin H J, van Ginkel M. The status of wheat diseases and disease and disease research in the warmer areas. Proc. Of the Wheat for Non-traditional Warm Areas Conference, Foz de Iguazu, Brail, 1990; Ed. Saunders DA. UNDP/CIMMYT, Mexico.1991; 125.
5. Duveiller E, Gilchrist L. 1994. Productions constraints due to *Bipolaris sorokiniana* in wheat: Current situation and future prospects. In: *Proc. Of the Wheat in the Warmer Areas, Rice/Wheat Systems*. Ed. Saunders DA, Hettel. GP. CIMMYT/UNDP, Nashipur. (Dinajpur). Bangladesh, Feb 13-16, 1993; 343.
6. Saari EE. Leaf blight diseases and associated soil borne pathogens of wheat in south and South East Asia, In: *Helminthosporium Blights of Wheat: Spot blotch and Tan spot*. (Eds. E. Duveiller, H. J. Dubin, J. Reeves and A. McNab), CIMMYT, D.F.: Mexico, 1998; 37.
7. Dubin HJ, Duveiller E. Helminthosporium leaf blights of wheat: integrated control and prospects for the future :Proceedings of the International Conference on Integrated Plant Disease Management for Sustainable agriculture. Indian Phytopathological Society, New Delhi, India, 2000; 575.
8. Duveiller E. Helminthosporium blight of wheat: challenges and strategies for a better disease control. In *Advances of wheat breeding in china*. China Science and Technology Press, Jinan, Shandong, Peoples Republic of China. 2002; 57.
9. Asad S, Iftikhar S, Munir A, Ahmad I. *Pak. J. Bot.* 2009; **41**: 301.
10. Prescott JM, Burnett PA, Saari EE, Ransom J, Bowman J, Milliano W de, Singh RP, Bekele G. *Wheat Disease and Pests: A Guide for Field Identification*. Mexico, D.F.: CIMMYT. 1986; 135.
11. Mathur SB, Cunfer BM. Ed. *Seed-Borne diseases and Seed Health Testing of Wheat*. Danish Government Institute Seed Pathology for Developing Countries. Copenhagen, Denmark. 1993; 168.
12. Joshi LM, Srivastava KD, Singh DV, Goel LB, Nagrajan S. *Annotated Compendium of Wheat Diseases in India*. ICAR, New Delhi, India.1978; 332.
13. Nema KG..Foliar diseases of wheat- leaf spots and blights. In : L. M. Joshi, D. V. *Problems and progress of wheat pathology in South Asia*, 162. New Delhi: Malhotra publishing House. 1986; 401.
14. Sharma, R. C., Dubin, H. J., Devkota, R. N., and Bhatta, M. R. *Plant Breeding*.1996; **116**: 64.
15. Alam KB, Shaheed MA, Ahmed AU, Malaker PK. *Bipolaris* leaf blight (spot blotch) of wheat in Bangladesh. In: Saunders DA, Hettel GP, Ed. *Wheat in Heat - stressed Environments: Irrigated, Dry Areas and Rice – Wheat Farming Systems*, Mexico, DF CIMMYT. 1994; 339.
16. Sharma S. 1996 Wheat diseases in western hills of Nepal. In: proceedings of the national Winter- Crops Technology Workshop. 1995; 339.

17. Hafiz A. *Plant Diseases*. Islamabad: Pakistan Agricultural Research Council. 1986; 552.
18. Prasada R, Prabhu AS. *Indian Phytopath.* 1962; **15**: 292.
19. Mehta YR. Constraints on the integrated management of spot blotch of wheat. In: *Helminthosporium Blights of Wheat: Spot Blotch and Tan Spot* (Duveiller, E., Dubin, H.J., Reeves, J. and McNab A., eds). Mexico, D.F., Mexico: CIMMYT. 1998; 18.
20. Singh DV, Srivastava KD. Foliar blights and *Fusarium* scab of wheat: Present status and strategies for management. In: *Management of threatening plant disease of national importance*, Malhotra Publishing House, New Delhi. 1997; 1.
21. Chowdhury AK, Garain PK, Mukharjee S, Datta S, Bhattacharya PM, Singh DP, Singh G. *J. Mycopathol. Res.* 2005; **43**: 139.
22. Chowdhury AK, Mukherjee S, Bandyopadhyaya S, Das J, Mondal NC. *J. Mycopathol. Res.* 2008; **46**: 59.
23. Crowe AJ, *Appl. Organomet. Chem.* 1987; **1**: 143.
24. Pellerito L, Nagy L. *Coord. Rev.* 2002; **224**: 111.
25. Basu Baul TS. *Appl. Organomet. Chem.* 2008; **22**: 195.
26. Parakhia AM, Vaishnav MU, Pandya, NK. *Indian J. Plant Prof.* 1980; **8**: 62.
27. Singh M, Shukla TN. *Pesticides.* 1985; **19**: 72.
28. Reddi MK, Mohan RC. *Pesticides.* 1984; **18**: 51.
29. Das CM, Mahanta IC. *Pesticides.* 1985; **19**: 37.
30. Lal S, Nath K, Saxena SC. *Trop. Pest Manage.* 1980; **26**: 286.
31. Anilkumar TB, Gowda KTP. *Pesticides.* 1984; **18**: 43.
32. Rai RC, Singh A. *Seed Res.* 1979; **7**: 186.
33. Singh A, Virk SK. *Ind. J. Mycol. Plant Pathol.* 1980; **10**: 115.
34. Yadav RKS, Agnihotri JP, Prasada. R. *Indian Phytopathol.* 1980; **33**: 16.
35. Raju CA, Singh RA. *Pesticides.* 1981; **15**: 26.
36. Ramaiah KS, Sastry MNL. *Mysore J. Agric. Sci.* 1983; **17**: 141.
37. Naidu PH, Mukhopadhyay AN. *Pesticides.* 1982; **16**: 20.
38. Srivastava TN, Sengupta AK, Jain SP. *J. Antibact. Antifung. Agents* 1981; **9**: 285.
39. Sengupta AK, Anurag A. *Ind. J. Chem. Sect. B.* 1983; **22B**: 263.
40. Srivastava TN, Sengupta AK, Jain SP. *Ind. J. Chem. Sect. A.* 1982; **21A**: 384.
41. Kamruddin SK, Chattopadhyaya TK, Roy A, Tiekink ERT. *Appl. Organomet. Chem.* 1996; **10**: 513.
42. Chakrabarty A, Kamruddin SK, Chattopadhyaya TK, Roy A, Chakraborty BN, Molloy KC, Tiekink ERT. *Appl. Organomet. Chem.* 1995; **9**: 357.
43. Sen Sarma M, Mazumder S, Ghosh D, Roy A, Duthie A, Tiekink ERT. *Appl. Organomet. Chem.* 2007; **21**: 890.
44. Tian L, Zhou Z, Zhao B, Sun H, Yu W, Yang P. *Synth. React. Inorg. Met. -Org. Chem.* 2000; **30**: 307.
45. Singh HL, Sharma M, Varshney AK. *Synth. React. Inorg. Met. -Org. Chem.* 2000; **30**: 445.
46. Blunden SJ, Cusack PA, Hill R. The Royal Society of Chemistry, London. 1985.
47. Molloy KC, Hartley FR. Ed. *The Chemistry of metal-carbon bond: Bioorganotin Compounds*, John Willey, New York, 1989.
48. Davies AG, Smith PJ. The synthesis, reactions and structure of organometallic compounds. In *Comprehensive Organometallic Chemistry*, Pergamon Press, New York. 1982.

49. Willem R, Biesemans M, Boualam M, Delmotto A, Ei-Khloufi A, Gielen M. *Appl. Organomet. Chem.* 1993; **7**: 311.
50. Rehman W, Baloch MK, Muhammad B, Badshah A, Khan KM. *Chin. Sci. Bull.* 2004; **49**: 119.
51. Godwin AA, Josiah JB, Shettima SA, Philip FO, Joseph OE, Serge K, Stephen Y. *Appl. Organomet. Chem.* 2003; **17**: 749.
52. Ng SW, Kuthubutheen AJ, Kumar Das VG, Linden A, Tickink ERT. *Appl. Organomet. Chem.* 1994; **8**: 37.
53. James BD, Gioskos S, Chandra RJ, Magee JD, Cashion J. *J. Organomet. Chem.* 1992; **436**: 155.
54. Eng G, Whalen YZ, Zhang A, Kirksey M, Otieno LE, Khoo T, James BD. *Appl. Organomet. Chem.* 1996; **10**: 501.
55. Eng G, Whalen D, Musingarimi P, Tierney J, DeRoss M. *Appl. Organomet. Chem.* 1998; **12**: 25.
56. Chandra S, Gioskos S, James BD, Macauley BJ, Magee RJ. *J. Chem. Tech. Biotechnol.* 1993; **56**: 41.
57. Kalsoom A, Mazhar M, Ali S, Mahon MF, Mollloy KC, Chaudhary MI. *Appl. Organomet. Chem.* 1997; **11**: 47.
58. Wharf I, Lamparski H, Reeleder R. *Appl. Organomet. Chem.* 1997; **11**: 969.
59. Srivastava TN, Kumar V, Srivastava OP. *Natl. Acad. Sci. Lett (India)*. 1978; **1**: 97.
60. Shahzadi S, Ali S, Wurst K, Najam-ul-Haq M. *Heteroatom Chem.* 2006; **18**: 664.
61. Shahzadi S, Ali S, Bhatti MH, Fettouhi M, Athar M. *J. Organomet. Chem.* 2006; **691**: 1797.
62. Shahzadi S, Ahmad SU, Ali S, Yaqub S, Ahmed F. *J. Iranian Chem. Soc.* 2006; **3**: 38.
63. Chaudhary A, Agarwal M, Singh RV. *Appl. Organometal. Chem.* 2006; **20**: 295.
64. Koopmans MJ. *Dutch Patent*, 96 805, 16 January 1961; *Chem. Abstr.* **55**: 27756f.
65. Kochkin DA, Verenikina SG. *Tr. Vses. Nauchn.-Issled. Vitamin. Inst.* 1961; **8**: 39.
66. Kochkin DA, Verenikina SG, Chekmareva IB. *Dokl. Akad. Nauk S.S.S.R.* 1961; **139**: 1375.
67. Brückner H, Hartel K. *German Patent*, 1 061 561, 16 July 1959; *Chem. Abstr.* **55**: 6772d.
68. Nath M, Yadav R. *Bull. Chem. Soc. Jpn.* 1998; **71**: 1355.
69. Nath M, Yadav R, Eng G, Musingarimi P. *J. Chem. Res.* 1998; **409**: 1730.
70. Nath M, Yadav R, Eng G, Musingarimi P. *Appl. Organometal. Chem.* 1999; **13**: 29.
71. Nath M, Goyal S. *Metal-Based Drugs* 1995; **2**: 297.
72. Nath M, Goyal S, Eng G, Whalen D. *Bull. Chem. Soc. Jpn.* 1996; **69**: 605.
73. Kuch TK, Khew KL. *Malays. Agric. J.* 1980; **52**: 263.
74. Cheah LH, Corbin JB, Hartil WFT. *N.Z.J. Agril Res.* 1981; **24**: 391.
75. Ramos RS, Issa E, Sinigaglia C, Chiba S. *Biologica.* 1984; **50**: 97.
76. Oladiran AO. *Trop. Pest Manage.* 1980; **26**: 396.
77. Schneider CL, Potter HS. *J. Amer. Soc. Sugar Beet Technol.* 1983; **22**: 54.
78. Rolim PRR, Oliveria DA. *Arg. Inst. Biol. Sao Paulo.* 1982; **49**: 37.
79. Large FC. *Ann. Rev. Phytopath.* 1966; **4**: 9.
80. Grainger JP. Economic aspects of crop losses caused by diseases. Food and Agriculture Organization Symposium on Crop Losses. Rome, 1967.
81. James WC. *Ann. Rev. Phytopathol.* 1974; **12**: 27.

82. James WC, Teng PS. The quantification of production constraints associated with plant diseases. Ed. Coaker TH. Academic Press, New York, *Appl. Biol.* 1979; **4**:201.
83. Teng PS. Ed. Crop loss assesment and pest management. American Phytopathological Society, St. Paul. 1987; 270.
84. Atwal AS, Singh B. Pest population and Assessment of crop losses. ICAR, New Delhi-12. 1990; 131.
85. Duveiller E, Garcia I, Franco J, Toledo J, Crossa J, Lopez F. Evaluating spot blotch resistance of wheat: Improving disease assessment under controlled condition and in the field. In: *Helminthosporium Blights of Wheat: Spot Blotch and Tan Spot*, Ed. Duveiller E, Dubin HJ, Reeves J, McNab A. CIMMYT, Mexico, D.F. 1998; 171.
86. Osorio L, Garcia I, Lopez F, Duveiller E. Improving the control of tan spot caused *Pyrenophora tritici-repentis* in the Mixteca Alta of Oaxaca, Mexico. *Proc. Of the International Workshop on Helminthosporium Disease of Wheat: Spot Blotch and Tan spot*, (Eds. Duveiller, E, Dubin, HJ, Reeves J, McNab A). CIMMYT, El Batan, Feb. 9-14, 1997, Mexico.
87. Anonymous. Annual Report of All India Coordinated research project on wheat and barley, ICAR, 1997.
88. Pedretti R, Viedma LQ. Estrategia de la DIEAF-PARAGUAY para el Mejoramiento para Resiatencia a Enfermedades. In: Seminario sobre Mejoramiento Genetico sobre Resiatencia a Enfermedades de Trigo. Passo Fundo, PR, Brasil: IICA/PROCISUR/BID, 1988.
89. Viedma LQ. Importancia y distribucion de la fusariosis del trigo en el Paraguay. In: dialogo XIII, Royas de Cerales de invierno, PROCISUR, 1989; 153.
90. Bhatti MAR, Ilyas MB. Wheat diseases in Pakistan. In: Problems and progress of Wheat in South Asia. Ed. Joshi LM, Singh DV, Srivastava KD. New-Delhi, India. Malhotra publishing house. 1986; 20.
91. Ali S, Francel LJ, Iram S, Ahmad I. *Plant Disease*. 2001; **85**: 1031.
92. Iftikhar S, Shahzad A, Munir A, Iftikhar I, Amir S. *Pak. J. Bot.* 2006; **38**: 205.
93. Shrestha KK, Timila RD, Mahto BN, Bimb HP. Disease incidence and yield loss due to foliar blight of wheat in Nepal. *Helminthosporium* blight of wheat: apot blotch and tan spot. In: Proceedings of an International Workshop held at CIMMYT El Batan, Maxico. (Ed. Duveiller E, Dubin HJ, Reeves J, McNab A) 1997; 67.
94. Alam KB, Banu SP, Shaheed MA. The occurrence and Significance of spot blotch disease in Bangladesh. *Proc. Of the International workshop on helminthosporium Disease of wheat: spot Blotch and Tan spot*, Ed. Duveiller E, Dubin HJ, Reeves J, McNab A. CIMMYT, El Batan, Feb. 9-14, 1997, Mexico.
95. Razaque MA, Hossain ABS. The wheat development programme in Bangladesh. In: Wheat for the Non Traditional warm areas, DA. Saunders (ed.) Mexico, D. F.: CIMMYT, 199; 144.
96. Badaruddin M, Saunders DA, Siddique AB, Hossain MA, Ahmed MU, Rahman MM, Parveen S. Determining yield constrains for wheat Production In Bangladesh. In : Wheat in Heat -Stressed Environments: Irrigated, Dry Areas and Rice-Wheat Systems. Ed. Saunders DA, Hettle GP. Mexico, DF CIMMYT. 1994; 265.
97. Hossain I, Azad AK. 1992. *Prog. Agric.* 1992; **5(2)**: 63.
98. Devkota RN. Wheat Breeding objectives in Nepal: The National Testing system and Recent progress. Wheat in Heat stressed Environment: Irrigated, dry area

- and rice wheat farming systems. Ed. Saunders DA, Hettel GP. Mexico CIMMYT. 1993; 216.
99. Chenulu VV, Singh A. *Indian Phytopath.* 1967; **17**: 256.
 100. Nema KG, Joshi LM. The spot blotch disease of wheat caused by *Hilminthosporium sativum*. Proc. Second Int. symp. Plant Path. IARI, New Delhi, 1971; 42.
 101. Prabhu AS, Singh A. *Indian phytopath.* 1974; **27**: 632.
 102. Goel LB, Nagarajan S, Singh RV, Sinha VC, Kumar J. *Indian Phytopath.* 1999; **52**: 398.
 103. Parashar M, Nagarajan S, Goel LB, Kumar J. Report of the coordinated Experiments 1994 -95. Crop protection (pathology) AICWIP, Directorate of wheat Research, Karnal. 1995; 206.
 104. Anonymous, 2003 Annual report of NATP (MM) project. Directorate of wheat Research, ICAR, Karnal, India.
 105. Zillinsky FJ. Common Diseases of small Grain Cereals. A Guide to Identification Mexico DF.: CIMMYT.1983; 141.
 106. Duveiller E, Dubin HJ. Helminthosporium Leaf blights:Spot blotch and Tan Spot. In: Bread Wheat Improvement & Production Series, No. 30 Ed. Curtis BC, Rajaram S, Gomez MH, F.A.O., Rome, 2002.
 107. Hait GN, Sinha AK. *J. Phytopath.* 1986; **115**: 97.
 108. Stack RW, McMullen M. Root and crown rots of small grains. NDSU extension service, Fargo, ND. USA. 1988; 8.
 109. Mehta YR. Spot blotch (*Bipolaris sorokiniana*). In: Seed-Borne Diseases and Seed Health Testing of Wheat Ed. Mathur SB, Kunfer BM Copenhagen, Denmark: Institute of Seed Pathology for Developing Countries, 1993: 168.
 110. Schilder, Bergstrom G. Tan spot. In: Seedborne diseases and seed health testing of wheat, (Eds. Mathur SB and Cunfer BM) Copenhagen, Denmark. Jordburgsförlaget 1993: 113.
 111. Pavlova VV, Dorofeeva LL, Kozhukhovskaya VA. Effectiveness of seed treatments against root rots of cereals. Moscow Russia; Izdatel stvokolos [Ru] All Russian Research Institute of Phytopathology, Russia, 2002; (CAB International) **8**: 21.
 112. Domanov NM. Kolfugo Duplet for seed treatment of cereals *Zashchita Karantin Rasteni.* 2002; **6**: 29 Moscow, Russia. (CAB International)
 113. Korobov VA, Korobova LN. Raxil in the south of West Siberia. *Zashchita Karantin Rasteni.* novosivirec Agrarian University, Siberia ,Russia.(CAB International) 2002; **6**: 29.
 114. Sharma-Poudyal D, Duveiller E, Sharma RC. *J. Phytopathol.* 2005; **153**: 401.
 115. Meisner CA, Badaruddin M, Saunders DA, Alam KB. Seed Treatment as a Means to Increase Wheat Yields in Warm Areas. In: Saunders DA and Hettel GP, eds. 1994. Wheat in Heat-Stressed Environments: Irrigated, Dry Areas and Rice-Wheat Farming Systems, Mexico, D.F.: CIMMYT, 1994; 402.
 116. Malaker PK, Mian IH. *Ban. J. Agril. Res.* 2009; **34**: 425.
 117. Singh DP, Chowdhury AK, Kumar P. *Indian J. Agri. Sci.* 2007; **77**: 101.
 118. Loughman R, Wilson RE, Roake JE, Platz GJ, Rees RG, Ellison FW. Crop Management and breeding for control of *Pyrenophora tritici repentis* Causing yellow spot of wheat in Australia. In Dubin HJ, Duveiller E. (2000). Proceedings of (*Indian phytopathological Society Golden Jubilee*). IARI, New Delhi, 1998; 571

119. Mehta YR, Igarashi S. Chemical control measures for major diseases of wheat with special attention to spot blotch. In: Proceedings of the International symposium Mexico, D.F. CIMMYT. 1985; 364.
120. Viedma LQ, Kohli MM. Spot blotch and Tan spot of wheat in Paraguay. In: Helminthosporium Blights of Wheat: Spot Blotch and Tan Spot (Ed. Duveiller E, Dubin HJ, Reeves J, McNab A), CIMMYT/UCL/BADC 1998; 126.
121. Annone J. Tan spot of wheat in Argentina: Importance and prevailing disease management strategies: *Proc.Of the International Workshop on Helminthosporium Diseases of wheat: Spot Blotch and Tan Spot*, Ed. Duveiller E, Dubin HJ, Reeves J, McNab A. CIMMYT, El Batan, Feb. 9-14, Mexico, 1997.
122. Tewari AN, Wako K. *Plant Dis. Res.* 2003; **18**: 39.
123. Rashid AQMB, Sarker K, Khalequzzaman KM. *Ban. J. Plant Pathol.* 2001; **17**: 45.
124. Colson ES, Platz GJ, Usher TR. *Aus. Plant Path.* 2003; **32**: 241.
125. Singh DP, Sharma AK, Kumar P, Chowdhury AK, Singh KP, Mann SK, Singh RN, Singh AK, Kalappanvar IK, Tewari AN. *Indian J. Agric. Sci.* 2008; **78**: 513.
126. Rahman MM, Barma NCD, Malaker PK, Karim MR, Khan AA. *Int. J. Sustain. Crop Prod.* 2009; **4**: 10.
127. Bochow H, Kogel KH, Poehling H, Von Alten H, Wyss U. *J. Plant Dis. Prot.* 2001; **108**: 626.
128. Sticher L, Mauch-Mani B, Mettraux JP. *Annu. Rev. Phytopathol.* 1997; **35**: 235.
129. Bello DG, Sisterna MN, Monaco CI. *Intl. J. Pest Manag.* 2003; **49**: 313.
130. Christensen JJ. *Phytopath.* 1925; **15**: 785.
131. Mitra M. *Trans. Brit. Mycol. Soc.* 1931; **16**: 115.
132. Hrushovetz SB. *Can. J. Bot.* 1956; **34**: 321.
133. Wilson VE, Murphy HC. *Phytopath.* 1964; **54**: 147.
134. Tinline RD. *Adv. Plant Pathol.* 1986; **6**: 113.
135. Zhong S, Steffenson BJ. *Mycologia.* 2001a; **93**: 852.
136. Zhong S, Steffenson BJ. *Phytopath.* 2001b; **91**: 469.
137. Zhong S, Steffenson BJ, Martinez JP, Ciuffetti LM. *Mol. Plant Microbe Interact.* 2002; **15**: 481.
138. Sinha A K. Basic research in induced resistance for crop disease management. In : " Basic Research for Crop Disease Management" ed. Vidyasekharan P. Daya Publishing House, New Delhi. 1989; 187.
139. Bashyal BM, Chand R, Kushwaha C, Sen D, Prasad LC, Joshi AK. *World J. Micro Biotech.* 2010; **26**: 309.
140. Newton R, Anderson JA. *Can. J. Res.* 1929; **1**: 86.
141. Matern U, Kneusel RE. *Phytopara* 1988; **16**: 153.
142. Sridhar R. *II Riso.* 1975; **25**: 37.
143. Hait GN, Sinha AK. *Z. pflkrankh. Pflschutz.* 1987; **94**: 360.
144. Reddy MN, Ramagopal G, Rao AS. *Phytopath. Medi.* 1976; **15**: 78.
145. Brahamachari BK, Kolte SJ. *Indian Phytopath.* 1983; **36**: 149.
146. Mahadevan A. *Phytopath. Z.* 1966; **57**: 96.
147. Van Loon LC. *Plant Mol. Biol.* 1985; **4**: 111.
148. Andebrhan T, Coutts RHA, Wagih EE, Wood RKS. *Phytopath. Z.* 1980; **98**: 47.
149. Gianinazzi S, Ahl P, Cornu A, Scalla R. *Physiol. Plant Path.* 1980; **16**: 337. 150. de Wit PJGM, Buurlance MB, Hammond KE. *Physiol. Mol. Plant Path.* 1986; **29**: 159.

151. Farkas GL, Kiraly Z. *Phytopath. Z.* 1958; **31**: 251.
152. Kosuge T. *Ann. Rev. Phytopath.* 1969; **7**: 195.
153. Fric F. Oxidative enzymes. In "Physiological Plant Pathology". Ed. Heitefuss R, Williams PM. Springer-Verlag 1976; 617.
154. Heitefuss R, Buchanan-Davidson DJ, Stahman MA, Walker JC. *Phytopath.* 1960; **50**: 198.
155. Ekbote AU, Mayee CD. *Indian J. Plant Path.* 1984; **2**: 21.
156. Sridhar R, Ou SH. *Phytopath. Z.* 1974a; **69**: 222.
157. Sridhar R, Ou SH. *Biol. Plant* 1974b; **16**: 67.
158. Patykowski J, Urbanek H, Kaczorowska T. *J. Phytopath.* 1988; **122**: 126.
159. Peltonen S. *Acta Agri. Scandi. Soil and Plant Sci.* 1998; **48**: 184.
160. Kervinen T, Peltonen S, Teeri TH, Karjalainen R. *New Phytologist.* 1998; **139**: 293.
161. Peltonen S, Mannonen L. Karjalainen R. *Plant Cell Tissue Organ Culture* 1997; **50**: 185.
162. Peltonen S, Karjalainen R. *J. Phytopath.* 1995; **143**: 239.
163. Manandhar HK, Mathur SB, Smedegaard-Petersen V, Thordal-Christensen H. *Physiol. Mol. Plant Path.* 1999; **55**: 289.
164. Sarkar B, Choudhury B, Sen Sharma M, Kamruddin SK, Choudhury AK, Roy A. *Archv. Phytopath. Plant Prot. (In Press)*, DOI: 10.1080/03235401003633667.
165. Saari EF, Prescott M. *Plant Dis. Rep.* 1975; 377.
166. Eyal Z, Scharen AL, Prescott JM, Van G. The (*Septoria*) disease of wheat: Concepts and methods of disease management. CIMMYT, Mexico city, 1987.
167. Das MK, Rajaram S, Mundt CC, Kronstad WE. *Crop Sci.* 1992; **32**: 1450.
168. Mahadevan A, Sridhar R. Method in Physiological Plant Pathology. 3rded Sivakami Publication, Madras. 1986
169. Lowry OH, Rosebrough NJ, Farr AL, Randall RJ. *J. Biol. Chem.* 1951; **193**: 265.
170. Addy SK, Goodman RN. *Indian Phytopath.* 1972; **25**: 575.
171. Bhattacharya MK, Ward EWB. *Physiol. Mol. Plant.* 1987; **31**: 407.
172. Laemmli UK. *Nature* 1970; **227**: 680.
173. Camm EL, Towers GHN. *Phytochemistry.* 1973; **12**: 961.
174. Novacky A, Acedo G, Goodman RN. *Physiol. Plant Pathol.* 1973; **3**: 133.
175. VanEtten HD, Mansfield JW, Bailey JA, Farmer EE. *Plant Cell.* 1994; **6**: 1191.
176. Tolbert NE. *Plant Physiol.* 1973; **51**: 234
177. Vidhyasekharan P. Phenolics and disease resistance. In Physiology of Disease Resistance in Plants (ed. Vidhyasekharan P.) CRS Press, Boca raton. 1988; 49.
178. Ride JP. Cell walls and other structural barriers in defence. In Biochemical plant pathology. (ed. Callow JA.) JohnWiley & Sons Ltd., New York. 1983; 215.
179. Bera S, Purkayastha RP. *Current science.* 1999; **76** (10): 1376.

List of publication

1. **Sarkar B.** Choudhury B, Sen Sarma M , Kamruddin Sk, Choudhury AK and Roy A. (2010). Potentiality of organotin (IV) compounds in the control of foliar blight disease of wheat (*Triticum aestivum*) caused by *Bipolaris sorokiniana*. **Archives of phytopathology and plant protection (In Press)**

DOI: 10.1080/03235401003633667

2. **Sarkar B.** Roy A, Ng SW and Tiekink ERT (2010) Bis (3,5-dinitrobenzoato- κO^1) tetramethanolicobalt (II) **Acta Cryst.** E66: m365.

3. **Sarkar B.** Choudhury AK, Roy A, Biesemans M, Willem R, Ng SW and Tiekink ERT (2010) Synthesis, characterization, crystal structure analysis, and anti-fungal and phytotoxicity activities of diorganotin compounds derived from dihalo-substituted [(2-hydroxyphenyl) methylideneamino] thiourea. **Applied Organometallic Chemistry.** (Article first published online: 27 JUL 2010, **DOI:** 10.1002/aoc.1698)

Poster presentation

a. **Sarkar B.** Roy A and Chowdhary, A (2007). Biocidal activities of newly synthesized organotin compounds against foliar blight of wheat. In: NATIONAL SYMPOSIUM ON PLANT PROTECTION: Technology Interface by Association for Advancement in Plant protection. 28th-29th Dec., 2007, Mohanpur, BCKV.

b. **Sarkar B.** Choudhury AK and Roy A. (2008) Synthesis of new Organotin (IV) compounds and its biocidal efficacy against some agriculturally important disease of North Bengal. 11th CRSI NATIONAL SYMPOSIUM IN CHEMISTRY, 6-8 February 2009, Indian Institute of Science Education & Research, Pune, India.

